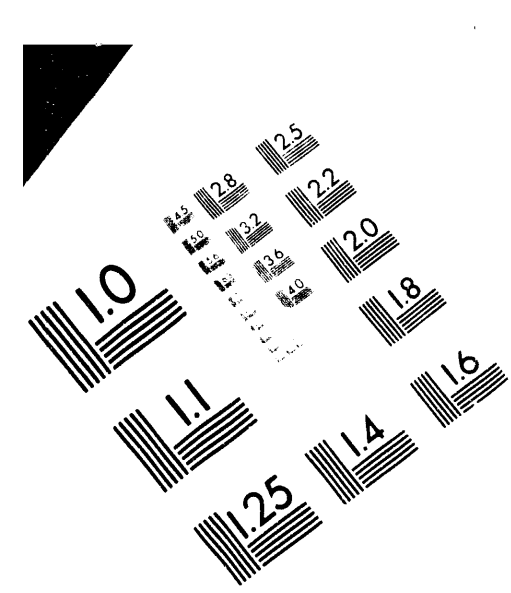

AIIM

Association for Information and Image Management

1100 Wayne Avenue, Suite 1100
Silver Spring, Maryland 20910

301/587-8202

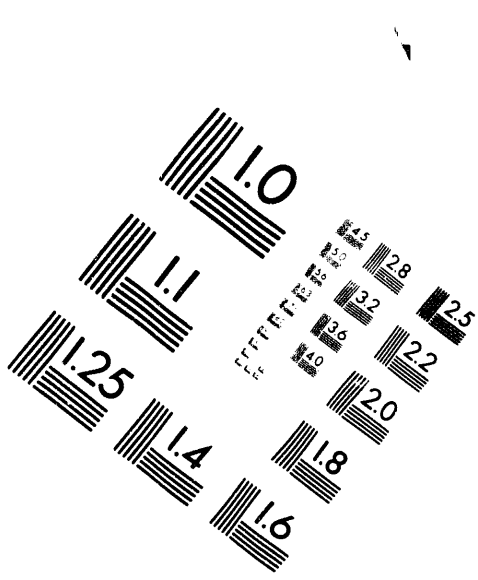

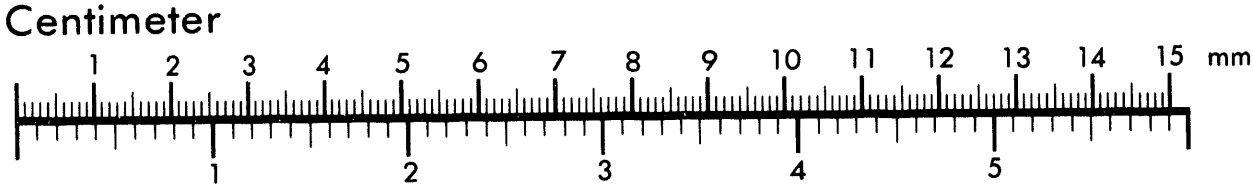

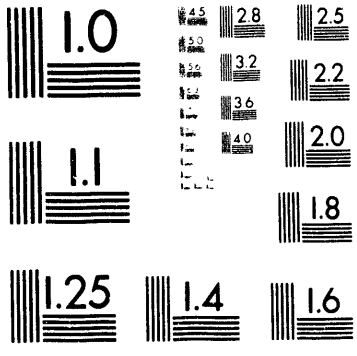

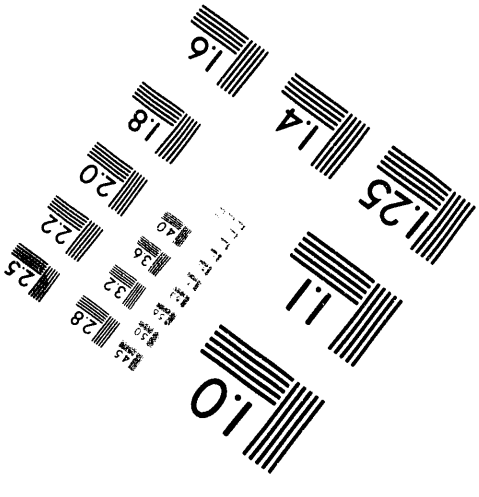

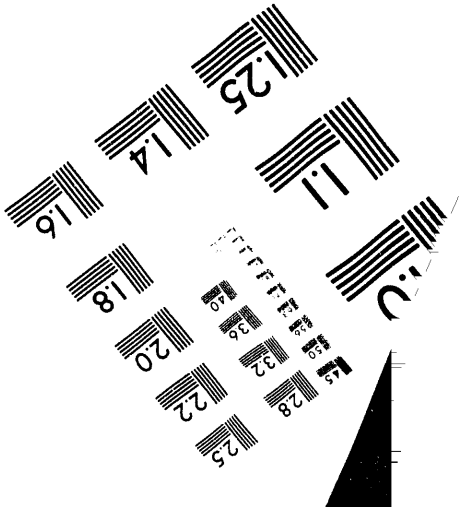

MANUFACTURED TO AIIM STANDARDS
BY APPLIED IMAGE, INC.

1 of 2

SAND88-1314
Unlimited Release
Printed April 1993

Distribution
Category UC-721

WASTE ISOLATION PILOT PLANT SIMULATED RH TRU WASTE EXPERIMENTS: DATA AND INTERPRETATION REPORT

Martin A. Molecke, J. Guadalupe Argüello, and Ricardo Beraún

Sandia National Laboratories
Albuquerque, New Mexico 87185

ABSTRACT

The simulated, i.e., nonradioactive remote-handled transuranic waste (RH TRU) experiments being conducted underground in the Waste Isolation Pilot Plant (WIPP) were emplaced in mid-1986 and have been in heated test operation since 9/23/86. These experiments involve the in situ, waste package performance testing of eight full-size, reference RH TRU containers emplaced in horizontal, unlined test holes in the rock salt ribs (walls) of WIPP Room T. All of the test containers have internal electrical heaters; four of the test emplacements were filled with bentonite and silica sand backfill materials. We designed test conditions to be "near-reference" with respect to anticipated thermal outputs of RH TRU canisters and their geometrical spacing or layout in WIPP repository rooms, with RH TRU waste reference conditions current as of the start date of this test program. We also conducted some thermal overtest evaluations. This paper provides a: detailed test overview; comprehensive data update for the first 5 years of test operations; summary of experiment observations; initial data interpretations; and, several recommendations for future RH TRU waste emplacements in the WIPP. Details included are: current test status; experimental objectives -- how these tests support WIPP TRU waste acceptance, performance assessment studies, underground operations, and the overall WIPP mission; and, in situ performance evaluations of RH TRU waste package materials plus design details and options. We provide instrument data and results for in situ waste container and borehole temperatures, pressures exerted on test containers through the backfill materials, and vertical and horizontal borehole-closure measurements and rates. The effects of heat on borehole closure, fracturing, and near-field materials (metals, backfills, rock salt, and intruding brine) interactions were closely monitored and are summarized, as are assorted test observations. Predictive 3-dimensional thermal and structural modeling studies of borehole and room closures and temperature fields were also performed. Computed and measured borehole closure results indicate greater closure occurs near the middle- and back-end of the holes than at the (open) rib-end. Computed vertical closure results provide an upper bound estimate on borehole closure that is 1.5 - 2.5 times larger than the measured in situ values, but are in qualitative agreement. Based on our current data, results, observations, and interpretations, RH TRU waste packages, materials, and emplacement geometry in unlined salt boreholes appear to be quite adequate and safe for repository-phase isolation at WIPP. There should be no restrictions on RH TRU waste acceptance at WIPP due to observed waste package behavior.

ACKNOWLEDGMENTS

The authors would like to acknowledge and express appreciation to the following people and organizations for helping to make the installation, technical support, operations, maintenance, and data interpretations for the WIPP simulated RH TRU waste test program a success:

- All the personnel in the Sandia WIPP Instrumentation Department and the Test Planning and Fielding Department, for overseeing the cabling, instrument installation and maintenance, and on-site data acquisition systems for this, and all other Waste Package Performance tests conducted at the WIPP facility. In particular, we would like to give thanks to Tom Burford of Sandia for his excellent support in supervising the day-to-day, on-site conduct of this test program, by serving as the lead technician and on-site alternate for the test Principal Investigator, Martin Molecke. In addition, Jim Krumhansl of the Sandia Geochemistry Department provided essentially all of the geochemical support and posttest analyses for this test.

- All the personnel of RE/SPEC, Inc. at the WIPP site for assisting Sandia in the areas of gage installation and maintenance, data acquisition operations, and for supervising the underground drilling operations. We would also like to acknowledge the RE/SPEC, Inc. personnel in Albuquerque for conducting data manipulation, analysis, and presentation operations for all of the test remote-instrument data.

- Personnel from Tech Reps, Inc., in Albuquerque, led by Bob Jones, for providing many of the test plan and report illustrations, other support work, and for assisting in manual data analyses.

- Underground personnel in both the WIPP Experimental Operations and drilling crews, for providing high-quality, cooperative support in all underground, test-related operations.

CONTENTS

CONTENTS (continued)

LIST OF FIGURES

LIST OF FIGURES (continued)

LIST OF FIGURES (continued)

LIST OF FIGURES (continued)

LIST OF TABLES

LIST OF ACRONYMS

3D - three dimensional
ASME - American Society of Mechanical Engineers
B/S - bentonite clay and silica sand backfill material
CH TRU - contact-handled transuranic waste
DAS - data acquisition system
DHLW - defense-related high-level wastes
DOE - U. S. Department of Energy
DOT - U. S. Department of Transportation
drift - mined tunnel
DRZ - disturbed rock zone
EPA - U. S. Environmental Protection Agency
HEPA - high-efficiency particulate filter
IEEE - Institute of Electrical and Electronics Engineers, Inc.
LVDT - linear variable displacement transducer
MAD - measurand action data sheet for recording instrument problems, resolution, etc., for QA purposes
NOS - computer network operating system, term used at Sandia
NUCFIL HEPA -filter provided by Nuclear Filter Technology Co.
PA - performance assessment
PI - Principal Investigator for a test program
ppm - parts per million
ppt - parts per thousand
QA - quality assurance
RH TRU - remote-handled transuranic waste
RHO - Rockwell Hanford Operations (now Westinghouse Hanford Operations), Richland, WA
rib - the wall in a mined drift
SNL - Sandia National Laboratories
SPDV - Site Preliminary Design Validation, early phase in WIPP development
TC - thermocouple
TR*** - designation for a remote-reading instrument or gage in WIPP Room T, as part of the Simulated RH TRU Waste test program
TRH*** - designation for a remote-reading instrument or gage in WIPP Room T, as part of the Simulated RH TRU Waste test program
TRU - transuranic
UNDERDOG - Underground Nuclear Depository Evaluation, Reduction, and Detailed Output Generator, data reduction software program used by SNL
WID - Westinghouse Waste Isolation Division
WPIO - U.S. DOE WIPP Project Integration Office
WIPP - Waste Isolation Pilot Plant
WPSO - U.S. DOE WIPP Project Site Office
WISDAAM - WIPP In Situ Data Acquisition, Analysis, and Management system, used by SNL
WPP - Sandia Waste Package Performance program, for laboratory and in situ tests supporting the WIPP Project

WASTE ISOLATION PILOT PLANT SIMULATED RH TRU WASTE EXPERIMENTS: DATA AND INTERPRETATION REPORT

1.0 INTRODUCTION

The simulated remote-handled transuranic waste (RH TRU) experiments being conducted in the Waste Isolation Pilot Plant (WIPP) are documented in a formal Test Plan (Molecke, 1986). Sandia National Laboratories prepared this Test Plan for the Department of Energy/WIPP Project Office, now the WIPP Project Site Office, DOE/WPSO, to describe test purposes, justifications, technical details, and operations. The test program and Test Plan were authorized and approved by both Sandia and DOE/WPSO.

The simulated RH TRU waste experiments were an important segment of the Sandia-WIPP Waste Package Performance (WPP) subtask (Tyler et al., 1988). The WPP subtask included the planning, direction, and conduct of all materials-related (and associated operations-related) testing on both simulated (i.e., nonradioactive) remote-handled and contact-handled (CH) TRU waste containers. Several other types of waste packages and waste forms were also tested. The WPP testing encompassed multiple WIPP in situ tests and the supporting laboratory materials research, laboratory analyses (of in situ samples), and modeling efforts (Tyler et al., 1988). Our predominant goal for the WIPP WPP testing program was to provide the comprehensive data bases for waste package engineered barrier material selections and detailed evaluations, waste package designs and design options, test operational experience, long-term predictive modeling, and performance assessment studies. Another of our major intents was to provide relevant support to the WIPP facility operations, procedures, designs, and overall mission.

The simulated RH TRU waste experiments were emplaced into the WIPP Room T in mid-1986. A successful Mandatory Full Participation (MFP) test readiness walk-through procedure was conducted on September 22, 1986 to ensure that essentially all necessary test preparations and requirements were accomplished. The MFP procedure was attended by test, administrative, and safety personnel from both Sandia National Laboratories -- the test conductors, and the Department of Energy/WIPP Project Office -- the test sponsors. Following the MFP, the simulated RH TRU waste experiments were officially turned-on, i.e., the test electric heaters were energized, at 1:00 PM on September 23, 1986. This was a formal WIPP Project milestone. These experiments have been in heated operation for a total of more than six years. They are still operational and continue in a state of instrument monitoring and passive maintenance -- no

instrument maintenance, test observations, or sampling within the test room are possible due to the current lack of access.

These WIPP in situ, simulated RH TRU waste experiments involve the emplacement and testing of 8 full-size (0.66m-diameter by 3.0m-long), near-reference (thermal and geometrical) RH TRU containers in horizontal, unlined emplacement holes in the rock salt ribs of test Room T. These RH TRU waste containers were each electrically heated to about 120 W, approximately 2 to 4 times the average expected thermal output of actual RH wastes to be disposed of in the WIPP. After approximately three years of testing, on November 1, 1989, we raised the thermal output of each of the electrical heaters to about 300 W for the remainder of the test. The thermal output of 300 W is the maximum allowable heat output for RH TRU wastes. We consider this higher-power portion of the test to be an overtest, a credible test accelerant.

Four of the eight RH TRU emplacements are backfilled within the borehole, around the test container, with a granular mixture of 70 wt. % bentonite clay and 30 wt. % silica sand. This backfill emplacement allows for evaluations on: backfill sorption of any intruding brines; options for operational emplacement techniques; possible modification of waste container-borehole thermal conductance properties; and, the transference of pressures due to borehole salt creep closure onto the RH TRU waste container. The other four test emplacements have no backfill materials -- other than trapped air. Many of these emplacements are fully instrumented with remote-reading thermocouples, pressure gages (only in backfilled test emplacements), borehole vertical-closure gages, and vertical and horizontal borehole-diameter closure gages. All gages are connected to a computerized data acquisition system. We closely monitored the effects of heat on borehole closure and near-field materials interactions. We also periodically opened each test borehole for visual inspections, manual closure measurements, maintenance, and materials sampling. Full technical details on these experiments and related test operations are described in a separate Test Plan (Molecke, 1986).

The purpose of this data report is to provide a detailed overview, data summary, technical observations, and initial interpretations from these in situ WIPP RH TRU waste experiments. Details included are:

1. the test status and relevant test observations after approximately the first five years of operations; test termination activities have not been conducted and are not addresssed;
2. the experimental objectives -- how these tests support WIPP TRU waste acceptance, performance assessment studies, underground operations, and the overall WIPP mission;

3. instrument data histories on in situ temperatures, pressures exerted on the waste containers, and borehole closure measurements and rates;

4. predictive geomechanical modeling of room and borehole closures and temperature fields -- and how these calculations compare to the actual borehole measured values;

5. in situ performance of RH TRU waste package materials and design details; and,

6. observations on growth and extent of the near-field disturbed-rock zone within and around the boreholes as a function of time.

We summarized some of this information in a preliminary overview report (Tyler et al., 1988) after about one year of test conduct. It is our purpose in this Data and Interpretation Report to be comprehensive in nature and to present a thorough summary of quality assurance-checked data and relevant experimental observations. All available data and information for the first five years of test operation are included. This data report ensures that all of this information is appropriately documented and available to other users and analysts for further interpretations, and is presentatble to various WIPP Project reviewers.

These WIPP simulated RH TRU waste experiments were included as a significant part of the Sandia-WIPP Waste Package Performance (WPP) program. The WIPP WPP program involved the direction and performance of all materials-related, and associated technical operations-related testing on both contact-handled (CH) and remote-handled (RH) transuranic (TRU) waste containers (Tyler et al., 1988; Matalucci et al., 1982), as well as of several different types of defense high-level waste (DHLW) packages and materials (Tyler et al., 1988; Matalucci et al., 1982). While none of these previous tests are active, the DOE WIPP Project has stated a commitment to appropriately complete and document these test results for the overall benefit of the WIPP Project and possibly other repository programs.

The WPP program encompassed several WIPP (simulated, nonradioactive) in situ tests and the supporting laboratory materials research, laboratory analyses (of in situ samples), and modeling efforts. The overall relationship of the WIPP simulated RH TRU waste experiments to the simulated CH TRU waste experiments, the simulated DHLW experiments, and other in situ WIPP experiments, is covered in full detail elsewhere (Tyler et al., 1988; Matalucci et al., 1982). The relationship of these simulated RH TRU waste experiments to previously planned RH TRU waste ADD-On Tests (Molecke and Munson, 1987), with a heavy emphasis on facility rock mechanics and thermal-structural interactions concerns, is also presented elsewhere. The RH TRU waste ADD-On Tests were approved, but were never funded nor initiated.

Our predominant goals for the overall WIPP WPP testing program were to provide comprehensive data bases for waste package engineered barrier material selections and detailed evaluations, waste package designs and design options, test operational experience, long-term predictive modeling, and performance assessment studies. Relevant support is also being provided to the WIPP facility operations, procedures, designs, and mission. Previous, supporting background material from all WPP laboratory and field data and experience is provided elsewhere (Tyler et al., 1988; Matalucci et al., 1982). This Data and Interpretation Report focuses on the WIPP simulated RH TRU waste experiment data and results, and related thermal and geomechanical modeling.

2.0 TEST OBJECTIVES

The general and specific technical objectives for the WIPP simulated RH TRU waste experiments are listed below.

a) To help provide a technical basis for validating the concept of safe RH TRU waste emplacement, retrieval, and disposal in the WIPP. This is a supplement for, and precursor to, the shipment of actual RH TRU wastes to the WIPP.

b) To extend the state-of-the-art of TRU waste package technology, beyond laboratory testing, with the in situ emplacement and testing of simulated, but representative, RH TRU waste containers.

c) To evaluate and demonstrate the horizontal emplacement of simulated RH TRU canisters in unlined boreholes in salt, emplaced in a simple, cost-effective manner. Provide technical comparisons to separate mock-RH TRU handling and retrieval demonstrations conducted in thick-sleeved boreholes (U.S. DOE, 1986a; Nair et al., 1986; U.S. DOE, 1987). This information applies directly to the proposed initial WIPP 5-year waste retrievability period.

d) To provide in situ verification by demonstration of the adequate durability (corrosion, behavior of protective coatings) and physical behavior (i.e., deformation) of RH waste containers in the WIPP under near-reference and thermal overtest repository conditions.

e) To continue posttest evaluation of RH TRU materials sampled (containers, backfills, and brines). Provide interpretations of results and assess the potential performance impacts for both the short-term, repository operational-phase and the long-term, post-closure phase.

f) To evaluate the effects of backfill materials (interactions behavior, compaction and "crusting," and emplacement techniques) on TRU waste containers durability and related repository operations, etc., as well as for addressing proposed EPA engineered-barrier criteria.

g) To evaluate the use of tailored backfills as affected by moisture sorption (brine-wicking), creep closure, and swelling pressures -- by monitoring pressures exerted on the waste containers, as transmitted through the backfill materials. Also, to assess potential impacts of backfills on container emplacement and retrieval operations.

h) To monitor the inflow of moisture into RH TRU boreholes, both as free brine and as backfill-sorbed moisture, for impacts on container corrosion and backfill behavior.

i) To measure the vertical and horizontal closure of RH TRU boreholes as a function of time and temperature. To compare in situ measured closure values with values calculated with geomechanical predictive models. Also, to provide interpretations of results and assess the potential performance impacts.

j) To monitor borehole thermal environments as a function of RH TRU thermal output (120 W and, as an overtest, 300 W). Compare in situ measured temperature values with values calculated with predictive thermal models. Provide interpretations of results and assess potential performance impacts.

k) To monitor changes in the disturbed-rock zone (DRZ) as a function of time, i.e., to measure any rock salt fracturing or separations adjacent to the RH TRU emplacement holes. This monitoring is for evaluating impacts on short-term repository operations (e.g., needs for borehole sleeves or rock-fall liners) and for performance assessment.

3.0 EXPERIMENTAL DETAILS

3.1 Test Room Physical Plan

The simulated RH TRU waste tests were conducted in the WIPP underground test Room T. Room T, as mined, is 3.96 m-high x 10.1 m-wide x 45.7 m-long (13 x 33 x 150 ft) in size, and occupies the southern half of the original, 91.4 m-long (300 ft), Site Preliminary Design Validation (SPDV) Room 3. The general underground location of WIPP test Room T, in relationship to other WIPP rooms, is shown in **Figure 3.1-1**. **Figure 3.1-2** shows a plan view of the Room T RH TRU waste tests; the simulated CH TRU (contact-handled) waste technology experiments (Molecke, 1986) are also shown in this figure. More details of the test room can be found in the simulated TRU waste Test Plan(s) (Molecke, 1986; Molecke and Munson, 1987).

Test Room T is located within a relatively thick layer of competent rock salt, about 95% halite (clear to reddish-orange-brown), with traces of argillaceous (clay) materials, discontinuous clay partings, traces of polyhalite, and anhydrite impurities. Excavation of Room T (SPDV Room 3) extended from March 24 - April 3, 1983. The floor of the room is about 654 m (2147 ft) below ground level; the floor level is also about 1.2 m (4 ft) above the anhydrite Marker Bed 139. The horizontal stratigraphic level of Room T is identical to the TRU waste storage rooms in Panel 1, in the southern end of the WIPP.

The RH TRU test containers were emplaced into unlined, horizontal cored holes in the rock salt ribs of Room T, as illustrated in **Figure 3.1-3** (photograph taken during the test installation phase). These boreholes are 0.91 m (36 in.) in diameter and 4.88 m (16.0 ft) deep. The tolerances on the hole length are +/- 15 cm (6 in.). Specific, initial diameters for these boreholes were not obtained. However, information provided by W.C. Patrick, Westinghouse-WID (November 1987), indicated that similar holes, cored with the same core barrel, had initial, average diameter measurements of 0.919 m (36.17 in.). **Table 3.1** lists the completion dates (both standard and Julian dates) for the coring of each RH test borehole.

The emplacement hole centers are 1.68 m (5.5 ft) above the drift floor and 2.44 m (8 ft) apart, with 4 holes in each rib, as illustrated in **Figure 3.1-4**. The hole-to-hole spacing used in WIPP Room T coincides with that of the planned WIPP RH TRU "reference" scheme. The WIPP Operating Contractor inferred this "reference" spacing from the areal thermal load limitation of approximately 2.5 W/m^2 (10 kW/acre), specified in the Waste Isolation Pilot Plant Design Validation Final Report (U.S. DOE, 1986b).

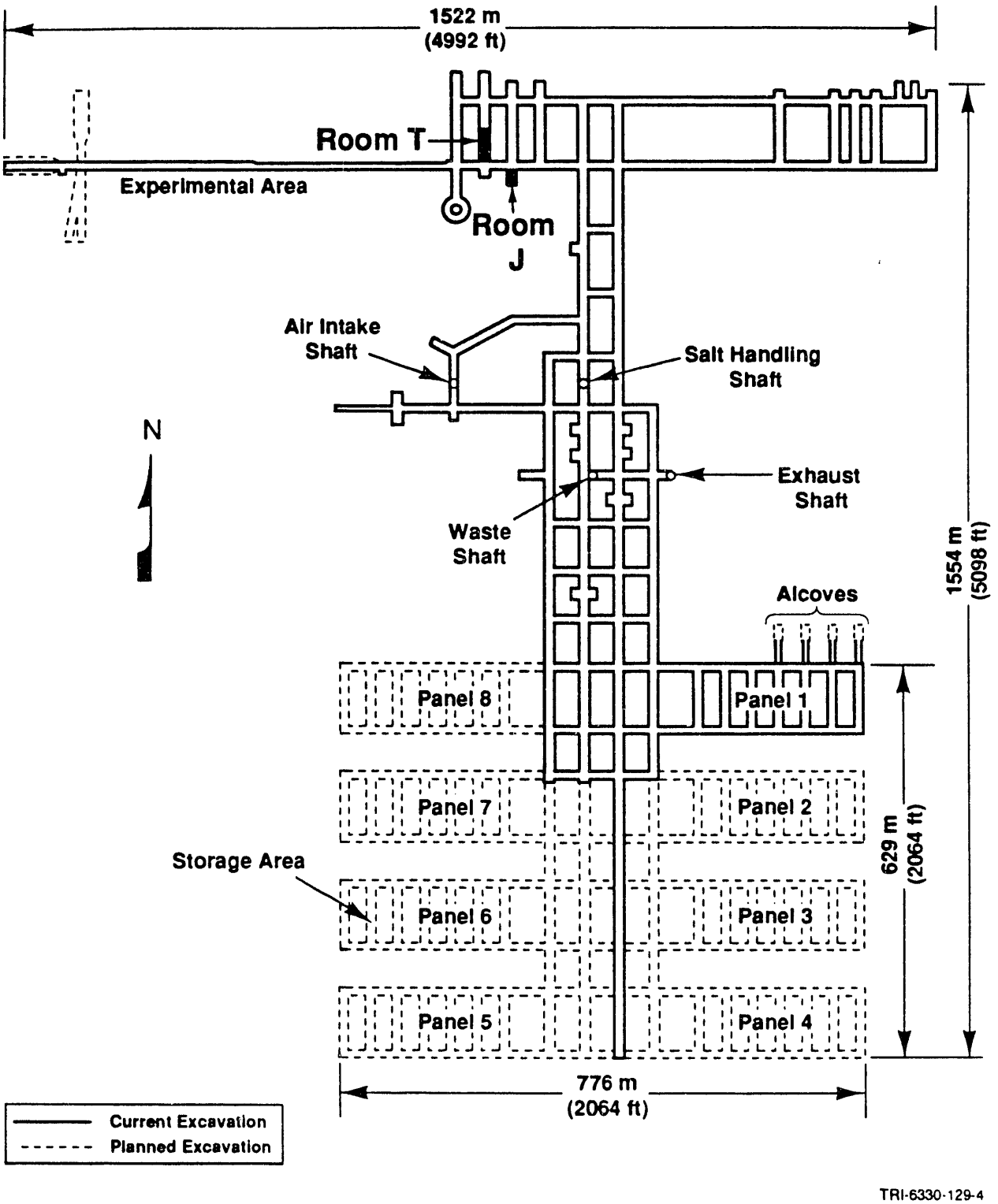

Figure 3.1-1. General underground layout of WIPP facility
(showing relative location of Simulated RH TRU Waste Experiments, Room T)

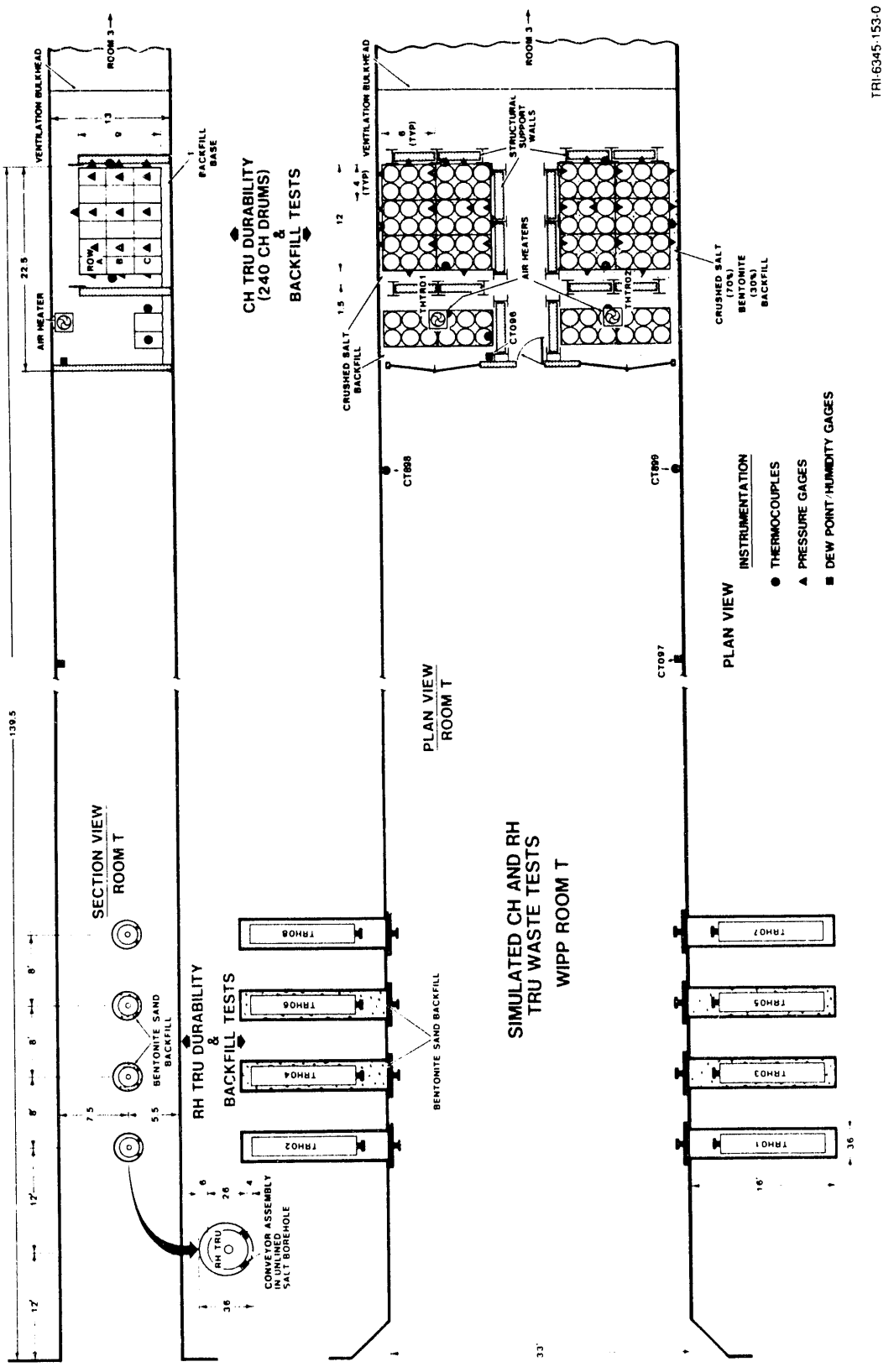

Figure 3.1-2 Plan view of Room T, with general details of Simulated RH and CH TRU Waste Tests

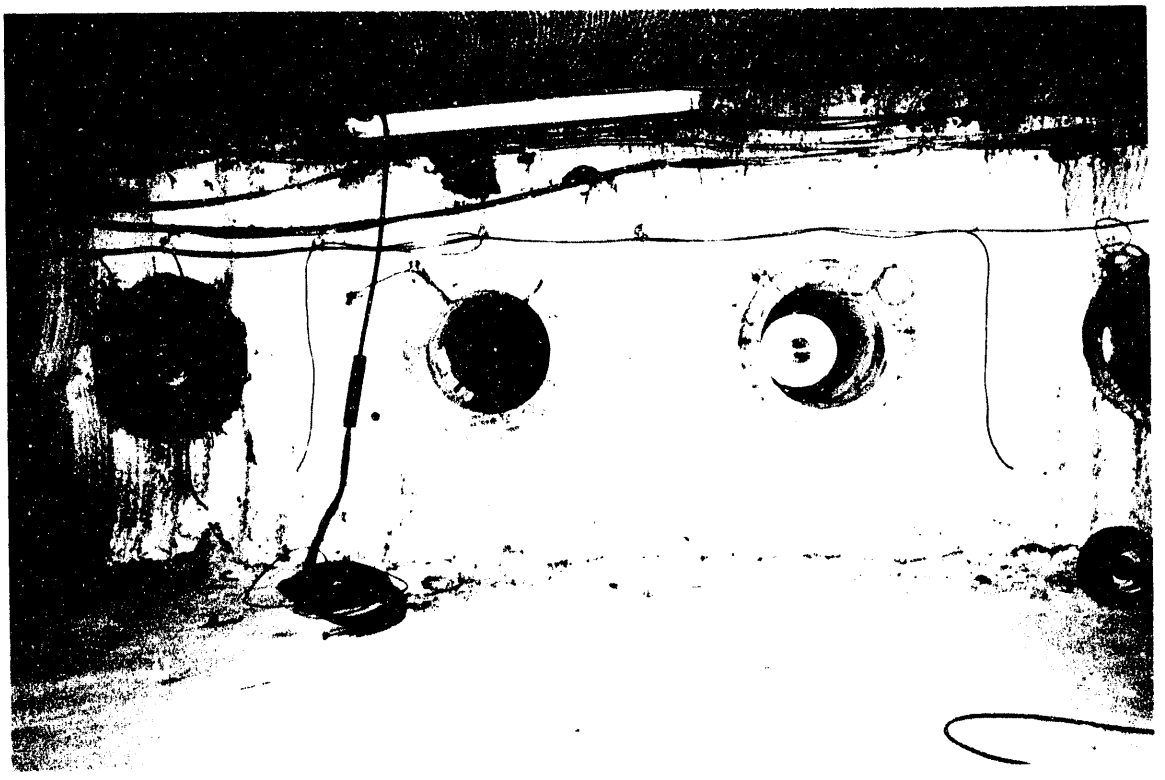

Figure 3.1-3 Photo of RH TRU test boreholes in Room T

Figure 3.1-4 Photo of simulated RH TRU waste test in Room T

The WIPP Operating Contractor has also interpreted this thermal load limitation to imply (Argüello and Torres, 1988) that as many as 70 "reference" canisters of RH TRU wastes could be emplaced into a maximum of 70 boreholes in the ribs of a waste storage room. There could thus be 35 canisters, with an average thermal output of 60 watts per canister, in each rib.

TABLE 3.1 Coring Completion Dates for Room T RH TRU Boreholes:

RH HOLE #	Completion Date	(Julian Date)
1	4-24-86	(6114)
2	4-15-86	(6105)
3	4-25-86	(6115)
4	4-26-86	(6116)
5	3-31-86	(6090)
6	3-25-86	(6084)
7	4-02-86	(6092)
8	3-10-86	(6069)

3.2 RH TRU Waste Containers and Heaters

Eight RH TRU waste containers were fabricated for test use in Room T. Fabrication was conducted by Seeley Enterprises, Inc., Albuquerque, NM, under subcontract to Sandia National Laboratories. Rockwell Hanford Operations (Hertelendy, 1984) provided the reference design (RHO drawing no. H-2-91273-1) for these containers, intended for use by defense waste generator sites in the US. This design is illustrated in **Figures 3.2-1** and **3.2-2**. Each container is 3.07 m-long (121 in.), 0.66 m (26 in.) in diameter, and has a maximum useful internal volume of 0.90 m^3 (31.7 ft^3). This internal volume was designed to incorporate 3 standard CH TRU DOT 17C drums, each 210 L (55 gallons) in volume, with dimensions of 0.884 m-high x 0.606 m-wide (34.8 in. x 23.8 in.). The empty weight of a reference RH TRU container is 799 kg (1760 lb.), the maximum gross weight is 3630 kg (8000 lb). Each RH TRU test container was fabricated out of ASTM A516-82, grade 70 mild steel, with an American Society of Mechanical Engineers (ASME) flanged-dome bottom head and an ASME flanged and reversed dish with flair head top. There is a crush ring or shroud on both ends of the container. These rings serve to protect the pintle on top, stabilize the container when it is stood upright, and absorb some energy by deforming -- in the case of an accidental drop. There is also a lead shield, or pig, at the top dome of the RH TRU container. Optional lead

pigs were not placed at the bottom of test containers, in order to make room for the installation of electric heaters, to be described. Leaving the bottom lead shield out also minimized the overall weight of the container. Obviously, no radiation shielding was necessary in these nonradioactive tests.

All test container welds were inspected by the dye penetrant method, per ASME SE165; acceptance standards are per ASME Section VIII division 1, appendix 8. The container exterior was painted with Amercote #86 primer and two coats of white, Amercote #33 enamel (Hertelendy, 1984). Prior to emplacement at the WIPP facility, the test containers were spot-painted with more of the original paint, Amercote #33. This spot painting was necessary to cover multiple paint scrapes and scratches, resulting from normal handling operations, in the relatively "soft" paint. Such painting touch-up would prove difficult if the containers had included actual, radioactive RH TRU wastes.

The RH TRU container pintle is fabricated out of bare, unpainted mild steel and has the same external dimensions as pintles used for defense high-level waste (DHLW) canisters at the Savannah River Plant. The RH TRU pintles incorporate a small carbon-composite, HEPA filter-assembly into the pintle head, as illustrated in **Figure 3.2-2,** as item 20. The RH TRU container, with the filter assembly, is designed to

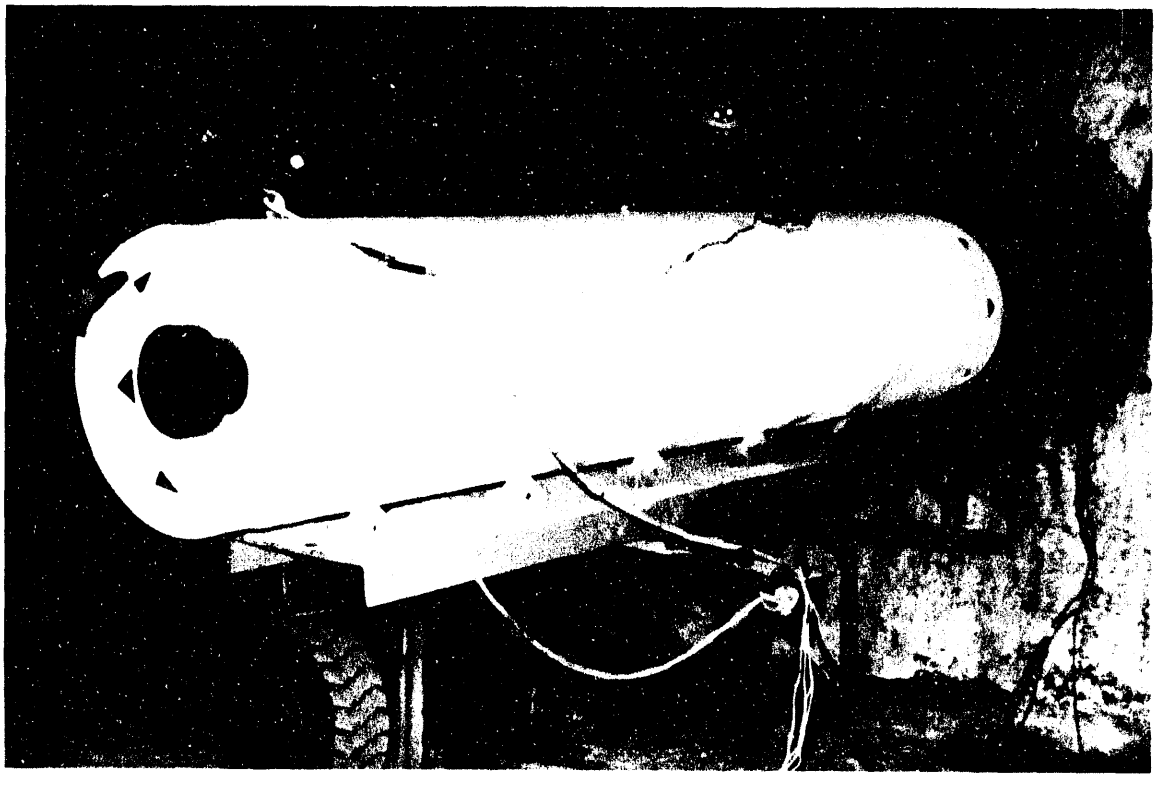

Figure 3.2-1 Photo of RH TRU test container, during emplacement

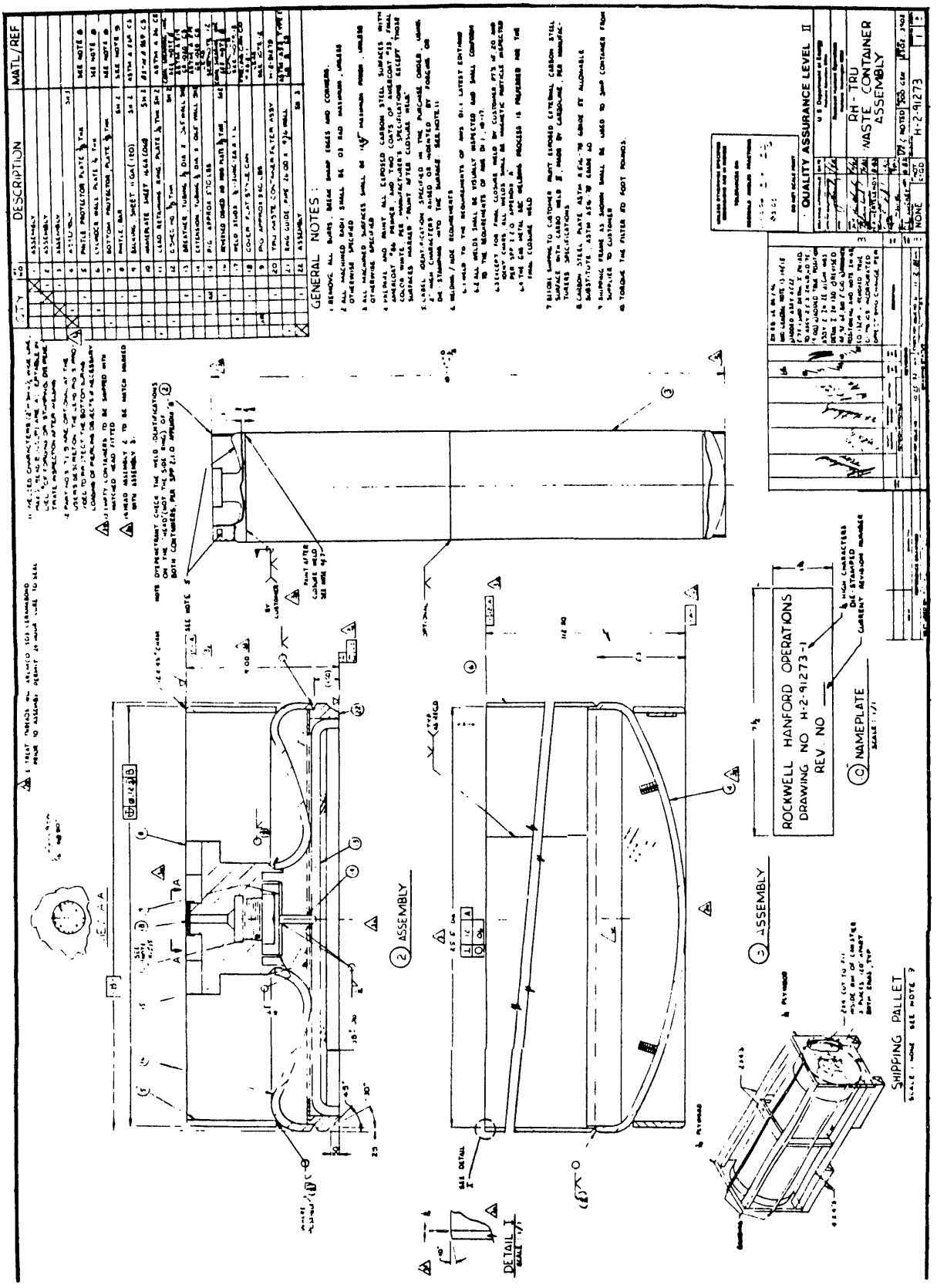

Figure 3.2-2 RH TRU waste test assembly

release any internal gases, but not particulates. The HEPA filter assemblies have a minimum flow capacity of 3000 cm^3/min and were obtained from Nuclear Filter Technology, Golden, CO. The entire, empty RH TRU container assembly cost $8100/each, as fabricated and delivered in 1985.

These RH TRU test containers have an internal, multiple rod-element electric-resistance heater inside, rather than actual TRU waste drums. The rod-heater assemblies incorporate four independently controllable Chromalox rods, have an active heated-length of 2.59 m (102 in.), and were identical to those used in the simulated DHLW test containers in Rooms B and A1 (Sandia drawing no. T95586) (Molecke, 1986; Molecke, 1984). The heater assemblies are illustrated schematically in **Figures 3.2-3** and **3.2-4**, shown inside of a RH TRU container, as modified for these experiments. The heater-rod assemblies were installed in the test container, as shown in **Figure 3.2-3,** and electrically checked-out by Sandia personnel at the fabricator site, before the container top head was welded on.

Each RH TRU test container was emplaced into a horizontal borehole. Each container rests on a preemplaced "borehole container conveyor assembly," as shown schematically in **Figure 3.2-5.** The conveyor assemblies are also visible in the two center boreholes shown in **Figure 3.1-3.** These assemblies have corrosion-resistant Inconel 600 roller wheels to facilitate container centering in the borehole. The

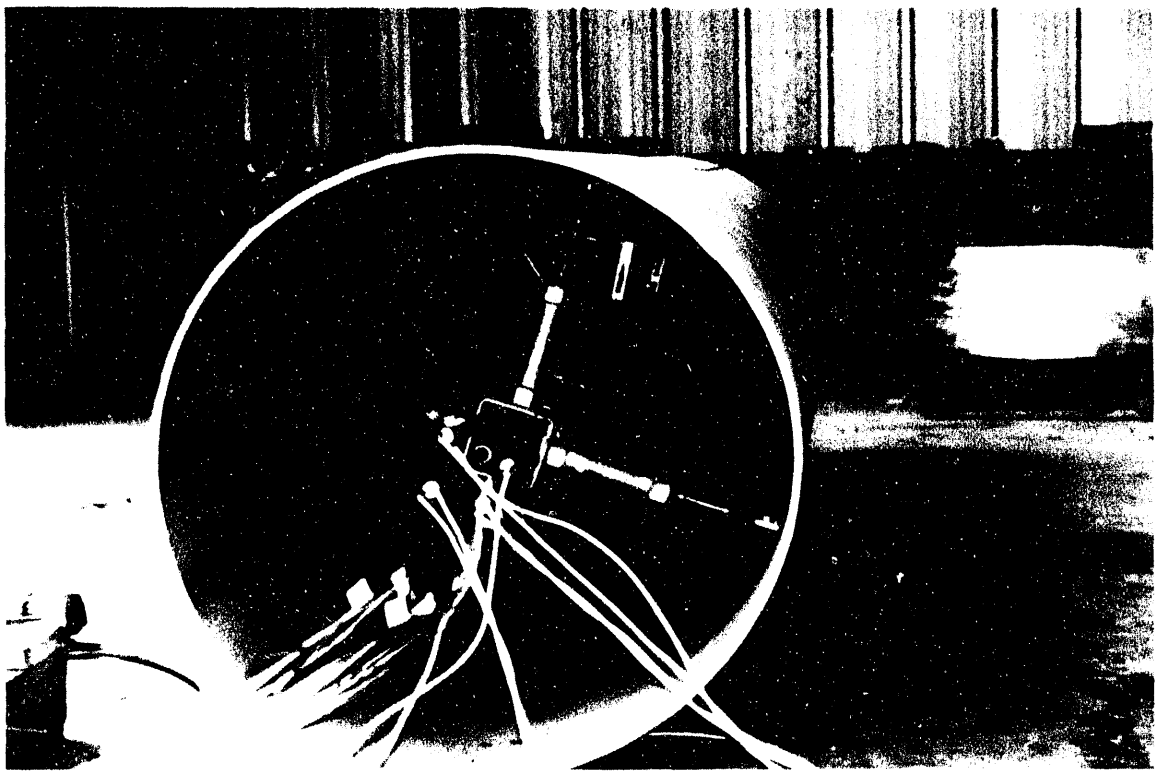

Figure 3.2-3 Photo of a RH TRU test heater assembly

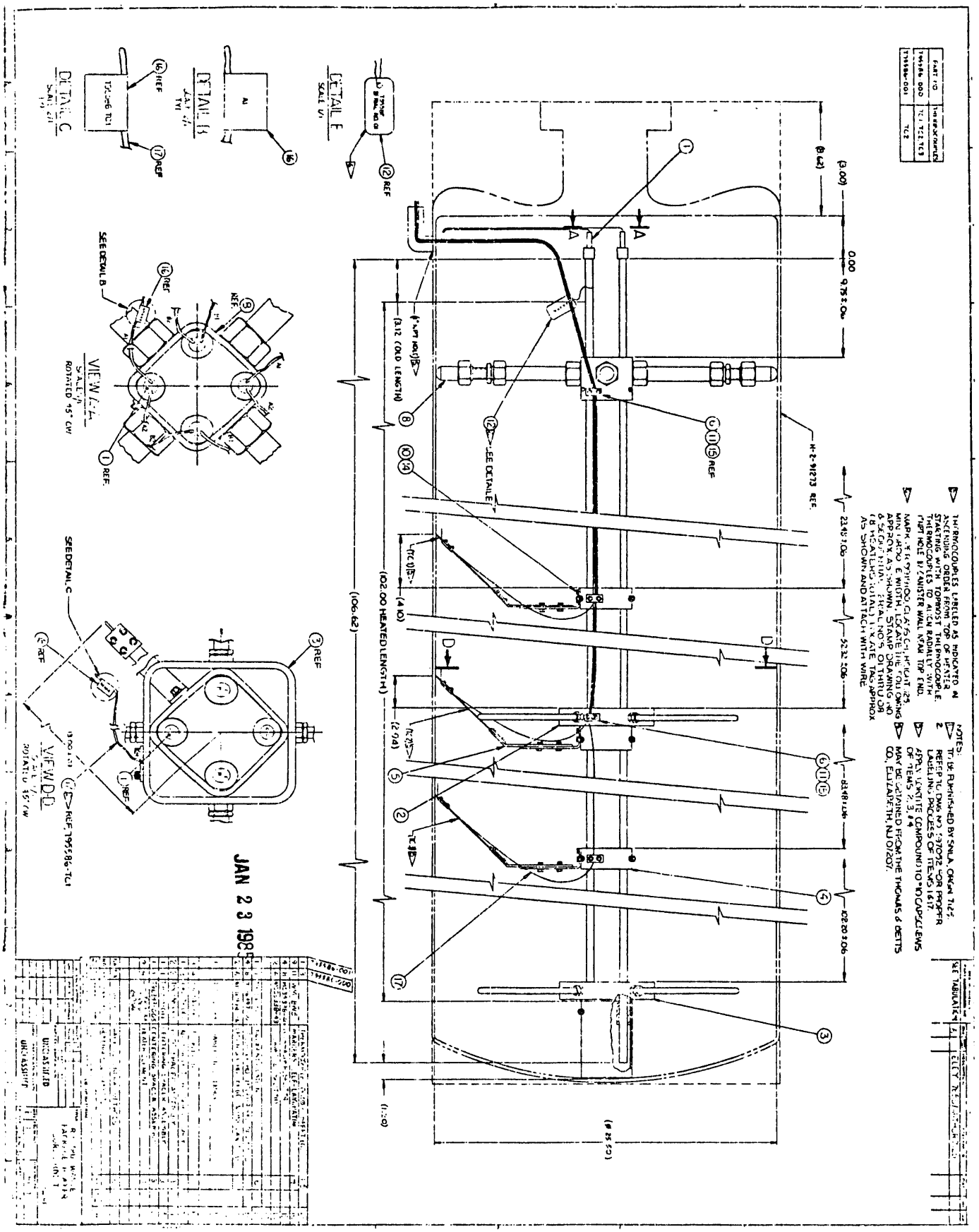

Figure 3.2-4 Schematic of a simulated RH TRU electric heater assembly

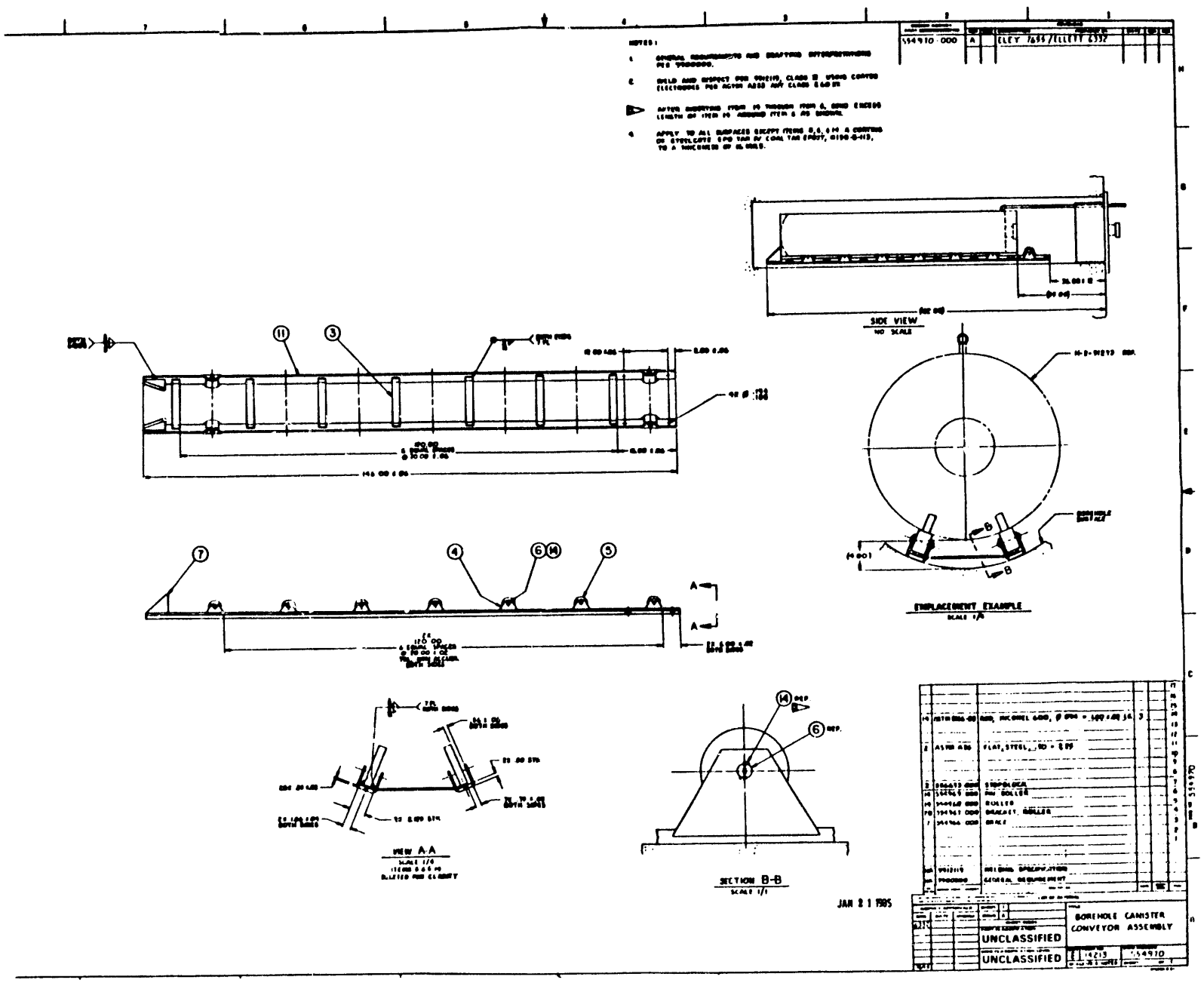

Figure 3.2-5 RH TRU test borehole conveyor assembly

bottom edge of the container rests 10 cm (4 in.) above the bottom of the salt borehole. This spacing prevents the container from laying in any potential accumulation of intruding brine, thereby mitigating potential short-term corrosion. The conveyor assembly rollers also facilitate container emplacement, periodic retrievals for examination, and reemplacements. In addition, we designed the conveyor assembly to position the test container in the borehole so that any added backfill material (Section 3.3) would completely encapsulate it.

3.3 Emplacement Hole Backfill, Materials, and Equipment

Four of the eight RH TRU waste test emplacements contain backfill materials; refer to **Table 3.3.** We used backfill in these tests to evaluate backfill materials performance (brine sorption, effects on container corrosion, compaction behavior, and possible modification of waste container-borehole thermal conductance properties) and impacts on emplacement and retrieval operations, all relative to the air/no-backfill case. The backfill material is a relatively low-density, granular mixture of 70 wt.% bentonite clay and 30 wt. % silica sand (abbreviated as B/S); it is described in more detail elsewhere (Pfeifle, 1987a). This is the same backfill material used in the simulated DHLW tests in Rooms B and A1 (Molecke, 1984). The bentonite clay is MX-80 granular Volclay Bentonite, purchased from American Colloid Company, and originating in South Dakota and Wyoming. This is predominantly a sodium- (with calcium-, and magnesium-) montmorillonite clay. The clay and sand mixture has an initial, as emplaced bulk density of 1.26 kg/m^3. (Tyler et al., 1988). The maximum sorbed-moisture content is 7%, based on the supplier's maximum-allowable moisture specification. Our laboratory analyzed moisture content for 100% MX-80 bentonite was 5.56%; this can be converted to about 3.9 % moisture for the B/S mixture.

We emplaced the B/S backfill material around the horizontal RH TRU canisters using an auger-type apparatus, as schematically illustrated in **Figure 3.3-1** (Pfeifle, 1987a). Further details are found elsewhere (Pfeifle, 1987a,b) cn the specifications for all of the backfill materials used and on the descriptions of the overall backfill blending and emplacement equipment, including the auger. For reasons of practicality, the backfill material does not occupy all the void volume in the emplacement hole. The backfill was added almost up to the top, horizontal surface of the test container, so as to not interfere with or impede the remote-reading, vertical borehole-closure gages stationed on top of the container. Also, the backfill material does not extend all the way to the front hole plug, but covers essentially the entire length of the test container, then slopes forward toward the hole plug; refer to **Figures 3.5-1 to 3.5-8**. [NOTE: For RH TRU wastes to be emplaced with backfill in an actual repostory, the backfill would probably be pneumatically installed, and would occupy essentially all of the borehole volume behind the hole shield plug.]

TABLE 3.3 Summary of Simulated RH TRU Tests in WIPP Room T: Backfill Materials, Objectives, and WPP Instruments

Container I.D.	Backfill Material	Primary Test Objectives	Heater Thermo-couples	Near-Field Thermo-couples	Pressure Gages	Vertical Closure Gages	Borehole Diameter Gages
TRH01	No Backfill	WPP Durability & Vert. Hole Closure	3	3	0	5	1-horiz. 1-vert.
TRH02	No Backfill	WPP Durability & Vert. Hole Closure	3	3	0	5	1-horiz. 1-vert.
TRH03	Partial B/S Backfill	WPP & Backfill-Brine Impacts, and Vert. Hole Closure	3	3	12	3	0 0
TRH04	Partial B/S Backfill	WPP & Backfill-Brine Impacts, and Vert. Hole Closure	3	3	12	3	0 0
TRH05	Partial B/S Backfill	WPP, Backfill-Brine Impacts, Vert. Hole Closure & DEMO	1	1	0	0	0 0
TRH06	Partial B/S Backfill	WPP, Backfill-Brine Impacts, Vert. Hole Closure & DEMO	1	1	0	0	0 0
TRH07	No Backfill	WPP Durability, Vert. Hole Closure, & DEMO	1	1	0	2	1-horiz. 1-vert
TRH08	No Backfill	WPP Durability, Vert. Hole Closure, & DEMO	1	1	0	2	1-horiz. 1-vert
		TOTAL RH TRU Instruments:	16 (=72)	16	12	20	4-horiz. 4-vert.

3.4 Test Accelerant Techniques

We used higher temperature, or more correctly greater than reference thermal power output, as the only test accelerant technique in these simulated RH TRU tests. The power output was approximately 120 W/container for the first three years of test operation. This is about two, or by some estimates up to four times the thermal output of "reference" RH TRU wastes to be isolated at WIPP. For the following three years of the test, we raised the heater output to a level of about 300 W/container, to simulate the maximum allowable power output of an RH TRU waste container. We used this thermal test accelerant technique to force interactions and modes of degradation to occur faster, for test observation purposes. This acceleration permits data to be gathered during the multi-year time-frame of these experiments and to be

extrapolated more confidently to longer periods of time (e.g., decades or more) for use in performance assessment consequence and uncertainty analyses.

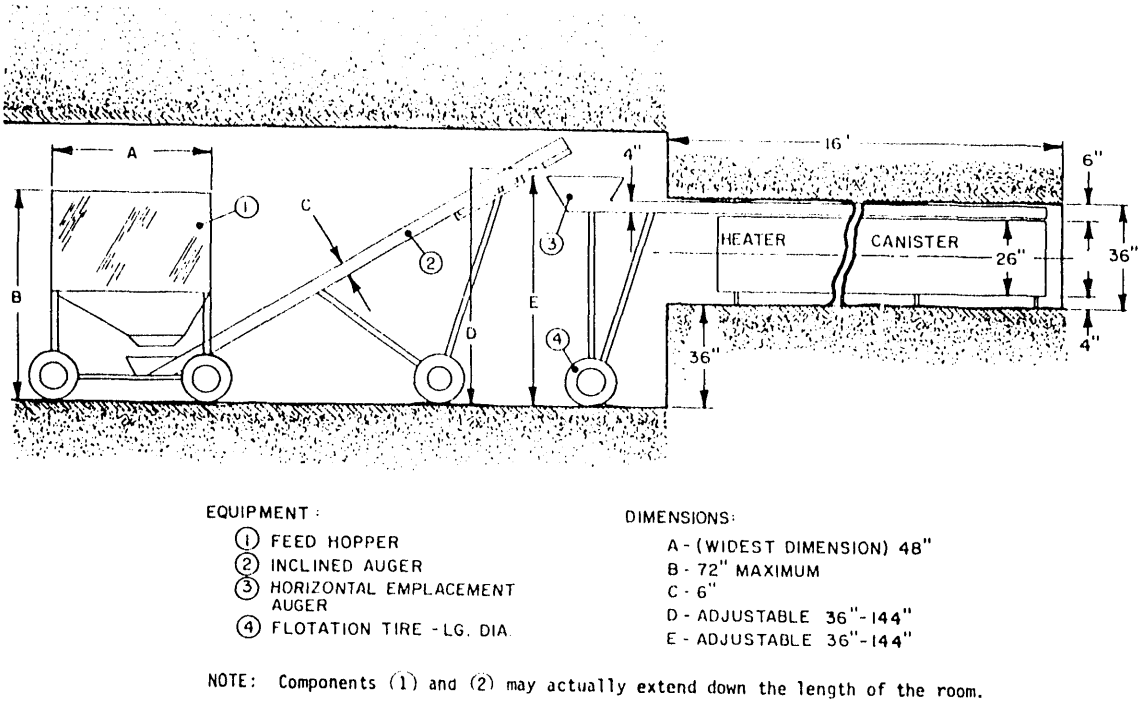

Figure 3.3-1 Horizontal-borehole backfill emplacement apparatus (Pfeifle, 1987a)

3.5 Test Instrumentation

There are basically 4 types of remote-reading instruments used in these RH TRU waste tests: thermocouples, pressure gages/stress transducers, vertical borehole-closure gages (to measure closure from the top of the RH TRU container to the top-center of the borehole surface), and vertical and horizontal borehole-diameter convergence gages. The quantities and types of installed gages, as well as a brief description and primary objectives of each RH TRU test emplacement are listed in **Table 3.3**. The detailed locations of each instrument in test emplacements TRH01 through TRH08 are illustrated in **Figures 3.5-1** to **3.5-8,** respectively (Molecke, 1986). The location of every waste package performance, WPP, instrument as installed in the test room is contained in a NOS (network operating system) computer file (Molecke, 1986) and is specified to, and installed within, ±0.1 ft (±3 cm) in the x, y, and z directions, relative to the test room geometric center. The "as built" instrumentation NOS file for this simulated RH TRU waste experiment (final revision, 1988) is duplicated in **Table 3.5.**

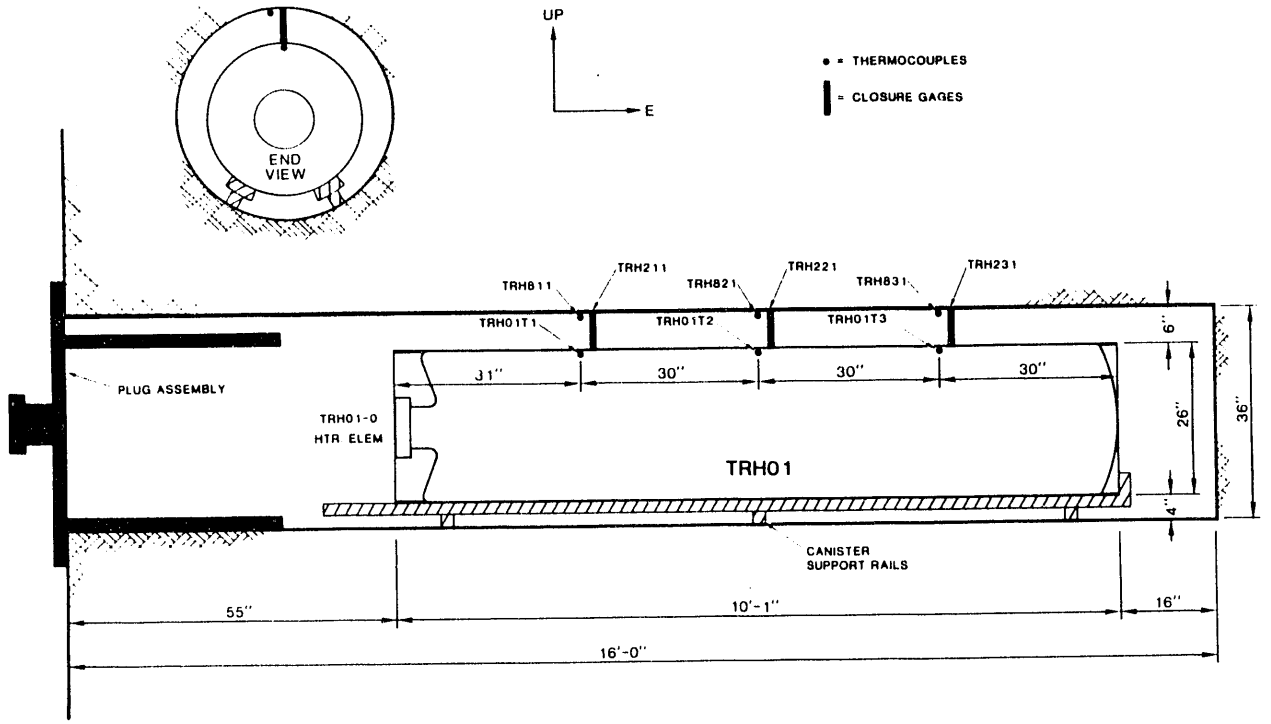

Figure 3.5-1 Simulated RH TRU Test Emplacement TRH01

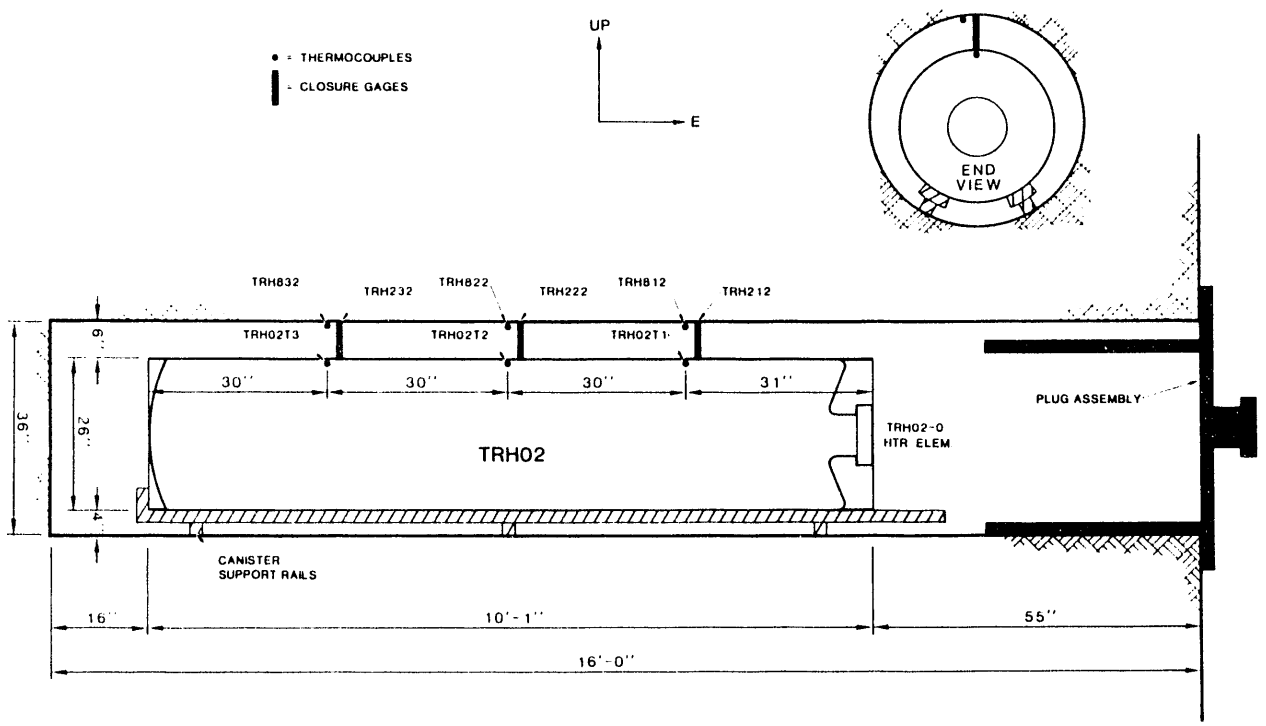

Figure 3.5-2 Simulated RH TRU Test Emplacement TRH02

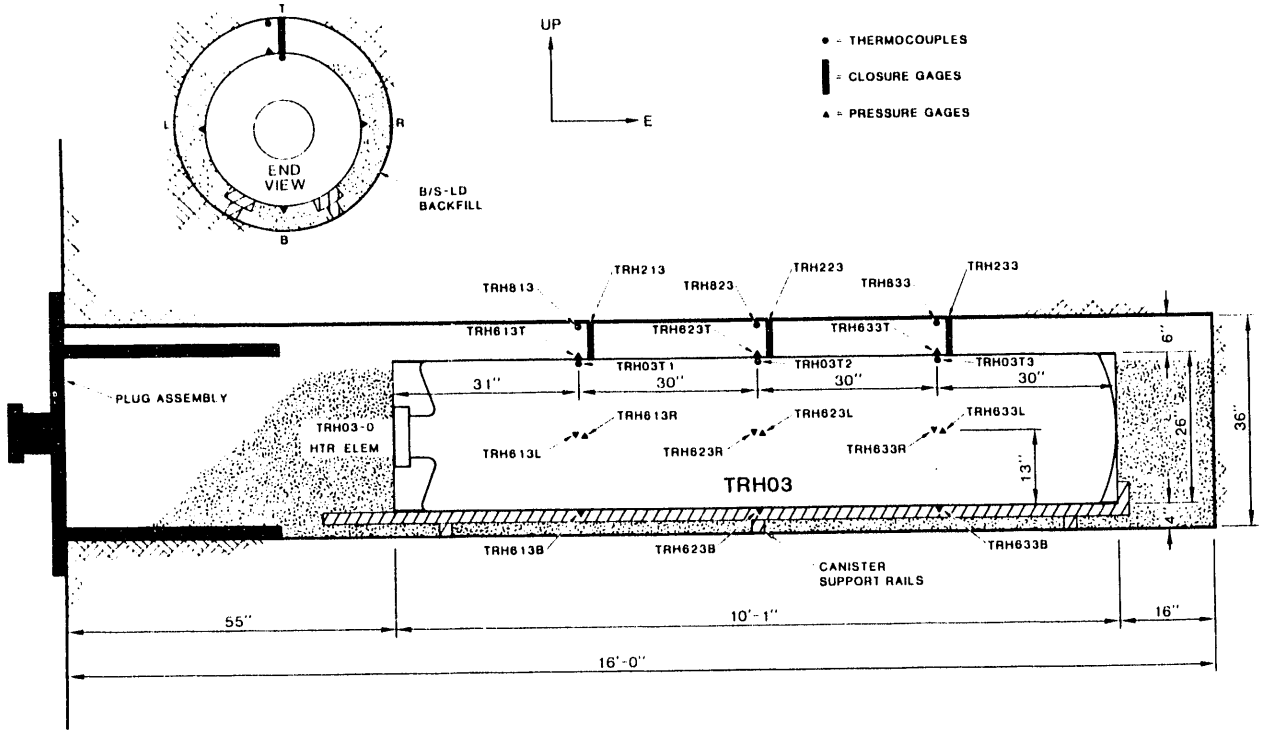

Figure 3.5-3 Simulated RH TRU Test Emplacement TRH03

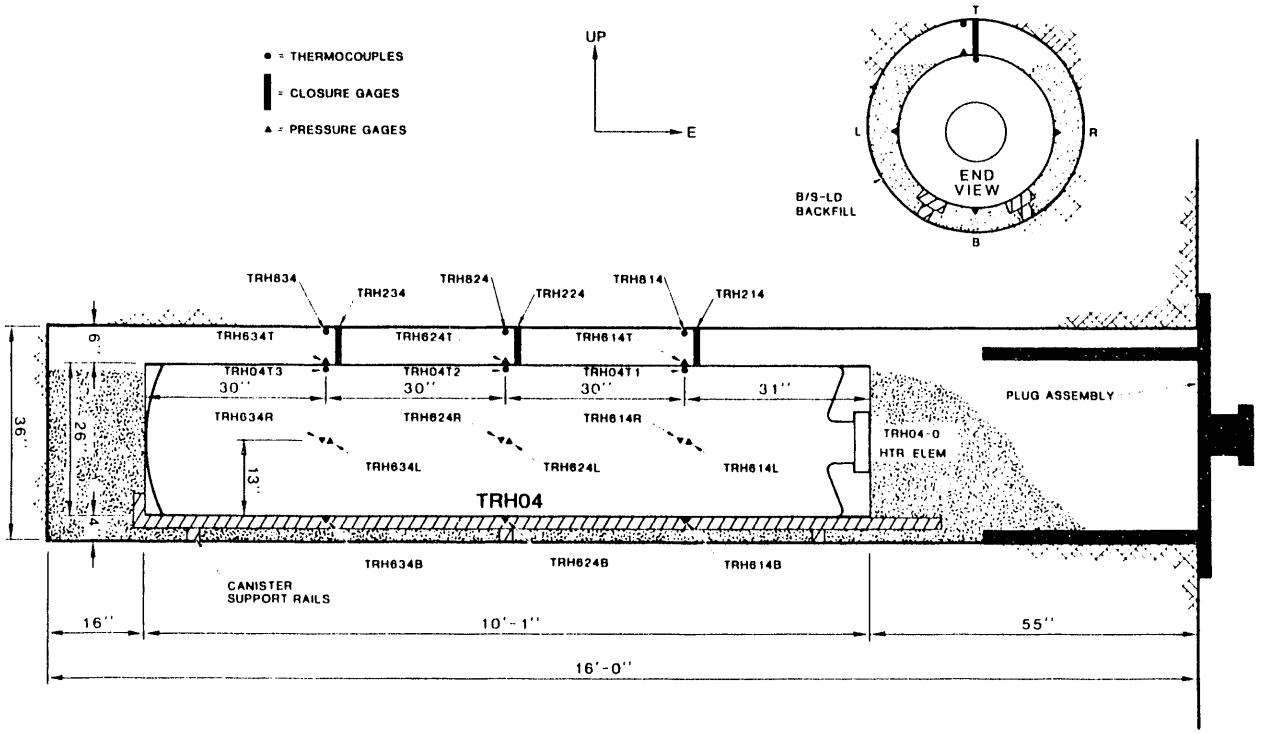

Figure 3.5-4 Simulated RH TRU Test Emplacement TRH04

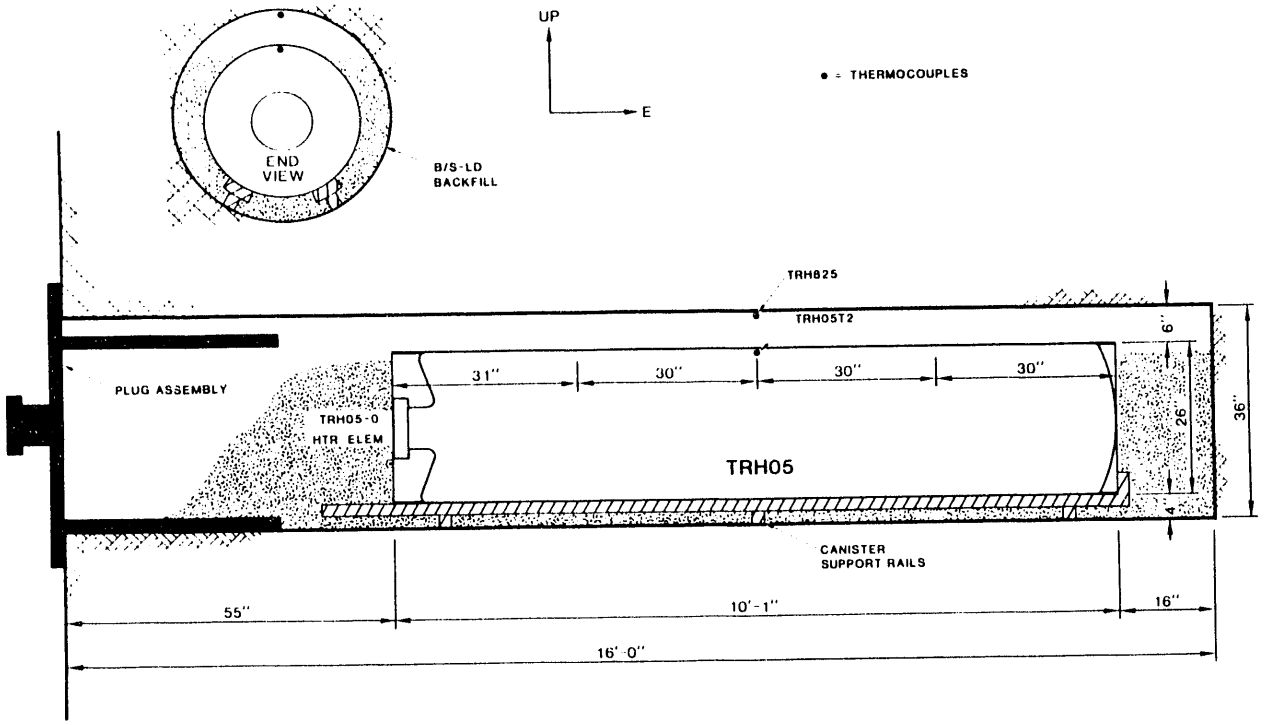

Figure 3.5-5 Simulated RH TRU Test Emplacement TRH05

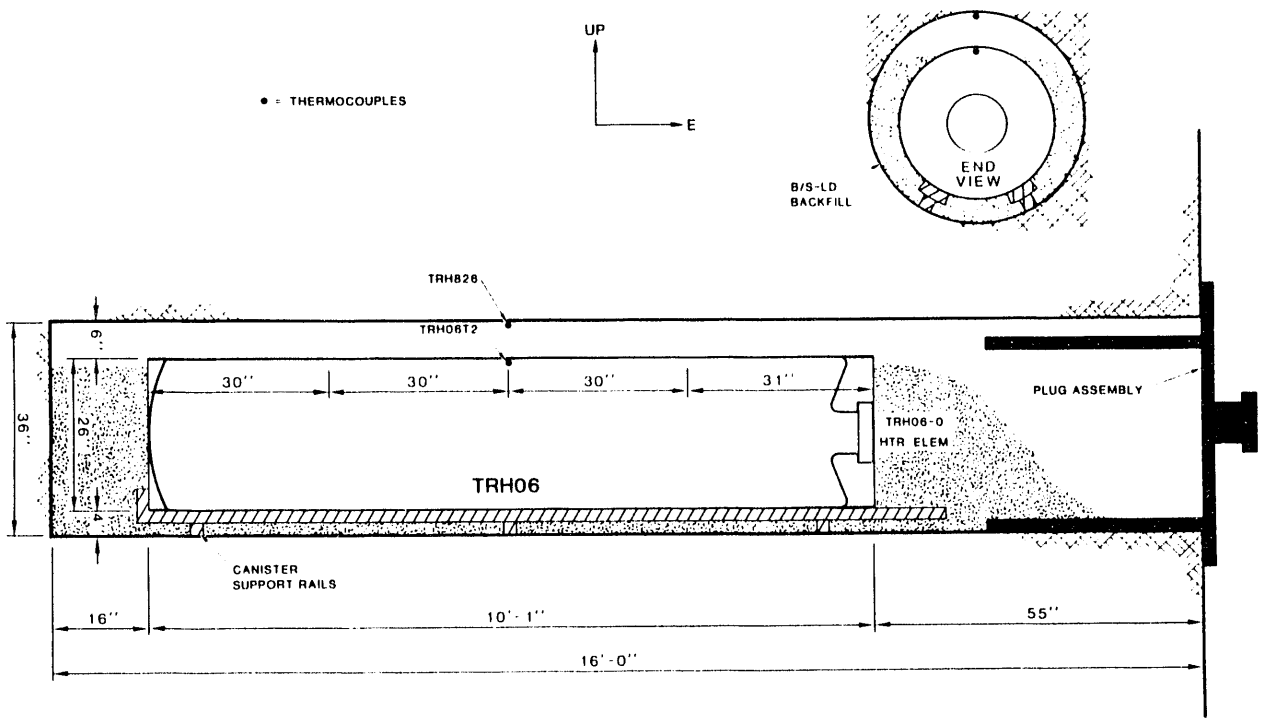

Figure 3.5-6 Simulated RH TRU Test Emplacement TRH06

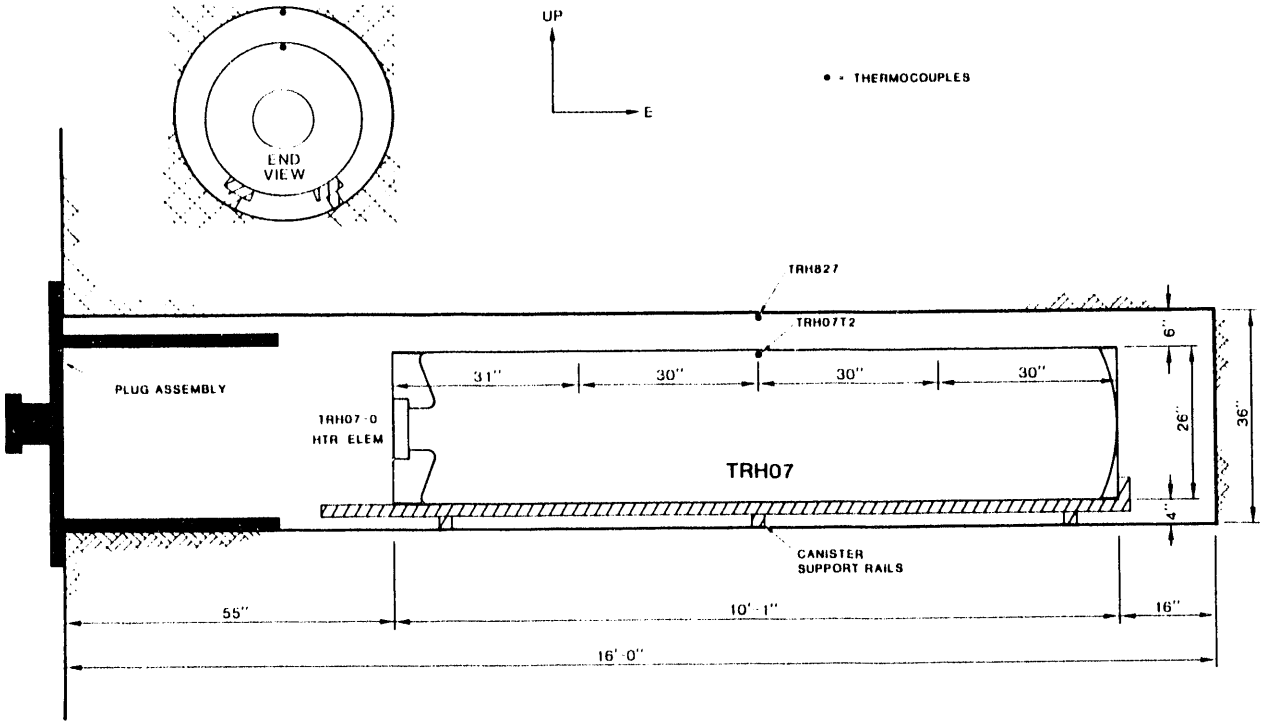

Figure 3.5-7 Simulated RH TRU Test Emplacement TRH07

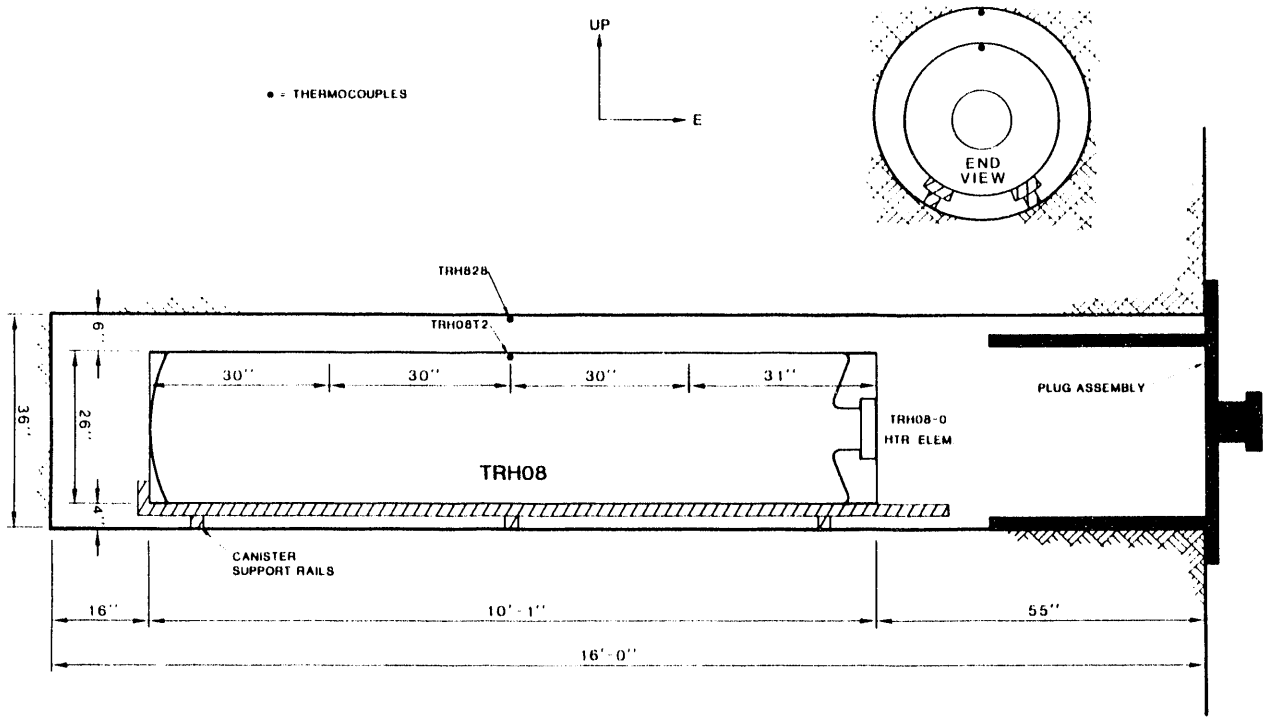

Figure 3.5-8 Simulated RH TRU Test Emplacement TRH08

Table 3.5

Instrumentation NOS File for the Simulated RH TRU Waste Test, WIPP Room T

SIM-TRU-ROOM T FILE DATED: 08/05/83 **AS BUILT** LAST REVISION: 10/88
APPROVED: M.A. MOLECKE, P.I., 6332 APPROVED FOR DISTRIBUTION: L.D. TYLER 6332

Notes:

IDs ARE AS FOLLOWS: (MODIFIED 10/16/86)

PREVIOUS ID	CURRENT ID
TRH01-0	TR001-0
TRH01T1	TR001T1
THTR01	TC001
CT506A	TC506A

Explanation of Gage Number
TR000-099 Special Gages
TR200-299 Closure or Displacement Gage
TR600-699 Stress Gage
TR700-899 Thermocouple - Temperature of Backfill or Canister Outer Shell

Gage Type Definition
CL - Closure or Displacement Gage
DEW - Dew Point/Humidity Sensor
HTR - Canister Heater
STR - Stress Gage
TC - Thermocouple

Orientation Definition
P - Point, No Defined Oreintation
H - Horizontal
V - Vertical

Coordinates X,Y,Z Refer to a Positive Distance East, North, and Above the Center of Room 3 (negative signs refer to west,south,and below center). X1, Y1, Z1 Locate One End of a Horizontal or Vertical Gage; X2, Y2, Z2 Locate the Other End. For Point Gages, X1, Y1, Z1 Define the Collar of the Hole that Contains the Gage. X2, Y2, Z2 Define the Point at Depth.

Gage Number	Gage Type	Orien-tation	X1 (m)	X2 (m)	Y1 (m)	Y2 (m)	Z1 (m)	Z2 (m)	Install Date
TC096-1	DEW	P	-1.2	-1.2	-9.8	-9.8	1.1	1.1	19-Mar-87
TC097-1	DEW	P	5.0	5.0	-21.3	-21.3	1.8	1.8	19-Mar-87
TC898-1	TC	P	-5.0	-5.0	-13.6	-13.6	-0.3	-0.3	9-Feb-87
TC899-1	TC	P	5.0	5.0	-13.6	-13.6	-0.3	-0.3	9-Feb-87
TR001-0	HTR	H	6.4	9.5	-38.4	-38.4	-0.3	-0.3	13-Jun-86
TR001T1	TC	P	5.0	7.2	-38.4	-38.4	0.0	0.0	13-Jun-86
TR001T2	TC	P	5.0	8.0	-38.4	-38.4	0.0	0.0	13-Jun-86
TR001T3	TC	P	5.0	8.7	-38.4	-38.4	0.0	0.0	13-Jun-86
TR002-0	HTR	H	-6.4	-9.5	-38.4	-38.4	-0.3	-0.3	22-May-86
TR002T1	TC	P	-5.0	-7.2	-38.4	-38.4	0.0	0.0	22-May-86
TR002T2	TC	P	-5.0	-8.0	-38.4	-38.4	0.0	0.0	22-May-86
TR002T3	TC	P	-5.0	-8.7	-38.4	-38.4	0.0	0.0	22-May-86
TR003-0	HTR	H	6.4	9.5	-36.0	-36.0	-0.3	-0.3	16-Jun-86
TR003T1	TC	P	5.0	7.2	-36.0	-36.0	0.0	0.0	16-Jun-86
TR003T2	TC	P	5.0	8.0	-36.0	-36.0	0.0	0.0	16-Jun-86
TR003T3	TC	P	5.0	8.7	-36.0	-36.0	0.0	0.0	16-Jun-86

Table 3.5 (continued)
Instrumentation NOS File for the Simulated RH TRU Waste Test, WIPP Room T

Gage Number	Gage Type	Orien-tation	X1 (m)	X2 (m)	Y1 (m)	Y2 (m)	Z1 (m)	Z2 (m)	Install Date
TR004-0	HTR	H	-6.4	-9.5	-36.0	-36.0	-0.3	-0.3	2-Jul-86
TR004T1	TC	P	-5.0	-7.2	-36.0	-36.0	0.0	0.0	2-Jul-86
TR004T2	TC	P	-5.0	-8.0	-36.0	-36.0	0.0	0.0	2-Jul-86
TR004T3	TC	P	-5.0	-8.7	-36.0	-36.0	0.0	0.0	2-Jul-86
TR005-0	HTR	H	6.4	9.5	-33.5	-33.5	-0.3	-0.3	13-Jun-86
TR005T2	TC	P	5.0	-8.0	-33.5	-33.5	0.0	0.0	13-Jun-86
TR006-0	HTR	H	-6.4	-9.5	-33.5	-33.5	-0.3	-0.3	13-Jun-86
TR006T2	TC	P	-5.0	-8.0	-33.5	-33.5	0.0	0.0	13-Jun-86
TR007-0	HTR	H	6.4	9.5	-31.1	-31.1	-0.3	-0.3	5-Jun-86
TR007T2	TC	P	5.0	8.0	-31.1	-31.1	0.0	0.0	5-Jun-86
TR008-0	HTR	H	-6.4	-9.5	-31.1	-31.1	-0.3	-0.3	3-Jun-86
TR008T2	TC	P	-5.0	-8.0	-31.1	-31.1	0.0	0.0	3-Jun-86
TR211-1	CL	V	7.2	7.2	-38.4	-38.4	0.0	0.2	29-May-86
TR212-1	CL	V	-7.2	-7.2	-38.4	-38.4	0.0	0.2	22-May-86
TR213-1	CL	V	7.2	7.2	-36.0	-36.0	0.0	0.2	16-Jun-86
TR214-1	CL	V	-7.2	-7.2	-36.0	-36.0	0.0	0.2	2-Jul-86
TR221-1	CL	V	8.0	8.0	-38.4	-38.4	0.0	0.2	29-May-86
TR222-1	CL	V	-8.0	-8.0	-38.4	-38.4	0.0	0.2	22-May-86
TR223-1	CL	V	8.0	8.0	-36.0	-36.0	0.0	0.2	16-Jun-86
TR224-1	CL	V	-8.0	-8.0	-36.0	-36.0	0.0	0.2	2-Jul-86
TR231-1	CL	V	8.7	8.7	-38.4	-38.4	0.0	0.2	29-May-86
TR232-1	CL	V	-8.7	-8.7	-38.4	-38.4	0.0	0.2	22-May-86
TR233-1	CL	V	8.7	8.7	-36.0	-36.0	0.0	0.2	16-Jun-86
TR234-1	CL	V	-8.7	-8.7	-36.0	-36.0	0.0	0.2	2-Jul-86
TR291-1	CL	V	6.3	6.3	-38.4	-38.4	-0.8	0.2	24-Jun-88
TR291-2	CL	H	6.3	6.3	-38.9	-37.9	-0.3	-0.3	24-Jun-88
TR292-1	CL	V	-6.3	-6.3	-38.4	-38.4	-0.8	0.2	19-Aug-88
TR292-2	CL	H	-6.3	-6.3	-38.9	-38.6	-0.3	-0.3	19-Aug-88
TR297-1	CL	V	6.3	6.3	-31.1	-31.1	-0.8	0.2	19-Aug-88
TR297-2	CL	H	6.3	6.3	-31.5	-30.6	-0.3	-0.3	19-Aug-88
TR298-1	CL	V	-6.3	-6.3	-31.1	-31.1	-0.8	0.2	22-Aug-88
TR298-2	CL	H	-6.3	-6.3	-31.5	-30.6	-0.3	-0.3	22-Aug-88
TR613B1	STR	P	5.0	7.2	-36.0	-36.0	-0.7	-0.7	16-Jun-86
TR613L1	STR	P	5.0	7.2	-35.4	-35.4	-0.3	-0.3	16-Jun-86
TR613R1	STR	P	5.0	7.2	-36.3	-36.3	-0.3	-0.3	16-Jun-86
TR613T1	STR	P	5.0	7.2	-36.0	-36.0	0.0	0.0	16-Jun-86

Table 3.5 (continued)
Instrumentation NOS File for the Simulated RH TRU Waste Test, WIPP Room T

Gage Number	Gage Type	Orien-tation	X1 (m)	X2 (m)	Y1 (m)	Y2 (m)	Z1 (m)	Z2 (m)	Install Date
TR614B1	STR	P	-5.0	-7.2	-36.0	-36.0	-0.7	-0.7	2-Jul-86
TR614L1	STR	P	-5.0	-7.2	-36.3	-36.3	-0.3	-0.3	2-Jul-86
TR614R1	STR	P	-5.0	-7.2	-35.6	-35.6	-0.3	-0.3	2-Jul-86
TR614T1	STR	P	-5.0	-7.2	-36.0	-36.0	0.0	0.0	2-Jul-86
TR623B1	STR	P	5.0	8.0	-36.0	-36.0	-0.7	-0.7	16-Jun-86
TR623L1	STR	P	5.0	8.0	-35.4	-35.4	-0.3	-0.3	16-Jun-86
TR623R1	STR	P	5.0	8.0	-36.3	-36.3	-0.3	-0.3	16-Jun-86
TR623T1	STR	P	5.0	8.0	-36.0	-36.0	0.0	0.0	16-Jun-86
TR624B1	STR	P	-5.0	-8.0	-36.0	-36.0	-0.7	-0.7	2-Jul-86
TR624L1	STR	P	-5.0	-8.0	-36.3	-36.3	-0.3	-0.3	2-Jul-86
TR624R1	STR	P	-5.0	-8.0	-35.6	-35.6	-0.3	-0.3	2-Jul-86
TR624T1	STR	P	-5.0	-8.0	-36.0	-36.0	0.0	0.0	2-Jul-86
TR633B1	STR	P	5.0	8.7	-36.0	-36.0	-0.7	-0.7	16-Jun-86
TR633L1	STR	P	5.0	8.7	-35.4	-35.4	-0.3	-0.3	16-Jun-86
TR633R1	STR	P	5.0	8.7	-36.3	-36.3	-0.3	-0.3	16-Jun-86
TR633T1	STR	P	5.0	8.7	-36.0	-36.0	0.0	0.0	16-Jun-86
TR634B1	STR	P	-5.0	-8.7	-36.0	-36.0	-0.7	-0.7	2-Jul-86
TR634L1	STR	P	-5.0	-8.7	-36.3	-36.3	-0.3	-0.3	2-Jul-86
TR634R1	STR	P	-5.0	-8.7	-35.6	-35.6	-0.3	-0.3	2-Jul-86
TR634T1	STR	P	-5.0	-8.7	-36.0	-36.0	0.0	0.0	2-Jul-86
TR811-1	TC	P	5.0	7.2	-38.4	-38.4	0.2	0.2	
TR812-1	TC	P	-5.0	-7.2	-38.4	-38.4	0.2	0.2	
TR813-1	TC	P	5.0	7.2	-36.0	-36.0	0.2	0.2	
TR814-1	TC	P	-5.0	-7.2	-36.0	-36.0	0.2	0.2	
TR821-1	TC	P	5.0	8.0	-38.4	-38.4	0.2	0.2	
TR822-1	TC	P	-5.0	-8.0	-38.4	-38.4	0.2	0.2	
TR823-1	TC	P	5.0	8.0	-36.0	-36.0	0.2	0.2	
TR824-1	TC	P	-5.0	-8.0	-36.0	-36.0	0.2	0.2	
TR825-1	TC	P	5.0	8.0	-33.5	-33.5	0.2	0.2	
TR826-1	TC	P	-5.0	-8.0	-33.5	-33.5	0.2	0.2	
TR827-1	TC	P	5.0	8.0	-31.1	-31.1	0.2	0.2	
TR828-1	TC	P	-5.0	-8.0	-31.1	-31.1	0.2	0.2	
TR831-1	TC	P	5.0	8.7	-38.4	-38.4	0.2	0.2	
TR832-1	TC	P	-5.0	-8.7	-38.4	-38.4	0.2	0.2	
TR833-1	TC	P	5.0	8.7	-36.0	-36.0	0.2	0.2	
TR834-1	TC	P	-5.0	-8.7	-36.0	-36.0	0.2	0.2	

Specific instrument alphanumeric names, or designations, listed in **Table 3.5** and illustrated in **Figures 3.5-1** through **3.5-8** have occasionally been modified or updated during the course of this test program. All modifications were made for reasons of consistency with other NOS instrument data files and other WIPP in situ test programs, e.g., the WIPP thermal-structural interactions tests (Munson, 1983). To minimize any confusion in this data report due to different instrument designations, cross-correlations on all different instrument names will be provided in Section 3.5.1 through 3.5.4 and in Section 5, Results, where appropriate.

3.5.1. Thermocouples

We used a total of 32 thermocouples, TCs, to monitor the temperatures in the RH TRU test system. Sixteen thermocouples monitor the temperature on the top, inner surface of the test containers; these are termed "heater thermocouples" in **Table 3.3.** These heater TCs were initially designated as TRH0XT-1, TRH0XT-2, and TRH0XT-3, where "X" represents test container 1 through 8. These TC identifiers have been redesignated as TR00XT-1, TR00XT-2, and TR00XT-3. The other sixteen TCs are at the top of the emplacement boreholes, at the salt-air interface; these are termed "near-field thermocouples" in **Table 3.3**. These near-field TCs were originally designated as TRH81X, TRH82X, and TRH83X, where "X" again represents test container 1 through 8; these have been redesignated as TR80X-1, TR80X-2, and TR80X-3. The exact locations of the "-1," "-2," and "-3" TCs within the test boreholes are illustrated in **Figures 3.5-1** through **3.5-8** and will be described in Section 5.2 and 5.3.

All of these heater and near-field thermocouples are Type E Chromel-Constantan and are clad in Inconel 600 sheaths, 3.2 mm in diameter, and are of various lengths. We selected Inconel 600 because of its known corrosion resistance in moderate-temperature salt environments (Molecke et al., 1983). The TCs have high purity MgO internal insulation and an ungrounded hot junction configuration. The thermocouples have a resolution of ±0.003°C, a calibrated range up to about 250°C, and an overall system accuracy of better than ±1.0°C.

3.5.2. Pressure Gages

A total of 24 pressure gage/stress transducers are located on the outer surfaces of RH TRU test containers TRH03 and TRH04, on the top (T), bottom (B), and left and right sides of the canister (L and R), at three longitudinal locations. These pressure gages are designated as TRH61X(T, B, L, or R), TRH62X(T, B, L, or R), and TRH63X(T, B, L, or R), where the "1, 2, or 3" again represent a specific location in the

test borehole, as illustrated in **Figures 3.5-3** and **3.5-4**. These pressure gages have more recently been re-designated as TR60X1(T, B, L, or R), TR60X2(T, B, L, or R), and TR60X3(T, B, L, or R). These pressure gages remotely measure the combined effects of borehole creep-closure pressures, backfill compaction and swelling pressures, and pressure from thermally induced expansion, all as experienced by the waste container.

Sandia instrumentation personnel designed, fabricated, and individually calibrated the pressure gages. These gages employ a full-bridge strain gage (transducer) that was chemically bonded to the inner surface of a stiff, but flexing diaphragm. The transducers used are commercially available, Endevco model 8510B-200 gages, and are 30.6 mm (1.25 in.) in diameter. The bonding agent used was Micro Measurements Division of Measurements Group, M-Bond 610 Adhesive. The flexing diaphragm is made of Inconel 600, and is 0.51 to 0.64 mm- (0.020 to 0.025 in.-) thick. The gage outer body or housing is constructed of Inconel 600. The space between the gage body and the flexing diaphragm is filled with air. These gages have a working range of up to 1.38 MPa (200 psi). They individually have been calibrated (hydrostatically) and temperature compensated with an accuracy of better than 1 %. The calibrations are essentially linear to 1.38 MPa. Power and signal leads for these gages are channeled out of the emplacement hole through thin-wall, 6 mm-diameter Inconel 600 tubing. These pressure gages are somewhat unique in that they have the capability to operate in a high-temperature (to about 190°C, or more) and potentially corrosive environment with long-term durability.

3.5.3 Vertical Displacement/Borehole Closure Gages

We used a total of 12 remote-reading, vertical displacement/borehole closure gages in RH TRU test emplacements TRH01, TRH02, TRH03, and TRH04. These closure gages were initially designated as TRH21X, TRH22X, and TRH23X, where "X" again represents test container 1 through 8. The locations of the "-1X," "-2X," and "-3X" gages within the test boreholes are illustrated in **Figures 3.5-1** through **3.5-4**. The more recent diameter-closure gage designations are TR20X-1V, TR20X-2V, and TR20X-3V, where the "V" stands for "vertical."

These closure gages use a LVDT (linear variable displacement transducer) with a maximum range of 0 to 76 mm (3 in.). The transducers are mechanically coupled to a spring-loaded scissors-jack apparatus that converts vertical closure (in the range of 0 to 127 mm, 0 to 5 in.) to horizontal motion within the range of the LVDT; refer to **Figure 3.5-9**. The overall vertical closure gage remotely monitors vertical closure

from the top of the heated RH TRU container to the top-center of the borehole surface, as a function of time, every 4 hours.

Vertical closure gages TRH21X (where X = 1 to 4), about 2.2 m in from the front or rib face-end of each borehole, were able to record borehole closure of the initial, about 152 mm, 6 in. gap immediately after gage installation. A Teflon spacer, about 30.2 mm- (1.19 in.-) high, was placed on top of the contact-end of the scissors-jack assembly (refer to **Figure 3.5-9**), with the spacer's upper end in contact with the borehole salt surface. Most of these spacers were removed after 18 months of heated test operation. The other closure gages, TRH22X and TRH23X, further back into the borehole (about 3.0 m and 3.7 m from the rib-face, respectively), did not have spacers.

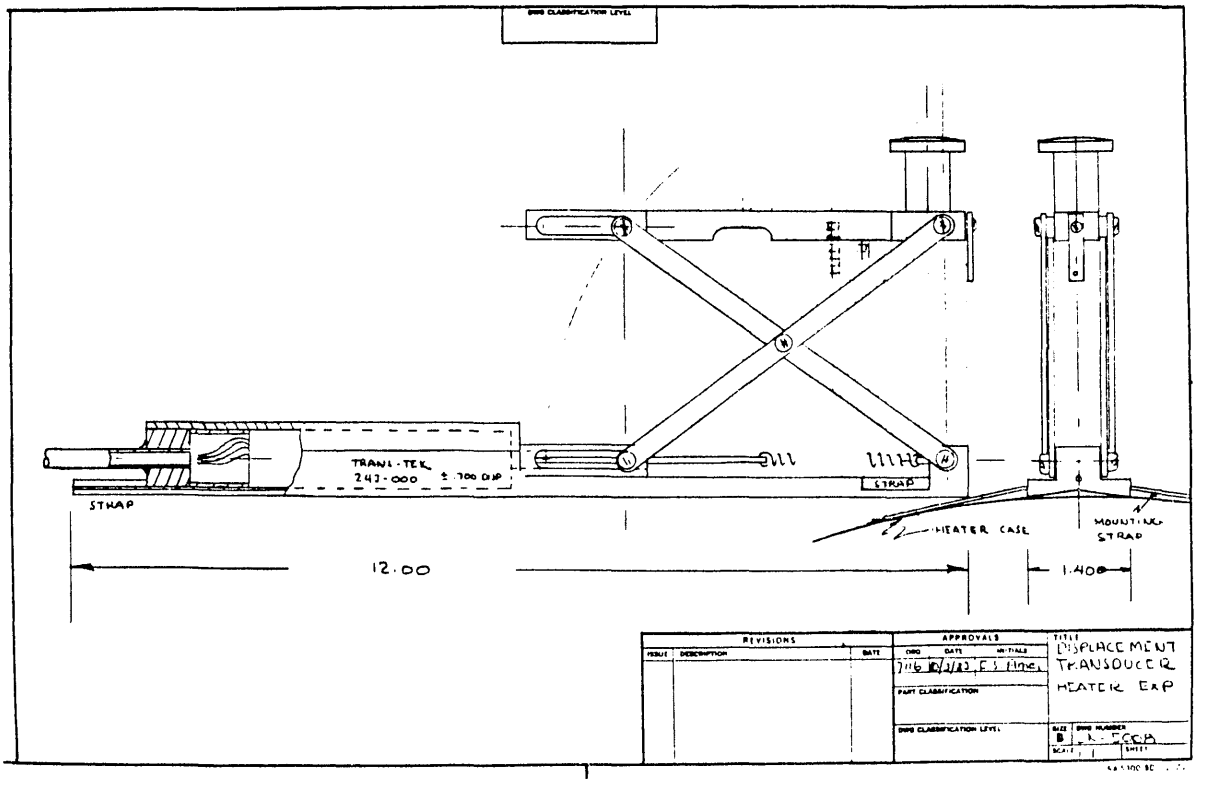

Figure 3.5-9 RH TRU vertical displacement/borehole closure gage

3.5.4 Borehole-Diameter Convergence Gages

We installed a total of 8 vertical and horizontal borehole diameter-convergence gages in test emplacement holes TRH01, TRH02, TRH07, and TRH08. These gages are designated as TR29X-1 and TR29X-2. There is a vertical diameter-convergence ("-1") and a horizontal diameter-convergence gage ("-2") pair in each of these holes, located 16.5 cm (6.5 in.) in front of the test container pintle. The full listing of all of

these convergence gages, and their specific locations, are listed in **Table 3.5**. These gages are basically wire extensometer-displacement transducers, with a range of 91 to 76 cm (36 to 30 in), and a sensitivity of 0.025 mm (0.001 in). We used the remotely-read diameter measurements to supplement the manually-read diameter data, as described in Section 3.5.5. We installed these borehole diameter-convergence gages for the test system in September 1988, shortly before the scheduled two-year RH TRU test sampling and examination period. The use of these wire extensometer-displacement transducers for RH TRU testing was originally noted in a planning document (Molecke and Munson, 1987). These gages are essentially identical to those used in the Thermal/Structural Interactions tests in both Rooms A and B of the WIPP (Munson, 1983).

3.5.5 Manual Closure and Diameter Measurements, Other Observations

We also conducted manual measurements of RH TRU container top-to-borehole closure during every sampling and examination period, using a snap-type caliper gage affixed to a long pole. These manual measurements were usually made in all test emplacements, including those with installed remote-reading closure and borehole-diameter convergence gages, for comparison and cross-calibration purposes.

Periodically, we rolled several of the RH TRU containers out of their emplacement holes, then made manual measurements of both current horizontal and vertical borehole diameters. These manual diameter measurements were made with a Starrett tubular, inside micrometer that has 0.001 inch graduations. The measurements were conducted at the same positions (horizontal depths) within the boreholes as the remote-reading closure and pressure gages; refer to **Figures 3.5-1** through **3.5-8**. Observations of any cracks, salt efflorescences, moisture inflow, corrosion, and general conditions within the test boreholes were also made at the same time as these manual measurements.

3.6 Data Acquisition and Analysis Systems

The RH TRU test heaters and instruments (thermocouples, pressure gages, and closure/displacement gages) are hooked-up to a WIPP-dedicated, computerized data acquisition system, DAS. Individual test-container heater voltages and watts, and borehole in situ temperatures, pressures, and closure values at multiple locations are monitored and recorded by the DAS every 4 hours. This DAS provides both easy access to test data for evaluation and permanent records for later detailed analyses.

Basically, the underground portion of the DAS consists of controlled-environment recording sheds that contain power supplies, signal conditioners, data scanners, digital voltmeters, and calibrators. The

analog voltage data from individual gages are periodically interrogated by digital voltmeters. Resulting digital signals are transmitted from the underground to the surface by means of a IEEE-488 interface data bus. The aboveground portion of the DAS consists of a multitasking and multi-user ModComp minicomputer system (ModComp Classic 7840) that converts the raw data to engineering units, stores the data in both raw and converted forms, provides plots and data listings, and manages remote (user) access via modem (McIlmoyle et al., 1987). This DAS has a capacity of more than 5,000 data channels and is adequate to operate all the Sandia-conducted underground WIPP experiments. It was designed, procured, installed, and is being operated by Sandia National Laboratories. Full details on this WIPP DAS can be found elsewhere (Tyler et al., 1988; McIlmoyle et al., 1987; Munson et al., 1990b).

A summary of the WIPP data reduction and analysis systems for remote-instrument data as discussed above is also detailed elsewhere (Tyler et al., 1988; Munson et al., 1990b). Essentially, this effort consists of: (a) an integrated database management system, WISDAAM (Munson et al., 1990b); and, (b) a data reduction software program, UNDERDOG (Tyler et al., 1988), to assist in performing the necessary functions for data corrections, adjustments, display, and output. "WISDAAM" is an acronym for the WIPP In Situ Data Acquisition, Analysis, and Management system. "UNDERDOG" is an acronym for the Underground Nuclear Depository Evaluation, Reduction, and Detailed Output Generator, and is documented elsewhere (Ball and Shepard, 1987). The WISDAAM system for the WIPP data reduction effort was developed especially for multiuser access to the database. This database is stored in a MicroVAX II computer at Sandia National Laboratories, in Albuquerque. The WISDAAM system and the UNDERDOG software were used to prepare the remotely-read instrumentation data presented in the Results and Observations section of this report. Further details on the data acquisition system and the data reduction processes are documented elsewhere (McIlmoyle et al., 1987; Munson et al., 1990a; Munson et al., 1990b).

This database management and reduction system provides data plots and displays that have been corrected appropriately for errors or gage adjustments, e.g., deletions due to maintenance activities, initial zero or other calibration shifts, scatter due to unknown causes, obviously erroneous data, etc. (Tyler et al., 1988; McIlmoyle et al., 1987; Munson et al., 1987; Munson et al., 1990b). All of the data corrections and final data presented in this report are "certified" as approved by the test Principal Investigator and are quality assurance (QA) stamped. The quality assured data output represents the actual in situ test measurements. Such QA-certified data are available for use in analyses or reviews by interested parties associated with the WIPP program.

4.0 MODELING TECHNIQUES AND PROCEDURES

We used three-dimensional (3D) thermal and geomechanical models to simulate the thermal/structural response of these RH TRU waste experiments in Room T. The modeling aided in the interpretation of the in situ measured borehole-closure results. We also evaluated some calculated predictions on vertical and horizontal room closure, and impacts of emplacement hole drilling. We used this modeling to help assess any potential operational or performance-related impacts in a typical waste storage room during the WIPP initial waste-retrieval period. This 3D model is briefly described and selected results from the analysis are presented.

4.1 Thermal Modeling

To properly assess the effects caused by the presence of the thermal load in the rock salt pillars, we assembled a 3D thermal model to predict both near-field and far-field temperature responses. A summary of this thermal model is presented herein. This thermal model is closely integrated to the geomechanical modeling work described in Section 4.2.

Assumptions: The thermal model is based on several assumptions, with the most important listed as follows:

1. There is an infinite array of equally spaced rooms and boreholes. The waste canisters are all simultaneously emplaced in the infinite array of equally spaced boreholes. With this assumption, the geometrical symmetry between boreholes and between rooms can be employed. A single slab, which symmetrically cuts through a canister and the midpoint between boreholes, represents the typical canister and its environment.
2. The components of the test container emplacement (i.e., the waste form, container, and backfill material) are made of isotropic and homogeneous materials .
3. Nonlinear effects, including pore water migration, were ignored. In practice, nonlinear effects, a more specific and detailed configuration of the container, the borehole, and the backfill material thermal behavior could strongly influence very-near-field conditions.
4. The (room) drift is unventilated and the radiative heat transfer taking place is approximated by ascribing equivalent thermal conductivity properties to air, as derived from an effective radiation conductivity analysis in the drift (Beraún and Molecke, 1987).

The uncertainties or errors potentially introduced by all the assumptions made in the thermal modeling are discussed in Sections 7.1.4 and 8.0.

Thermal Properties: The actual geometry of the region in which the RH TRU canisters are emplaced consists of many layers of dissimilar materials that vary in thickness from 19.39 m to 0.08 m. Because many of these regions are located at a distance greater than 10 m from the canister, we used average material properties to represent the actual strata (Krieg, 1984). Material density, specific heat, and the conductivity exponent, γ, were geometrically averaged. We averaged the thermal conductivities using a series model,

$$\sum \frac{L}{k} = \frac{L_1}{k} + \frac{L_2}{k} + \ldots \frac{L_i}{k} \qquad (1)$$

where L_i is the thickness of the i^{th} strata. The thermal conductivity of the materials in the stratigraphy was assumed to vary with temperature according to (Mufti, 1971):

$$k(T) = k_{300}\left(\frac{300}{T}\right)^{\gamma} \qquad (2)$$

where k is the material's thermal conductivity at a given temperature T, k_{300} is its conductivity value at some reference point (300 °K for this case, the ambient underground temperature at the WIPP facility), and γ is the conductivity exponent (Rohsenow and Hartnett, 1973). The thermal properties of materials used in the modeling calculations are listed in **Table 4.1.** Thermal properties for the waste canisters and the air in the drift ("equivalent thermal material") are also listed in this Table.

Table 4.1 Material Thermal Properties

Material	Density ρ, kg/m^3	Specific Heat C_p, J/kg-K	Thermal Conductivity k, w/m-K	Conductivity Parameter γ
Argillaceous Salt	2,167	860	4.0	1.14
Halite	2,300	860	5.0	1.14
Anhydrite MB136	2,170	860	4.14	1.14
Anhydrite MB139	2,167	860	4.5	1.14
Anhydrite	2,200	860	4.9	1.14
Polyhalite	2,167	860	3.6	1.14
Air	1	1,000	46.0*	0.00
RH TRU Canister	4,126	460	17.3	0.00

* effective radiation conductivity value (Beraún and Molecke, 1987)

Numerical Analysis: For situations where thermal radiation needed to be accounted for, we treated it indirectly by deriving an effective thermal radiation conductivity, k_{eff} (Beraún and Molecke, 1987; Bulmer, 1980; Rohsenow and Hartnett, 1973). To determine this parameter and simulate the thermal radiation heat transfer across the drift, one needs to set the radiation heat transfer between infinite parallel plates equal to the conductive heat transfer taking place between the plates. In doing this, the following relationship is found to be true:

$$\frac{\epsilon_1 A_1 \sigma_1 \left(T_1^4 - T_2^4\right)}{1+\left(\frac{\epsilon_1}{\epsilon_2}\right)(1-\epsilon_2)} = k_{eff} A_1 \left(\frac{T_1 - T_2}{L}\right) \qquad (4)$$

where the subscripts 1 and 2 represent plate-1 and plate-2, respectively; and L represents the spacing between plates. Solving for k_{eff} yields the effective radiation conductivity relationship for the drift:

$$k_{eff} = \frac{4T^3 \epsilon_1 \sigma_1 L}{1 + \left(\frac{\epsilon_1}{\epsilon_2}\right)(1-\epsilon_2)} \qquad (5)$$

Figure 4.1-1 depicts the three-dimensional finite-element mesh in the disposal room proximity, as used in these calculations. This mesh was generated with PATRAN (PDA, 1984), a finite-element pre- and post-processing and analysis package. Upon completion of the mesh, it was translated to the equivalent thermal resistor network for solving with P/THERMAL (Rockenbach, 1987), the thermal analysis module of PATRAN. P/THERMAL uses the traditional thermal network approach which allows skewed and irregularly spaced meshes for two-dimensional and three-dimensional problems to be handled with the ease of a finite-element code. We used a very fine mesh size (relative to the overall size) within the waste package to provide realistic temperature predictions. As the distance from the waste package increases, the mesh sizes also gradually increase. This approach is based on the fact that the thermal gradient diminishes as the distance from the heat source increases.

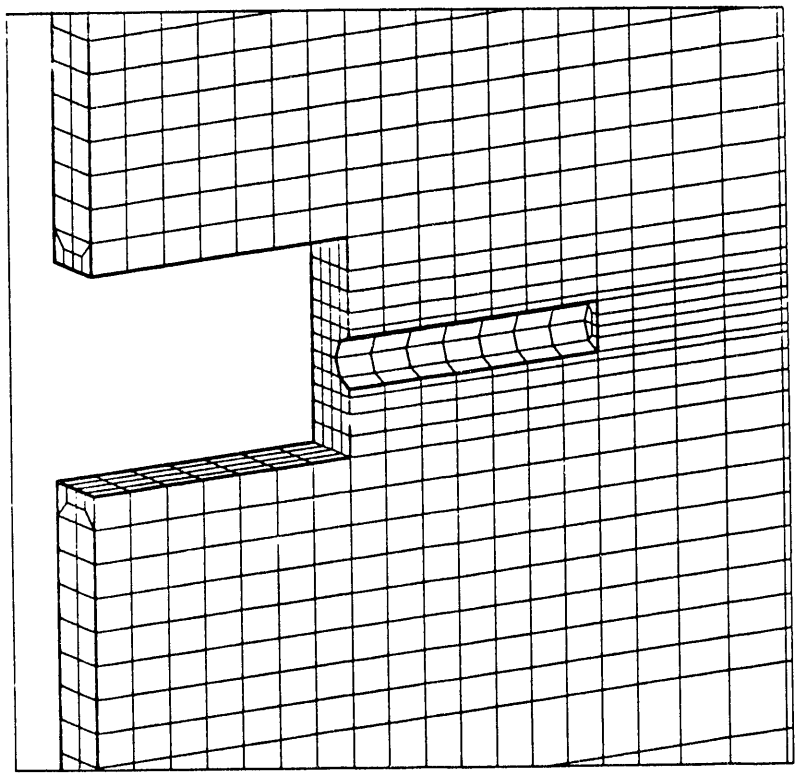

Figure 4.1-1 Finite-element mesh in vicinty of modeled room

4.2 Geomechanical Modeling

The experimental configuration modeled herein represents a typical disposal room in the WIPP waste storage area. We assumed, for purposes of calculational simplification, that there is an infinite array of equally spaced similar rooms that are also infinitely long and contain an infinite number of equally spaced horizontal boreholes. To simulate this infinite array of rooms, we used four symmetry planes. The 3D response of the room and boreholes of the Room T experiments were thus approximated by the idealization shown in **Figure 4.2-1**. The four side boundaries represent the symmetry planes, and the upper and lower boundaries were assumed to be approximately 50 m (164 ft) from the room to preclude their affecting the response of the room. The boundary conditions applied to the configuration were such that no displacement perpendicular to any of the four sides or the bottom was permitted. A pressure boundary condition of 13.57 MPa (the assumed lithostatic pressure) was applied at the top plane,and gravitational effects were represented as body forces. We assumed the initial stress to be lithostatic and to vary linearly with depth.

The modeled room was assumed to appear instantaneously as a void at time t = 0. The borehole was assumed to appear instantaneously as a void at t = 3 years. Also, there is no liner included in the

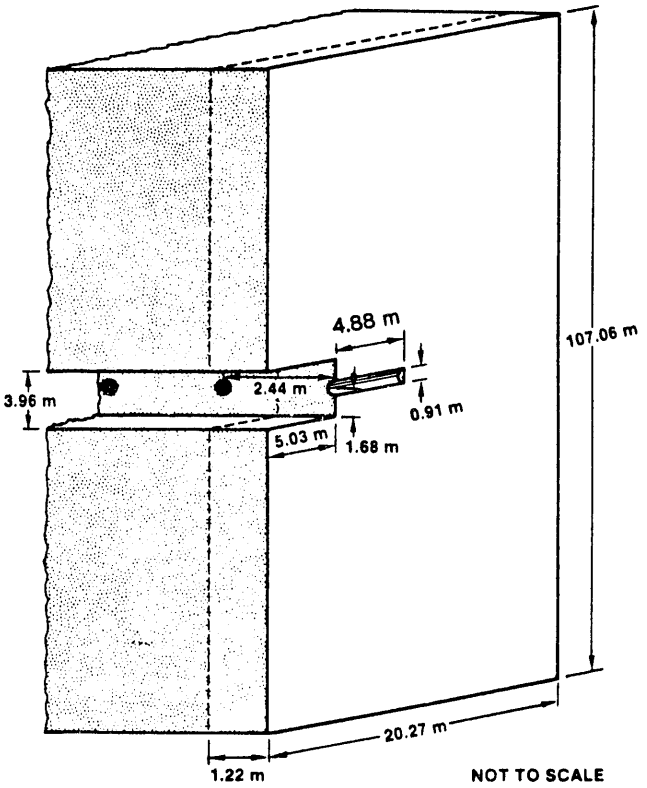

Figure 4.2-1 Geomechanical idealized three-dimensional configuration

We assumed the temperature of the configuration to be 300K for the first 3.48 years of the 6 year simulation period. At 3.48 years, the thermal power output of 117 W per RH TRU test canister (as compared to the actual average of 114.9 ± 4.5 W; refer to Section 5.1, **Table 5.1**) was applied and held constant for the remainder of the simulation period. This sequence of events represents:

1. an assumed instantaneous creation of the room (Room T) on 4/1/83 (compared to the actual 3/24 to 4/3/83 excavation);
2. an assumed instantaneous creation of all of the boreholes on 4/1/86 (compared to the actual 3/10/86 through 4/26/86 corings in Room T; refer to **Table 3.1**), and;
3. power to the heaters on 9/23/86 (actual date).

The simplifications inherent in all of the assumptions made in this thermal/structural modeling can be expected to introduce some potential uncertainties or errors. Resultant uncertainties become evident when calculations are compared to measured closures; this is discussed further in Sections 6.2 and 7.3.4.

The finite element mesh used in the calculations, in the vicinity of the room and borehole, is shown in **Figure 4.1-1**, with the rock salt material occupying the room and borehole removed. The finite element discretization of the idealization yielded a mesh consisting of 4301 nodal points and 2728 elements. We performed two separate analyses using this mesh, one thermal and one structural. The thermal analysis, using an "equivalent thermal material" (work performed by O.L. George, Sandia National Laboratories, 1984) for the room, was performed first with the P/THERMAL code (Rockenbach, 1987), a module of the PATRAN II system. We used the thermal results from that analysis, in terms of nodal temperatures, as input to the structural analysis code. As will be discussed later, the thermal effect on structural response was very small. A summary of calculated temperature contours will be presented in the Results section.

The finite-element computer code, JAC3D (developed by J. H. Biffle, Sandia National Laboratories) was used for the structural analysis. JAC3D is a code developed for quasistatic analysis of 3-dimensional non-linear solids, and was derived from its 2-dimensional counterpart, JAC (Biffle, 1984). It employs the conjugate gradient iterative technique to obtain a solution, and spatial integration is performed using a single Gauss point in each eight-node isoparametric hexahedral element. It used an hour-glass viscosity technique to control the zero energy modes that can typically occur with single point integration.

The model configuration was assumed to be all rock salt, and its structural material response was modeled as elastic/secondary creep. We used the WIPP reference secondary creep law (Krieg, 1984) along with the reference material parameters for the model, except that the value of Young's modulus was reduced by a factor of 12.5 (E/12.5) while holding the value of Poisson's ratio fixed. H.S. Morgan (Sandia National Laboratories), in calculations on the estimated time needed for TRU storage rooms to close, has shown that this artificial reduction in Young's modulus produces good agreement between computed and in situ closures. Further details on the geomechanical model, and its application to RH TRU waste emplacements, have been documented separately (Argüello, Beraún, and Molecke, 1989). Argüello and Beraún are continuing their work on a 3-dimensional finite element simulation of the thermal/structural responses for the WIPP Room T, RH TRU waste test emplacements; these studies will be documented in the near future.

5.0 RESULTS AND OBSERVATIONS

The eight simulated RH TRU waste emplacements in Room T have been in heated-test operation since September, 1986, for more than six years now. Remote instrument data have been acquired and evaluated continuously. The emplacements have, so far, been opened for examinations, maintenance, and for materials sampling after 6, 12, 18, 24, and 36 months of testing. In this section, we will present and summarize all available and QA-certified remote-instrument data plus manually-acquired data and observations for the first five years of this test program. We also will compare the measured data with thermal and geomechanical modeling calculations in Sections 7.1 and 7.3, respectively.

We will also present materials alterations results, laboratory analyses, and notable test and operational observations through the last sampling period at 36 months in this Section. Further materials-related results can be documented when this test program is terminated, after all material samples have been removed for posttest laboratory analyses. The date of termination of the simulated RH TRU waste test program is still to be determined, pending future availability of access into the underground WIPP test Room T.

NOTE: In the following sections of this report, we provide plots of data histories, calculated data averages and standard deviations, and other assorted calculations based upon the various data. We do not list the tens of thousands of individual data points. As described in Section 3.6, the entire "certified," quality assured database for this experiment is stored in a MicroVAX II computer (and associated storage media) at Sandia National Laboratories, in Albuquerque. Multi-user access to this database is available through the WISDAAM system (Tyler et al., 1988; Munson et al., 1990b).

5.1 Test Container Heater-Power Histories

For the first 1,135 days (3.1 years) of heated test operations, the thermal power output of each of the electric-heater assemblies within the simulated RH TRU waste test containers has remained within the range of 110 to 120 W, with a slightly decreasing long-term trend. Power fluctuations of less than ±10 W per day are common. As described in Section 3.4, we then raised heater power levels to about 300 W/each, the maximum allowable thermal output for RH TRU wastes, for the remainder of the testing period.

The average power values for each test container, plus or minus calculated standard deviations, are listed in **Table 5.1.** The overall average power for all eight test heaters was 114.89 W for the first 3.1 years, then 298.94 W for the subsequent 3.1 to 5.0 year period. The overall power histories for each test

container are illustrated in **Figures 5.1-1a** through **5.1-8a,** for heaters TR001-0, TR002-0, TR003-0, TR004-0, TR005-0, TR006-0, TR007-0, and TR008-0. These heater numbers (as listed in the instrumentation NOS file, **Table 3.5**, as TRH0X-0) correspond to test containers TRH01, TRH02, TRH03, TRH04, TRH05, TRH06, TRH07, and TRH08, respectively. It must be noted that these figures, and similar figures in following sections, show "sieved" data for the purpose of increased legibility. Adjacent but redundant data points, i.e., those that vary by less than a predetermined minimal amount, are not illustrated on these figures. However, all data points, not just the sieved values, were used for any numerical calculations. There have been multiple brief periods of power outages at the WIPP site, resulting in power loss to the heaters. We also deenergized individual test heaters (for several hours) to zero power during periodic sampling and examination times. These brief power outages also have been graphically filtered-out in **Figures 5.1-1a** through **5.1-8a**, for clarity.

Calculations of the average values and standard deviations listed in **Table 5.1** were made with the GRAFAID analysis tool (Adams, 1985). Calculated heater-power running averages and (±) standard deviations for heaters TR001-0, TR002-0, TR003-0, TR004-0, TR005-0, TR006-0, TR007-0, and TR008-0 are illustrated (as the three solid lines) in **Figures 5.1-1b** through **5.1-8b,** respectively.

Table 5.1 RH TRU Test Heater-Power Values

Test Container	Test Heater (& old I.D.)	Average Power ± Standard Deviation [0 to 1135 days, 3.1 yr]	Average Power ± Standard Deviation [3.1 to 5.0 years]
TRH01	TR001-0 (TRH01-0)	117.06 ± 3.74 W	304.14 ± 6.90 W
TRH02	TR002-0 (TRH02-0)	114.65 ± 3.70 W	298.57 ± 6.72 W
TRH03	TR003-0 (TRH03-0)	115.64 ± 4.55 W	292.40 ± 6.49 W
TRH04	TR004-0 (TRH04-0)	114.39 ± 4.52 W	288.92 ± 6.36 W
TRH05	TR005-0 (TRH05-0)	113.66 ± 5.22 W	308.51 ± 16.64 W
TRH06	TR006-0 (TRH06-0)	112.80 ± 5.11 W	306.36 ± 13.36 W
TRH07	TR007-0 (TRH07-0)	116.23 ± 4.48 W	297.84 ± 7.05 W
TRH08	TR008-0 (TRH08-0)	114.67 ± 4.44 W	294.76 ± 6.87 W
	Average:	114.89 ± 4.50 W	298.94 ± 9.54 W

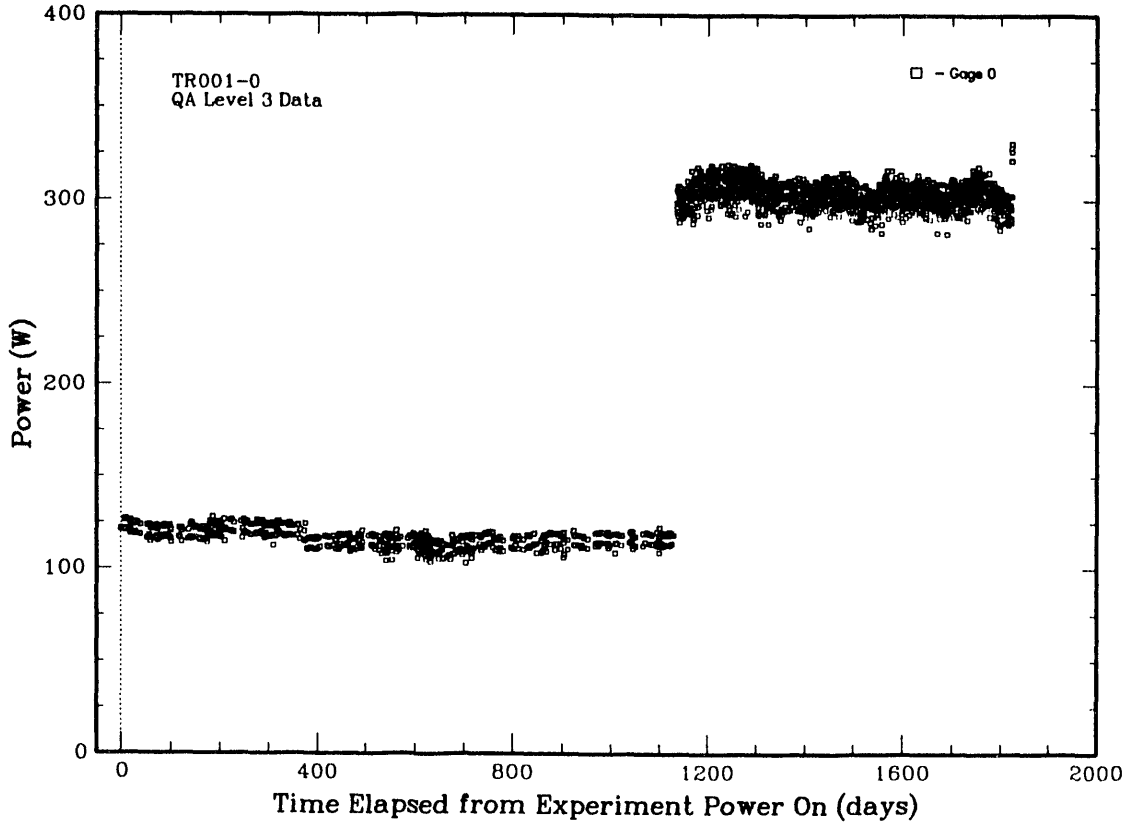

Figure 5.1-1a Simulated RH TRU Test TRH01 Power History

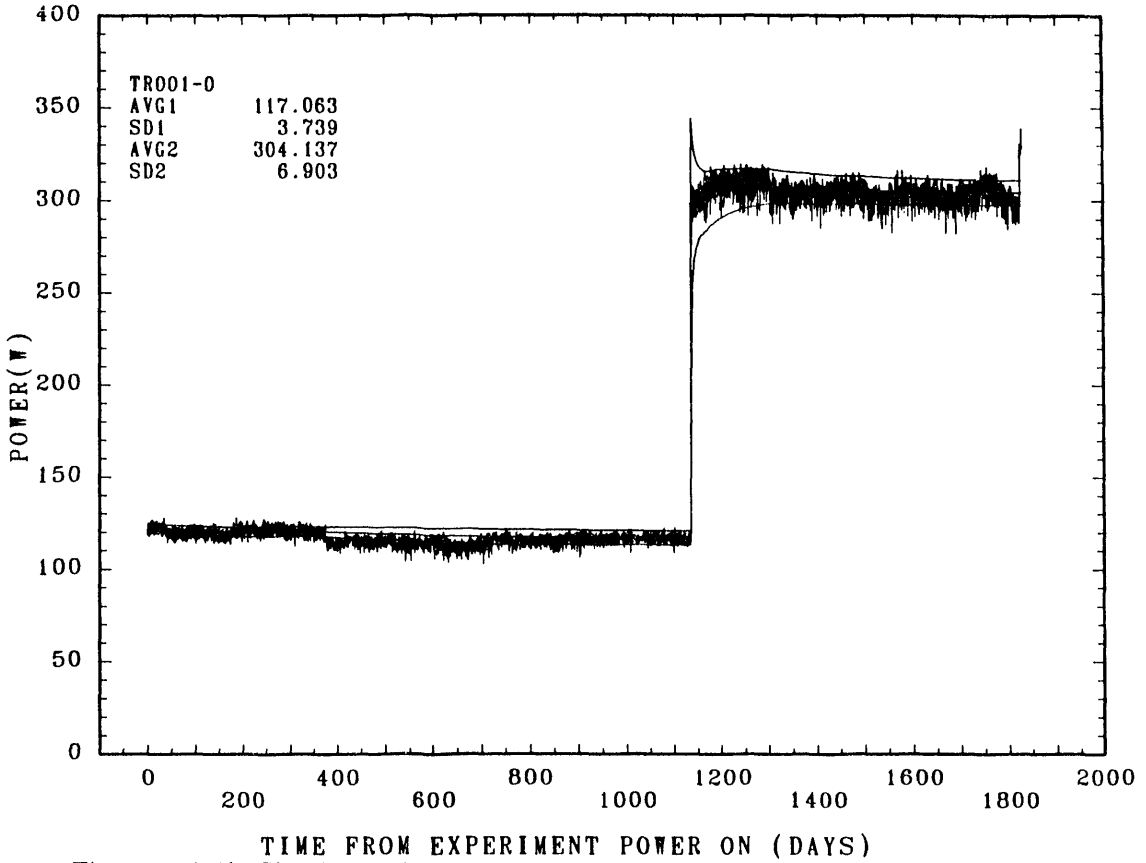

Figure 5.1-1b Simulated RH TRU Test TRH01 Calculated Power Averages

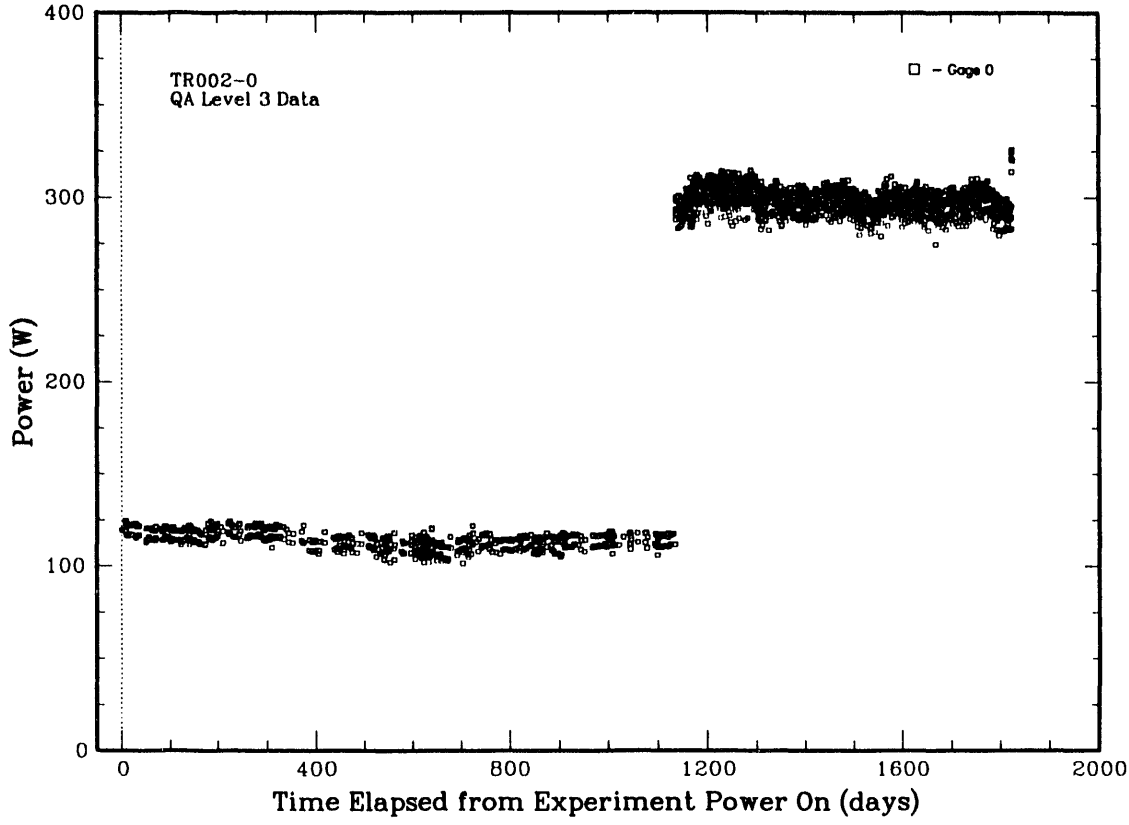

Figure 5.1-2a Simulated RH TRU Test TRH02 Power History

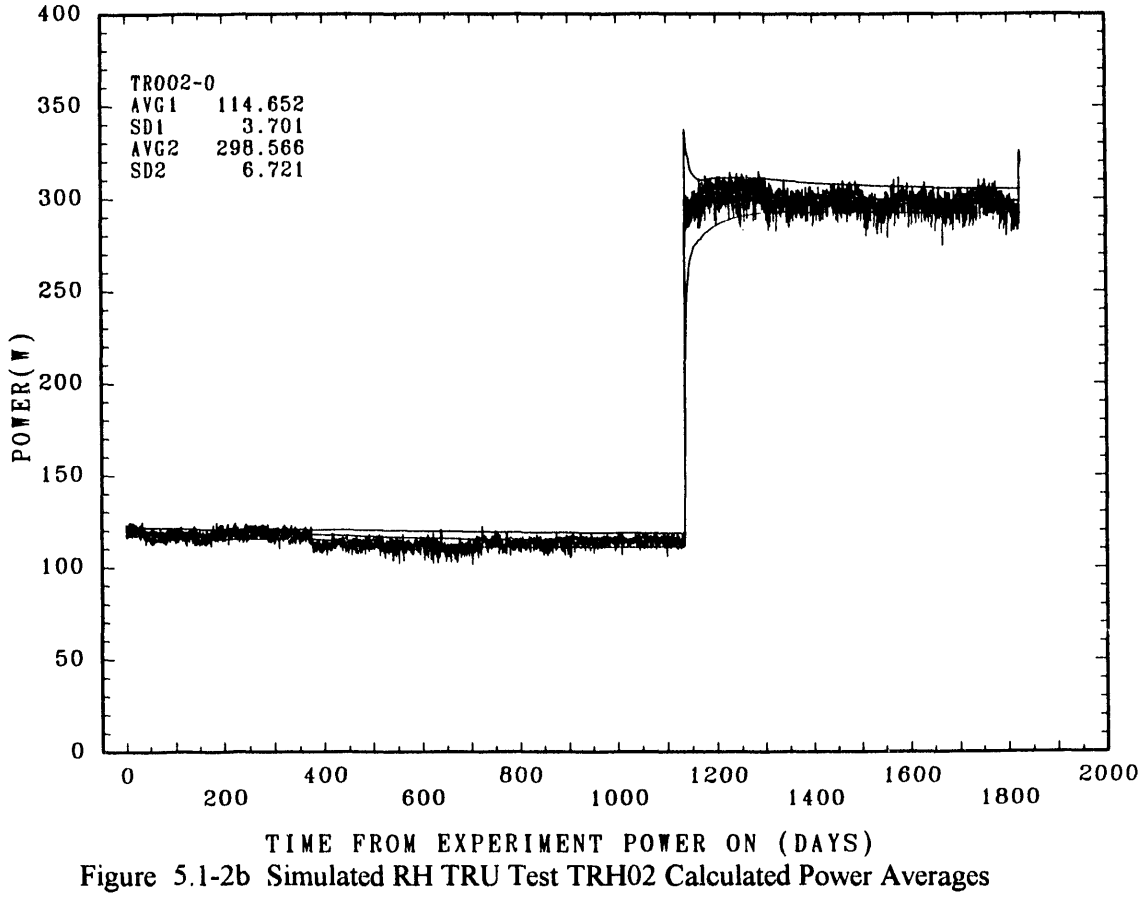

Figure 5.1-2b Simulated RH TRU Test TRH02 Calculated Power Averages

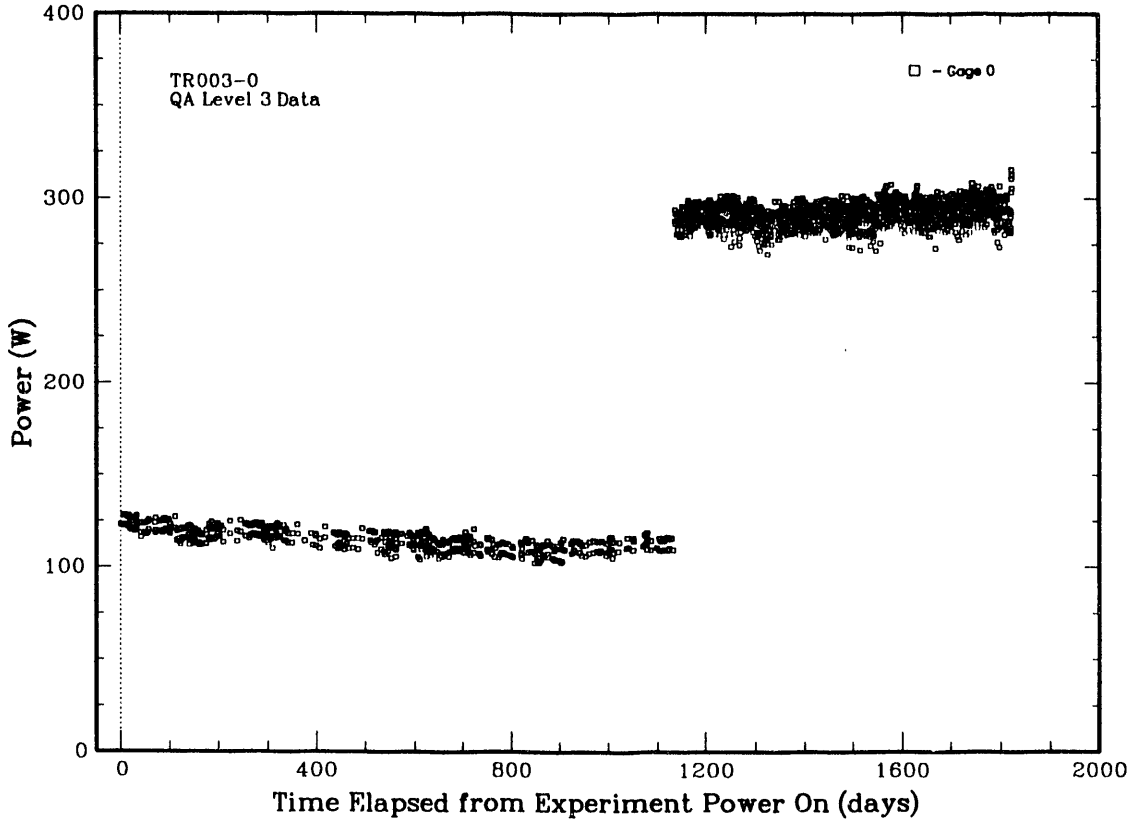

Figure 5.1-3a Simulated RH TRU Test TRH03 Power History

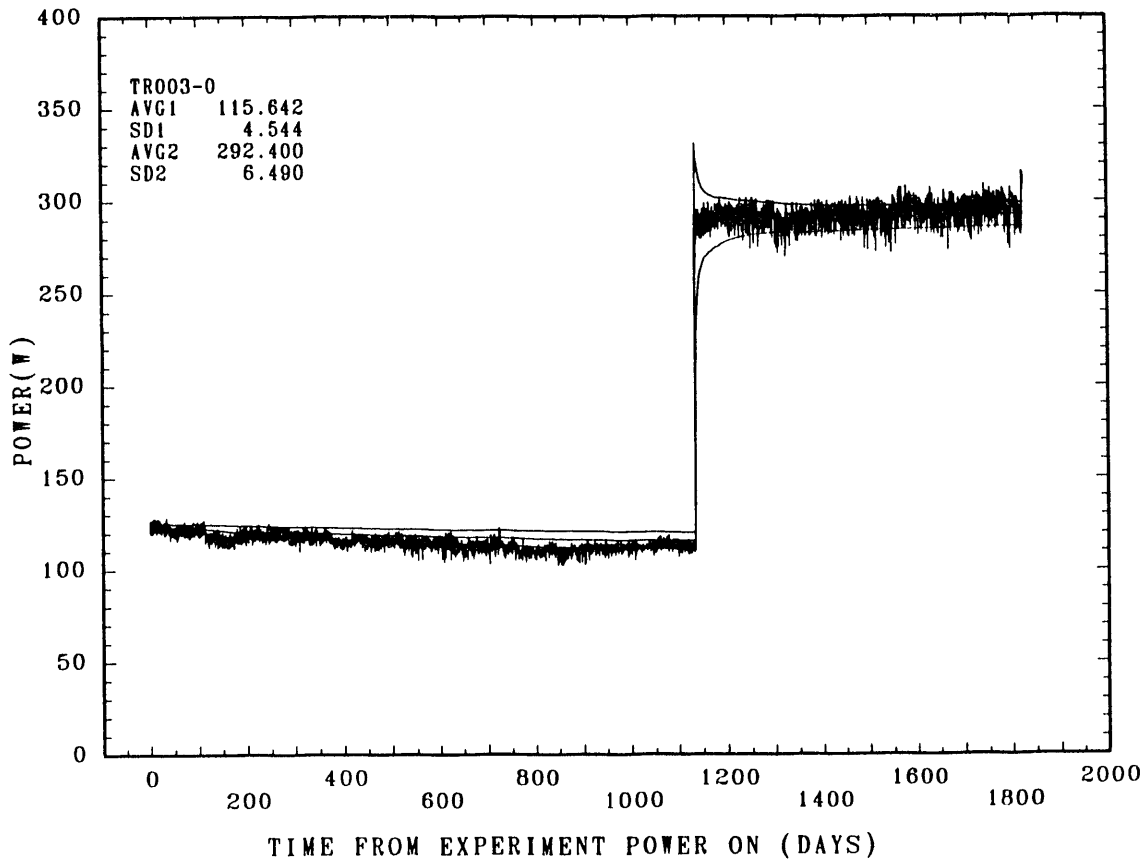

Figure 5.1-3b Simulated RH TRU Test TRH03 Calculated Power Averages

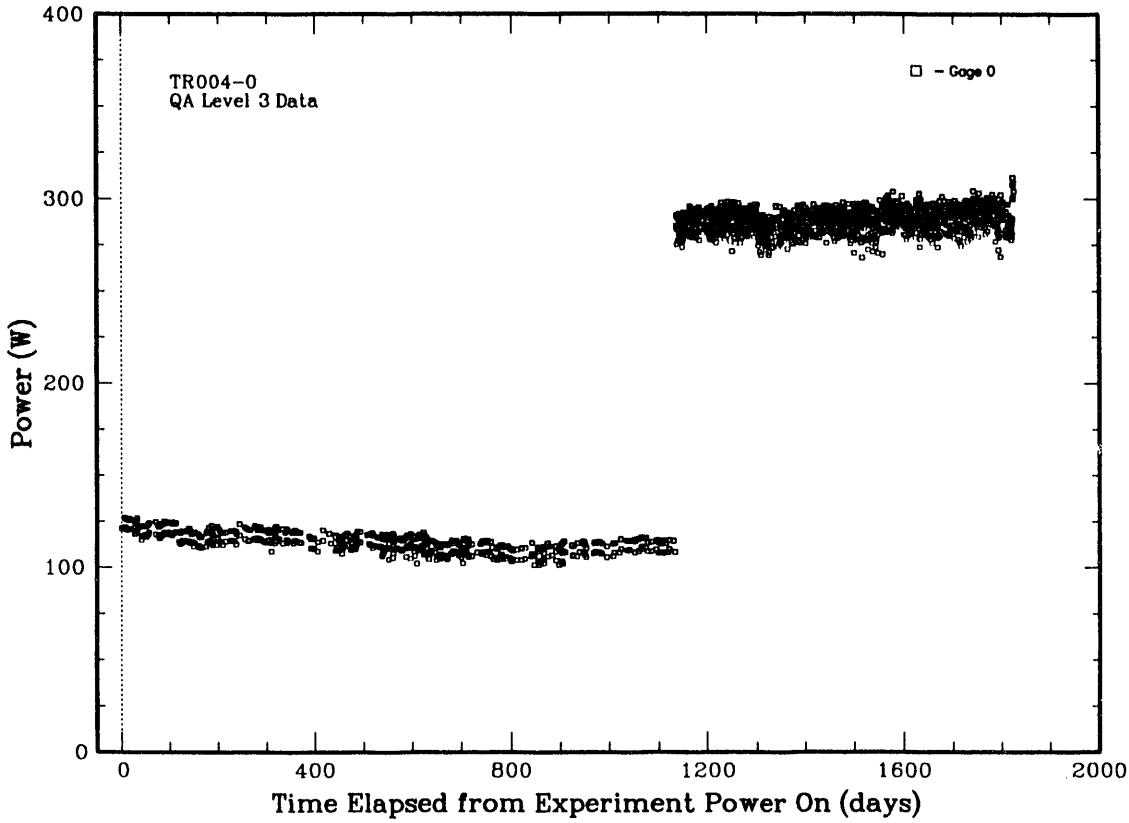

Figure 5.1-4a Simulated RH TRU Test TRH04 Power History

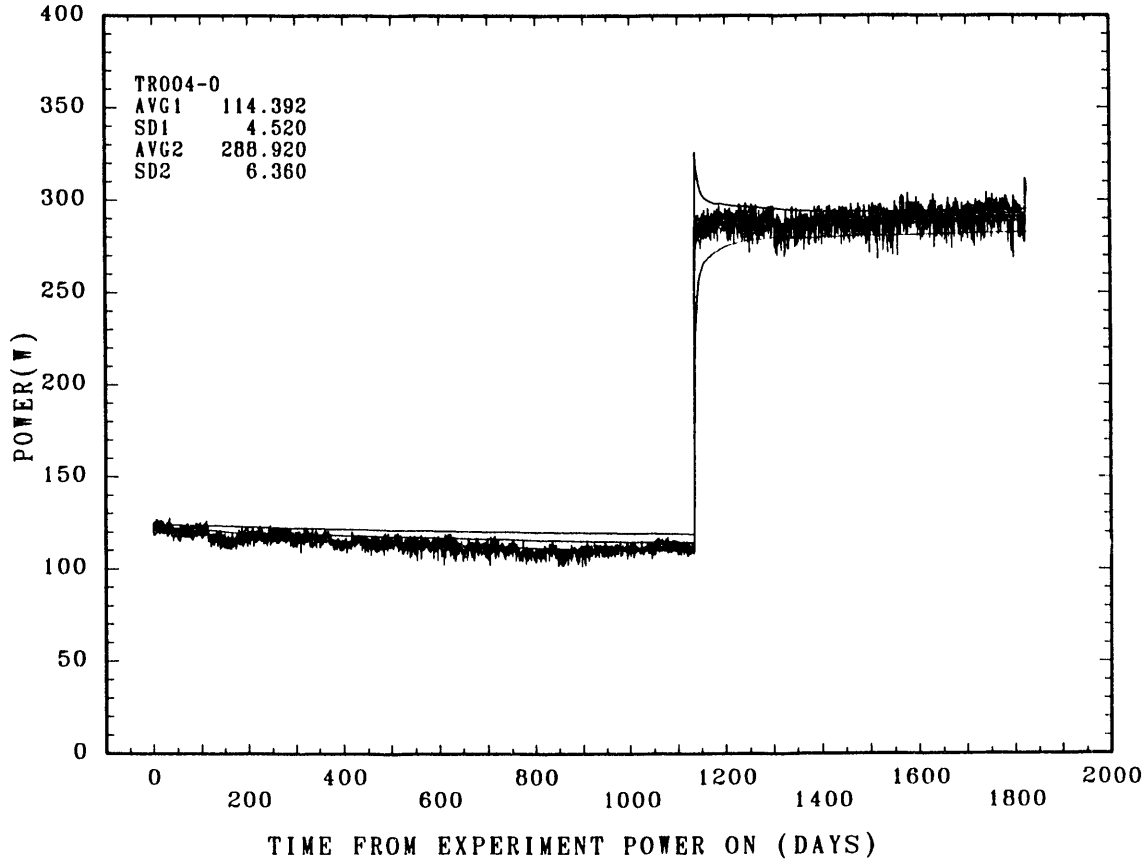

Figure 5.1-4b Simulated RH TRU Test TRH04 Calculated Power Averages

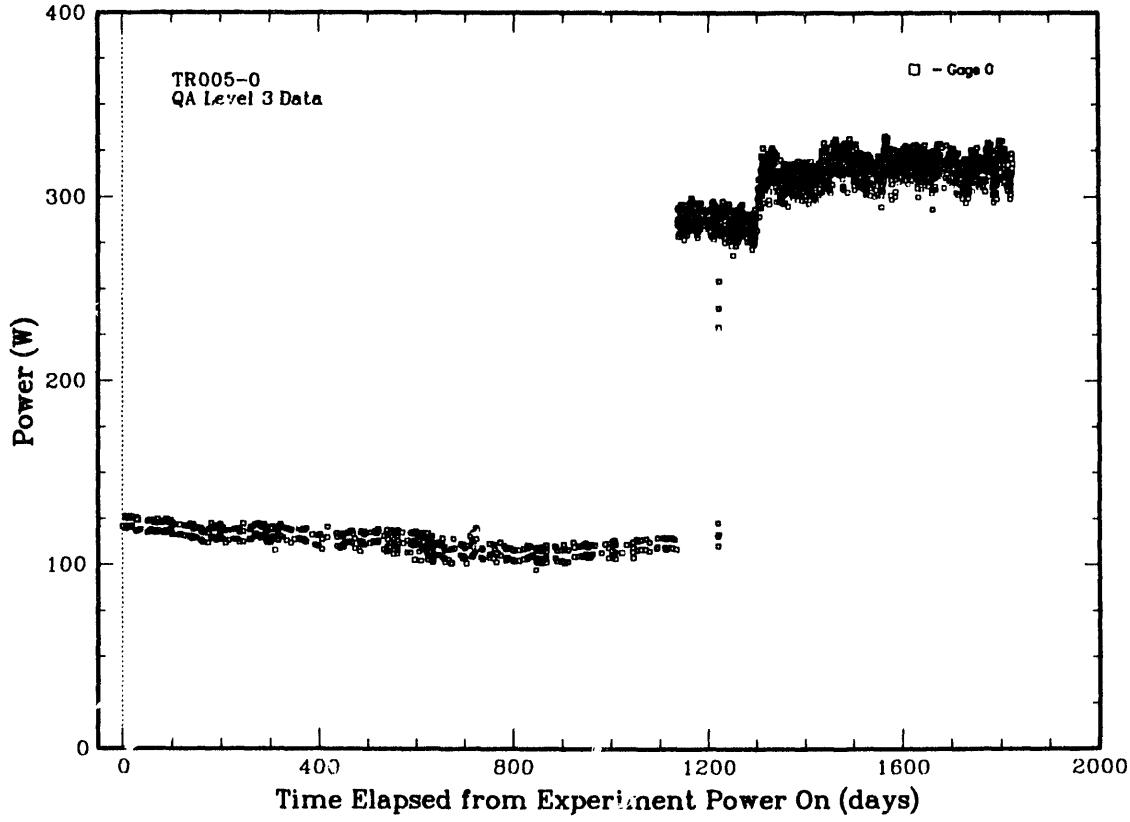

Figure 5.1-5a Simulated RH TRU Test TRH05 Power History

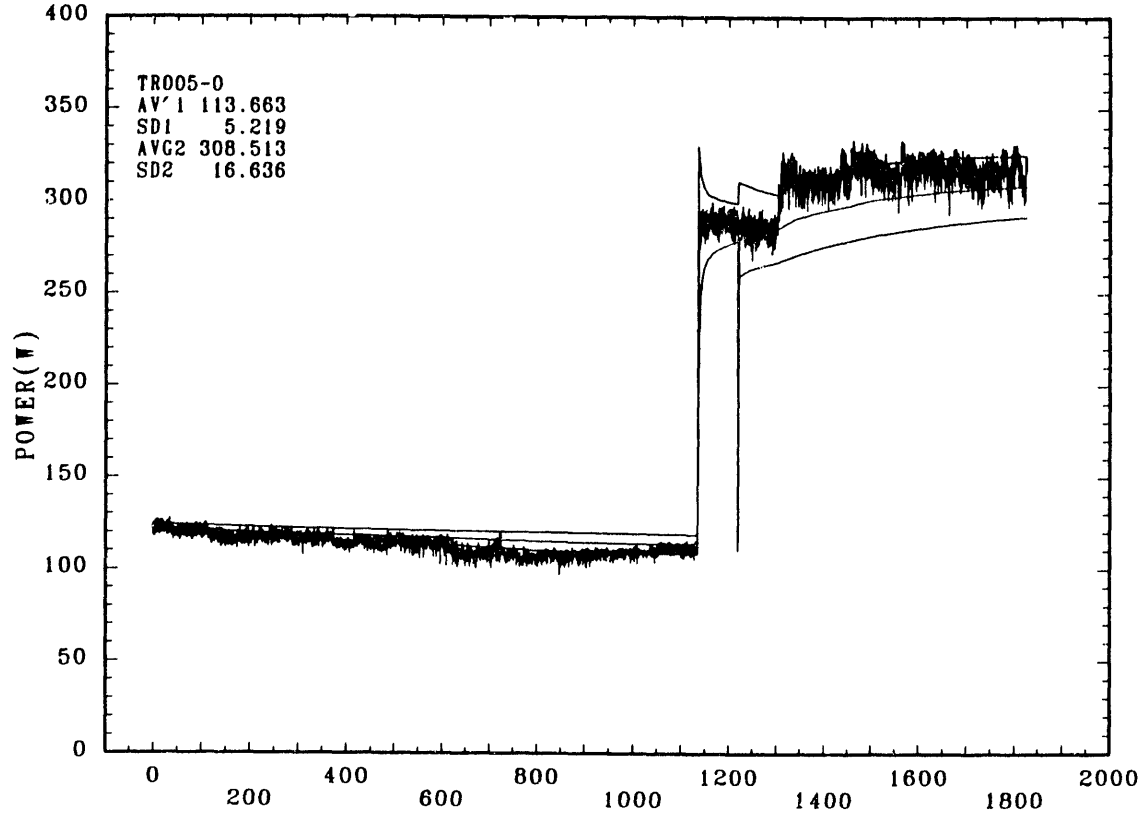

Figure 5.1-5b Simulated RH TRU Test TRH05 Calculated Power Averages

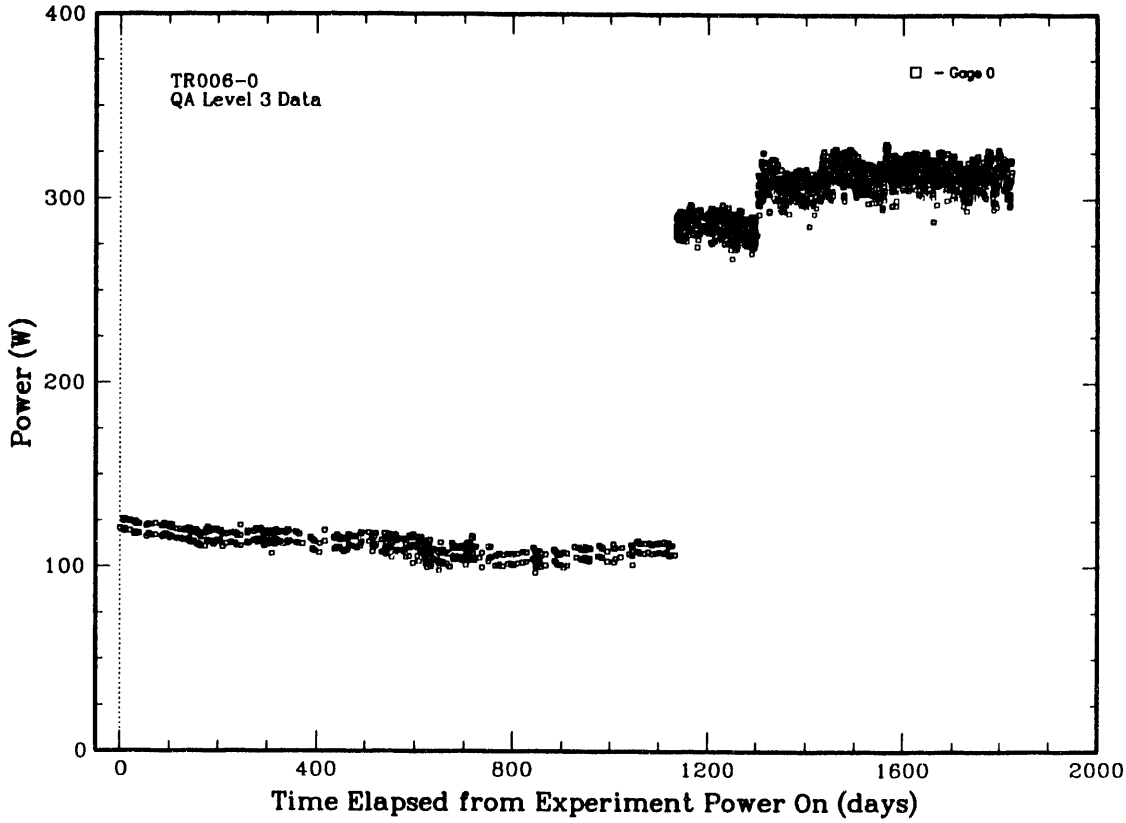

Figure 5.1-6a Simulated RH TRU Test TRH06 Power History

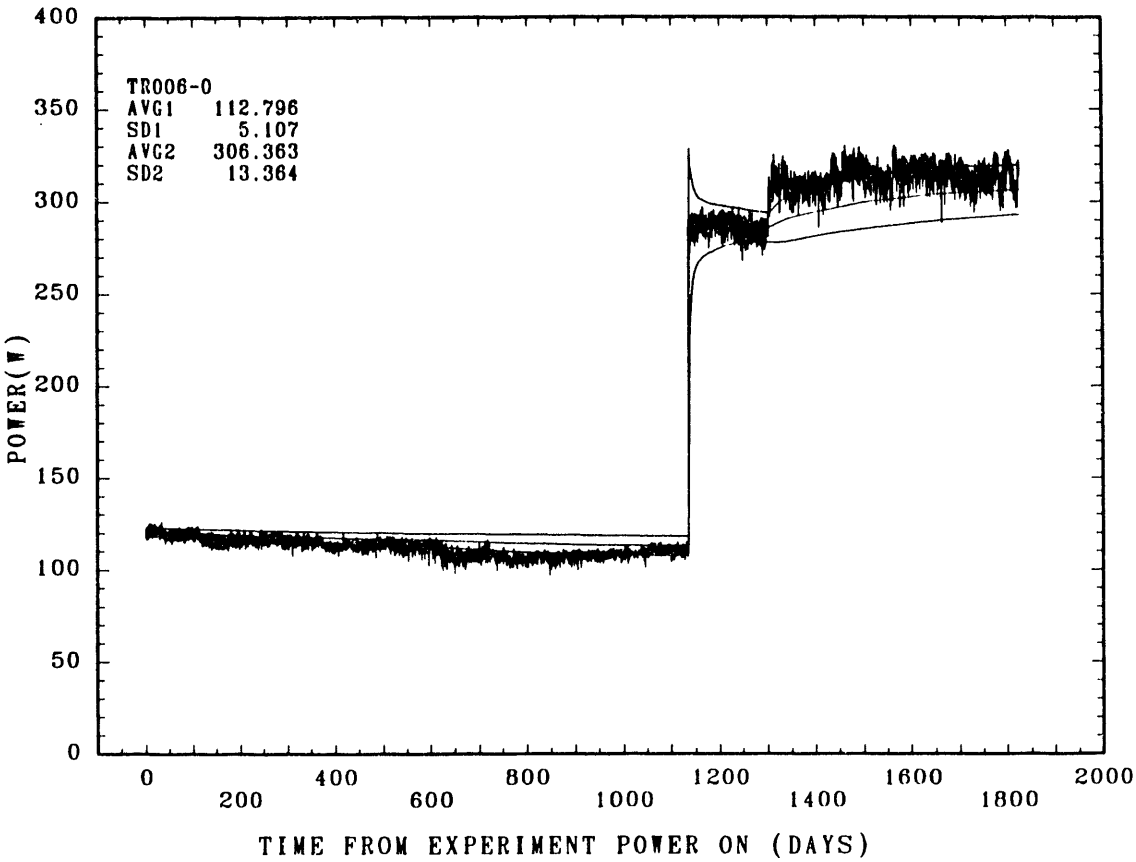

Figure 5.1-6b Simulated RH TRU Test TRH06 Calculated Power Averages

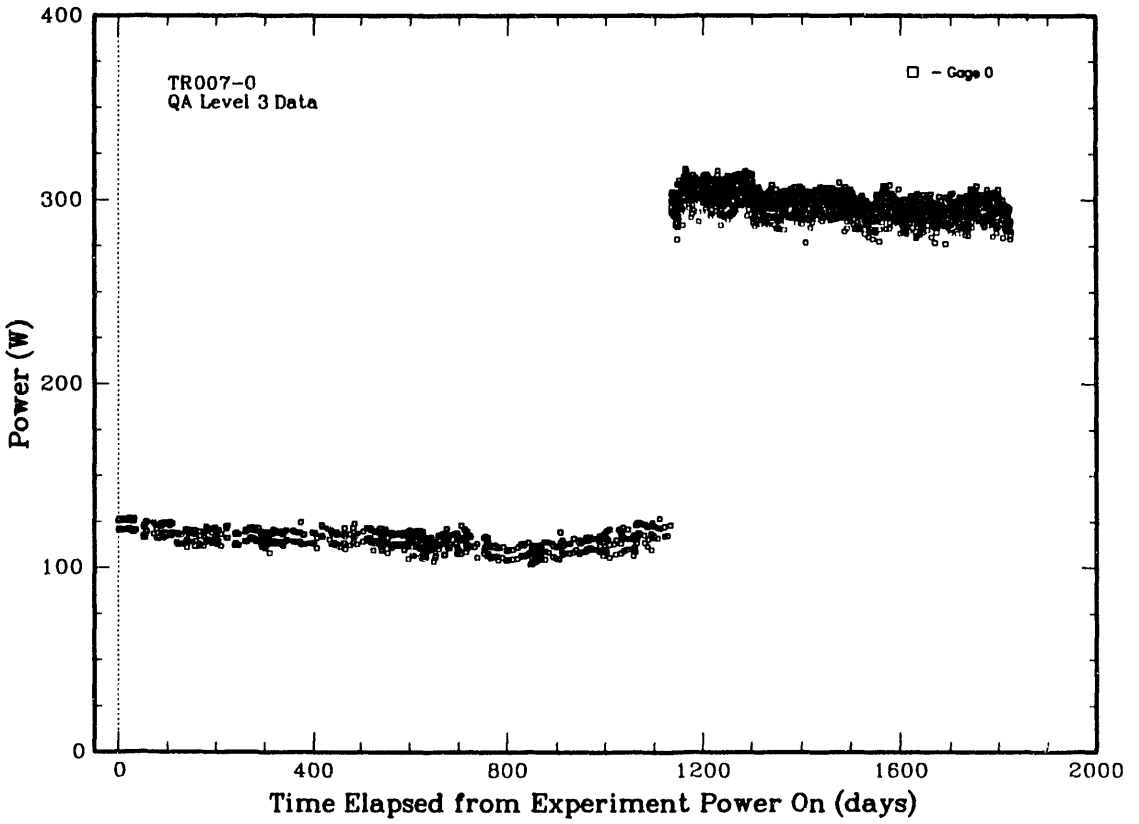

Figure 5.1-7a Simulated RH TRU Test TRH07 Power History

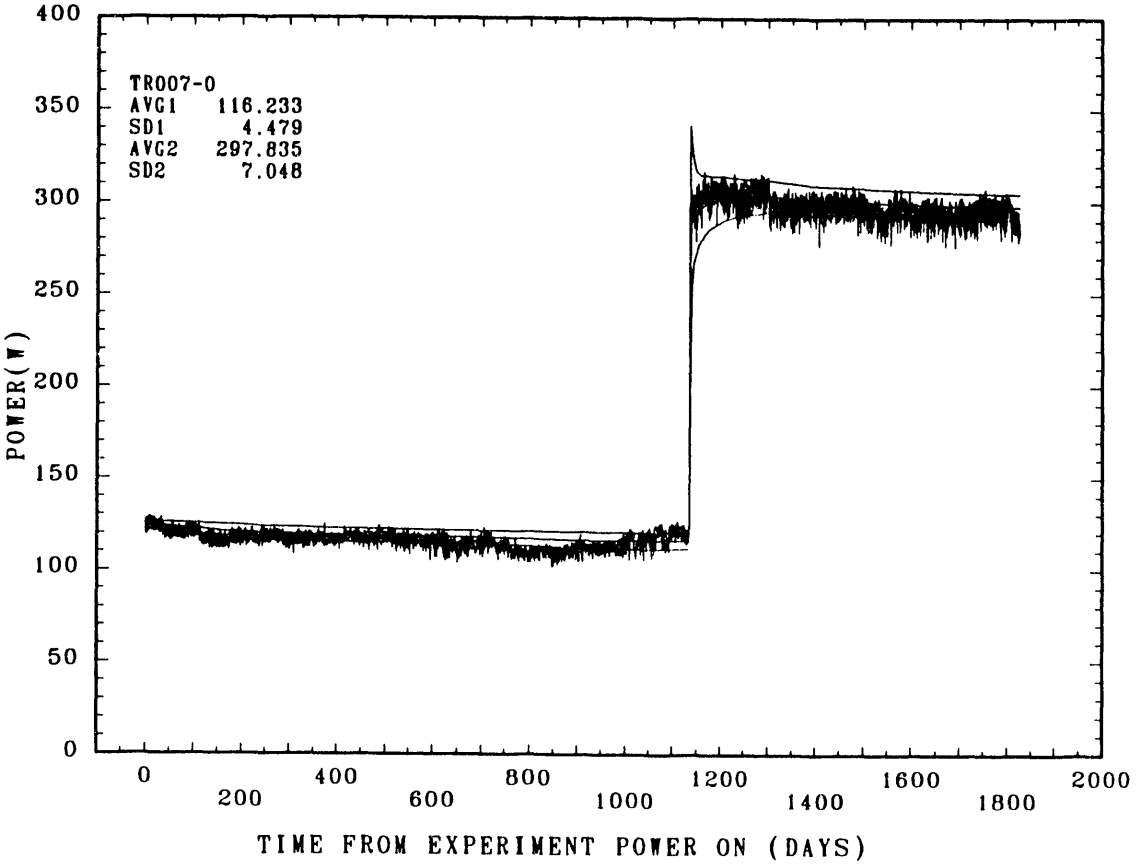

Figure 5.1-7b Simulated RH TRU Test TRH07 Calculated Power Averages

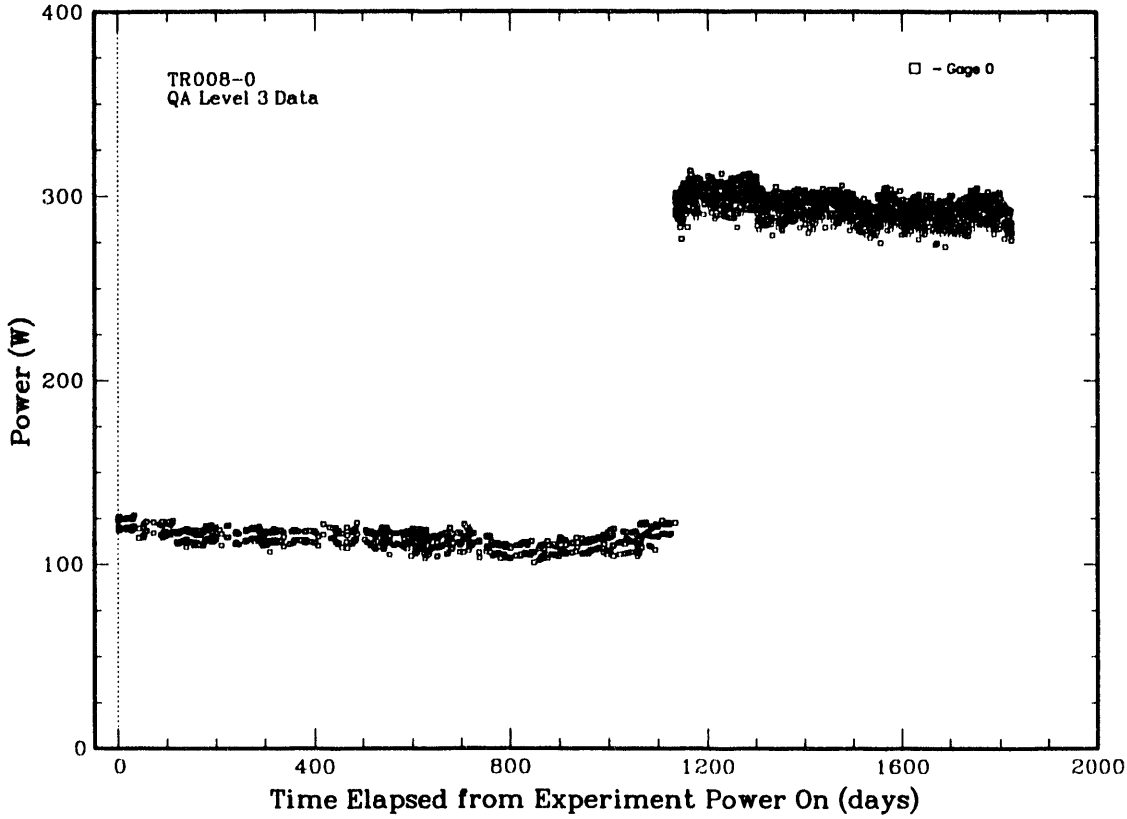

Figure 5.1-8a Simulated RH TRU Test TRH08 Power History

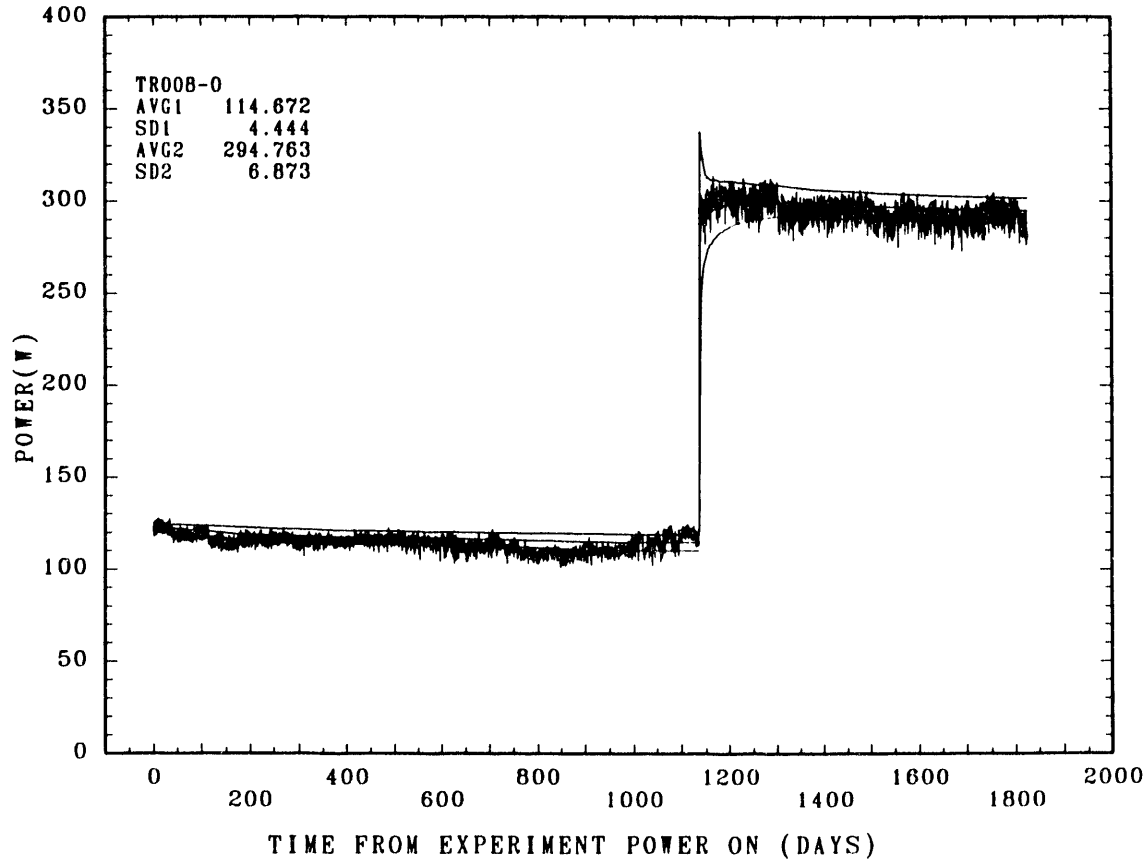

Figure 5.1-8b Simulated RH TRU Test TRH08 Calculated Power Averages

5.2 Test Container Temperature Histories

We measured temperatures on the top, inner surface of each test container with one to three "heater" thermocouples. These TCs are designated as TR00XT-1, TR00XT-2, and TR00XT-3, where "X" represents test container 1 through 8. Thermocouple "-2" is located at essentially the mid-length of each container. Thermocouple "-1" and "-3," present in containers TRH01 through TRH04 only, are located at the front (closest to the rib) top-25% (length) position and the back-75% position of the container, respectively. The exact test-room coordinates of each heater TC are listed in **Table 3.5,** the Instrumentation NOS file. The locations of each heater TC, relative to each test emplacement and borehole, are shown in **Figures 3.5-1** through **3.5-8.** These heater-TCs are identified in **Figures 3.5-1** through **3.5-8** by their original designations ("old I.D.") of TRH0XT-1,-2, or -3.

The heater-thermocouple temperature data histories on the top-inner surface of each RH TRU test container are illustrated in **Figures 5.2-1a** through **5.2-8a** for test containers TRH01 through TRH08, respectively. The corresponding calculated temperature running averages and standard deviations are illustrated in **Figures 5.2-1b,c,d** through **5.2-8b,c,d**. Calculations of the average values and standard deviations of all temperature data points were made with the GRAFAID analysis tool (Adams, 1985). As is evident in these figures, the heater-TC temperatures have risen from the initial Room T mine-ambient temperature of 28.0° to 28.3°C up to near their maximum values in a very few days after heater turn-on at day t = 0, and the heater power increase to about 300 W at day t = 1135.

The average temperature values for each test thermocouple, plus or minus calculated standard deviations, are listed in **Table 5.2.** Temperature are listed for the distinct (heater power-level) time periods of 0 through 1,135 days and 3.1 through 5.0 years (1,135 through 1,826 days). The GRAFAID calculations covered the time period of 10 to 1,135 days after test turn-on, and, independently, 1,145 to 1,826 days. The initial 10-day segment of each time period was not included, in order to minimize any effects of the initial heat-up period(s) on the overall temperature averages. Several of the calculated average temperatures listed in this table are enclosed in parentheses. These denoted temperatures cannot be considered as averages since the observable temperature trends (in the appropriate figures) are either increasing as a function of time or contain discontinuous "jumps," probably caused by adjustments to the heater powers.

Table 5.2 RH TRU Heater-Thermocouple (TR00XT) Temperature Values

Test Container X: (= 1 - 8)	0 to 1,135 Days 0 to 3.1 Years			3.1 to 5.0 Years		
	TR00XT-1 (TRH0XT-1)	TR00XT-2 (TRH0XT-2)	TR00XT-3 (TRH0XT-3)	TR00XT-1 (TRH0XT-1)	TR00XT-2 (TRH0XT-2)	TR00XT-3 (TRH0XT-3)
TRH01:	36.91° ± 0.55°C	36.89° ± 0.49°C	37.40° ± 0.55°C	46.57° ± 0.90°C	47.84° ± 0.73°C	48.73° ± 0.82°C
TRH02:	36.10° ± 0.49°C	(inoperable)	35.56° ± 0.51°C	45.17° ± 0.89°C	(inoperable)	44.28° ± 0.93°C
TRH03:	38.95° ± 0.47°C	39.39° ± 0.44°C	40.05° ± 0.47°C	51.69° ± 0.87°C	53.50° ± 1.40°C	54.85° ± 0.75°C
TRH04:	41.31° ± 0.57°C	40.20° ± 0.57°C	41.93° ± 0.51°C	(failed, inoperable)	(58.26° ± 1.24°C)	57.72° ± 0.67°C
TRH05:		38.91° ± 0.46°C			(55.64° ± 2.18°C)	
TRH06:		39.86° ± 0.54°C			(56.49° ± 1.60°C)	
TRH07:		36.33° ± 0.60°C			46.63° ± 0.60°C	
TRH08:		38.85° ± 0.57°C			50.32° ± 0.65°C	

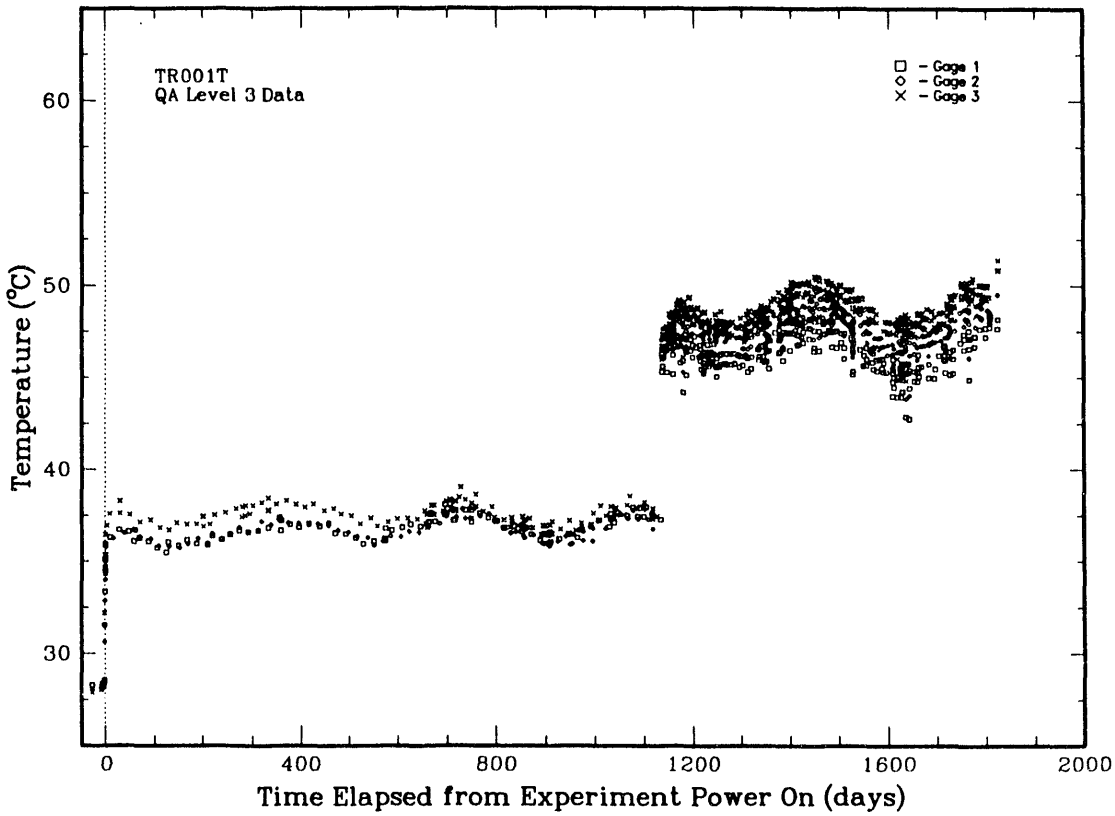

Figure 5.2-1a Heater-Thermocouple TR001T Temperature History

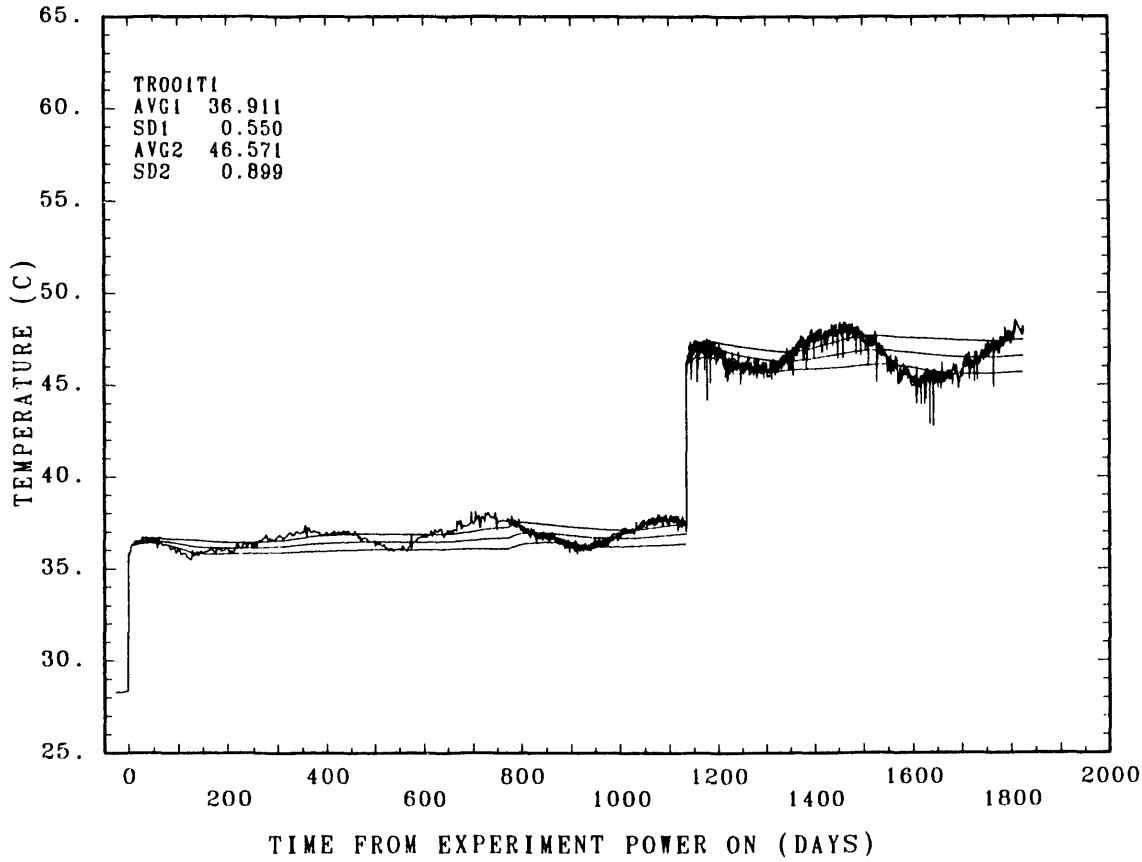

Figure 5.2-1b Heater-Thermocouple TR001T-1 Calculated Temperature Averages

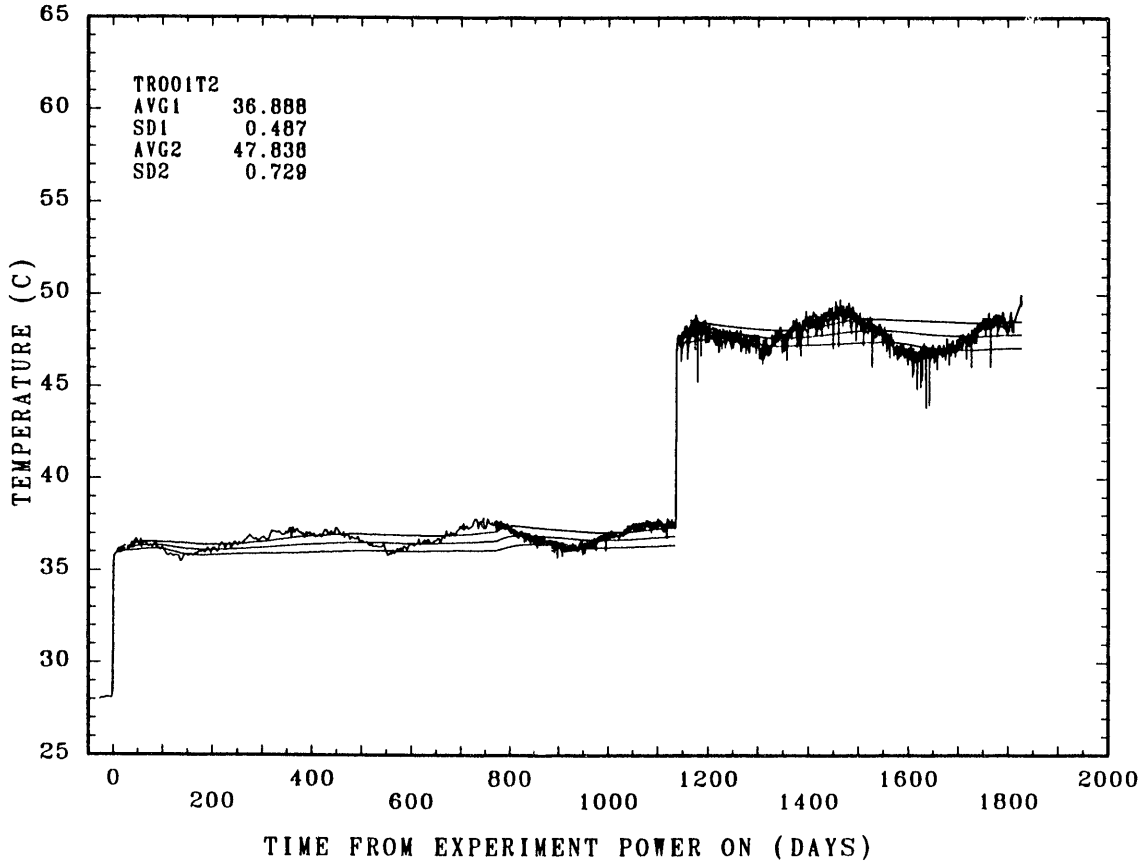

Figure 5.2-1c Heater-Thermocouple TR001T-2 Calculated Temperature Averages

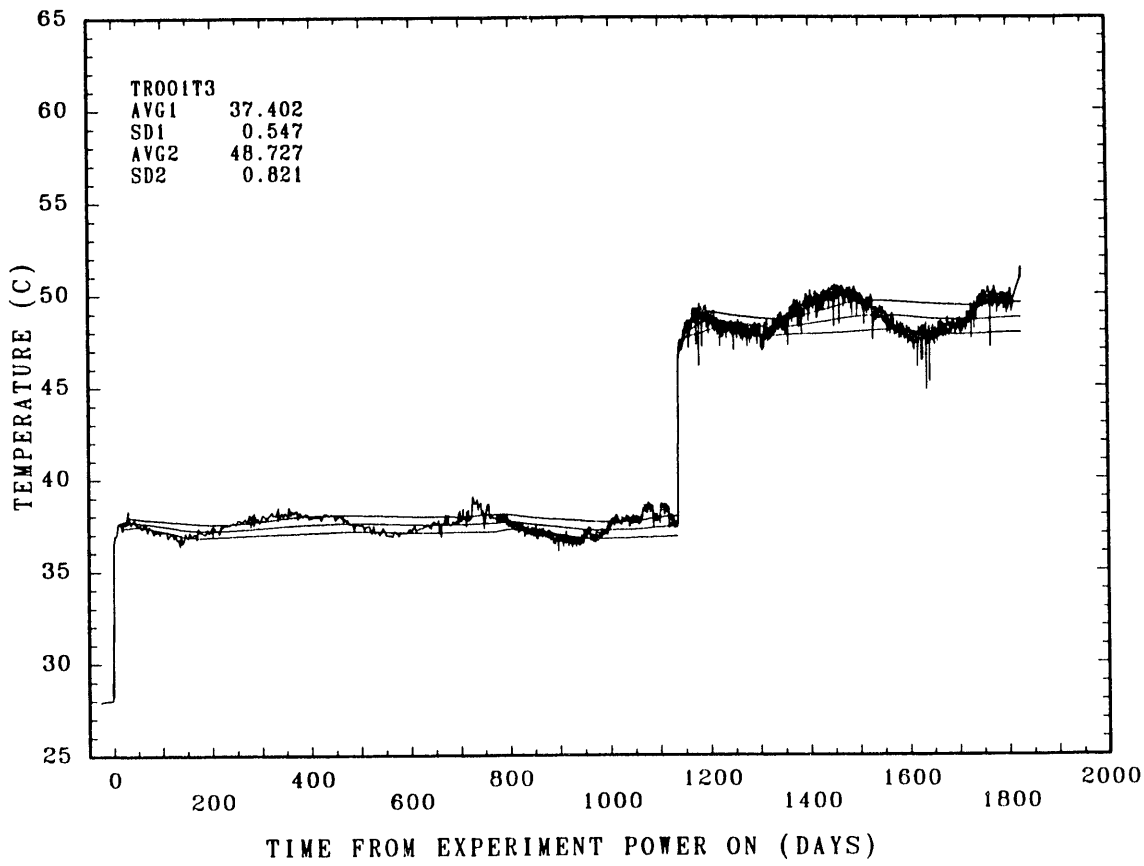

Figure 5.2-1d Heater-Thermocouple TR001T-3 Calculated Temperature Averages

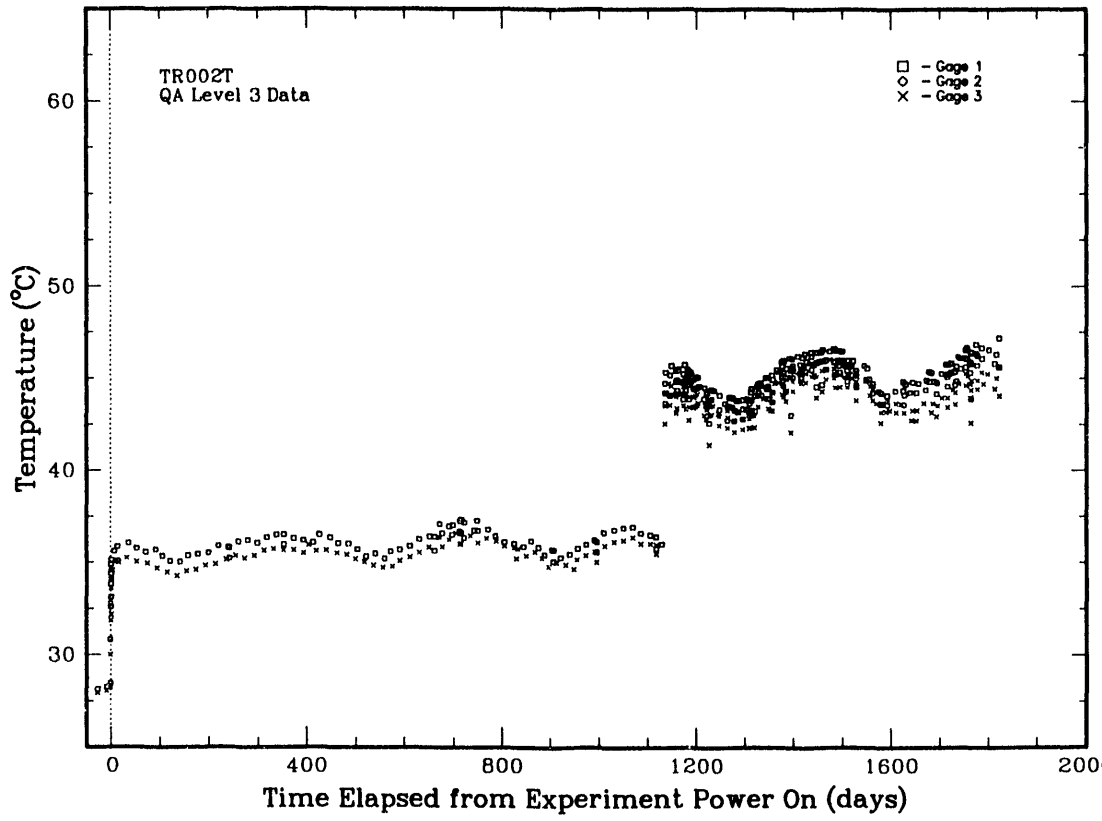

Figure 5.2-2a Heater-Thermocouple TR002T Temperature History

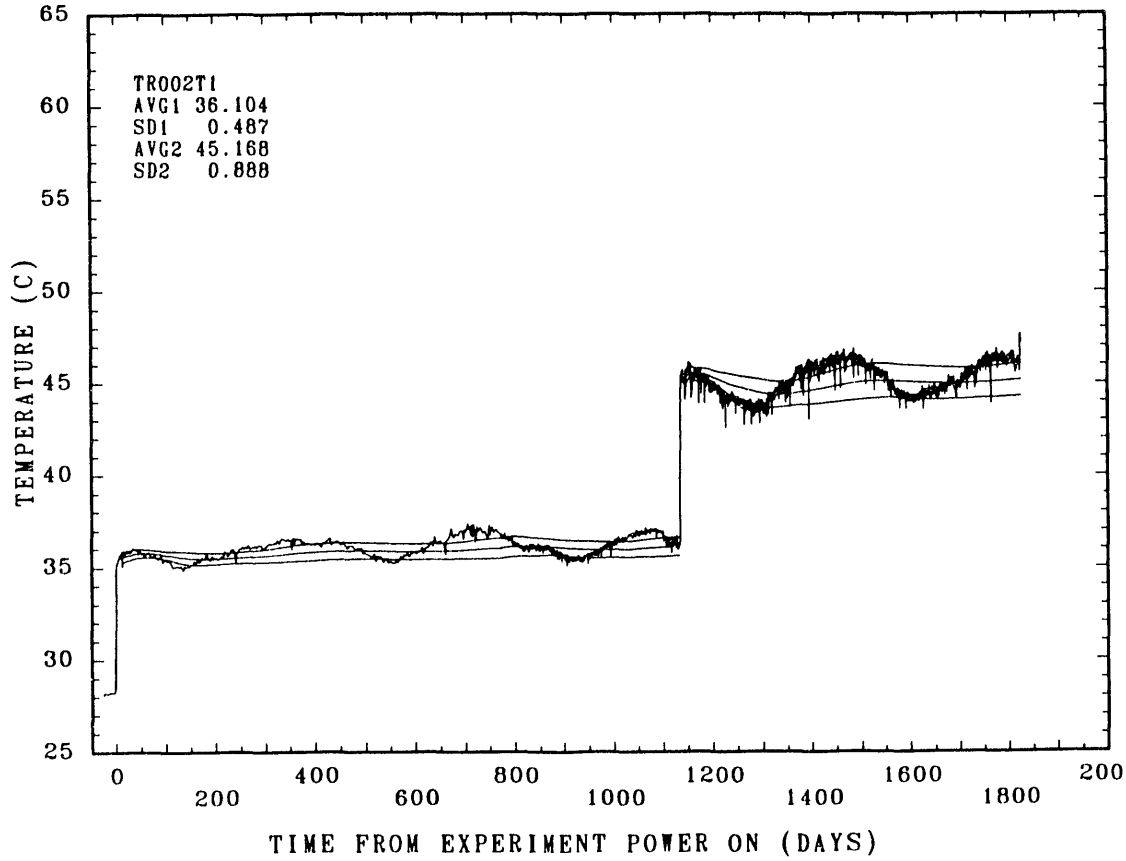

Figure 5.2-2b Heater-Thermocouple TR002T-1 Calculated Temperature Averages

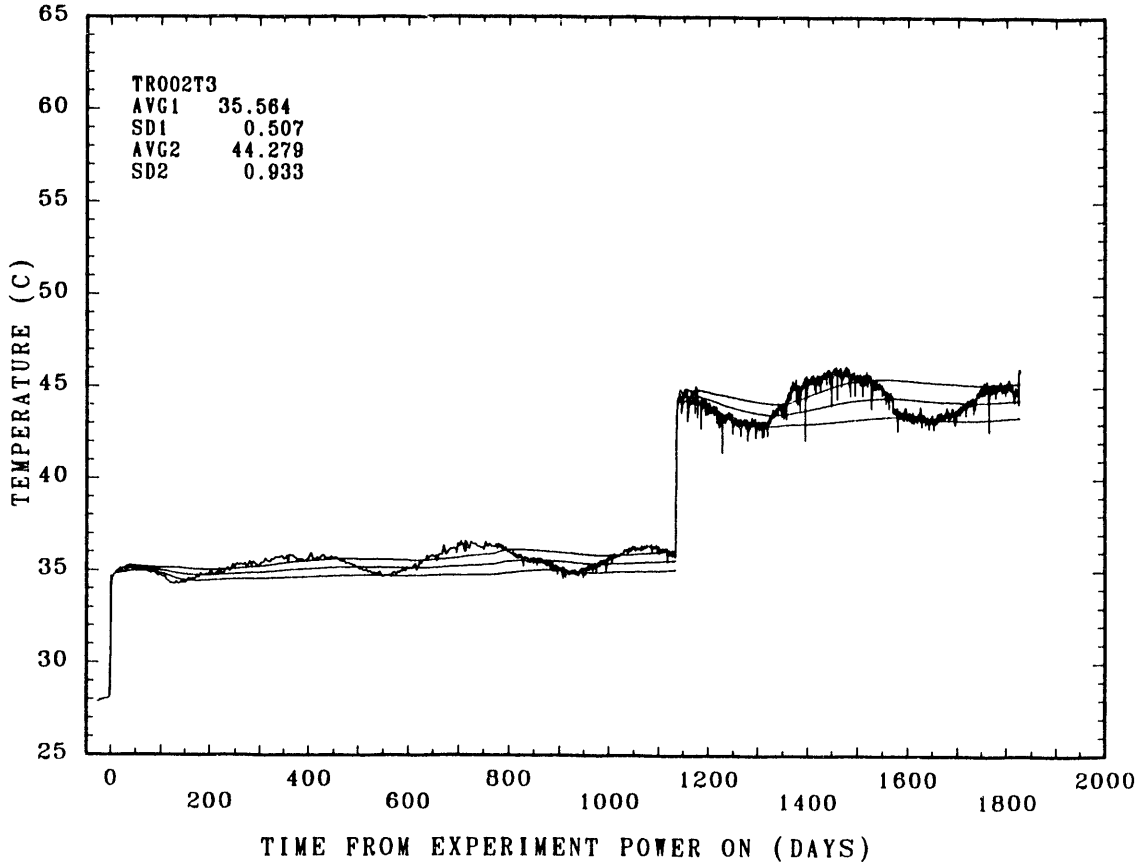

Figure 5.2-2d Heater-Thermocouple TR002T-3 Calculated Temperature Averages

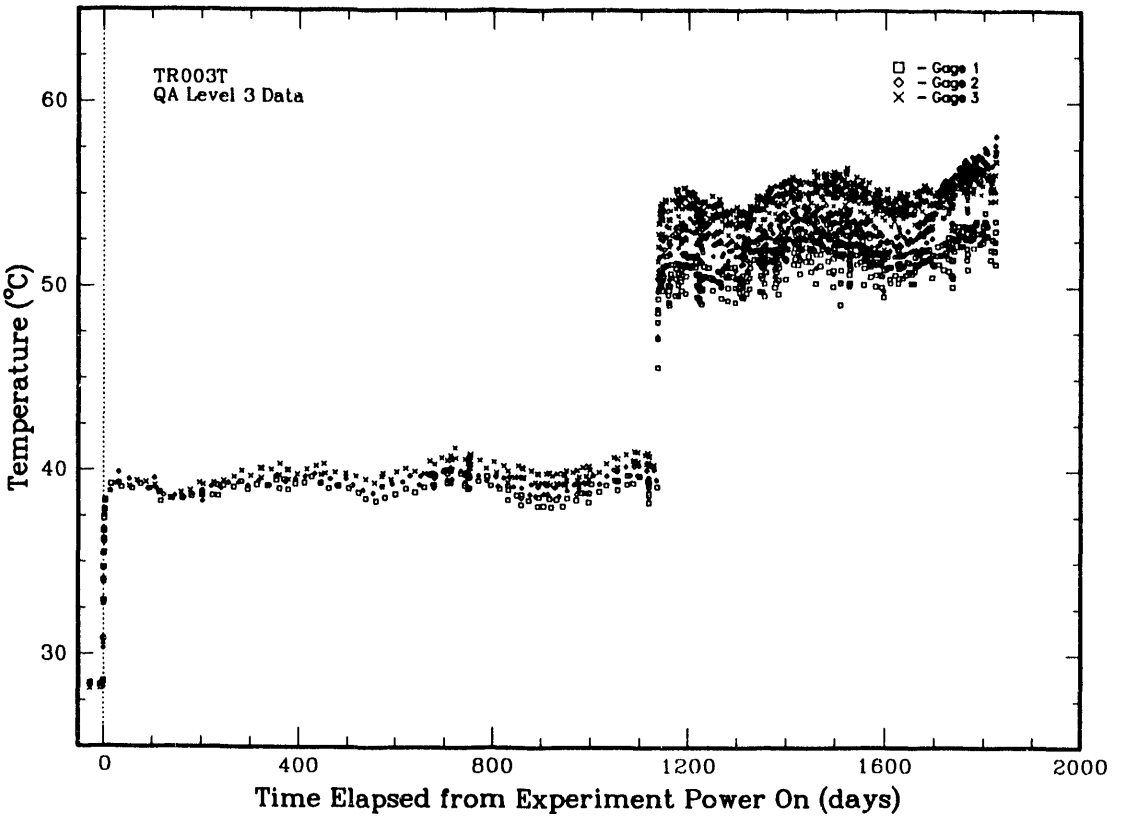

Figure 5.2-3a Heater-Thermocouple TR003T Temperature History

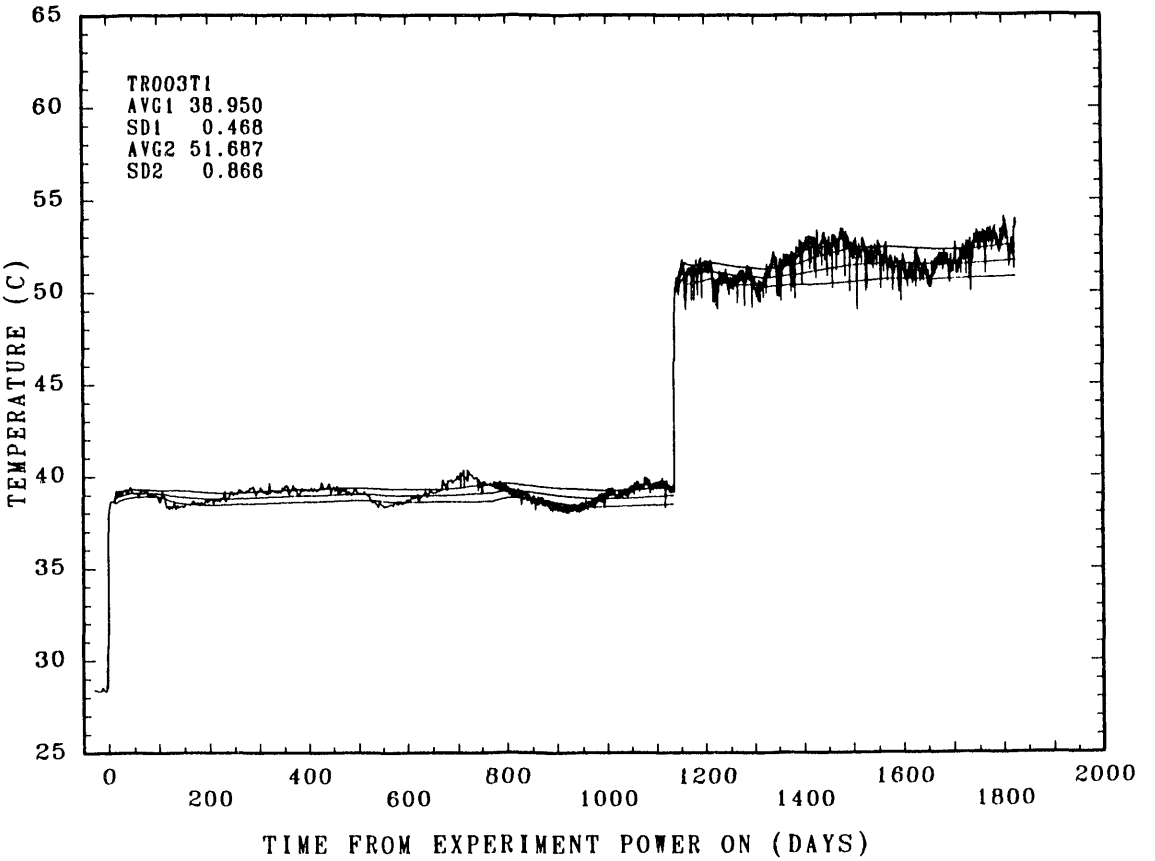

Figure 5.2-3b Heater-Thermocouple TR003T-1 Calculated Temperature Averages

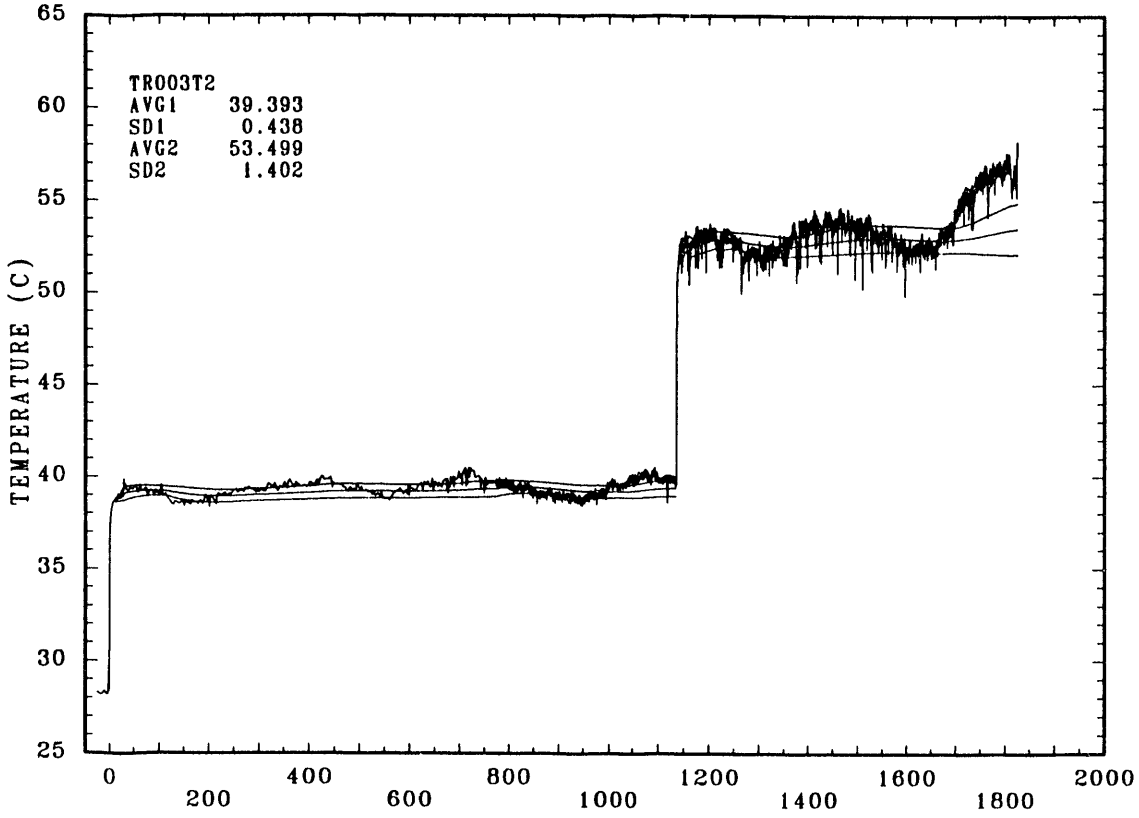

Figure 5.2-3c Heater-Thermocouple TR003T-2 Calculated Temperature Averages

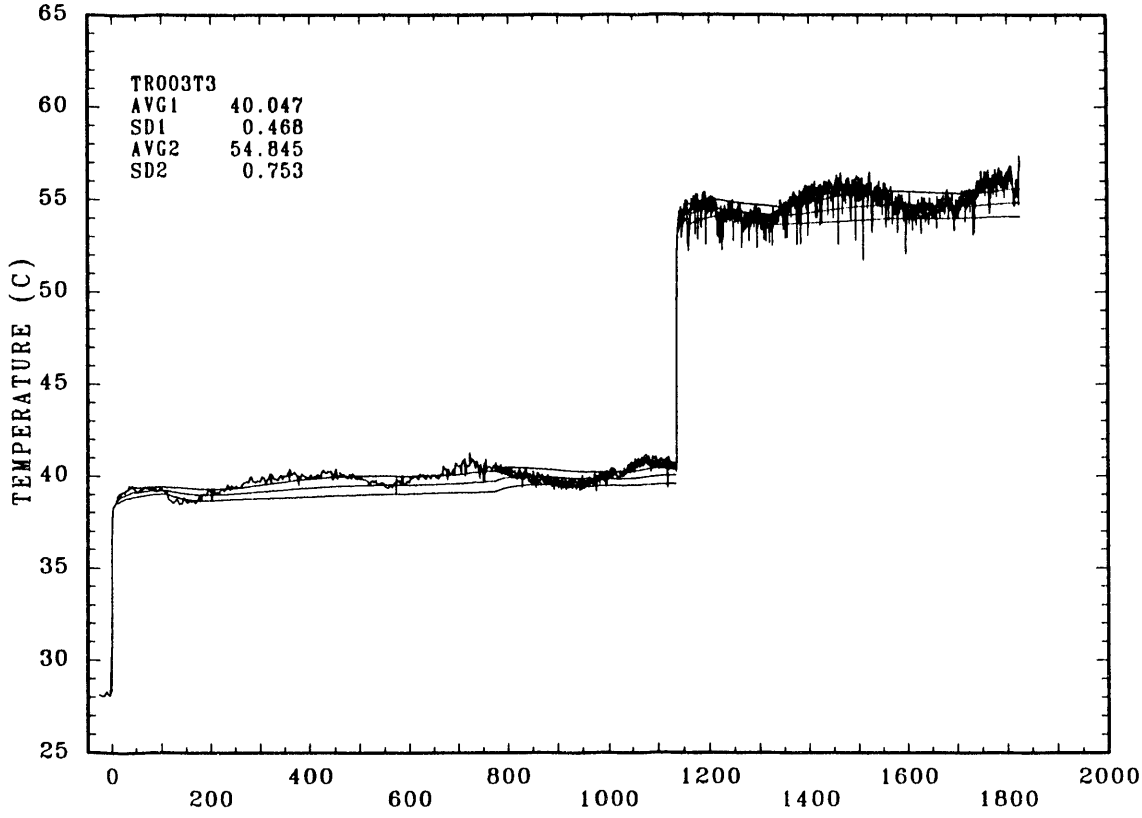

Figure 5.2-3d Heater-Thermocouple TR003T-3 Calculated Temperature Averages

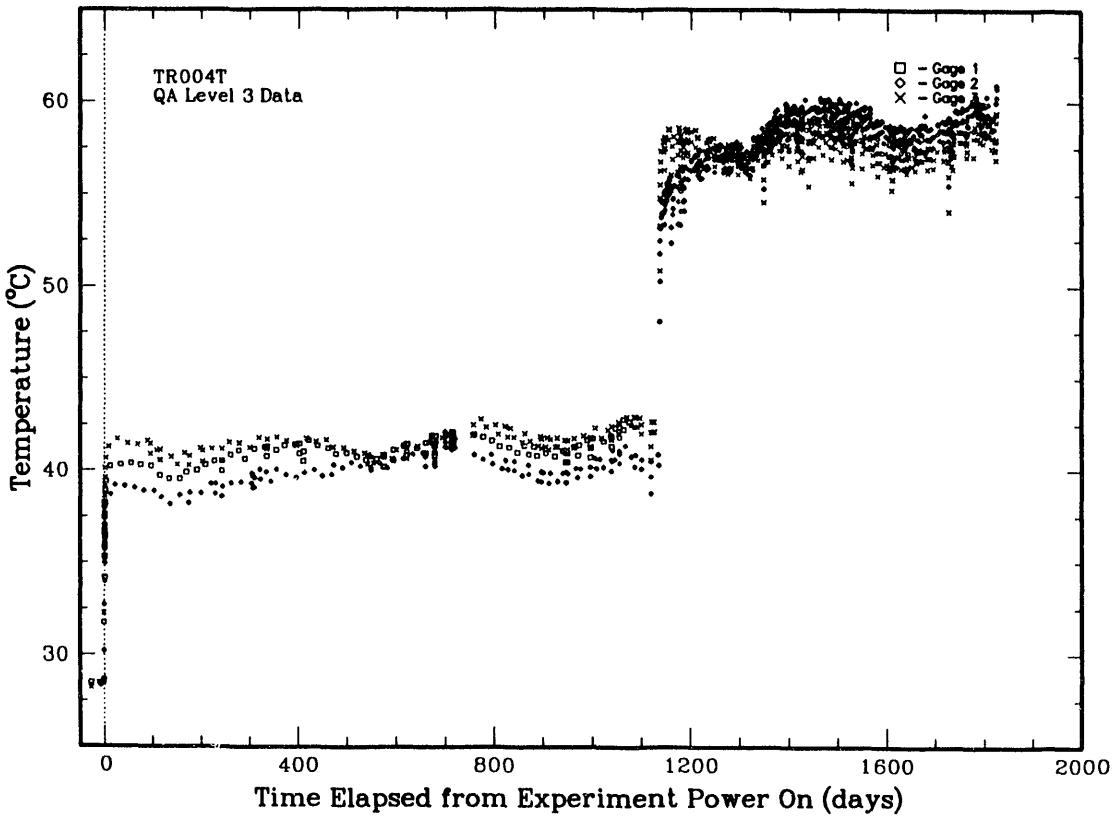

Figure 5.2-4a Heater-Thermocouple TR004T Temperature History

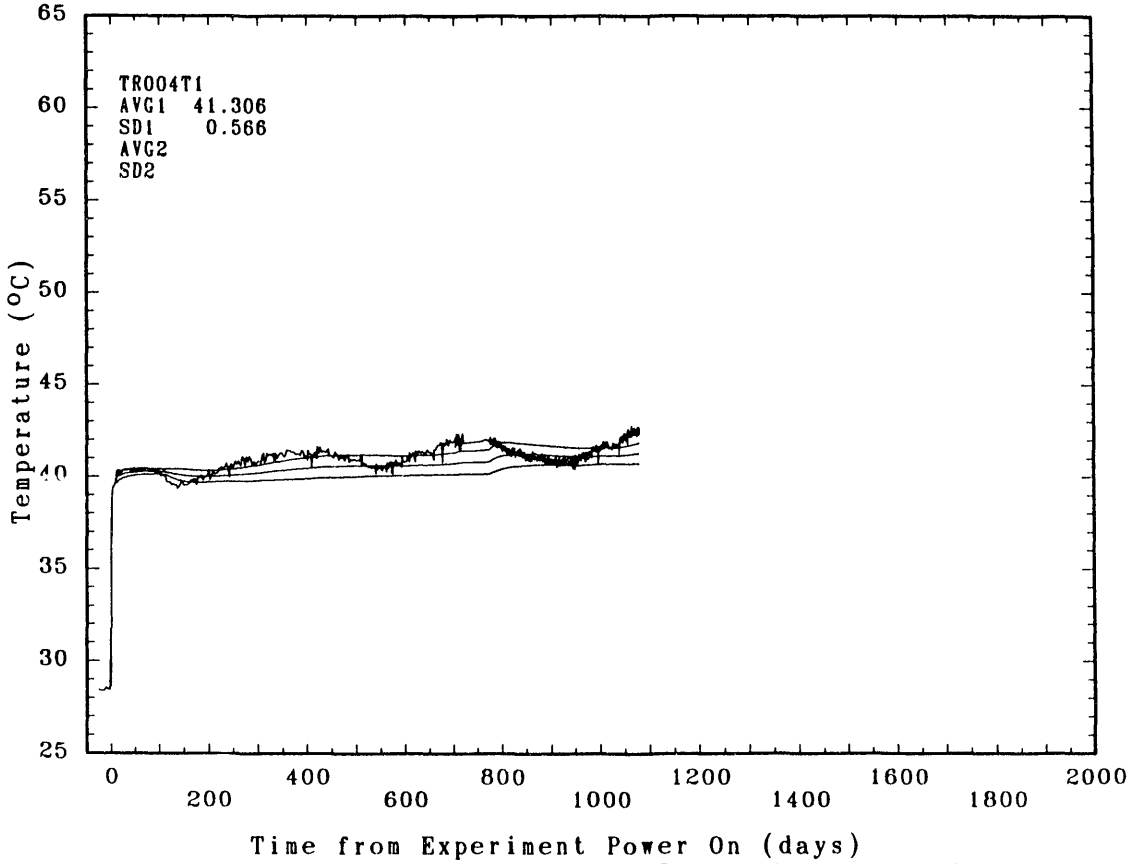

Figure 5.2-4b Heater-Thermocouple TR004T-1 Calculated Temperature Averages

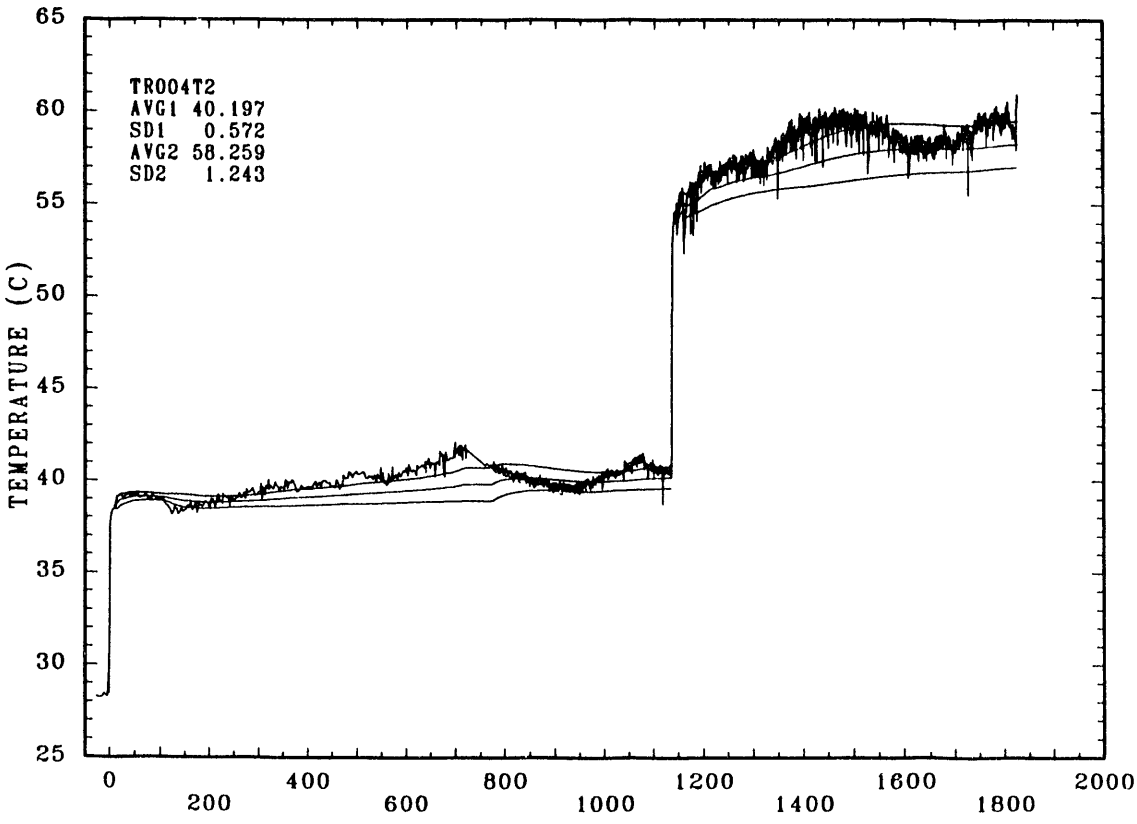

Figure 5.2-4c Heater-Thermocouple TR004T-2 Calculated Temperature Averages

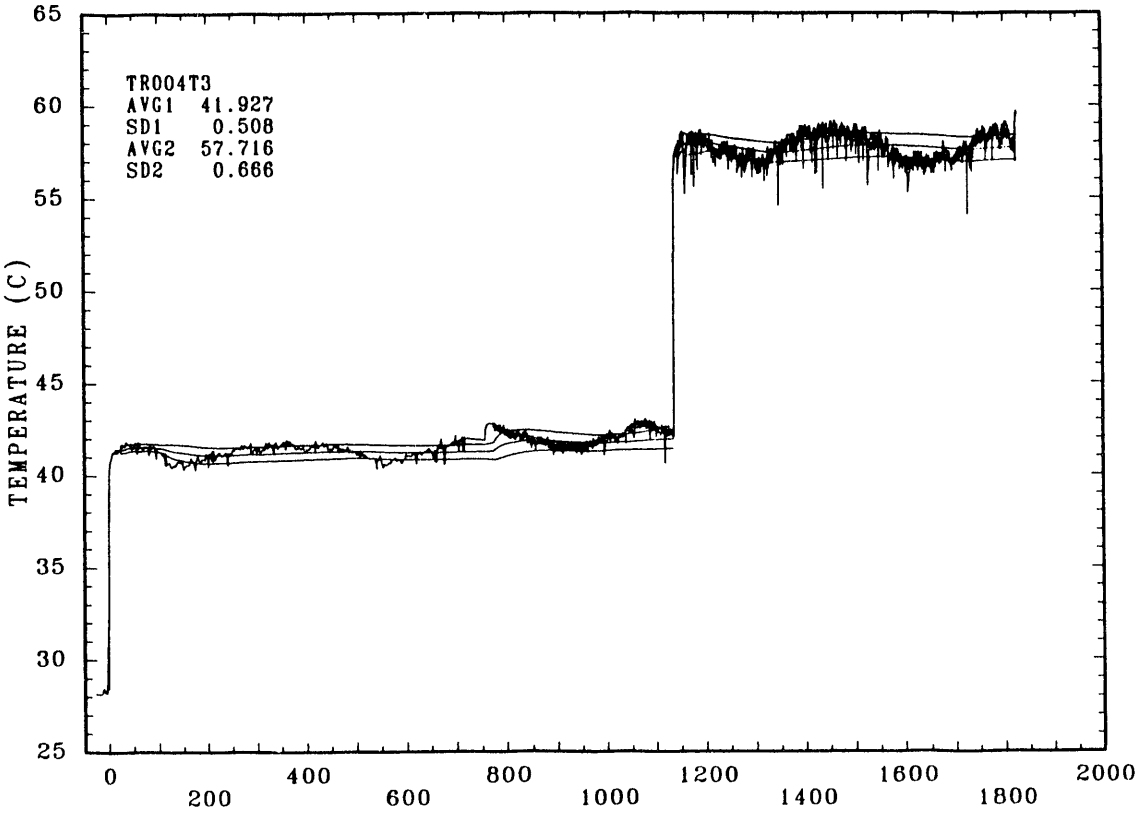

Figure 5.2-4d Heater-Thermocouple TR004T-3 Calculated Temperature Averages

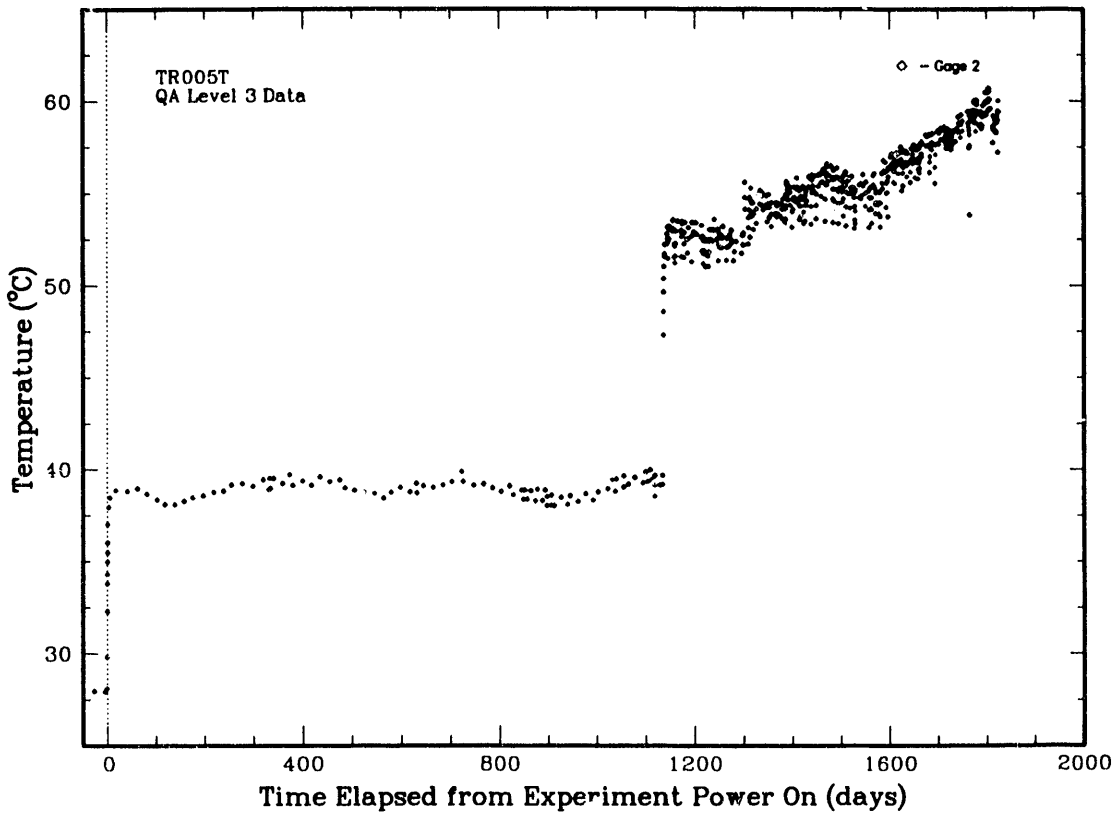

Figure 5.2-5a Heater-Thermocouple TR005T-2 Temperature History

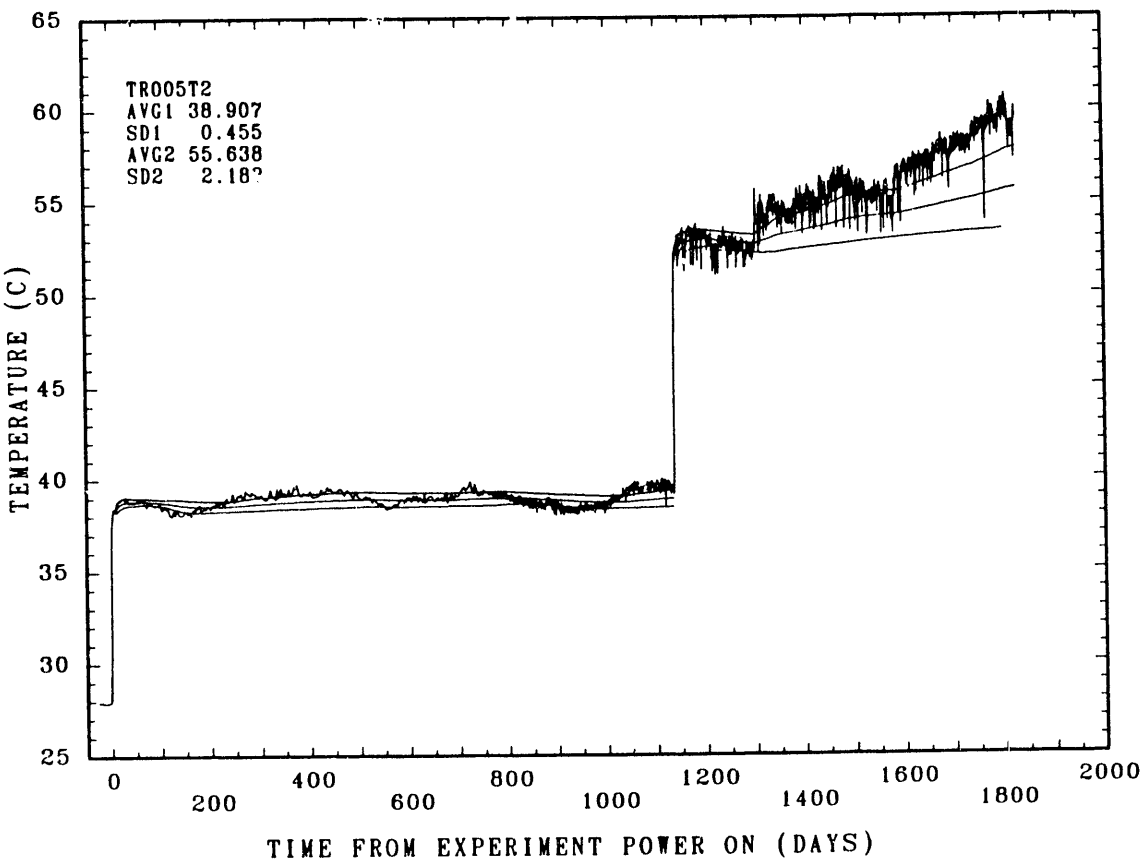

Figure 5.2-5b Heater-Thermocouple TR005T-2 Calculated Temperature Averages

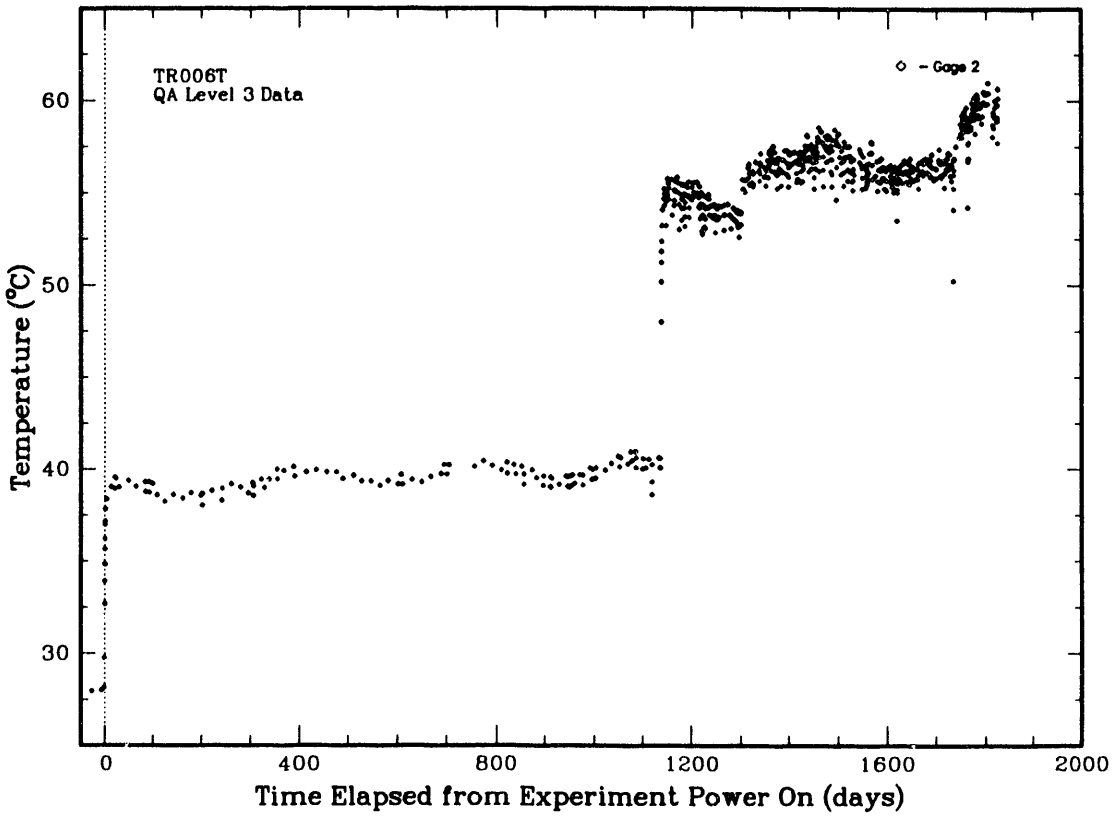

Figure 5.2-6a Heater-Thermocouple TR006T-2 Temperature History

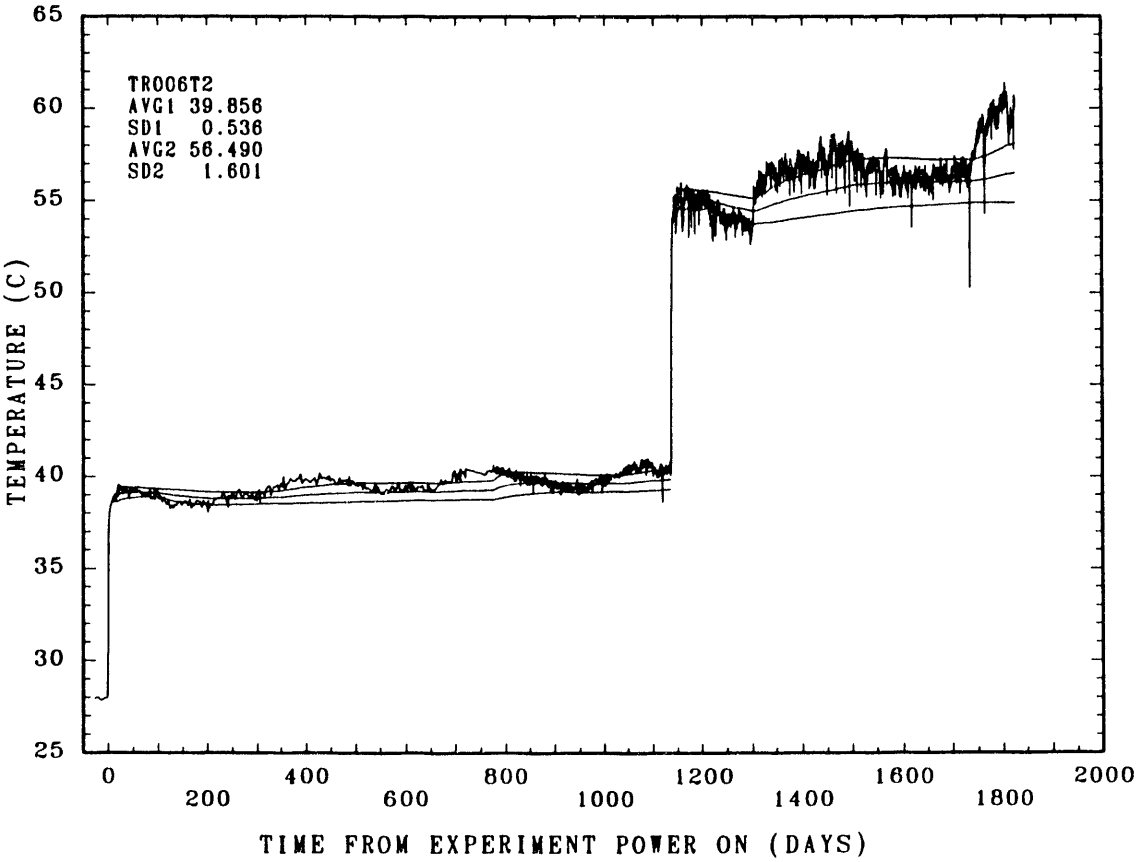

Figure 5.2-6b Heater-Thermocouple TR006T-2 Calculated Temperature Averages

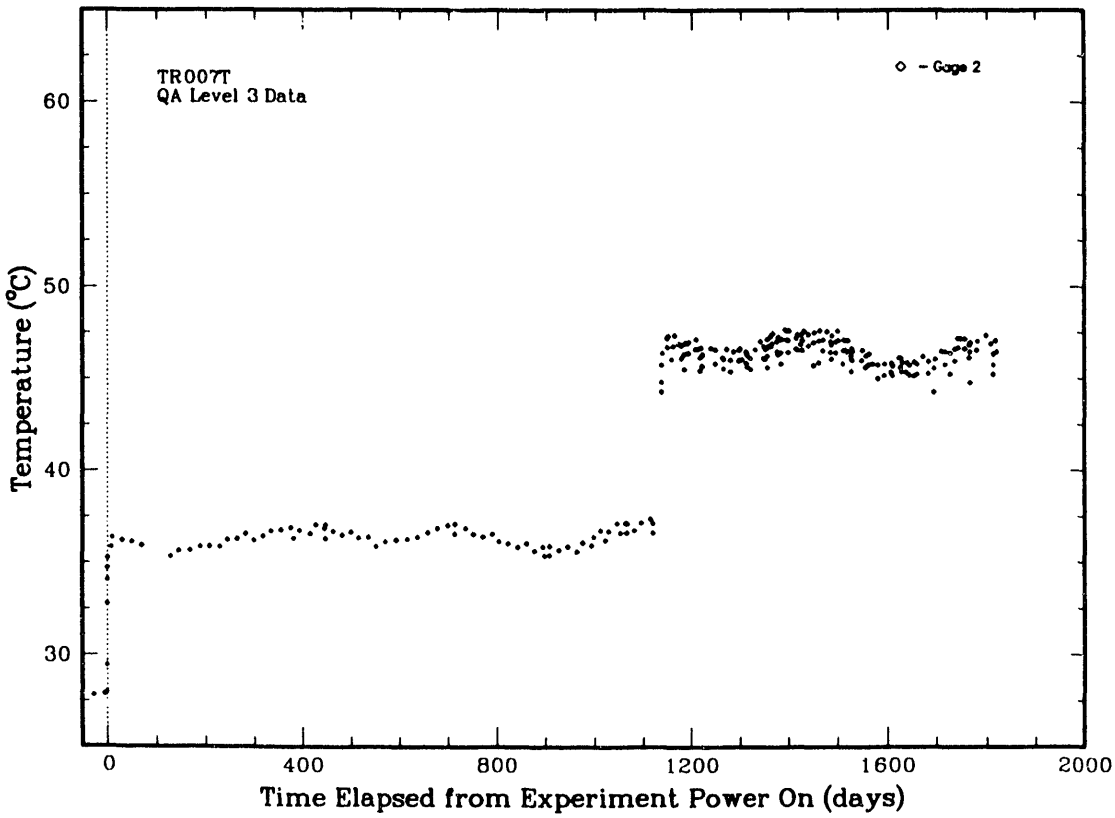

Figure 5.2-7a Heater-Thermocouple TR007T-2 Temperature History

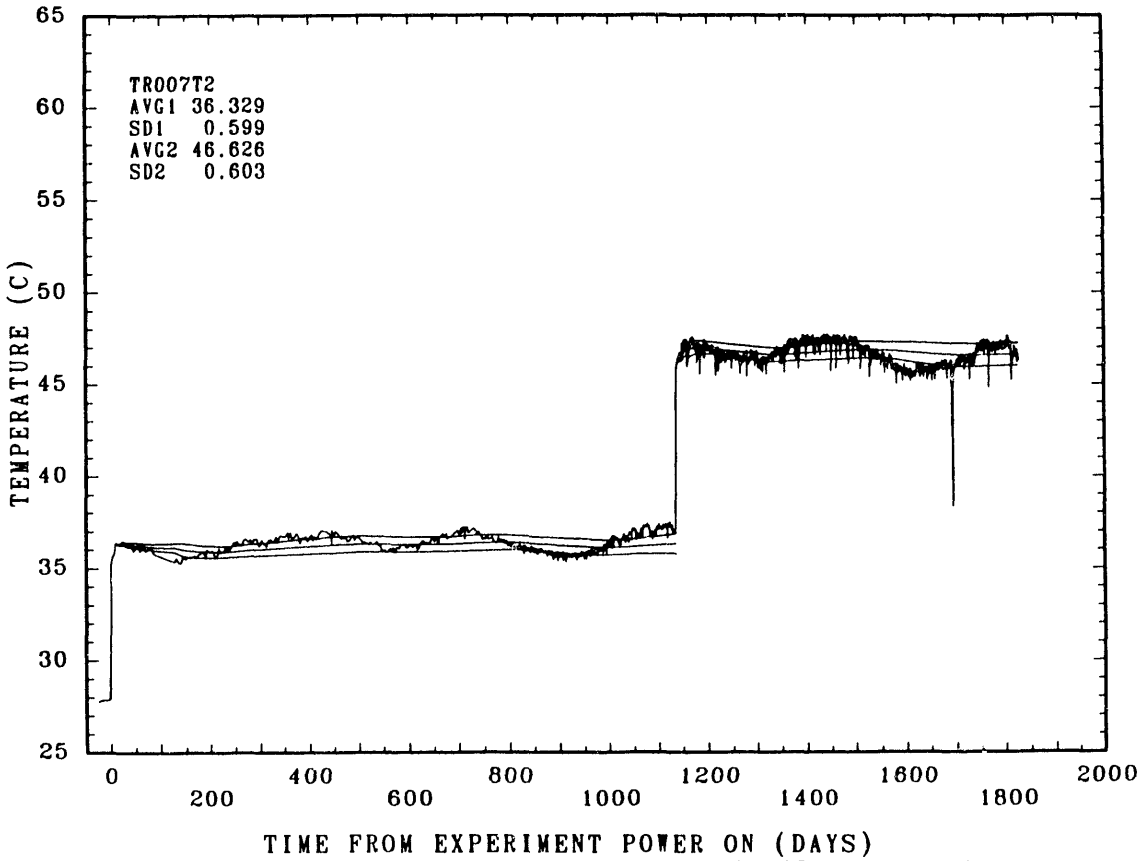

Figure 5.2-7b Heater-Thermocouple TR007T-2 Calculated Temperature Averages

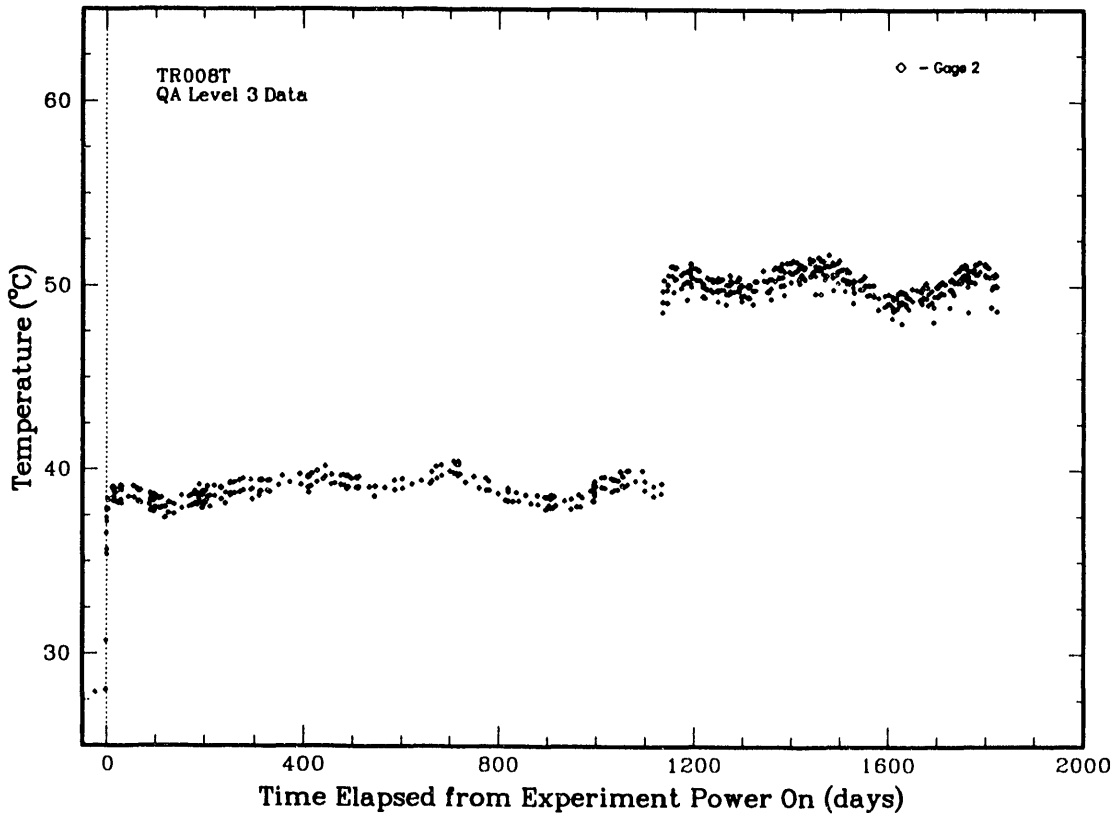

Figure 5.2-8a Heater-Thermocouple TR008T-2 Temperature History

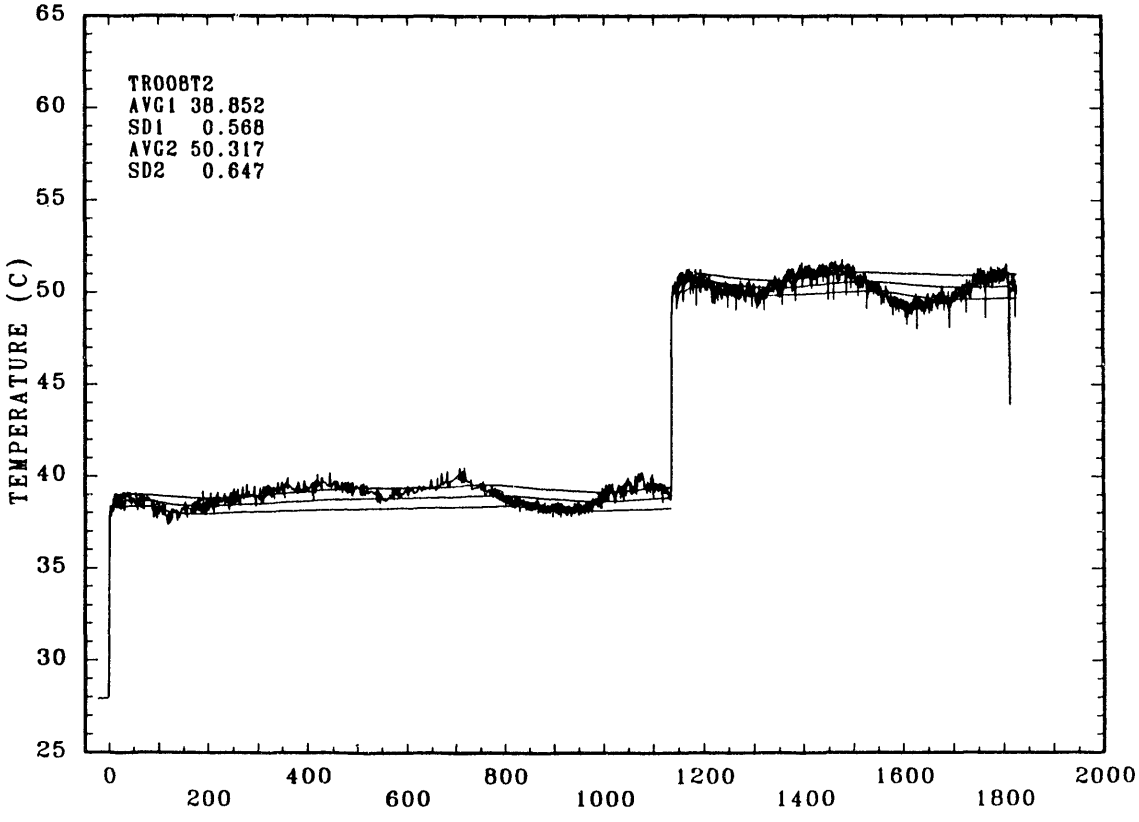

Figure 5.2-8b Heater-Thermocouple TR008-2 Calculated Temperature Averages

5.3 Borehole Near-Field Temperature Histories

We measured temperatures on the top surface of each RH TRU test borehole, at the rock salt-air interface, with one to three borehole "near-field" thermocouples. These TCs are designated as TRH81X, TRH82X, and TRH83X, where "X" represents test container 1 through 8. These three near-field thermocouples are located directly above (about 15 cm, 6 in., initially, above) the similarly designated heater-container TCs, TR00XT-1, -2, and -3, as described in Section 5.2. Thermocouples TR82X are located above the mid-length of each container. Thermocouples TRH81X and TRH83X are present in test emplacements TRH01 through TRH04 only. The exact test-room coordinates of each near-field TC are listed in **Table 3.5,** the instrumentation NOS file. The locations of each near-field TC, relative to each test emplacement and borehole, are shown in **Figures 3.5-1** through **3.5-8.**

The near-field thermocouple temperature data histories of each RH TRU test emplacement are illustrated in **Figures 5.3-1a** through **53-8a** for tests TRH01 through TRH08, respectively. The corresponding calculated temperature running averages and standard deviations are illustrated in **Figures 5.3-1b,c,d,e,f** through **5.3-8b,c,d,e,f**. We calculated the average values and standard deviations of all temperature data points, not "sieved" data, with the GRAFAID analysis tool (Adams, 1985).

The average temperature values for each near-field thermocouple, plus or minus calculated standard deviations, are listed in **Table 5.3.** Temperature are listed for the distinct (heater power-level) time periods of 0 through 1,135 days and 3.1 through 5.0 years (1,135 through 1,826 days). The GRAFAID calculations covered the time period of 20 to 1,135 days after test turn-on, and, independently, 1,155 to 1,826 days. The initial 20-day segment of each time period was not included, in order to minimize any effects of the initial heat-up period(s) on calculated, "steady state" averages. These calculated "averages" must be evaluated with some care. There appears to be a slight increase in temperatures as a function of time. There is also an obvious cyclical nature to the observed temperature histories. This observed temperature periodicity is discussed and interpreted in Section 7.1.3.

Table 5.3. RH TRU Near-Field Temperature Values, °C

Test Container X: (= 1 - 8)	0 to 1,135 Days 0 to 3.1 Years			3.1 to 5.0 Years		
	TRH81X (TR80X-1)	TRH82X (TR80X-2)	TRH83X (TR80X-3)	TRH81X (TR80X-1)	TRH82X (TR80X-2)	TRH83X (TR80X-3)
TRH01:	31.32 ± 0.65°	31.23 ± 0.95°	31.08 ± 0.56°	35.42 ± 0.77°	35.34 ± 0.70°	34.92 ± 0.70°
TRH02:	31.24 ± 0.70°	31.11 ± 0.61°	31.09 ± 0.57°	35.35 ± 1.00°	34.88 ± 0.81°	34.75 ± 0.81°
TRH03:	32.13 ± 0.56°	32.28 ± 0.49°	32.11 ± 0.45°	36.81 ± 0.75°	37.70 ± 0.66°	37.42 ± 0.57°
TRH04:	32.25 ± 0.59°	32.26 ± 0.46°	31.75 ± 0.43°	36.84 ± 0.83°	37.14 ± 0.70°	36.01 ± 0.60°
TRH05:		31.95 ± 0.50°			37.41 ± 0.68°	
TRH06:		32.08 ± 0.46°			37.07 ± 0.70°	
TRH07:		31.41 ± 0.55°			35.14 ± 0.55°	
TRH08:		31.58 ± 0.46°			35.52 ± 0.58°	

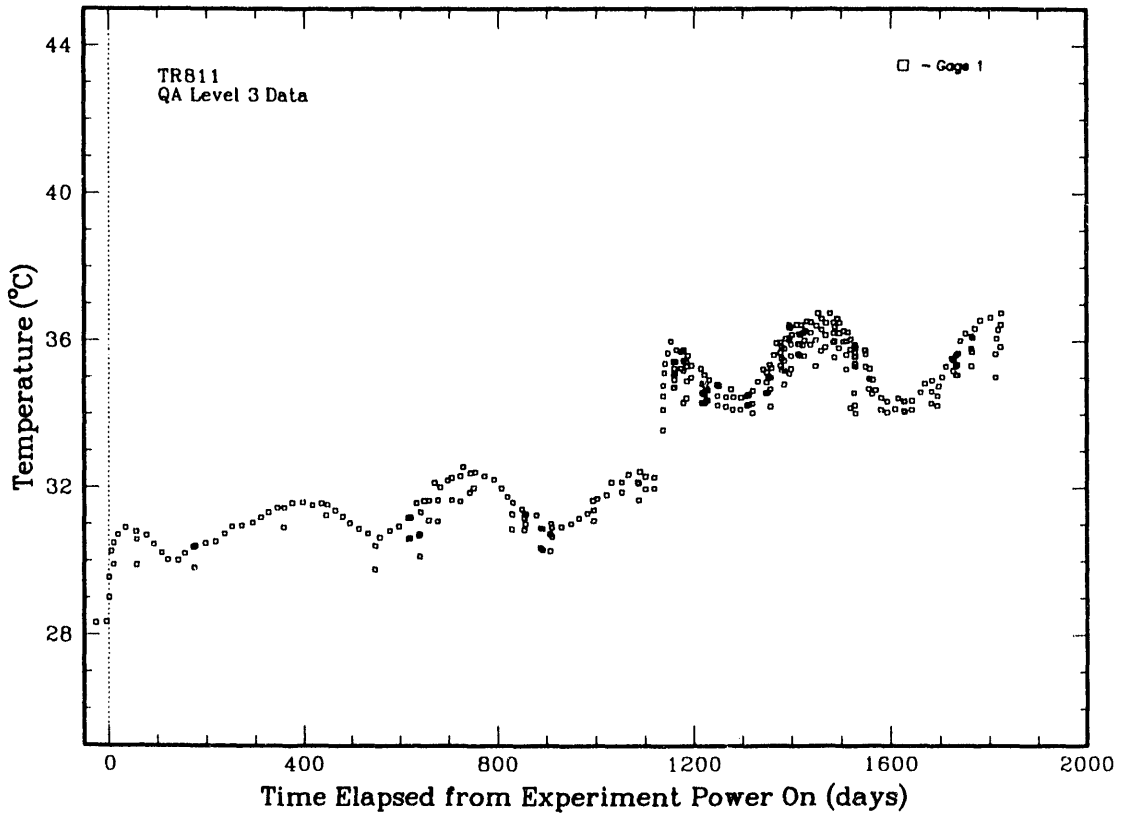

Figure 5.3-1a Near-Field Thermocouple TRH811 Temperature History (TRH01)

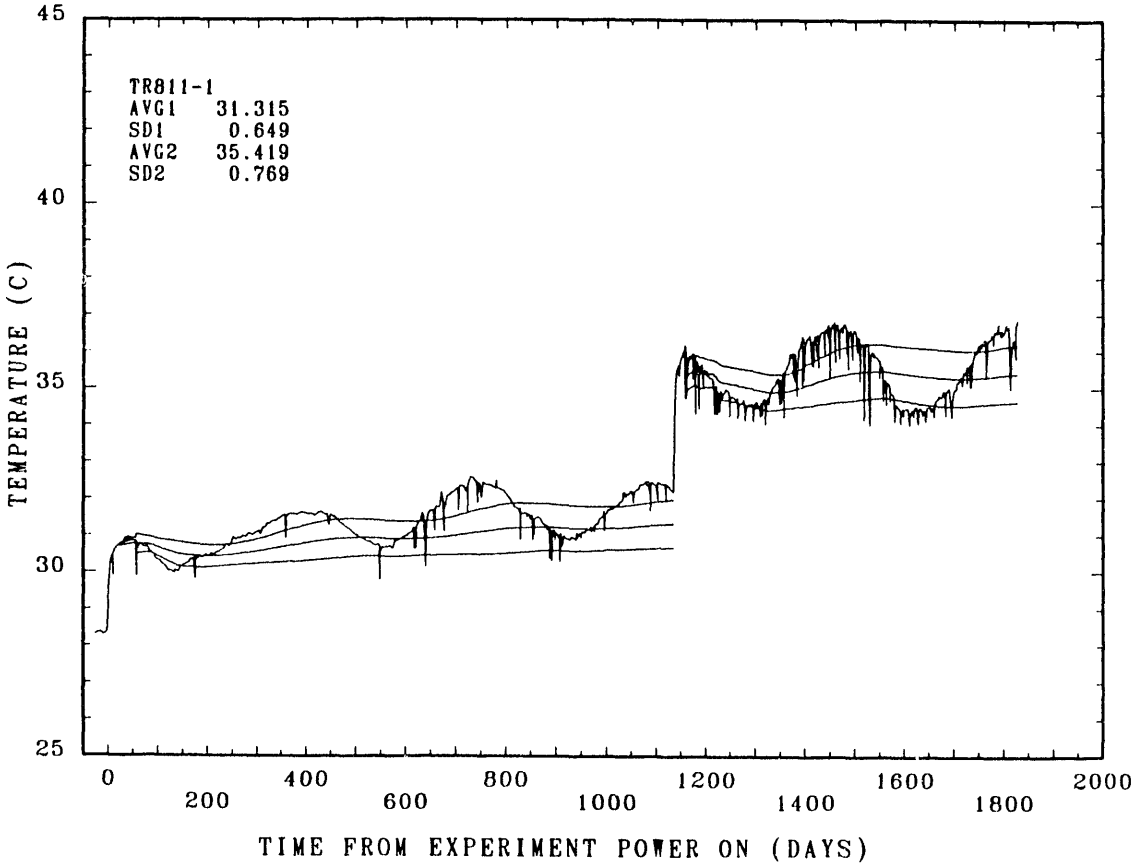

Figure 5.3-1b Near-Field Thermocouple TRH811 Calculated Temperature Averages

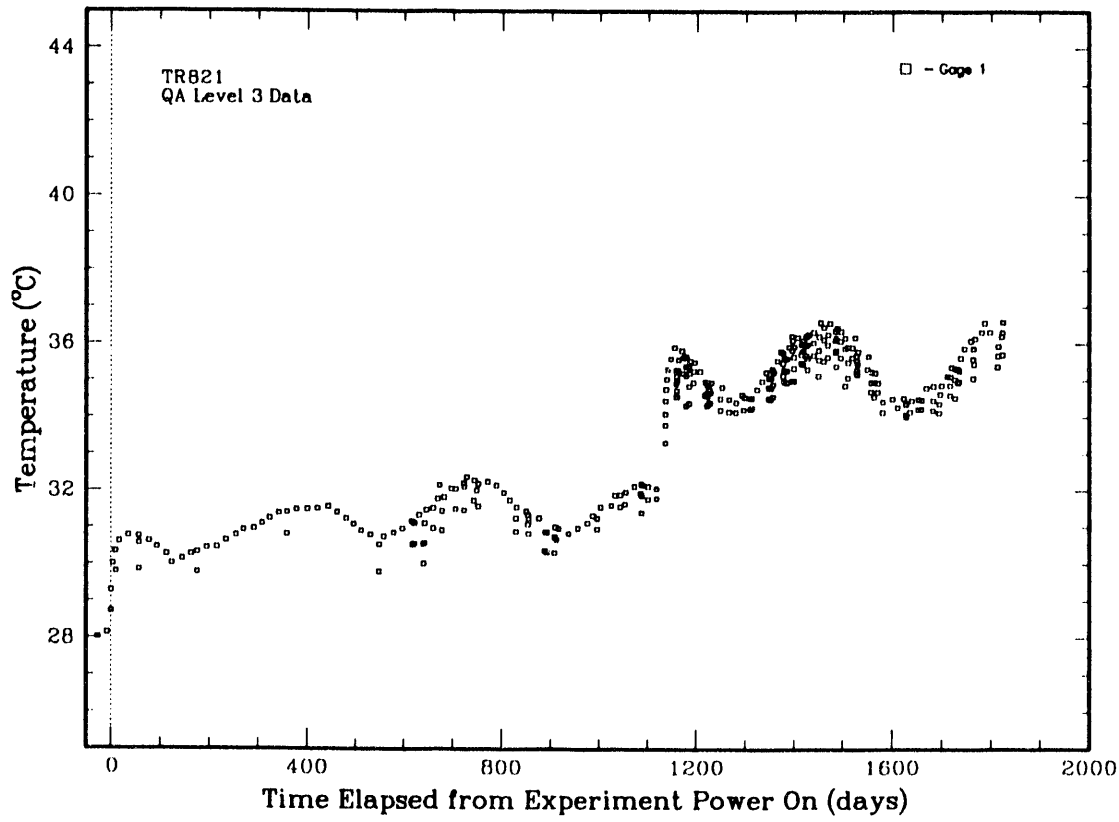

Figure 5.3-1c Near-Field Thermocouple TRH821 Temperature History (TRH01)

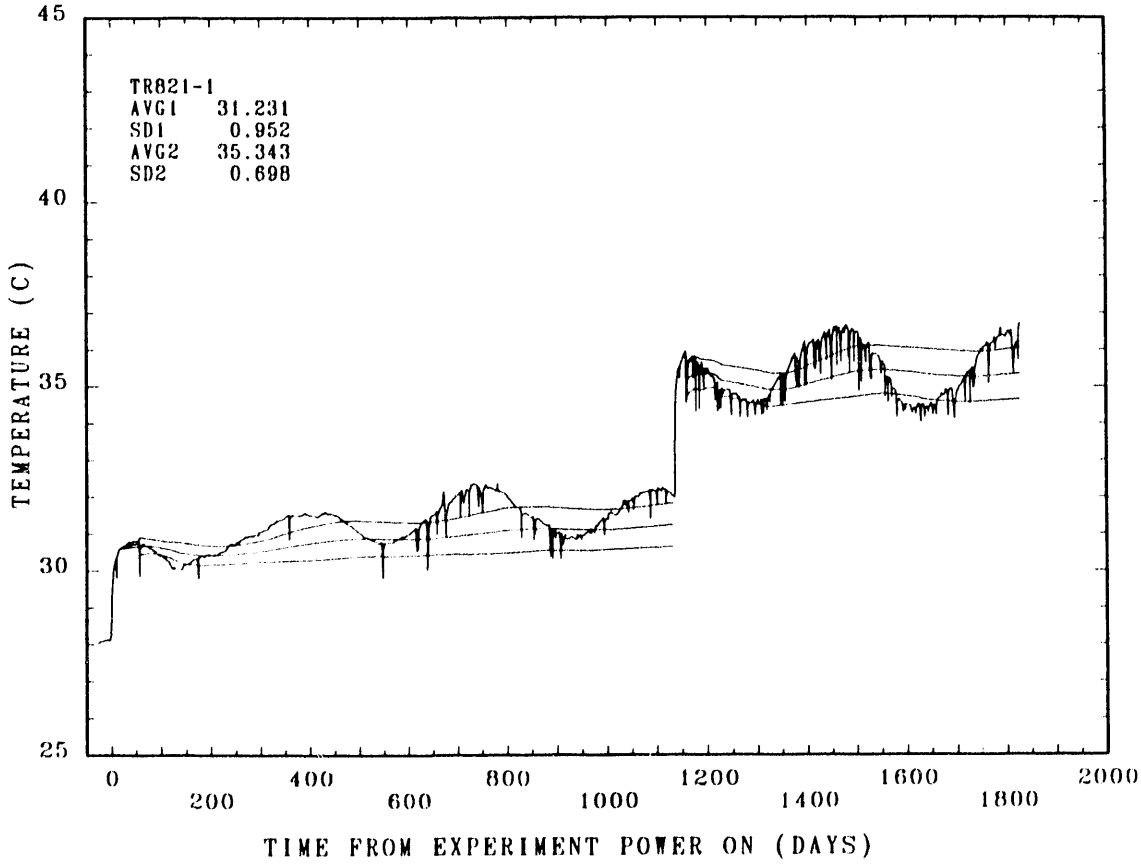

Figure 5.3-1d Near-Field Thermocouple TRH821 Calculated Temperature Averages

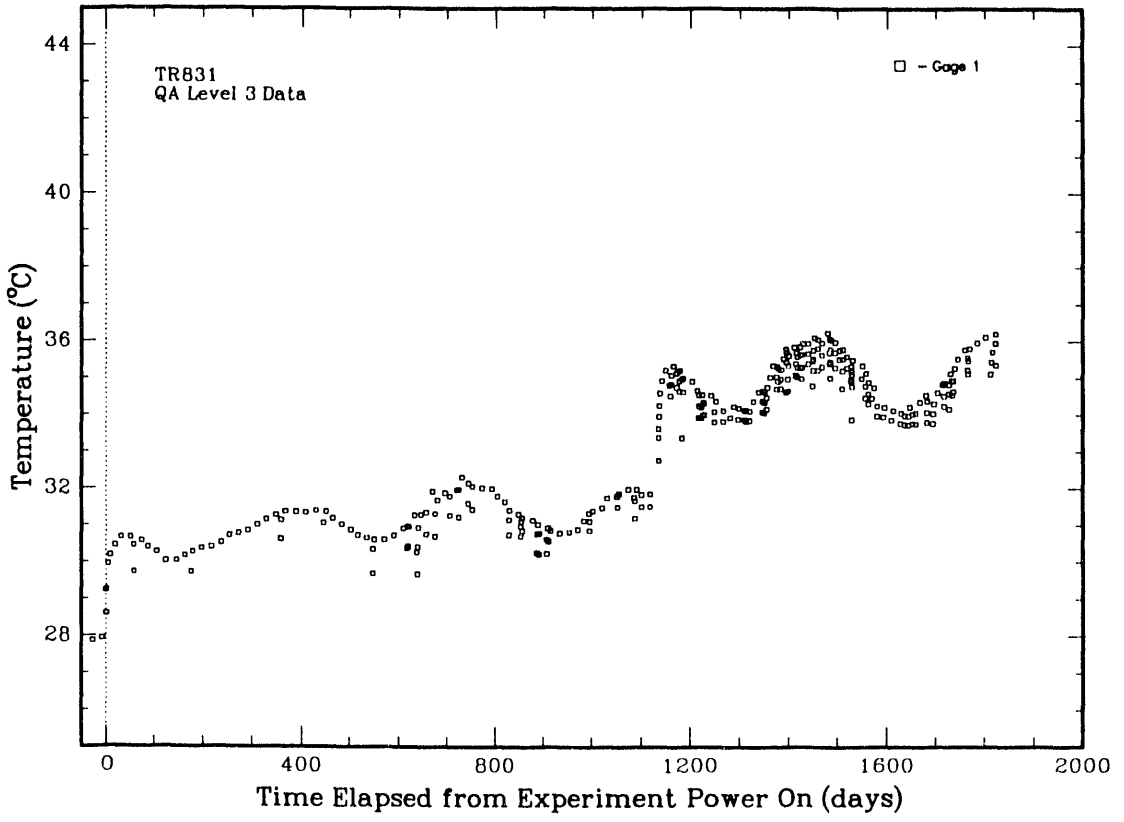

Figure 5.3-1e Near-Field Thermocouple TRH831 Temperature History (TRH01)

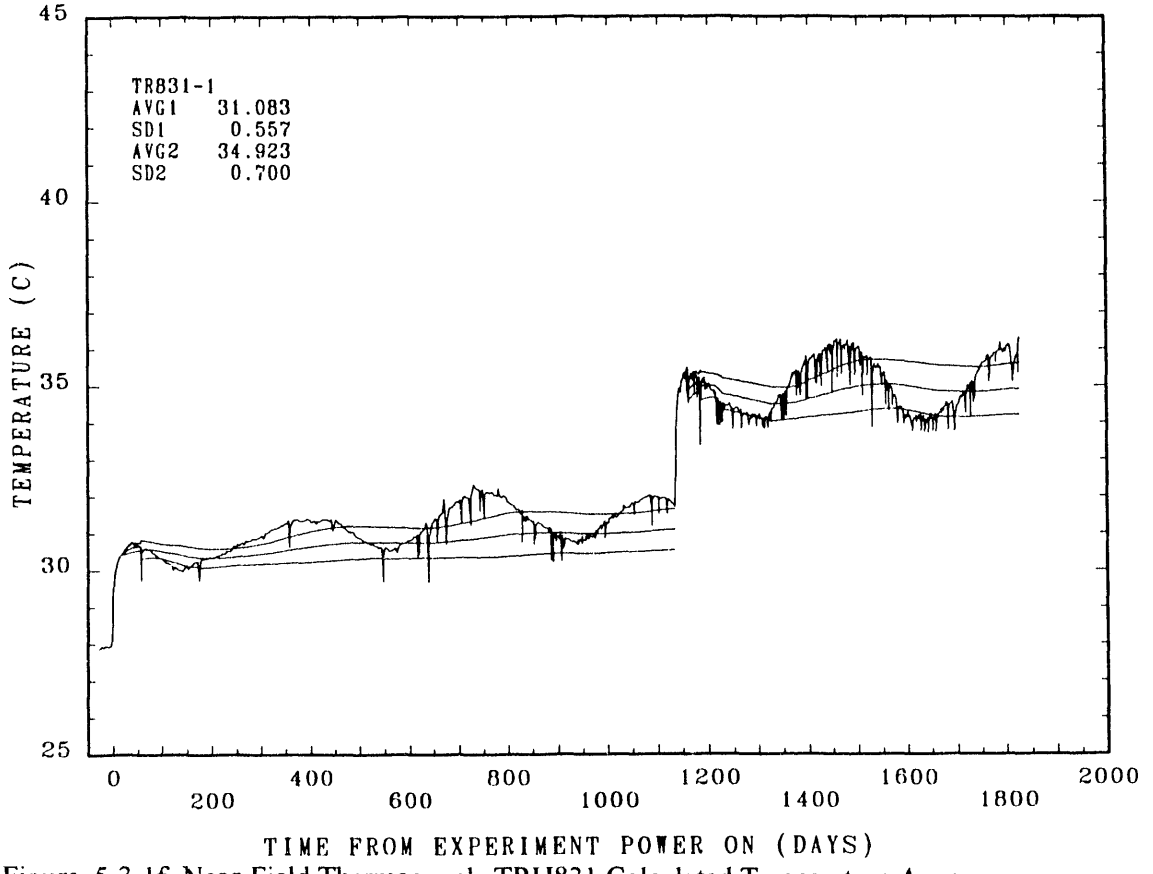

Figure 5.3-1f Near-Field Thermocouple TRH831 Calculated Temperature Averages

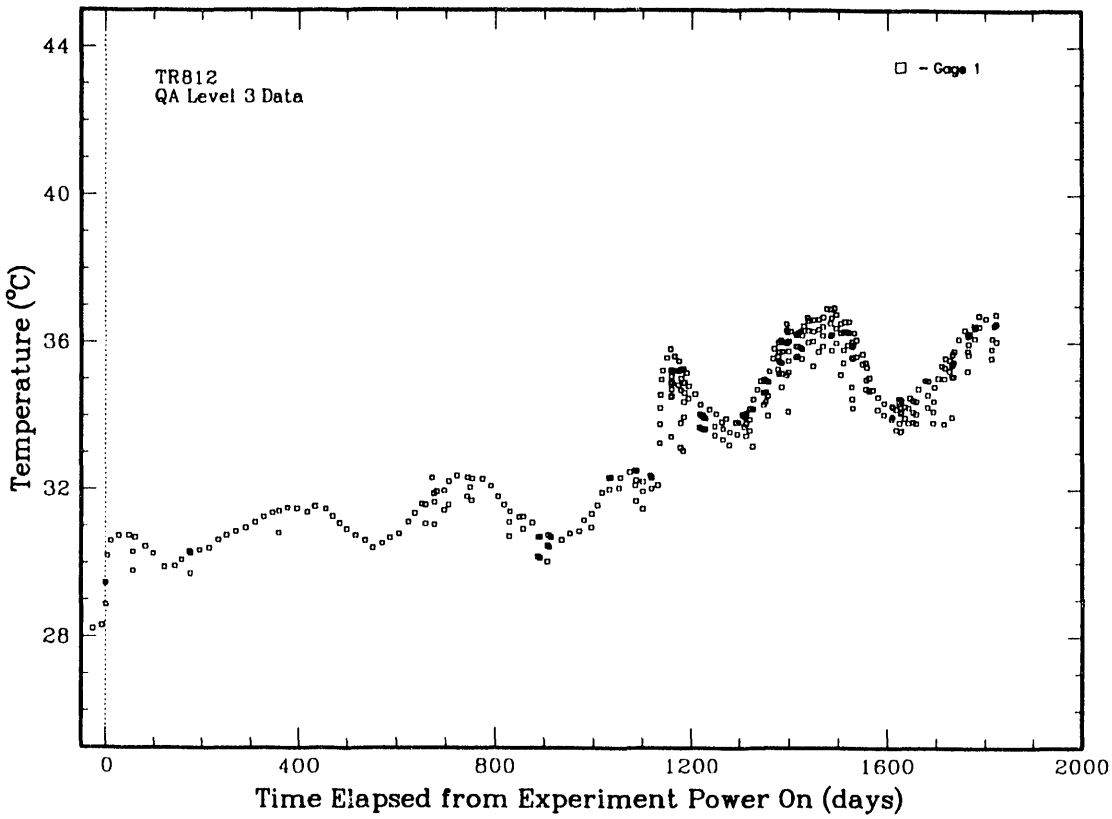

Figure 5.3-2a Near-Field Thermocouple TRH812 Temperature History (TRH02)

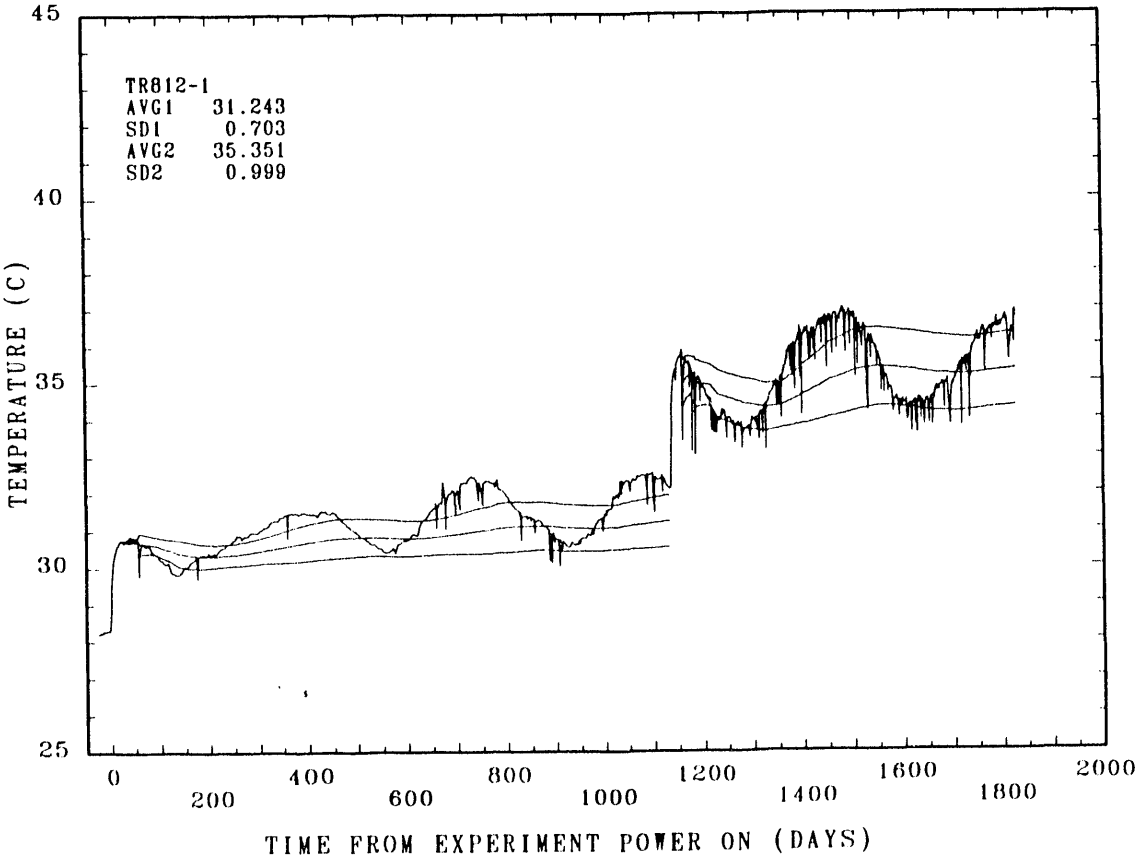

Figure 5.3-2b Near-Field Thermocouple TRH812 Calculated Temperature Averages

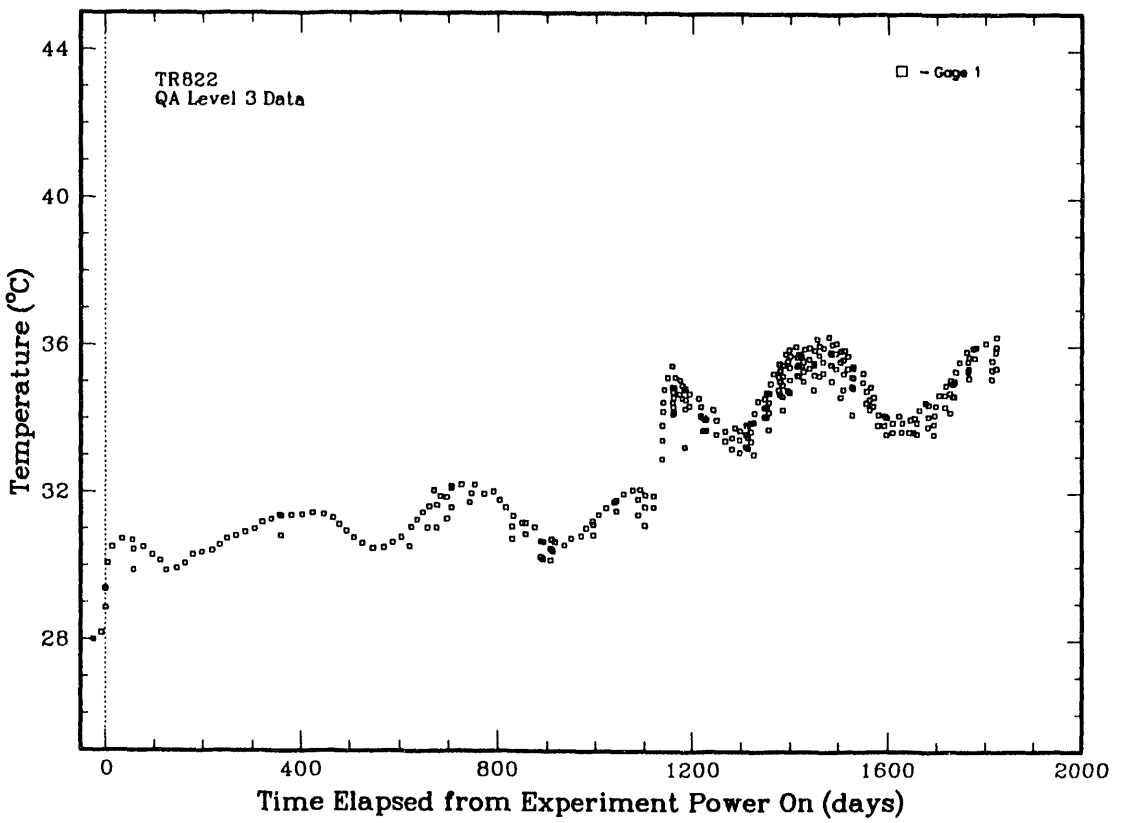

Figure 5.3-2c Near-Field Thermocouple TRH822 Temperature History (TRH02)

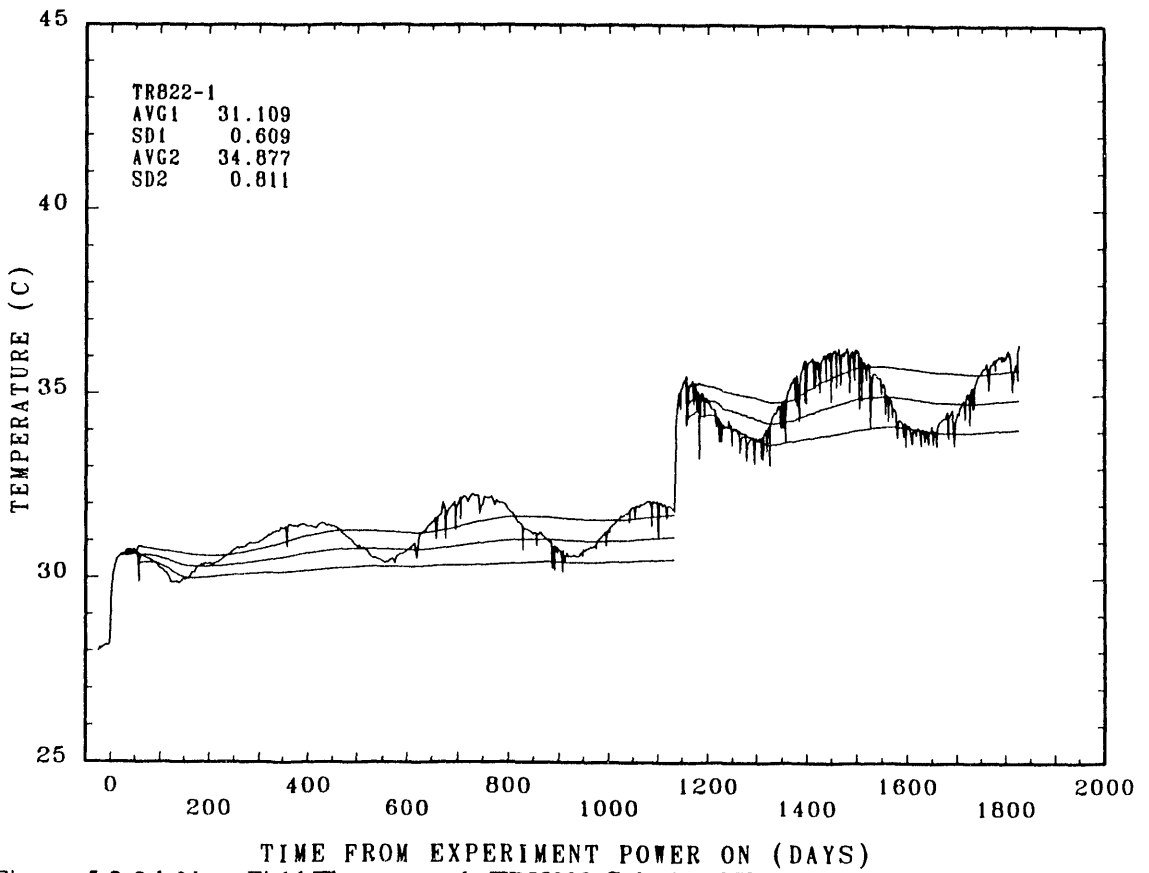

Figure 5.3-2d Near-Field Thermocouple TRH822 Calculated Temperature Averages

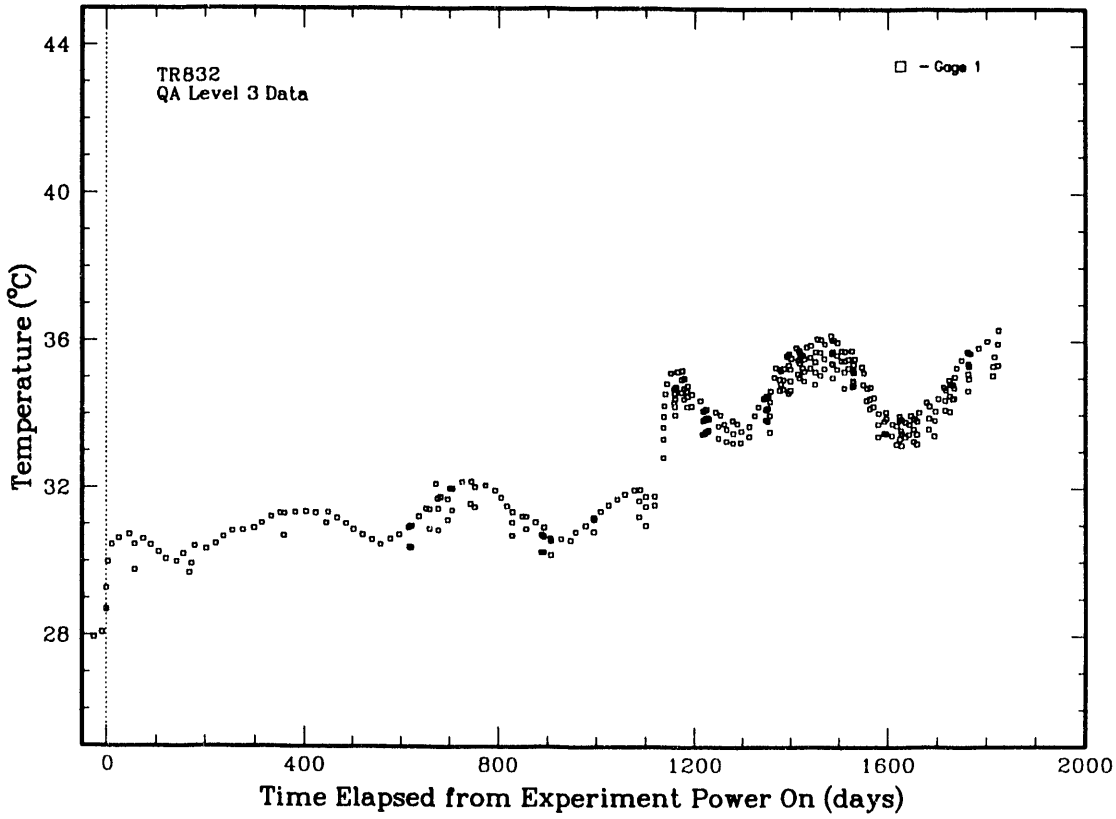

Figure 5.3-2e Near-Field Thermocouple TRH832 Temperature History (TRH02)

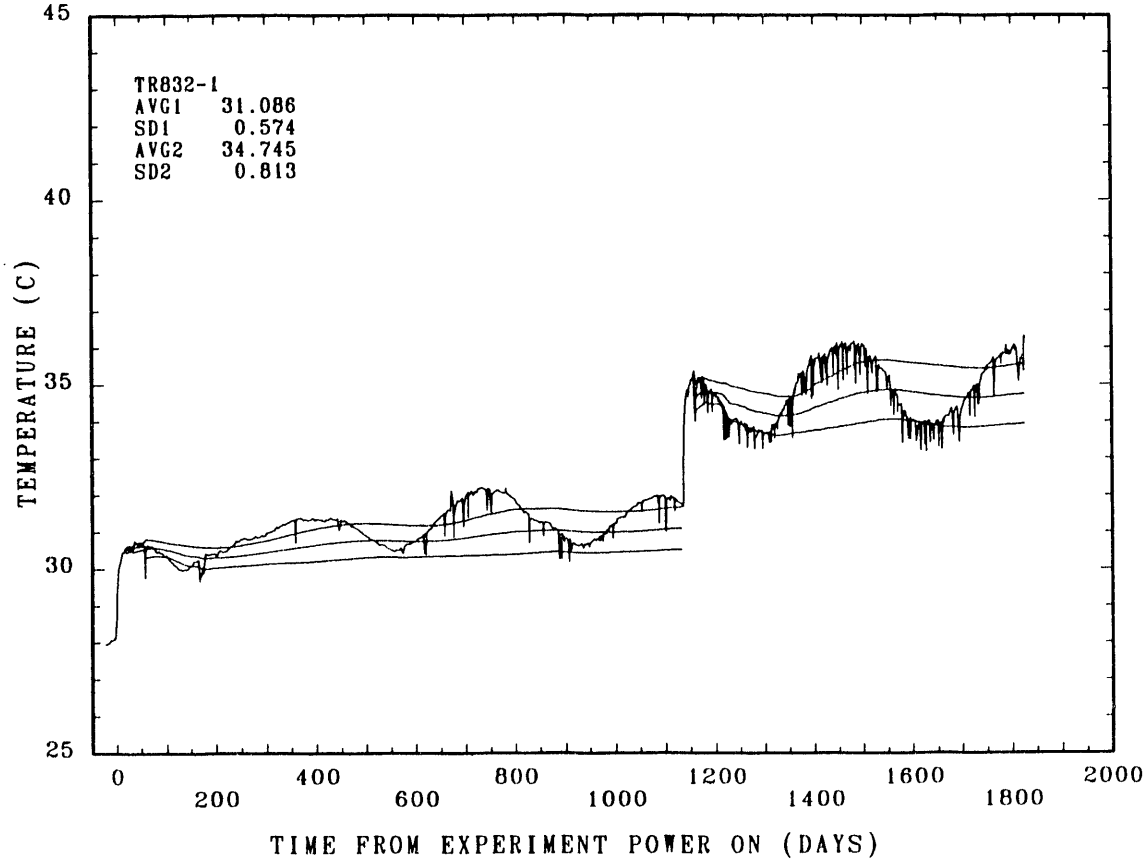

Figure 5.3-2f Near-Field Thermocouple TRH832 Calculated Temperature Averages

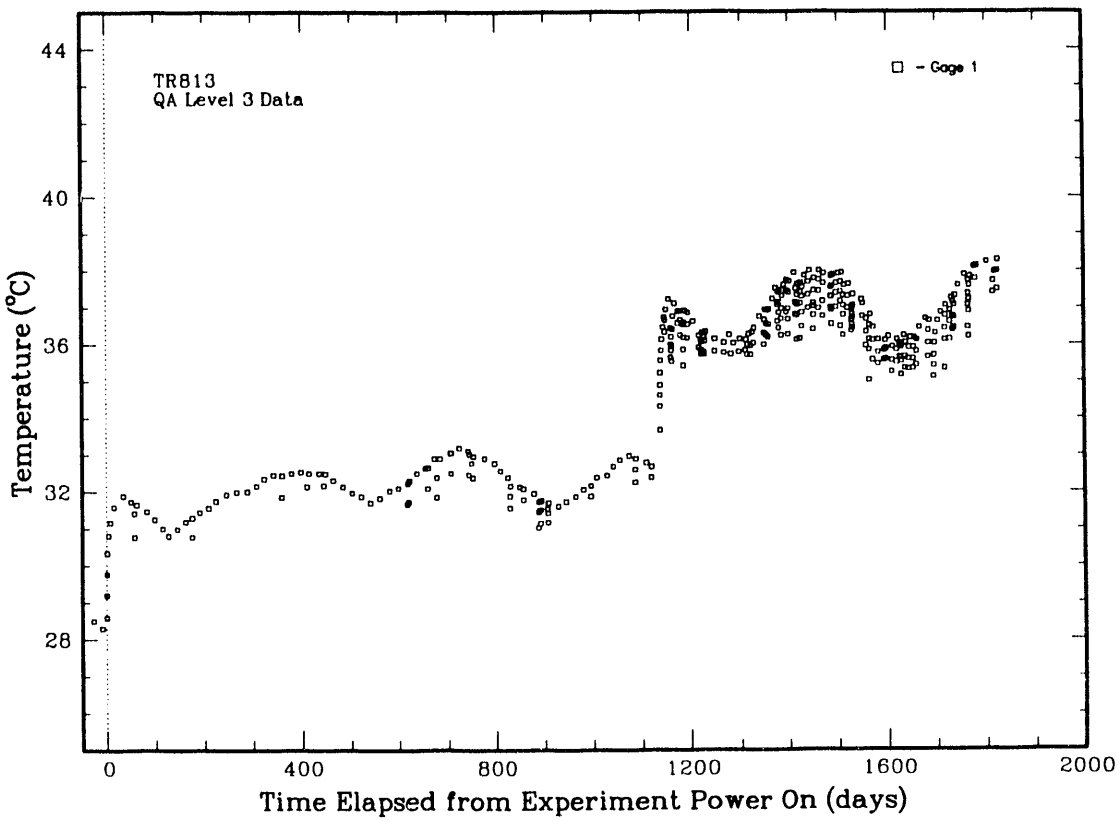

Figure 5.3-3a Near-Field Thermocouple TRH813 Temperature History (TRH03)

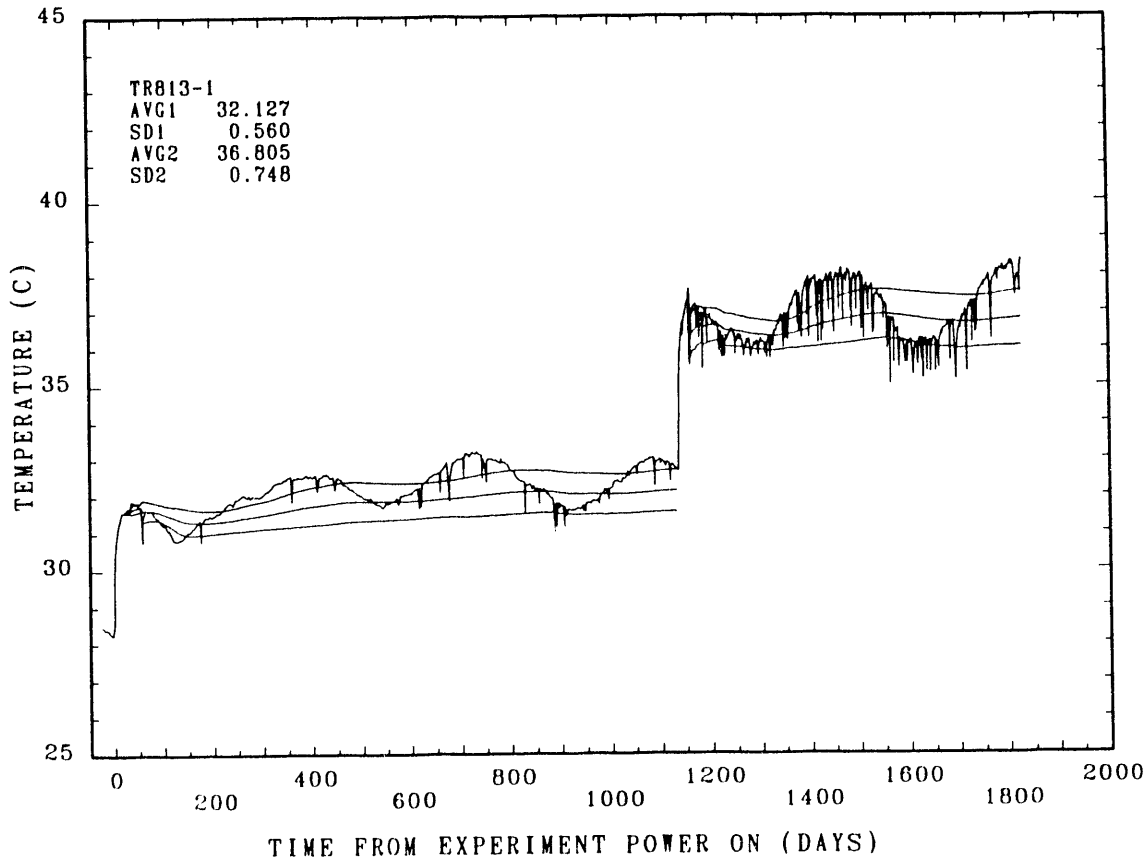

Figure 5.3-3b Near-Field Thermocouple TRH813 Calculated Temperature Averages

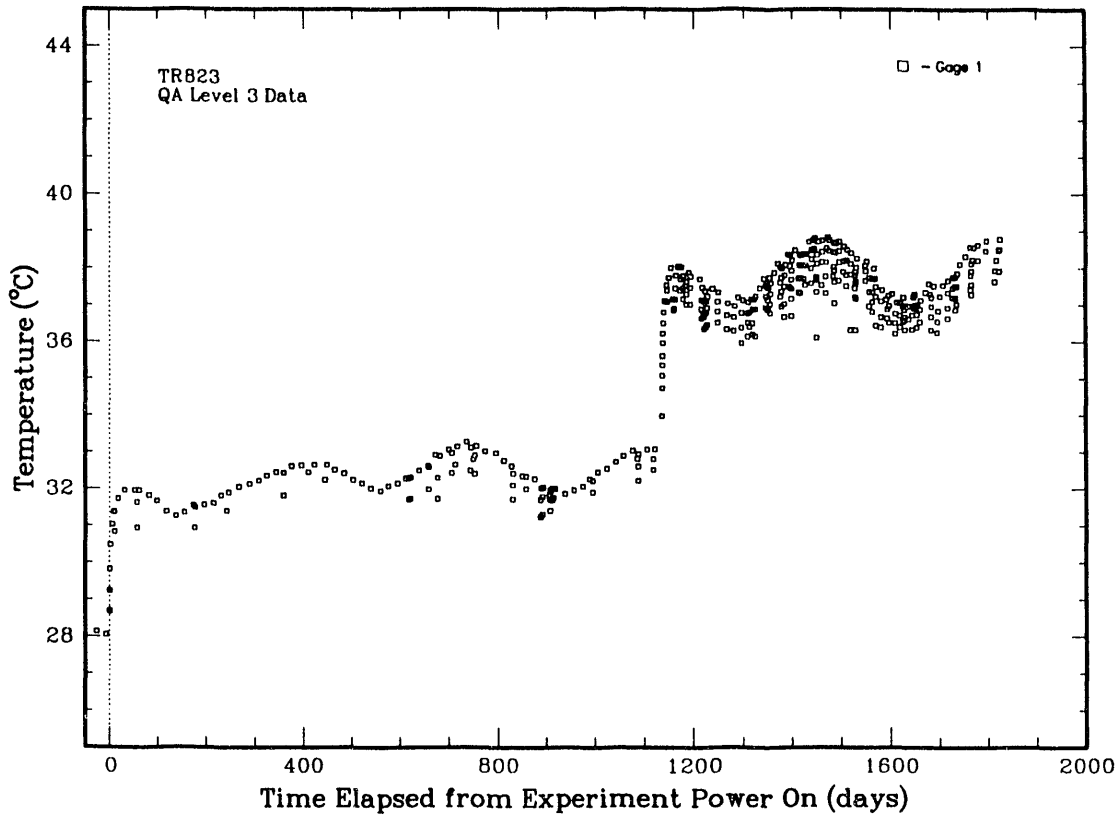

Figure 5.3-3c Near-Field Thermocouple TRH823 Temperature History (TRH03)

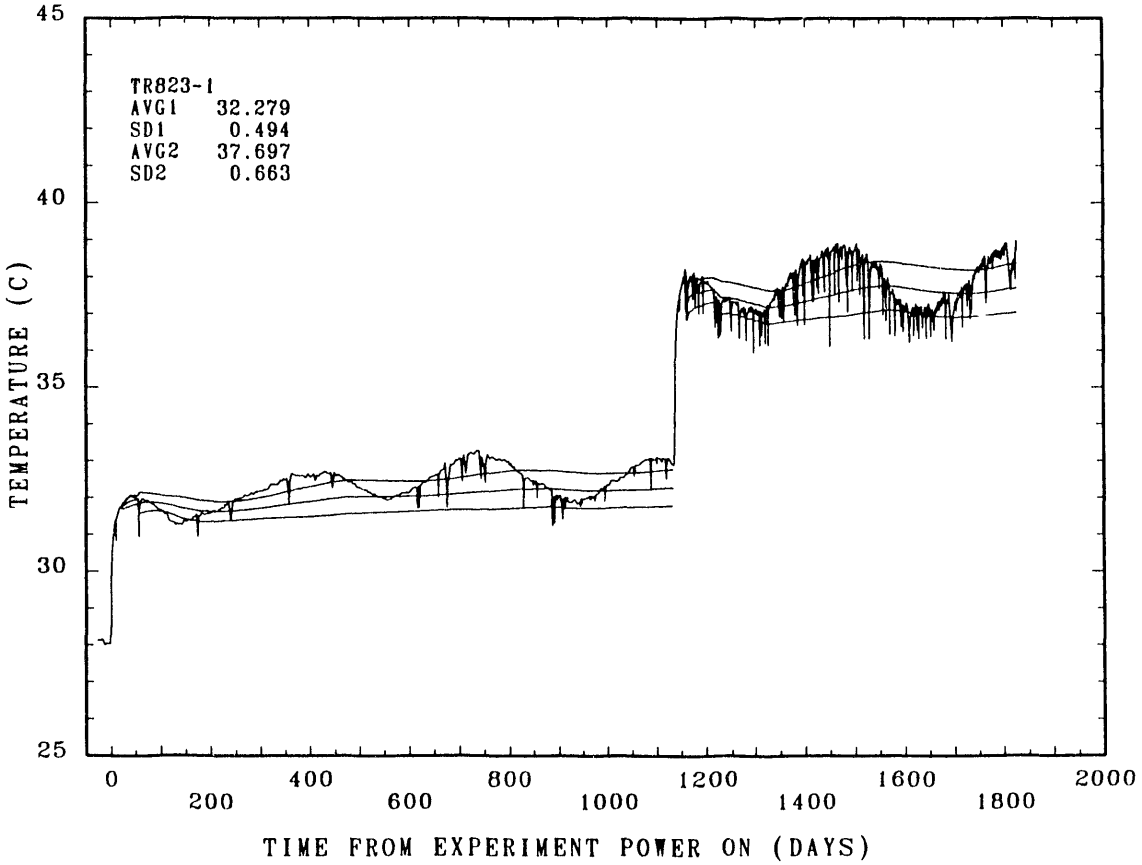

Figure 5.3-3d Near-Field Thermocouple TRH823 Calculated Temperature Averages

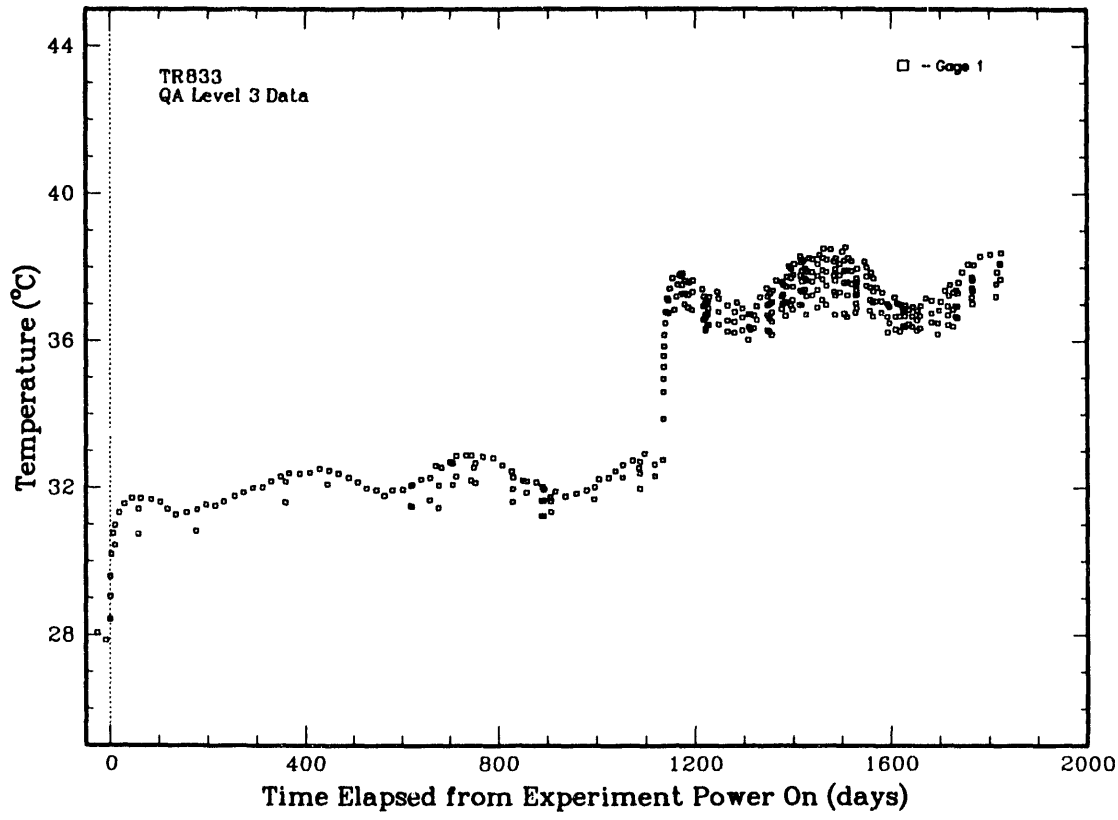

Figure 5.3-3e Near-Field Thermocouple TRH833 Temperature History (TRH03)

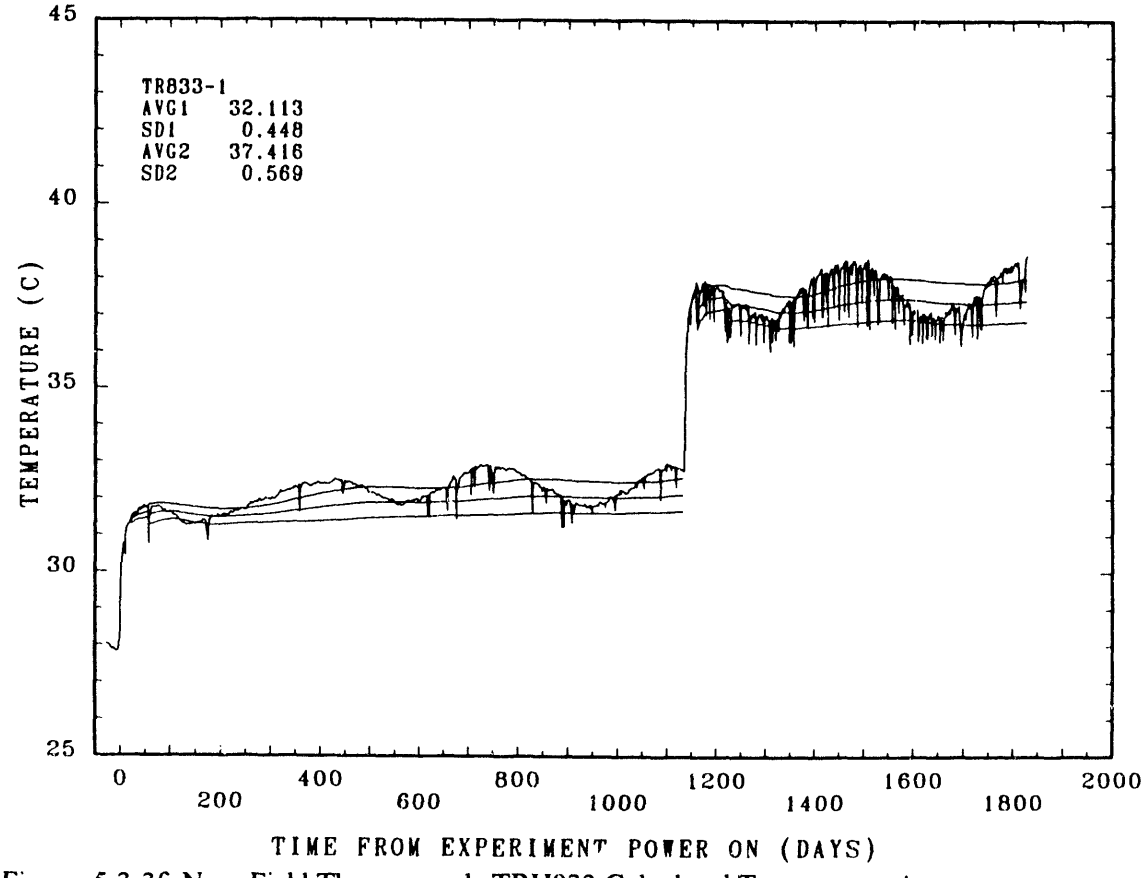

Figure 5.3-3f Near-Field Thermocouple TRH833 Calculated Temperature Averages

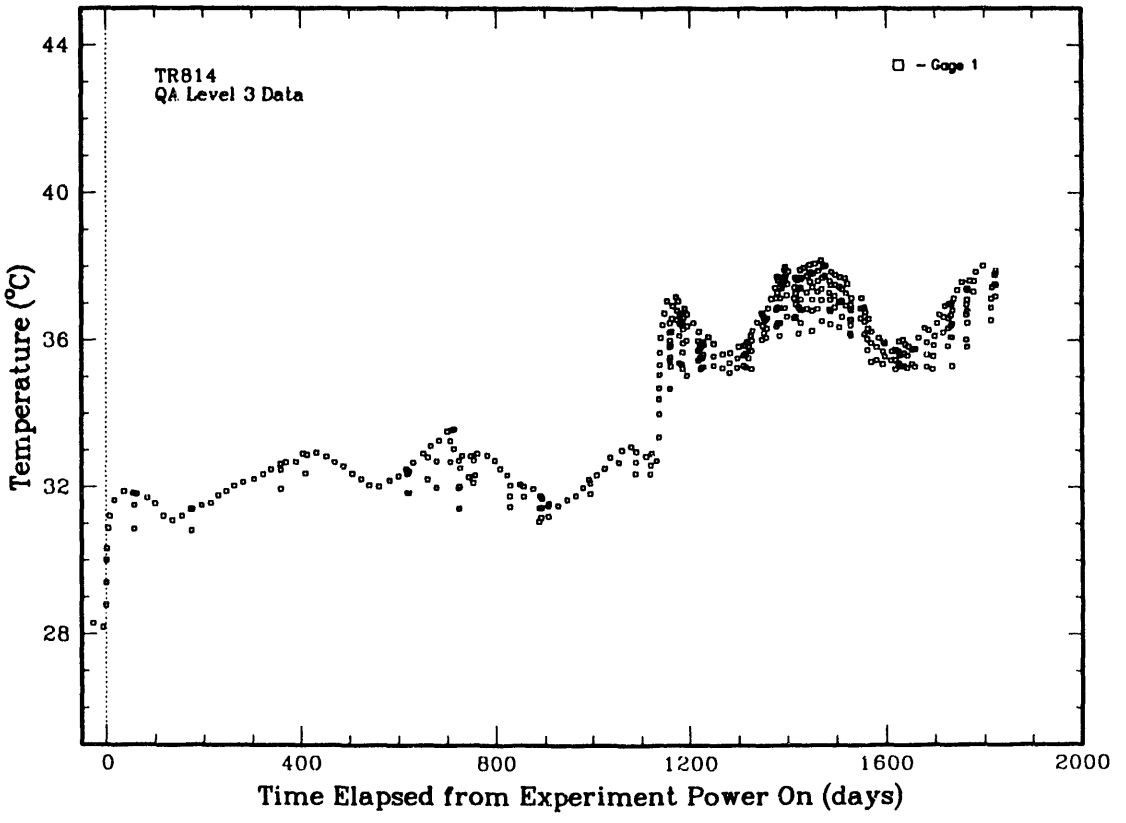

Figure 5.3-4a Near-Field Thermocouple TRH814 Temperature History (TRH04)

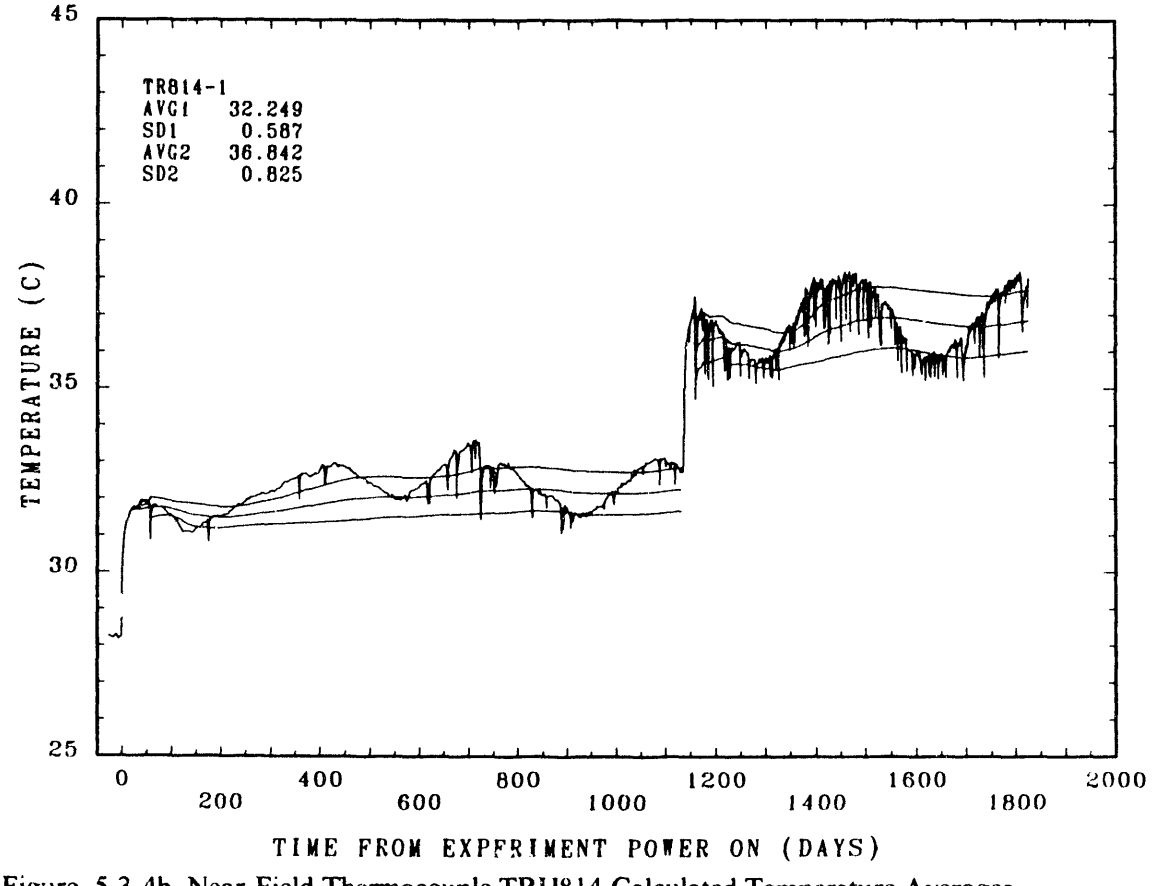

Figure 5.3-4b Near-Field Thermocouple TRH814 Calculated Temperature Averages

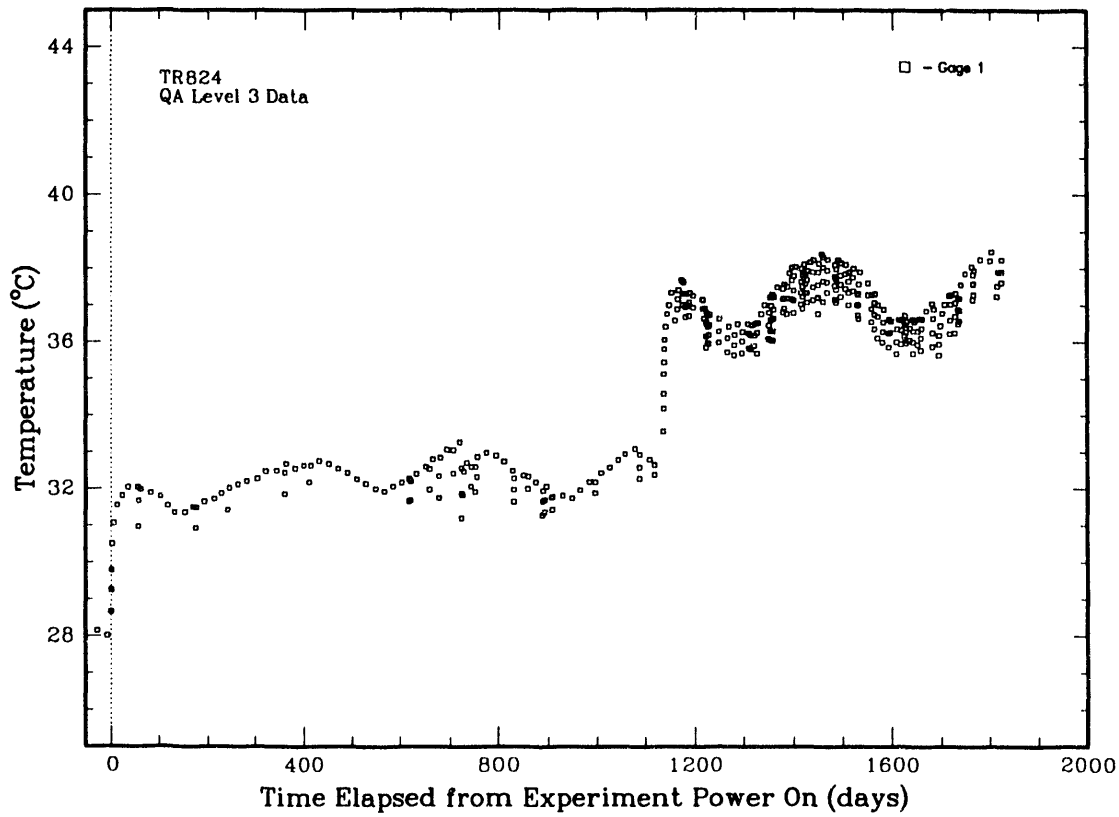

Figure 5.3-4c Near-Field Thermocouple TRH824 Temperature History (TRH04)

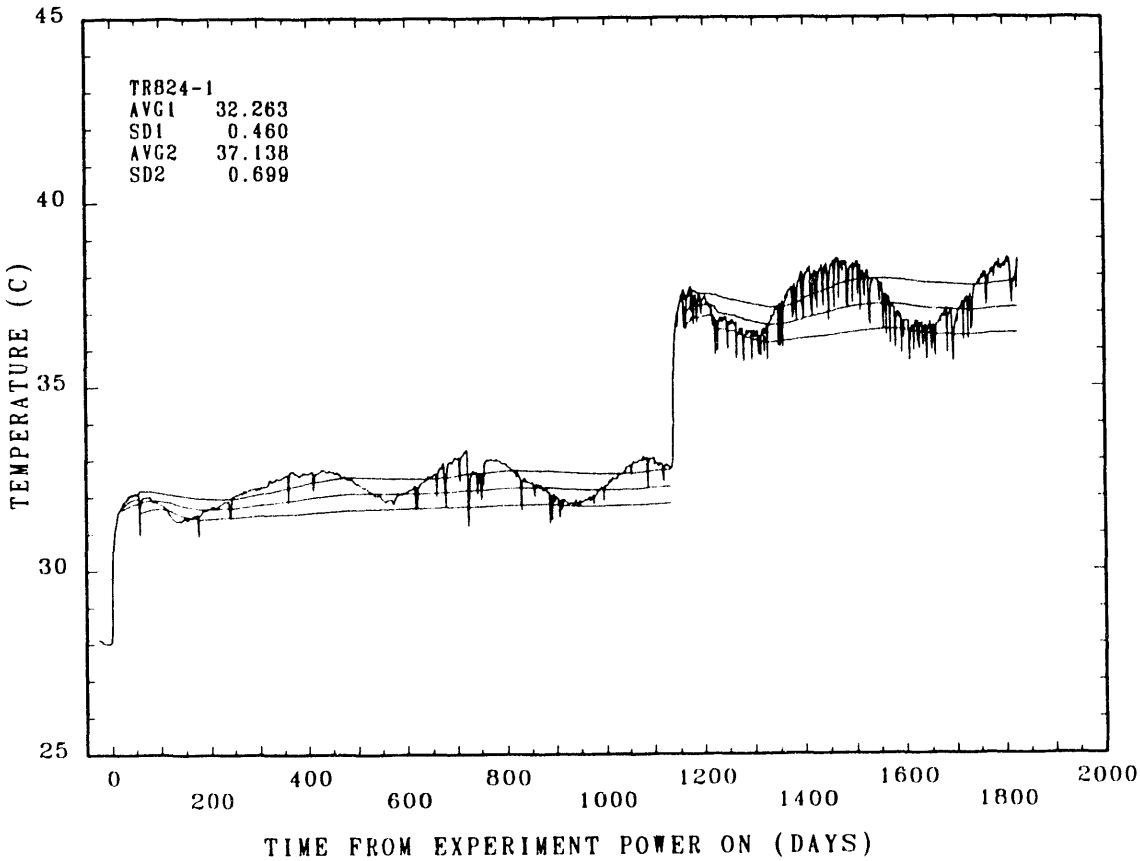

Figure 5.3-4d Near-Field Thermocouple TRH824 Calculated Temperature Averages

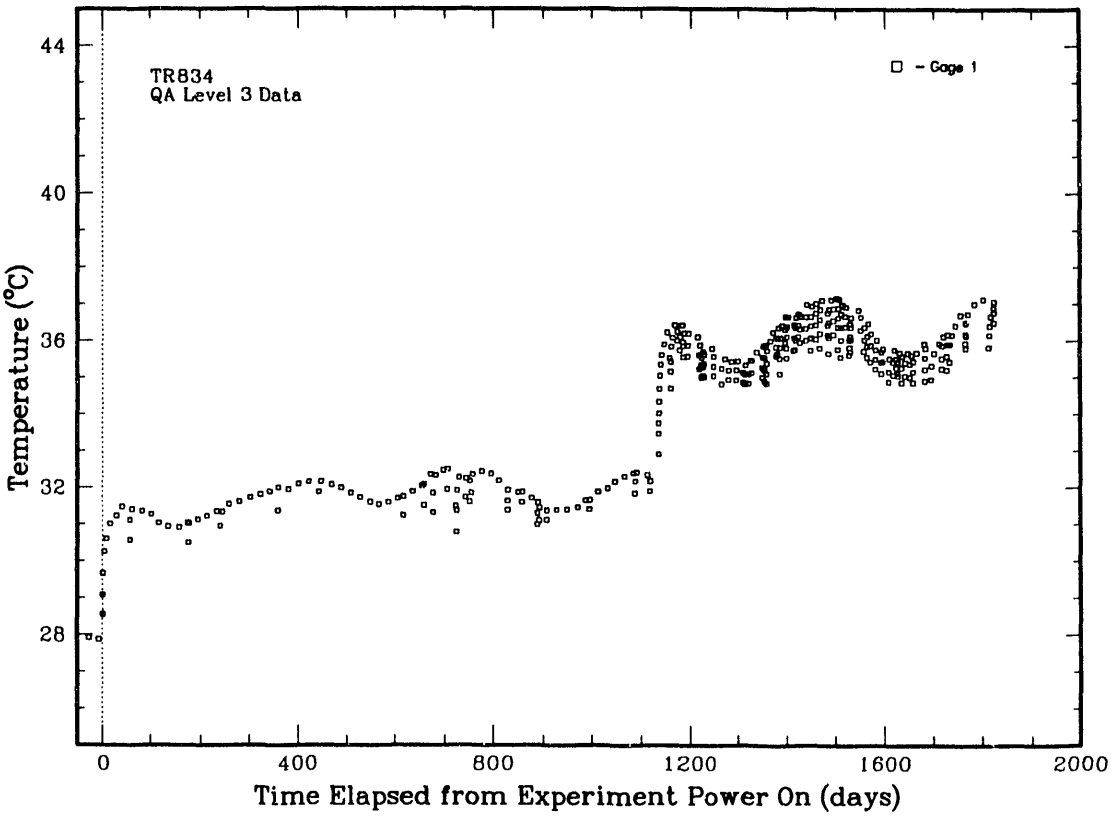

Figure 5.3-4e Near-Field Thermocouple TRH834 Temperature History (TRH04)

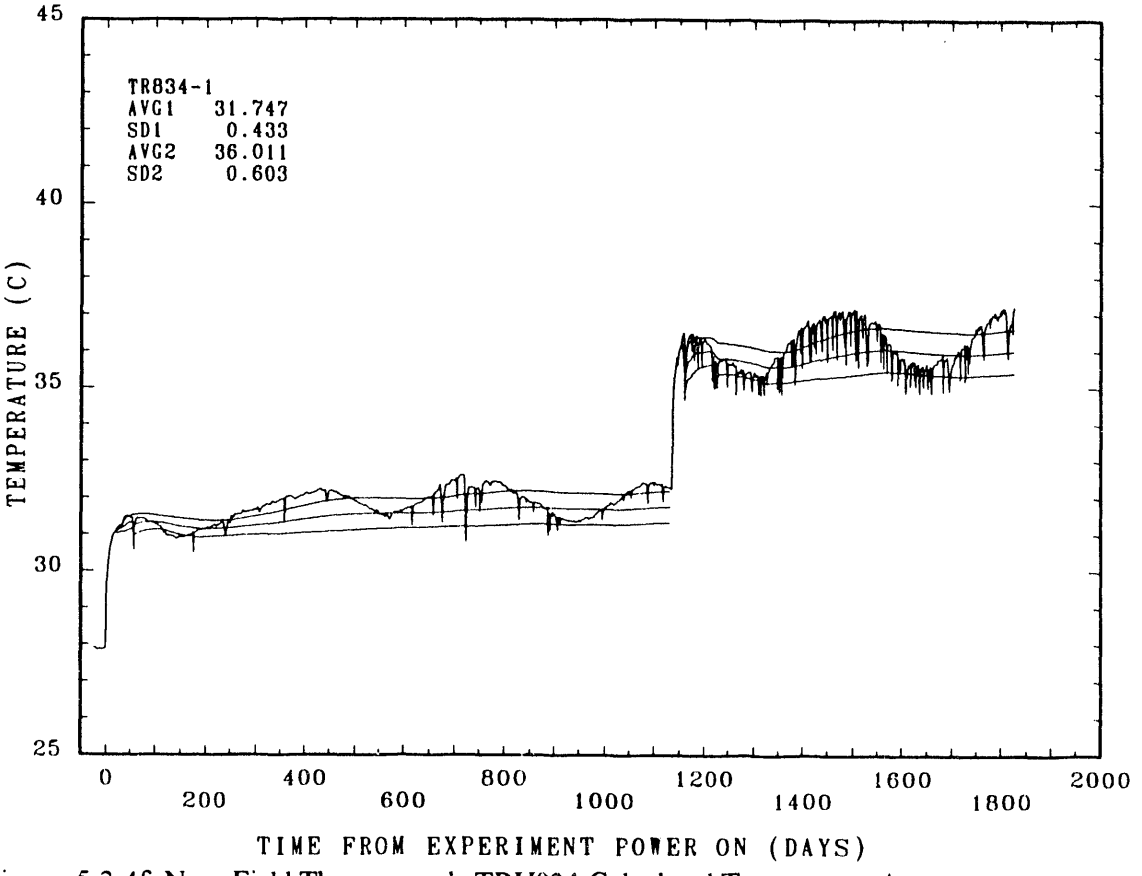

Figure 5.3-4f Near-Field Thermocouple TRH834 Calculated Temperature Averages

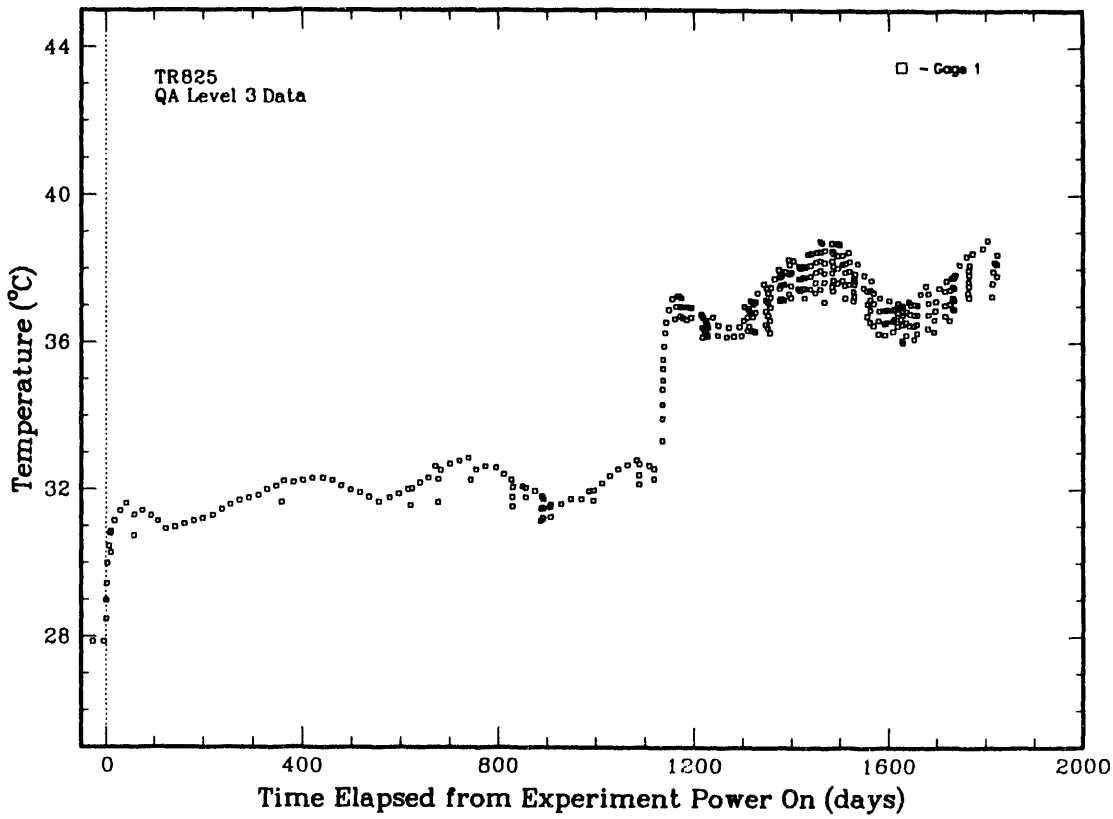

Figure 5.3-5a Near-Field Thermocouple TRH825 Temperature History (TRH05)

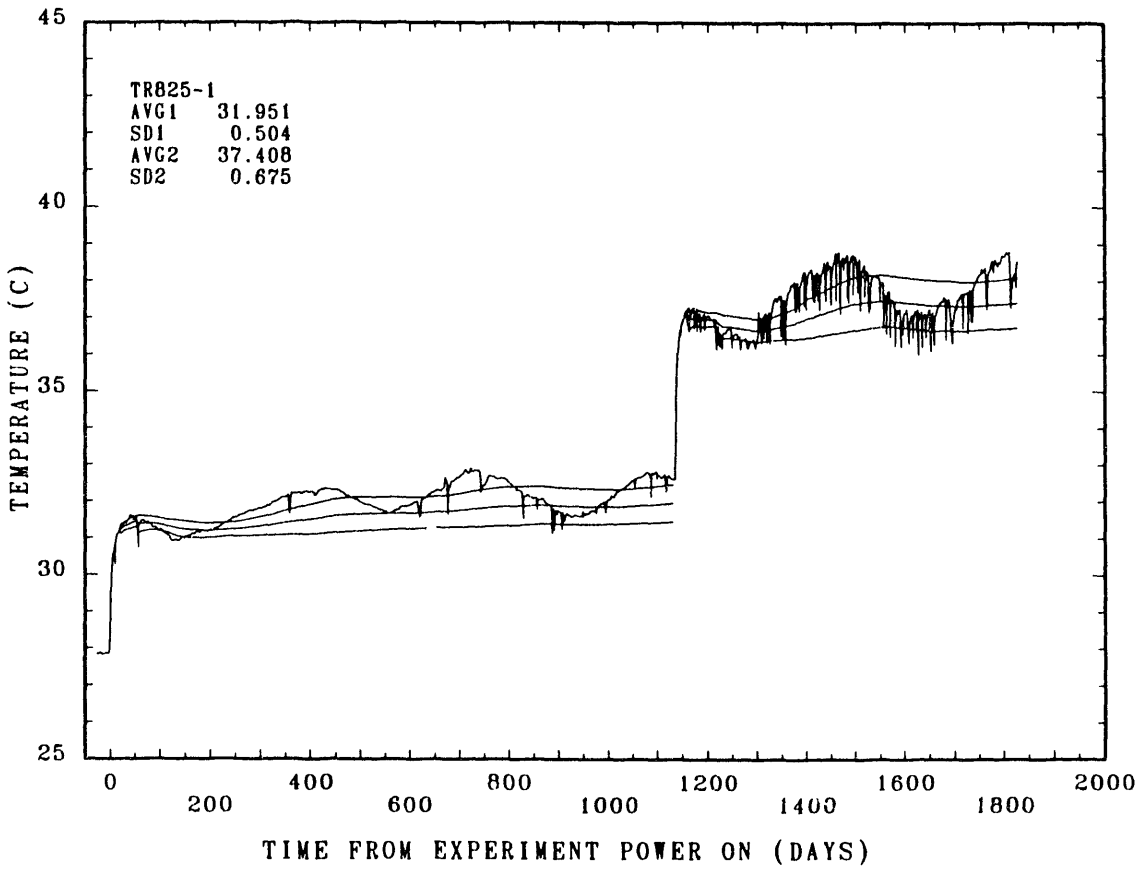

Figure 5.3-5b Near-Field Thermocouple TRH825 Calculated Temperature Averages

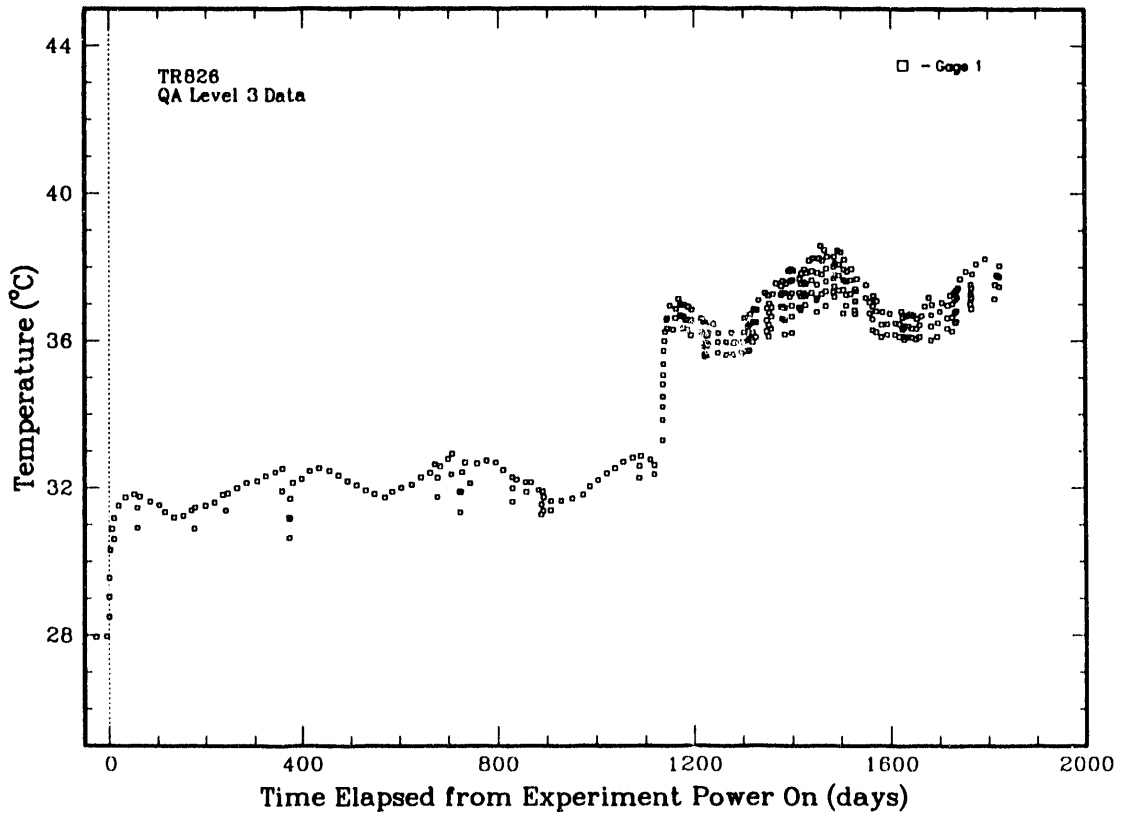

Figure 5.3-6a Near-Field Thermocouple TRH826 Temperature History (TRH06)

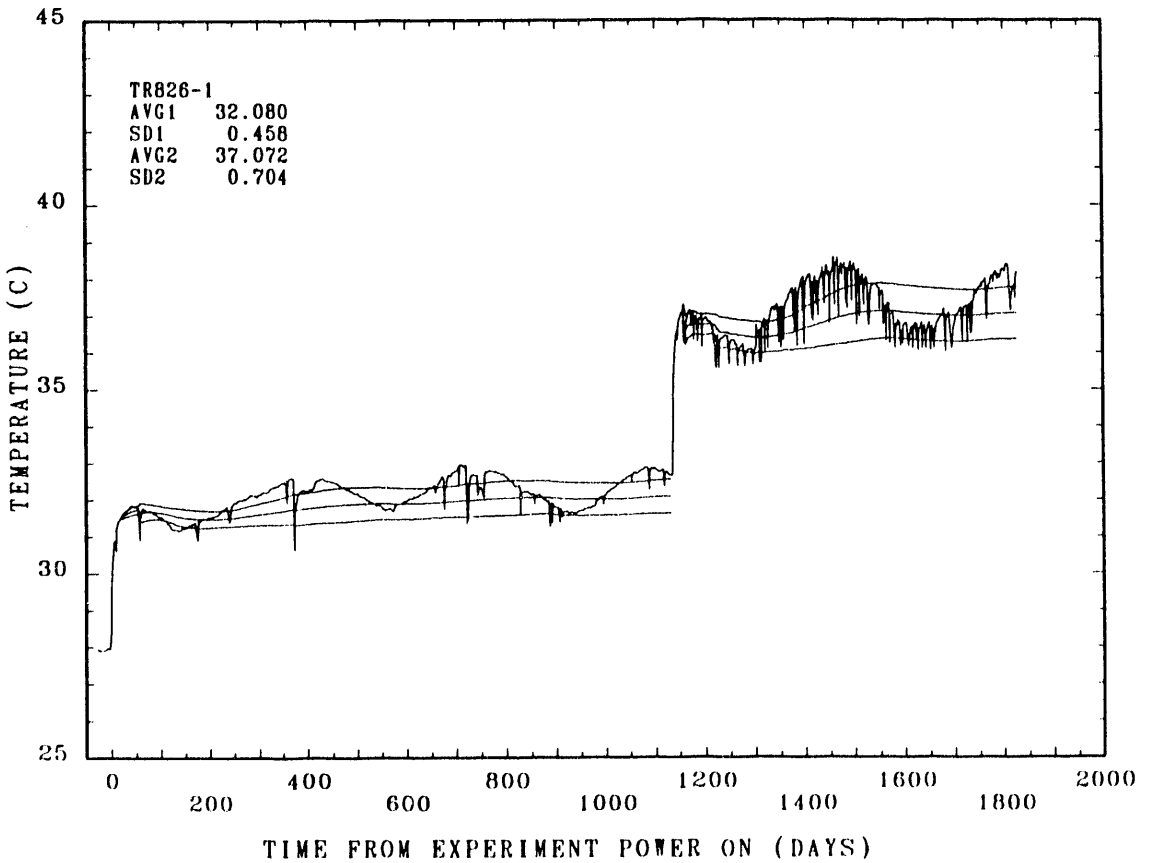

Figure 5.3-6b Near-Field Thermocouple TRH826 Calculated Temperature Averages

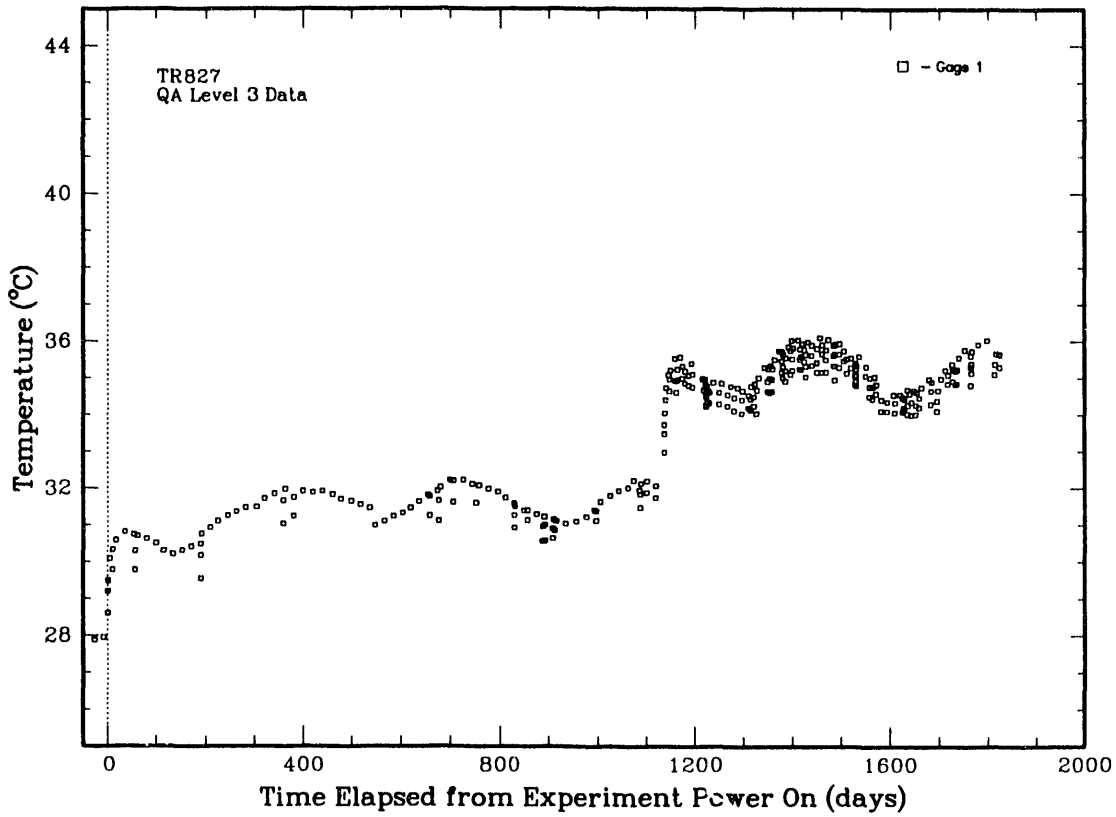

Figure 5.3-7a Near-Field Thermocouple TRH827 Temperature History (TRH07)

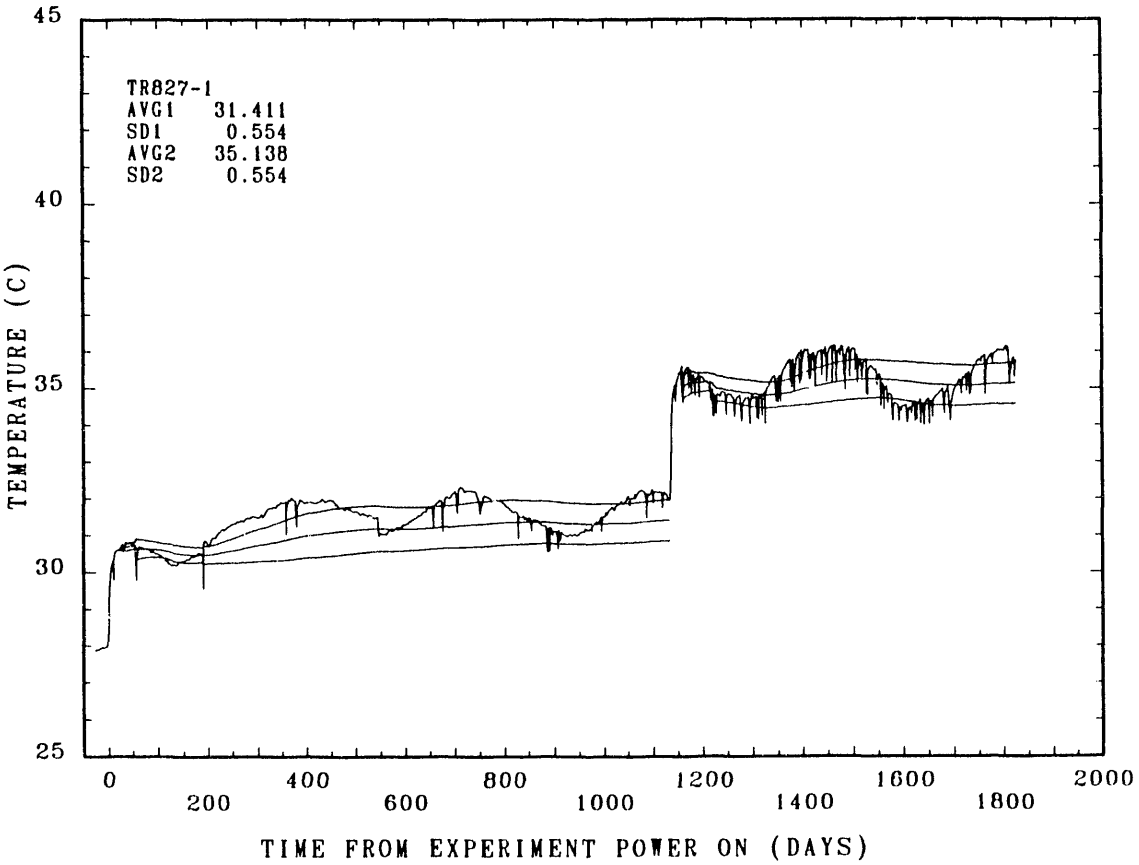

Figure 5.3-7b Near-Field Thermocouple TRH827 Calculated Temperature Averages

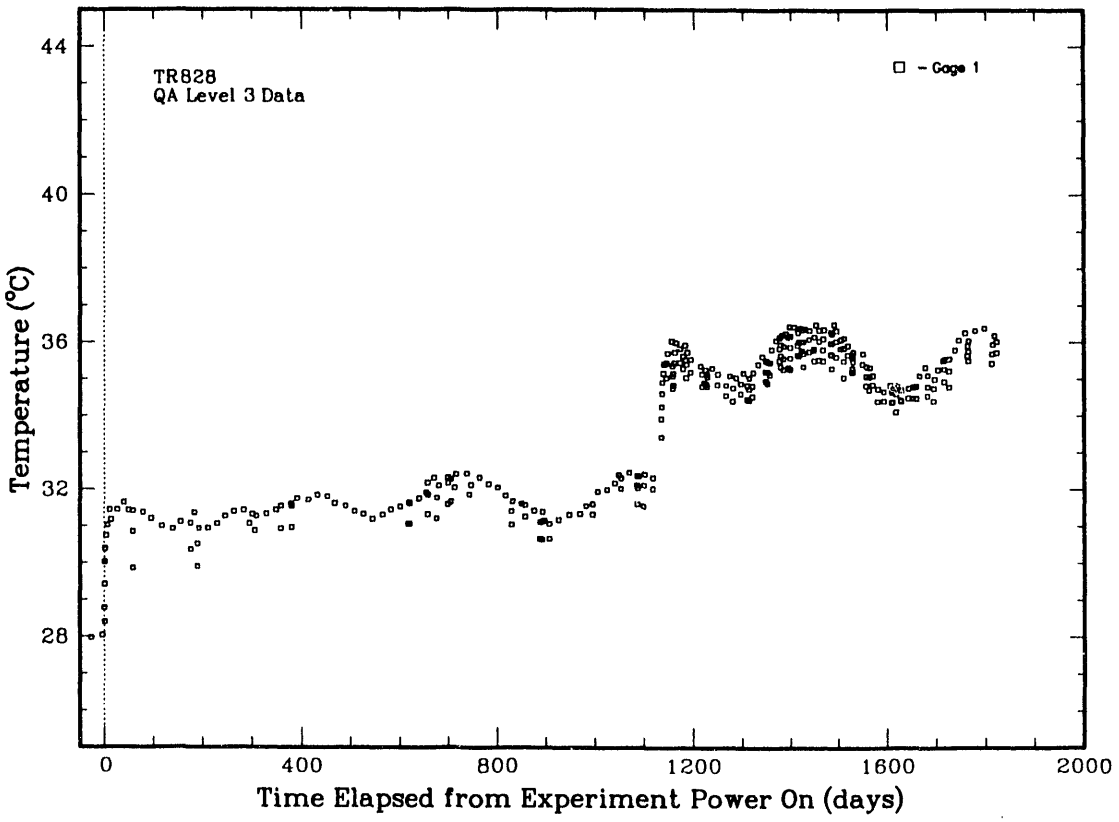

Figure 5.3-8a Near-Field Thermocouple TRH828 Temperature History (TRH08)

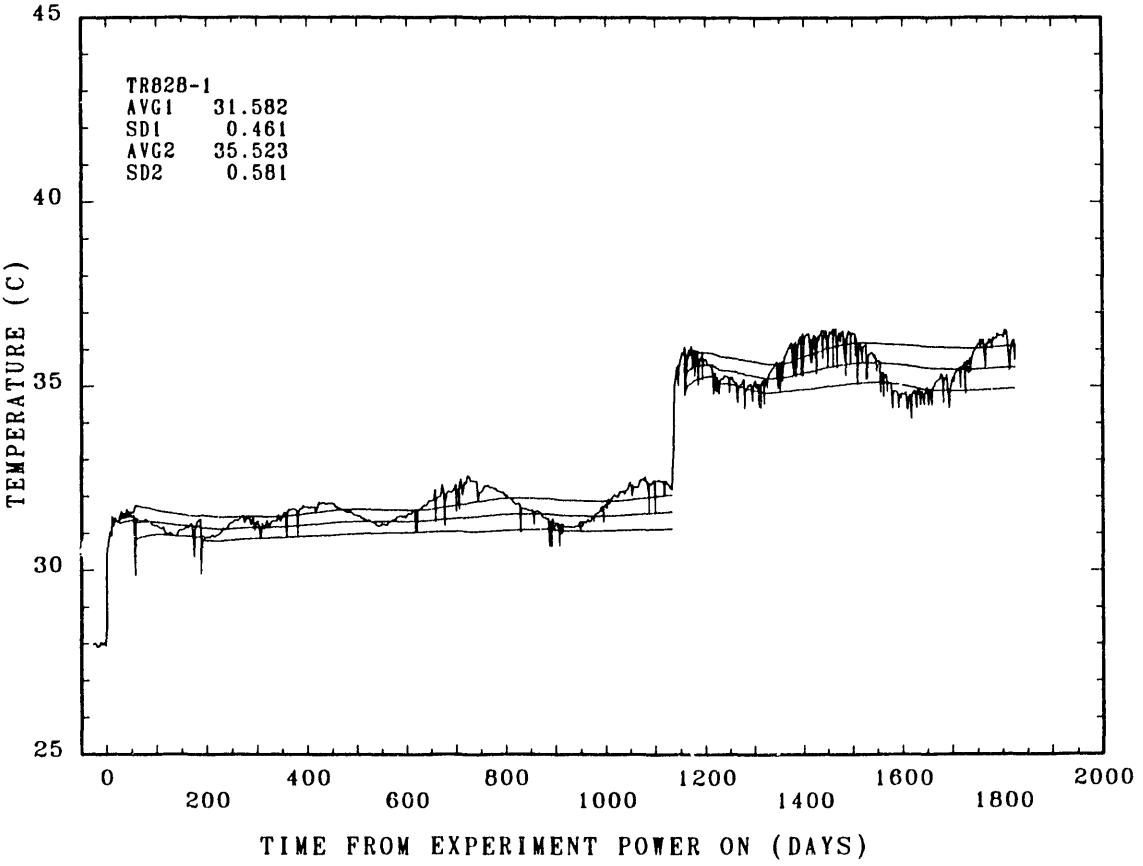

Figure 5.3-8b Near-Field Thermocouple TRH828 Calculated Temperature Averages

5.4 Container-Pressure Histories

The remotely-monitored pressures on the outer surfaces of RH TRU test containers TRH03 and TRH04 are summarized in **Tables 5.4.1** and **5.4.2.** Both test containers are located in partially-backfilled emplacement holes with multiple pressure gages located on the left (L), right (R), top (T), and bottom (B) of the container; refer to **Figures 3.5-3** and **3.5-4**. The "L" and "R" pressure gages, totally surrounded by backfill materials, have the most pressure exerted on them, with pressures originating from borehole closure, being transmitted through the compacting backfill. The "T" pressure gages are surrounded by air only; as such, they are primarily indicators of minor long-term drift and potential temperature effects.

Table 5.4.1 gives the maximum pressure measured by each gage over the period of heated-test operation, through about 1,800 days. It also provides the rate of pressure increase, in units of both MPa/year and psi/year, calculated as a linear slope over a selected time period (slope period). Only (observed, assumed) "near-linear" data time periods were used for these calculations. **Table 5.4.2** is similar to **Table 5.4.1** but gives the maximum pressure measured by each gage over two distinct time periods, from 0 through 722 days and from 722 through about 1,800 days. We physically removed test container TRH04 from its emplacement hole at the "two-year" sampling/examination period; this actually occurred after 722 days of heated test operation. We removed most of the backfill material from the test hole at this time. Then, following detailed examinations of the test container and the emplacement hole, and reemplacement of the test container, we reinstalled the same material within about one day. (Test container TRH03 was not removed for examinations.) All pressure gages in emplacement hole TRH04 were reset to zero pressure immediately following the reemplacement of the backfill material.

A computerized linear regression analysis program, LINREGS, was used to calculate the slopes of "sieved" pressure data points. LINREGS was written (by D.A. Labreche, RE/SPEC) in FORTRAN for, and computed on, a VAX/VMS computer. The LINREGS program reads gage data extracted from the WISDAAM database (Munson, et al., 1990b; as described in Section 3.6) and performs a linear least-squares fit to this data. This program calculates regression coefficients for each gage time interval, as well as the correlation coefficient, the error of the estimate, the 95% confidence interval (upper and lower bounds) on the slope of the linear best fit, intercept at time zero, etc. The calculated confidence interval, essentially the error bars, were generally less than $\pm$ 1 $\times 10^{-5}$ MPa/year ($\pm$ 0.001 psi/year) for the top (T) and bottom (B) gages and $\pm$ 1 $\times 10^{-3}$ MPa/year ($\pm$ 0.1 psi/year) for the left (L) and right (R) gages, respectively. These small calculated uncertainties are not shown in the tables.

Table 5.4.1 RH TRU Emplacement TRH03

Measured Maximum Pressures and Pressure Rates of Increase

Gage #	MPa	MPa/year	psi	psi/year	slope period	Comments
TR613T	0.03	4.8×10^{-3}	4	0.70	0 - 1700 d	upward drift
TR613B	-0.04	- - -	-6	- - -	0 - 1800 d	not linear
TR613L	0.66	0.23	96	33	719 - 1519 d	subsequent decrease
TR613R	0.54	0.16	78	23	719 - 1519 d	subsequent decrease
TR623T	0.08	9.3×10^{-3}	12	1.3	0 - 1700 d	upward drift
TR623B	0.03	-1.2×10^{-3}	4	- 0.17	0 - 1700 d	downward drift
TR623L	0.54	0.16	78	23	200 - 1400 d	dual peaks
TR623R	0.28	0.08	41	12	200 - 1200 d	dual peaks
TR633T	-0.03	-7.8×10^{-3}	-4	- 1.1	0 - 1700 d	downward drift
TR633B	0.09	15×10^{-3}	13	2.2	0 - 1700 d	excludes temp. spikes
TR633L	0.87	- - -	126	- - -	0 - 1800 d	not linear, dual peaks
TR633R	0.72	0.15	104	22	200 - 1300 d	subsequent decrease

The pressure histories for the gages installed on the top, bottom, left, and right surfaces of test containers TRH03 and TRH04 (designated as TR613T, B, L, and R; TR623T, B, L, and R; TR633T, B, L, and R; TR614T, B, L, and R; TR624T, B, L, and R; and TR634T, B, L, and R, respectively) are illustrated in **Figures 5.4-1T, B, L, R; 5.4-2T, B, L, R; 5.4-3T, B, L, R; and 5.4-4T, B, L, R; 5.4-5T, B, L, R**; and **5.4-6T, B, L, R**, respectively.

Table 5.4.2 RH TRU Emplacement TRH04

Measured Maximum Pressures and Pressure Rates of Increase

Gage #	MPa	MPa/year	psi	psi/year	slope period	Comments
TR614T *	0.03	12×10^{-3}	4	1.7	0 - 722 d	upward drift
**	0.02	4.6×10^{-3}	3	0.67	722 - 1798 d	upward drift
TR614B *	0.02	7.6×10^{-3}	3	1.1	0 - 722 d	upward drift
**	0.03	6.7×10^{-3}	4	1	722 - 1796 d	upward drift
TR614L *	0.18	0.12	26	17	360 - 722 d	steady increase
**	0.52	0.25	75	36	1200 -1797 d	steady increase
TR614R *	0.12	0.096	17	14	360 - 722 d	steady increase
**	0.39	0.23	57	33	1200 -1600 d	short-term drop
TR624T *	0.02	-0.53×10^{-3}	3	- 0.08	50 - 722 d	downward drift
**	-0.03	-6.3×10^{-3}	-4	- 0.91	722 - 1622 d	downward drift
TR624B *	0.01	0.46×10^{-3}	1	0.07	50 - 722 d	downward drift
**	0.06	2.0×10^{-3}	9	0.29	722 - 1722 d	spurious end peak?
TR624L *	0.08	0.069	12	9.7	360 - 722 d	steady increase
**	0.21	0.085	30	12	722 - 1622 d	later decrease
TR624R *	0.12	0.072	17	10	360 - 722 d	steady increase
**	0.18	0.079	26	11	722 - 1622 d	later decrease
TR634T *	0.13	22×10^{-3}	19	3.1	100 - 722 d	upward drift
**	0.02	9.2×10^{-3}	7	1.3	722-1122 d	upward drift, dual
**	0.05	17×10^{-3}	7	2.5	1150 -1722 d	slope, & noisy
TR634B *	0.03	4.8×10^{-3}	4	0.70	100 - 722 d	steady increase
**	0.03	7.3×10^{-3}	4	1.1	722 - 1722 d	steady increase
TR634L *	0.40	0.21	58	30	100 - 722	steady increase
**	0.52	0.25	75	36	1122- 1722 d	steady increase
TR634R *	0.32	0.20	46	29	360 - 722 d	steady increase
**	0.44	0.24	64	35	1122- 1722 d	steady increase

[* = 0 to 722 days, ** = 722 to 1800 days]

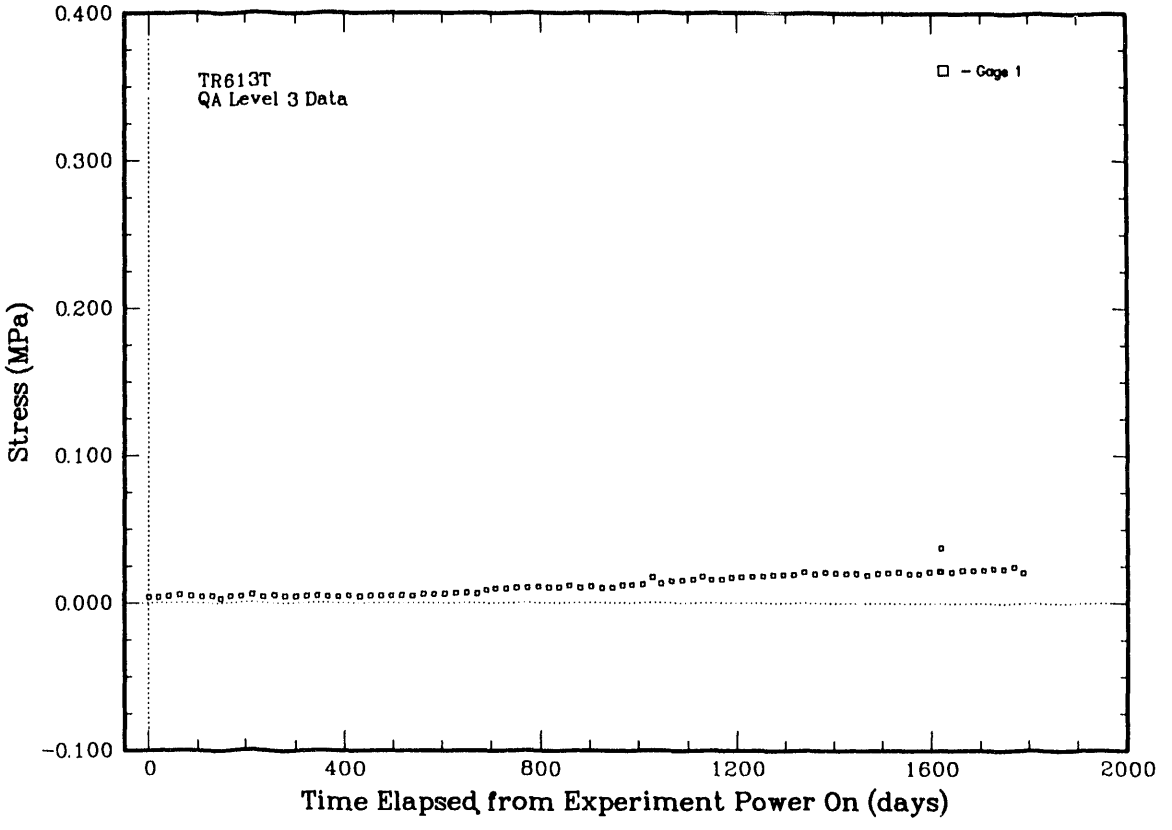

Figure 5.4-1T Pressure Gage TR613T History (TRH03)

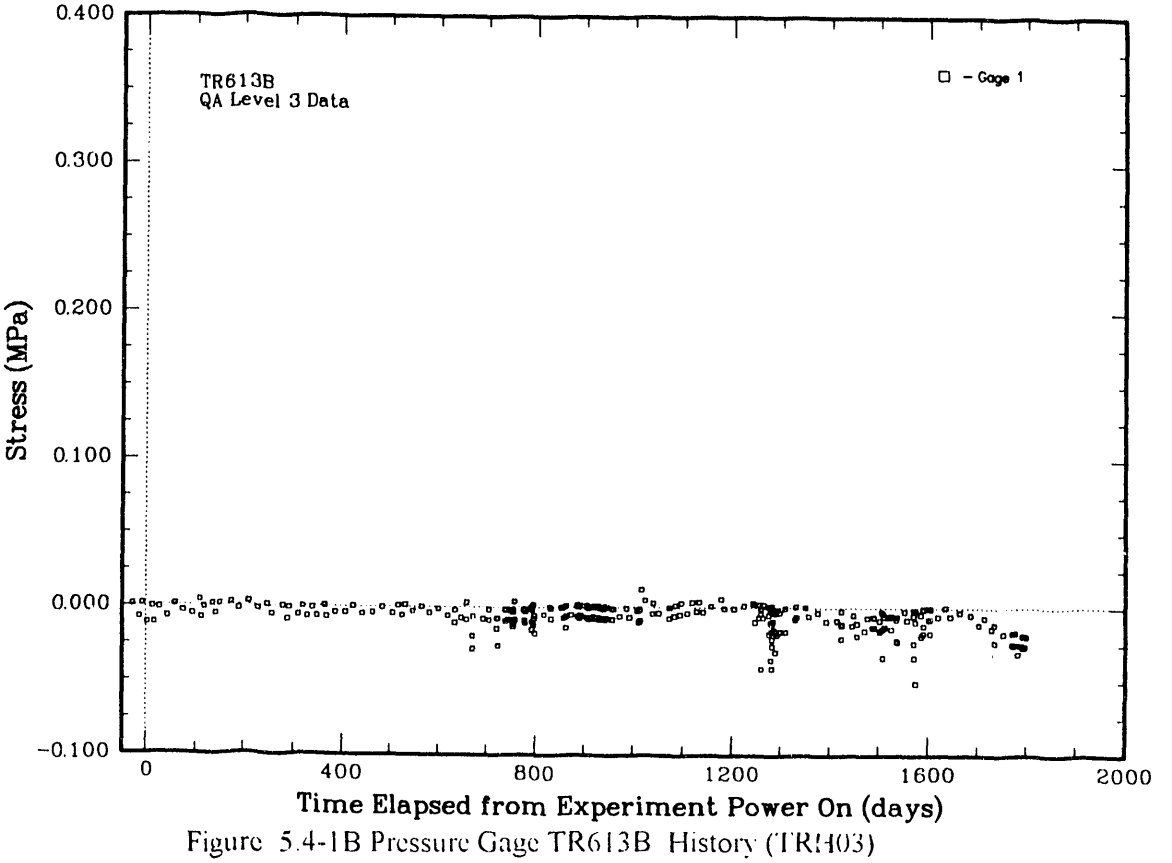

Figure 5.4-1B Pressure Gage TR613B History (TRH03)

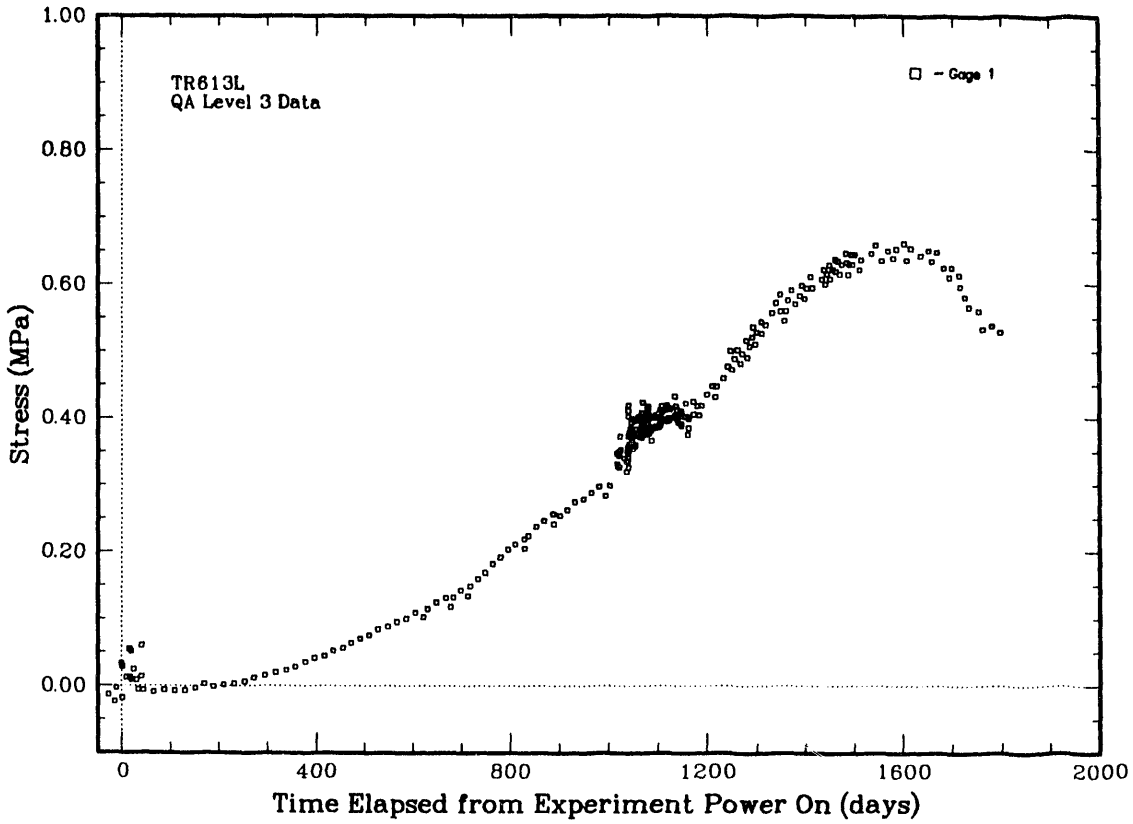

Figure 5.4-1L Pressure Gage TR613L History (TRH03)

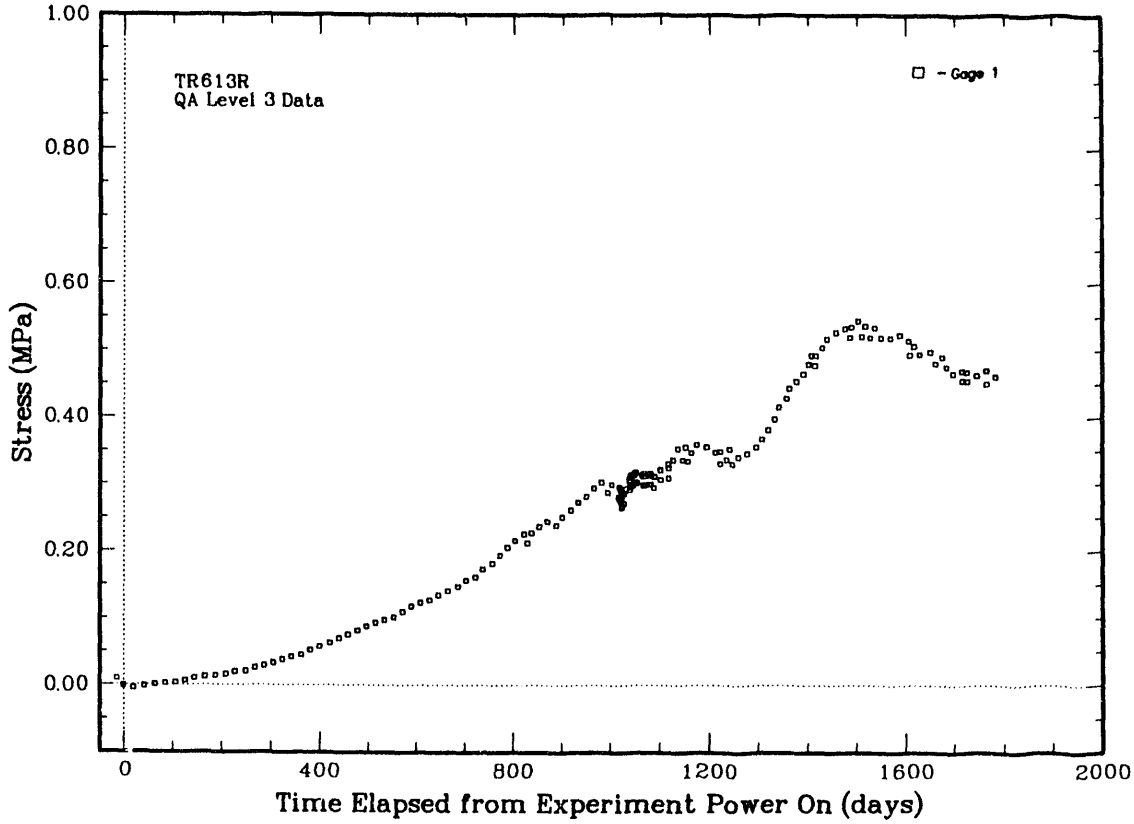

Figure 5.4-1R Pressure Gage TR613R History (TRH03)

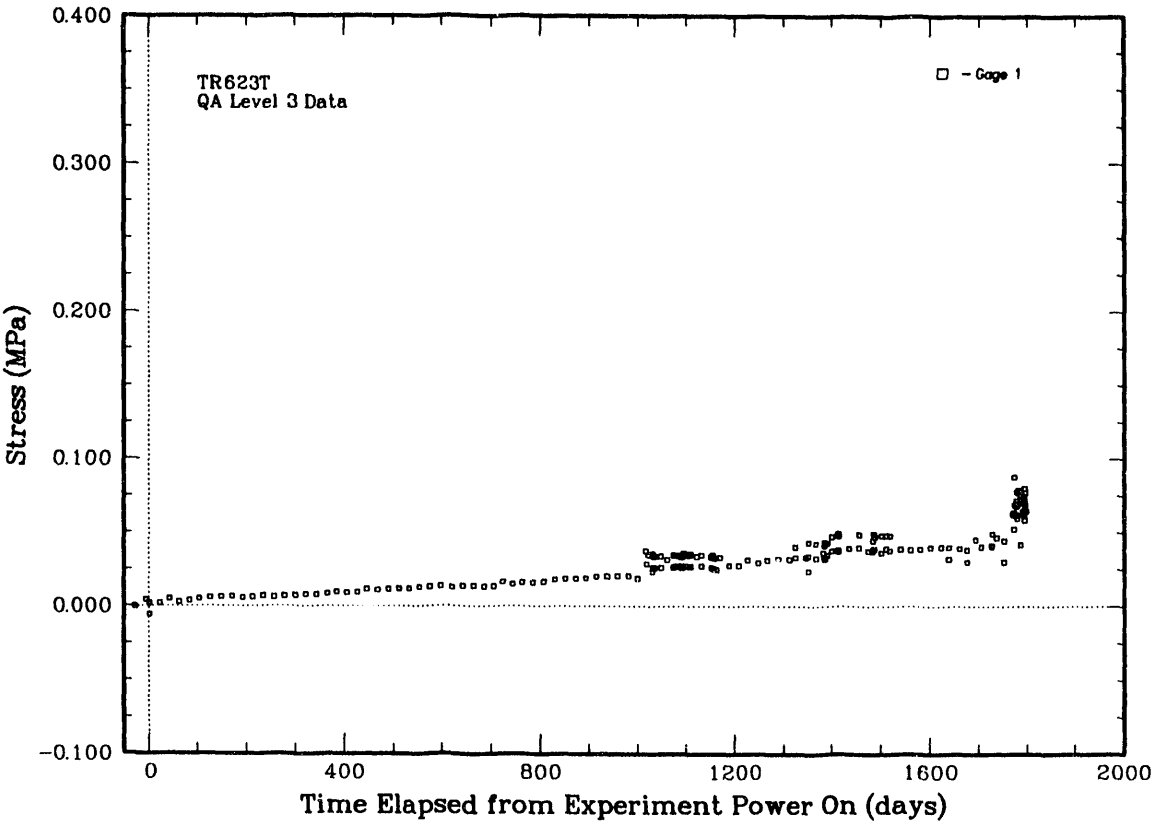

Figure 5.4-2T Pressure Gage TR623T History (TRH03)

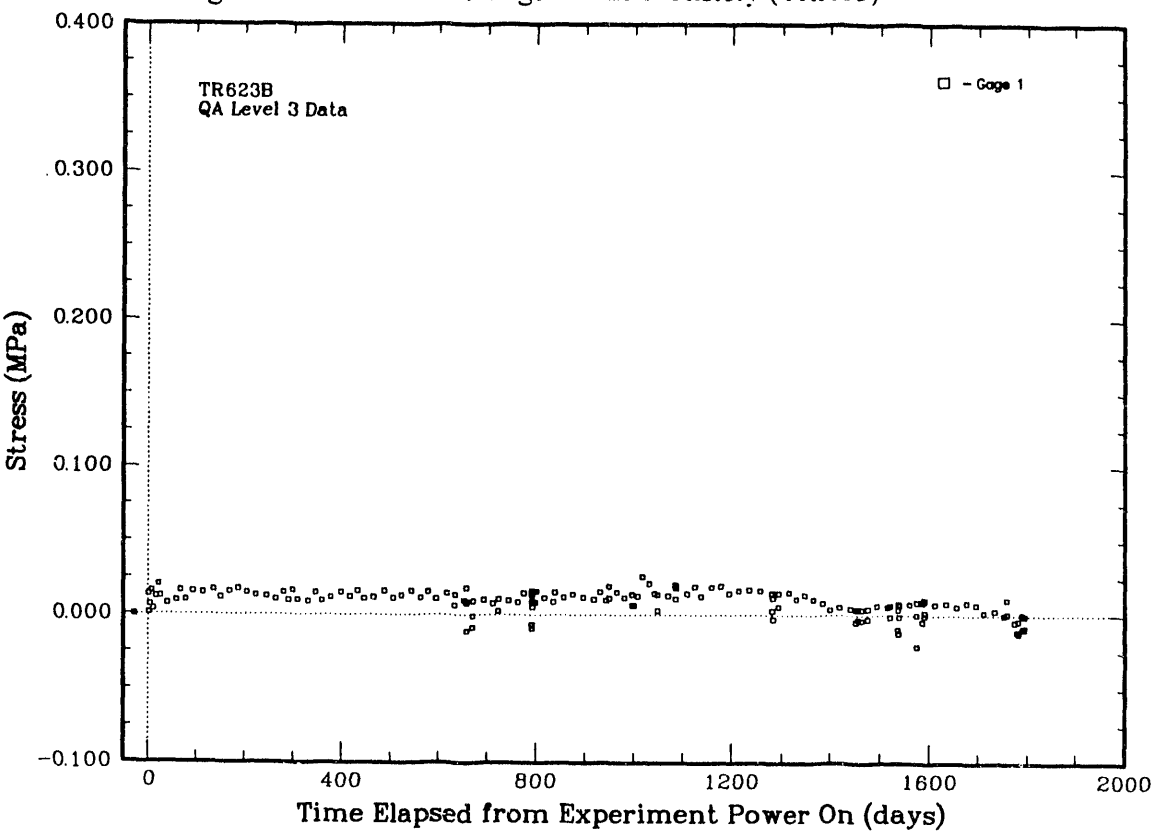

Figure 5.4-2B Pressure Gage TR623B History (TRH03)

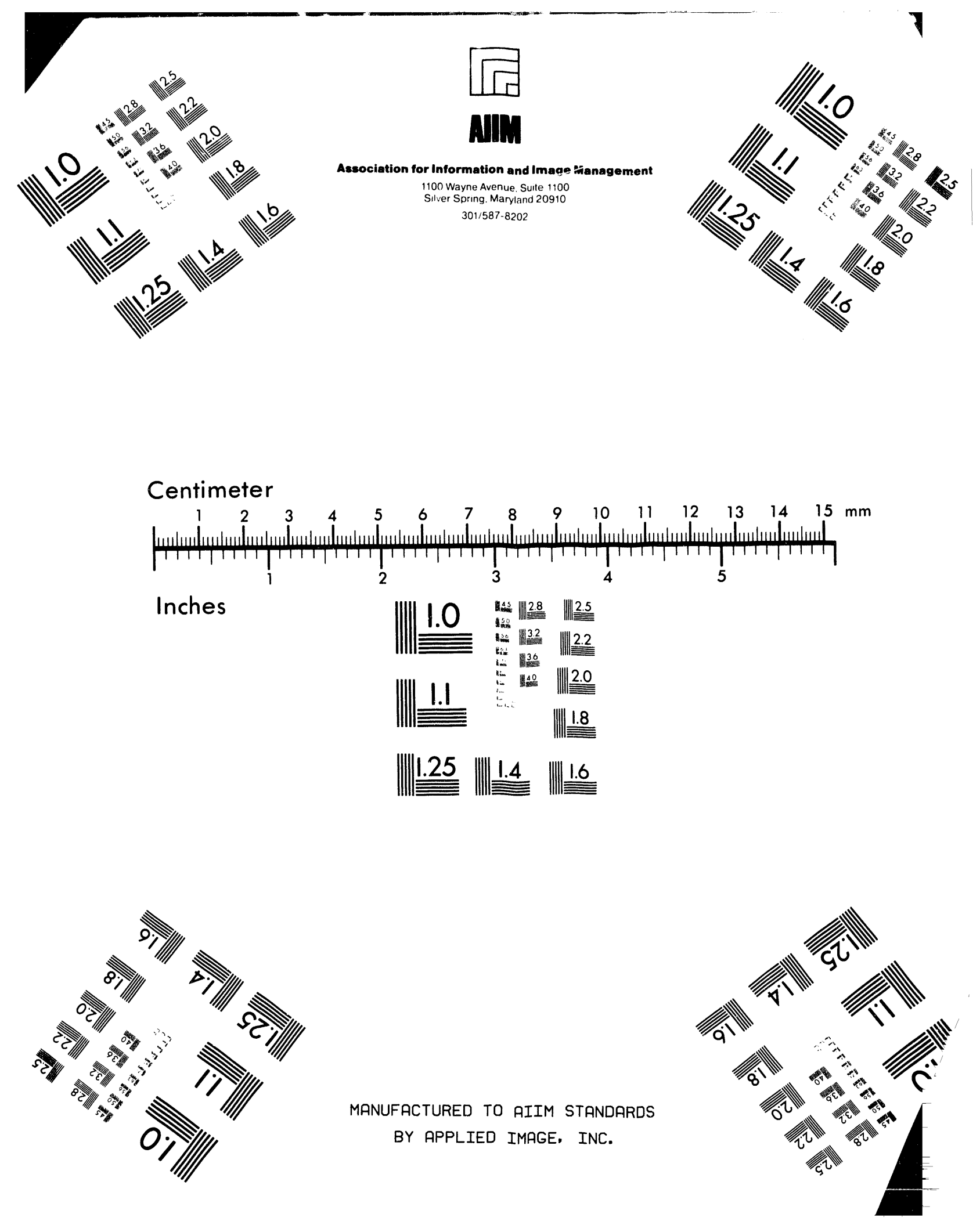
AIIM
Association for Information and Image Management
1100 Wayne Avenue, Suite 1100
Silver Spring, Maryland 20910
301/587-8202
Centimeter
Inches
MANUFACTURED TO AIIM STANDARDS
BY APPLIED IMAGE, INC.

2 of 2

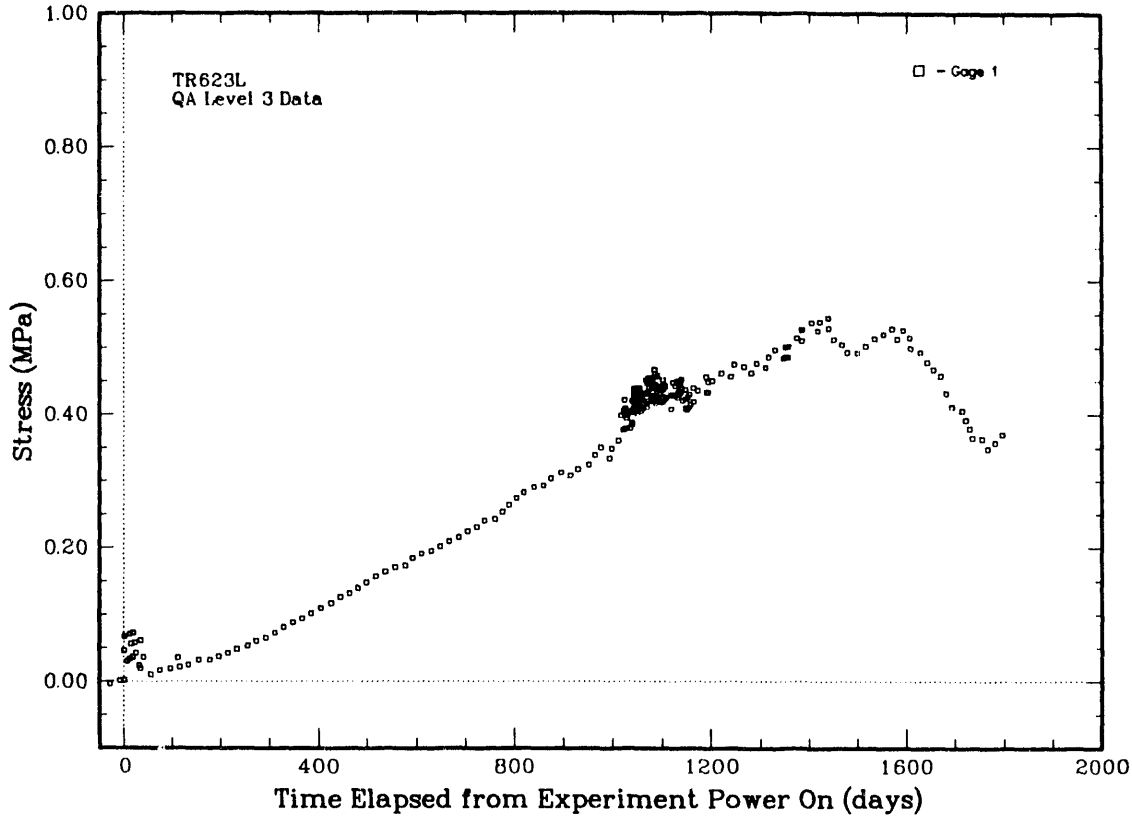

Figure 5.4-2L Pressure Gage TR623L History (TRH03)

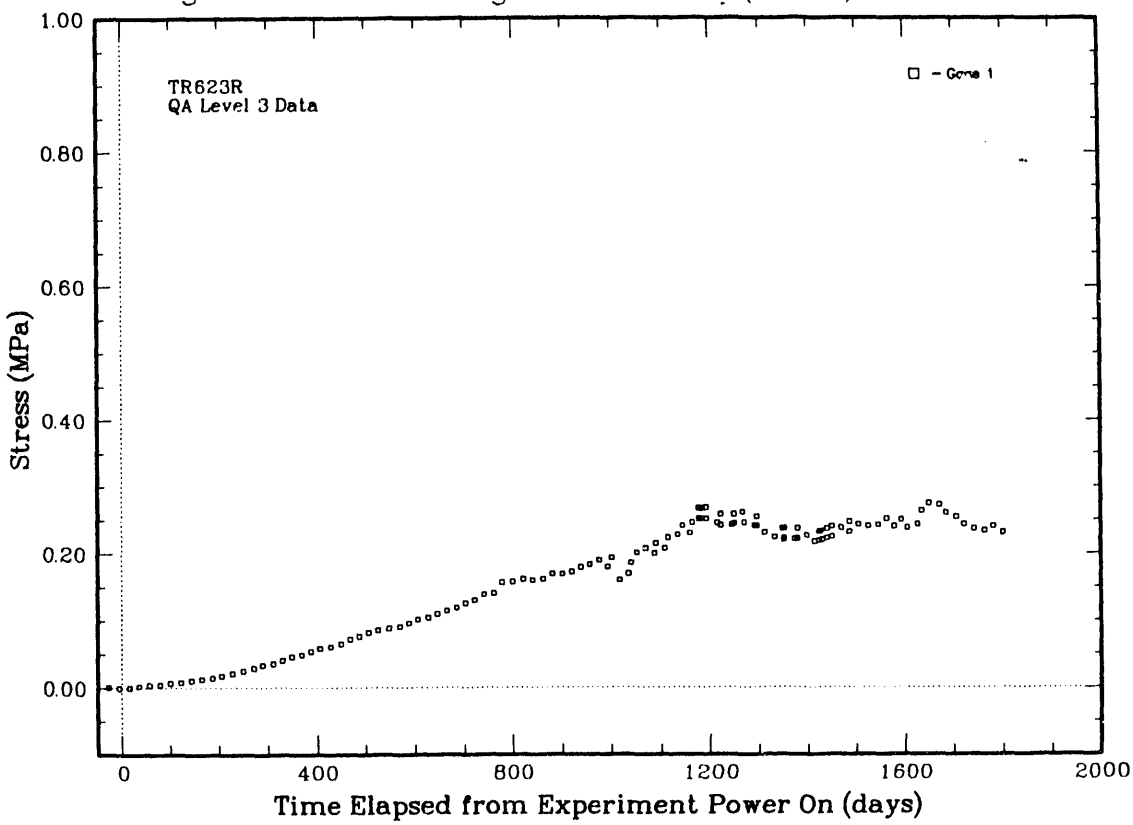

Figure 5.4-2R Pressure Gage TR623R History (TRH03)

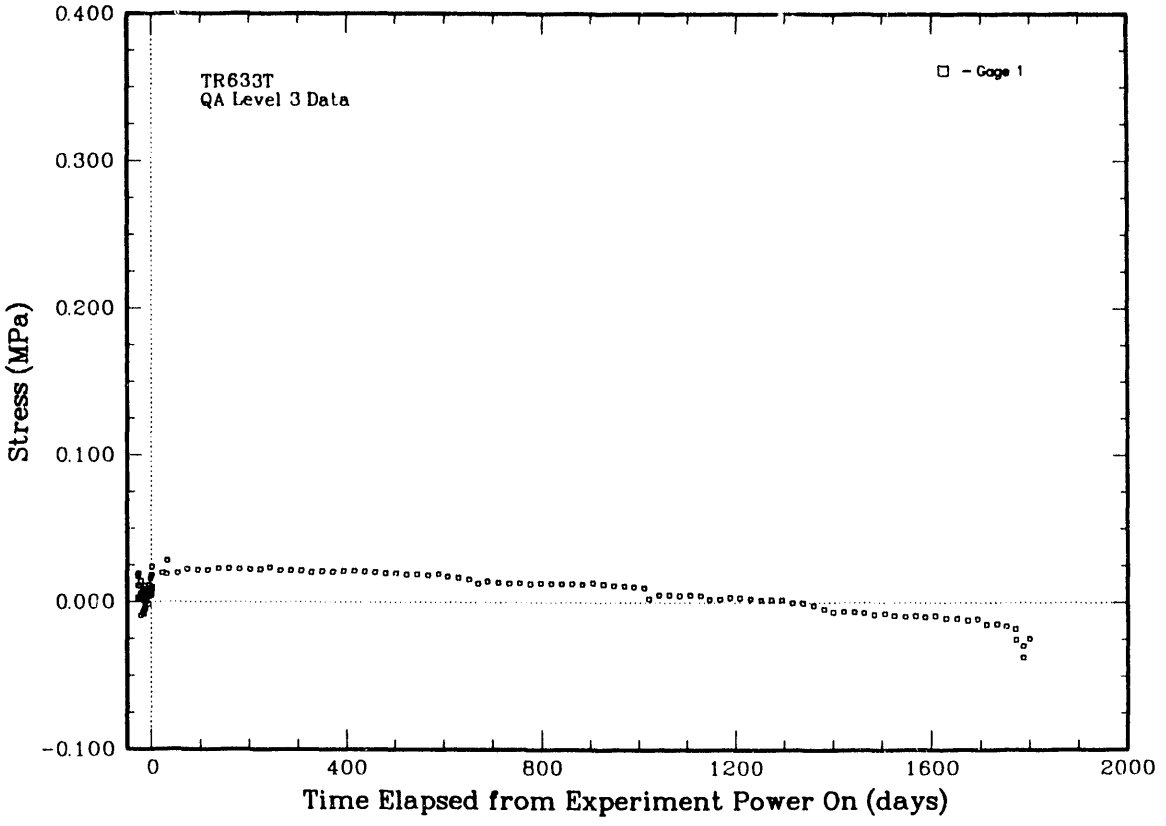

Figure 5.4-3T Pressure Gage TR633T History (TRH03)

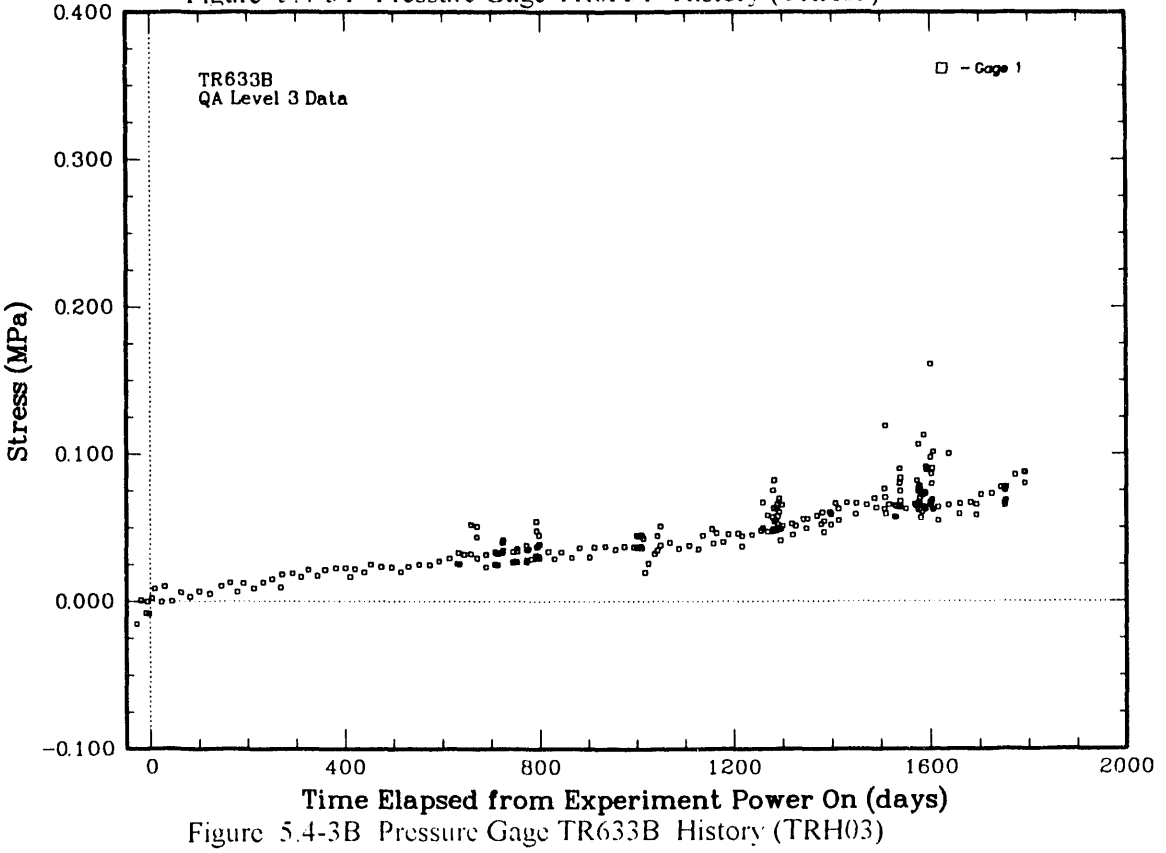

Figure 5.4-3B Pressure Gage TR633B History (TRH03)

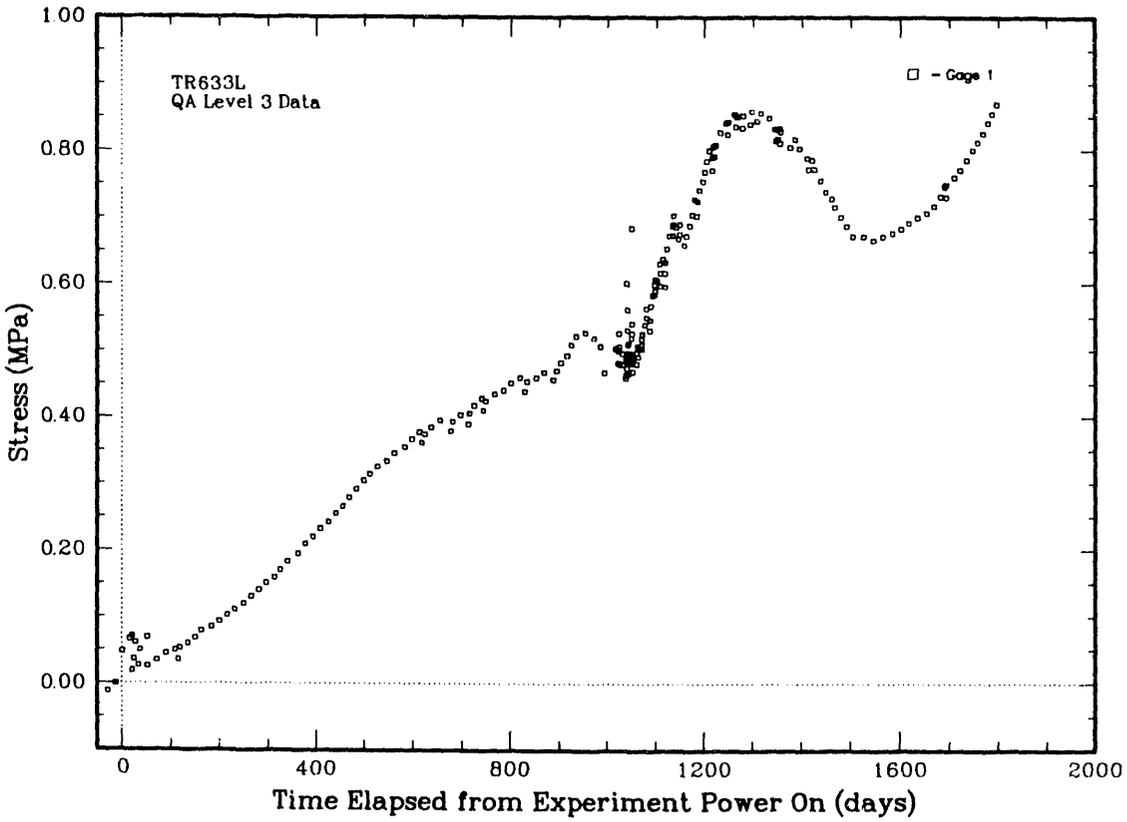

Figure 5.4-3L Pressure Gage TR633L History (TRH03)

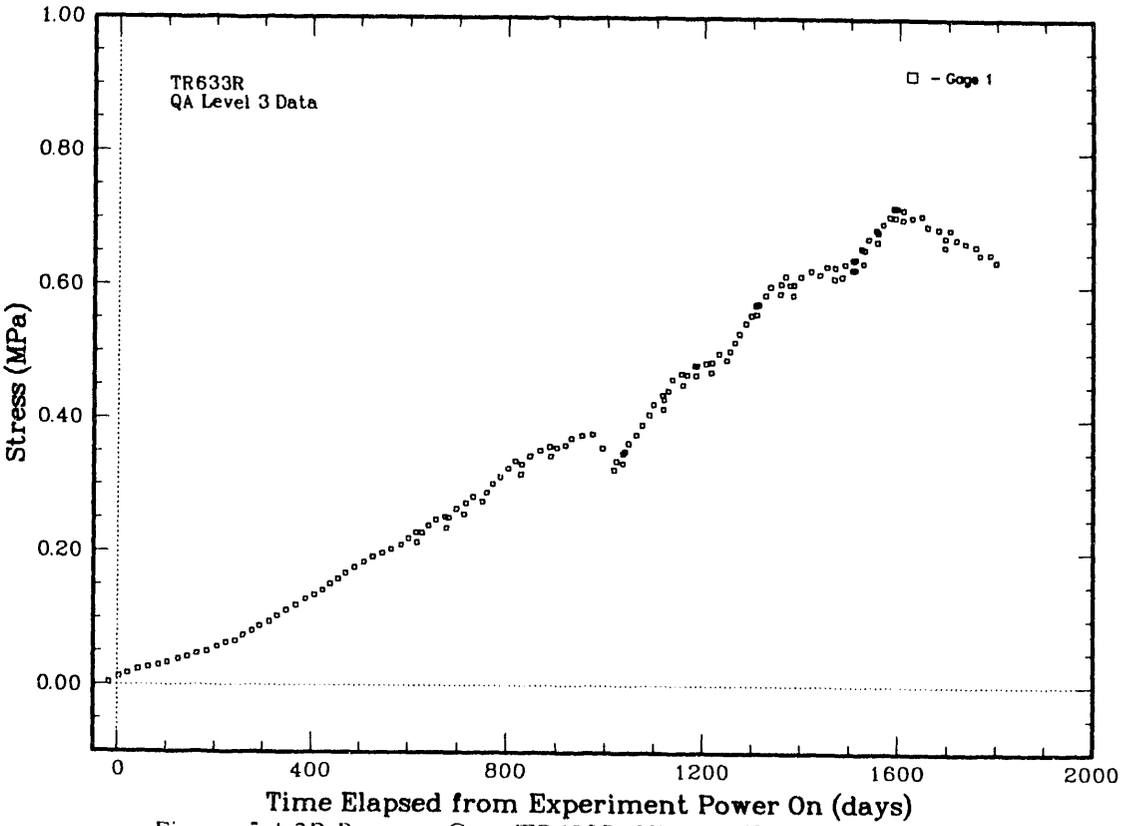

Figure 5.4-3R Pressure Gage TR633R History (TRH03)

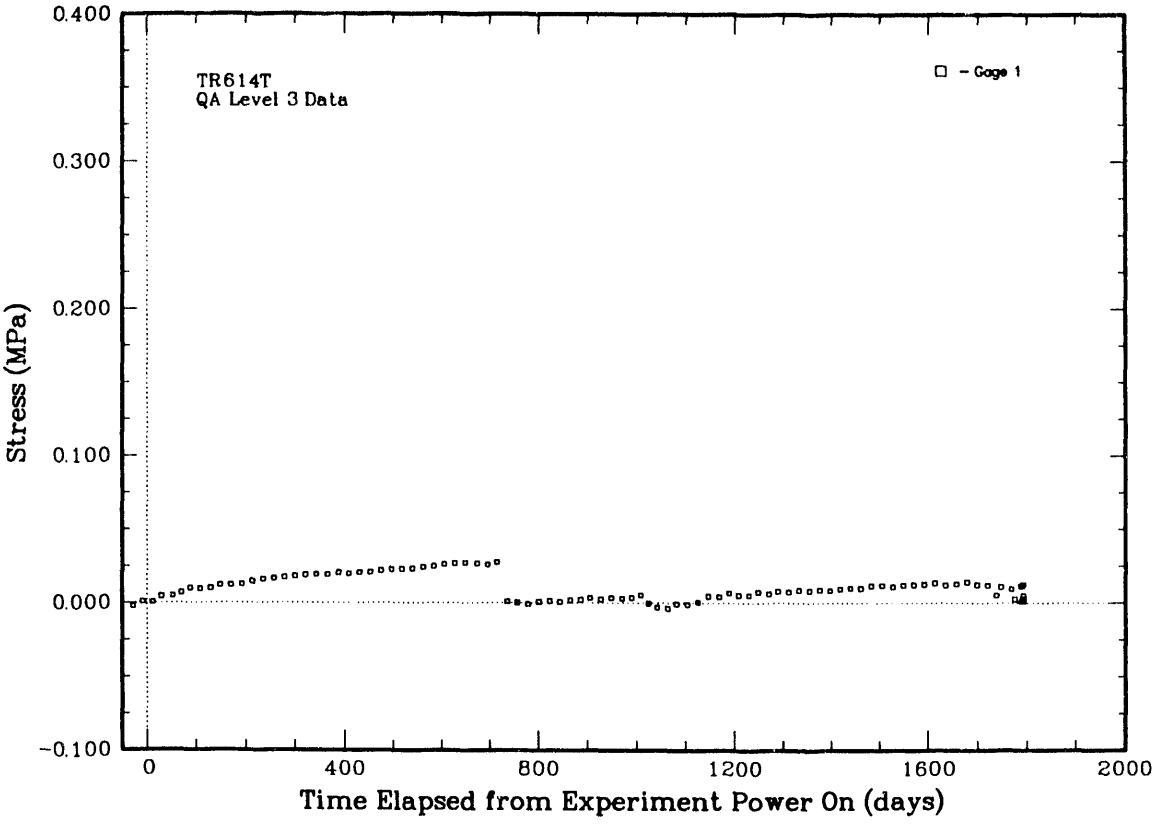

Figure 5.4-4T Pressure Gage TR614T History (TRH04)

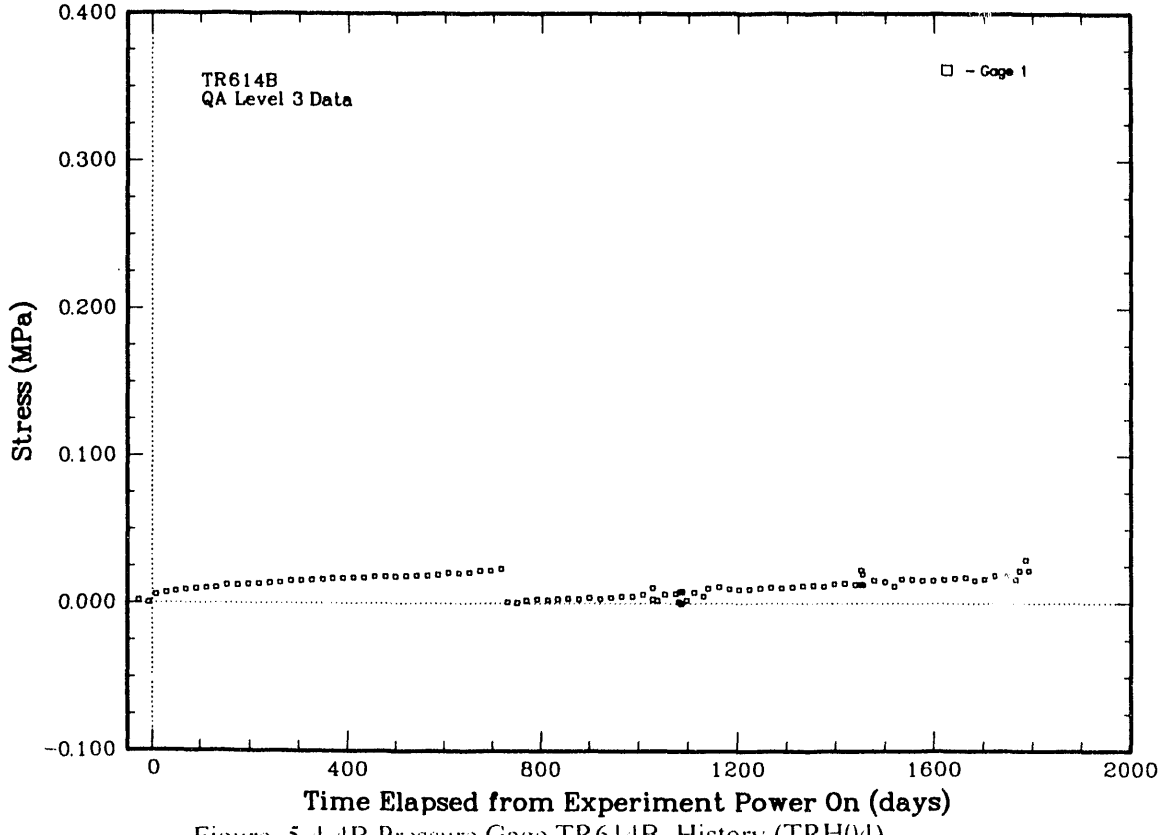

Figure 5.4-4B Pressure Gage TR614B History (TRH04)

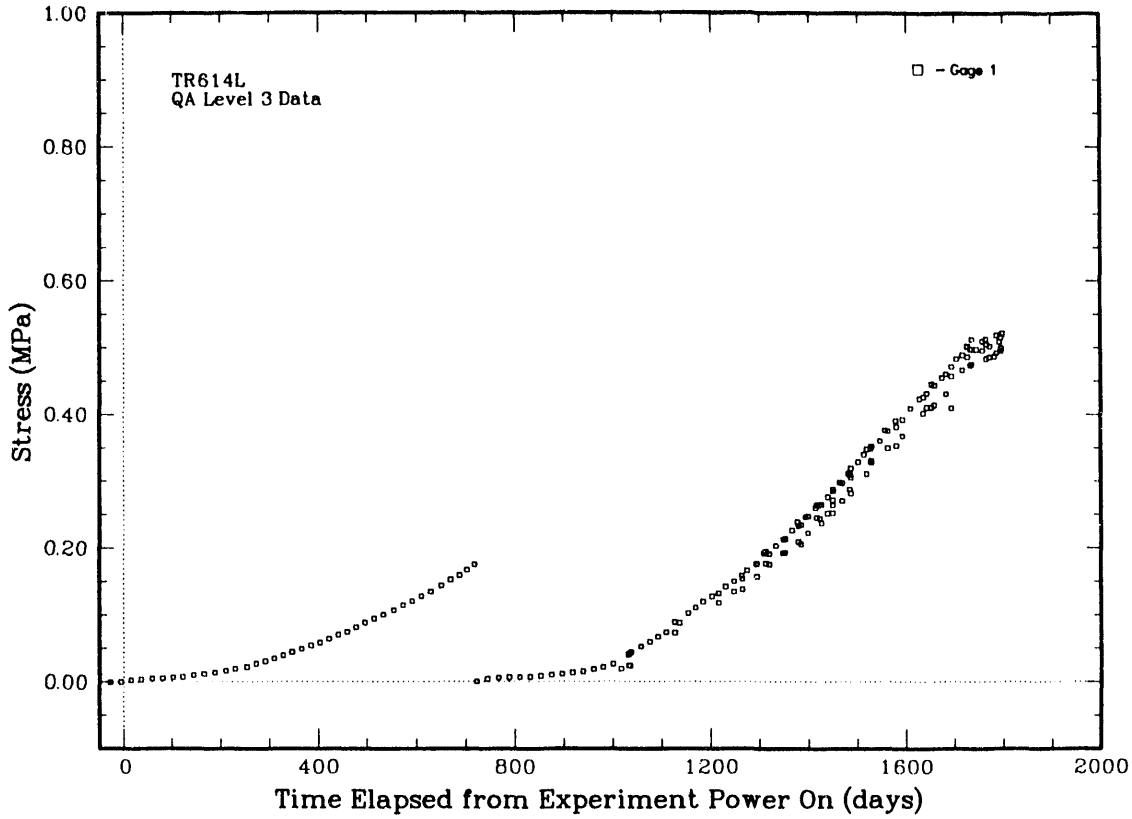

Figure 5.4-4L Pressure Gage TR614L History (TRH04)

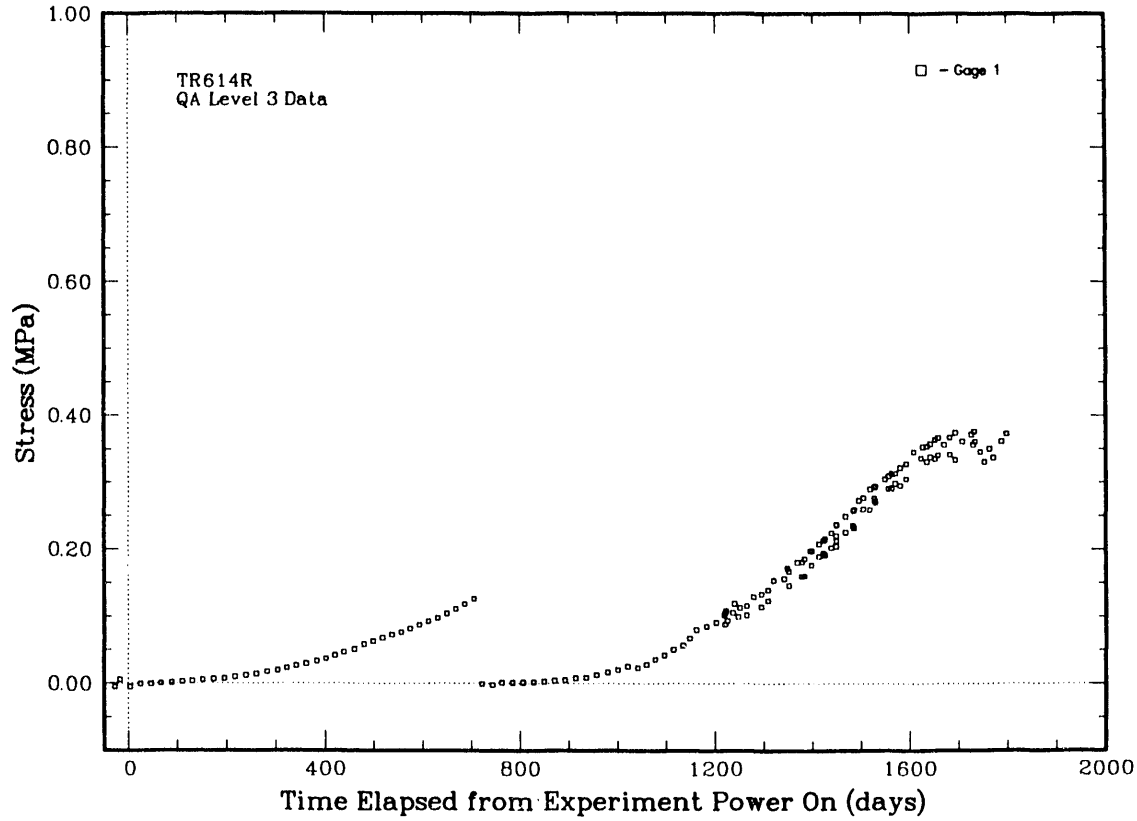

Figure 5.4-4R Pressure Gage TR614R History (TRH04)

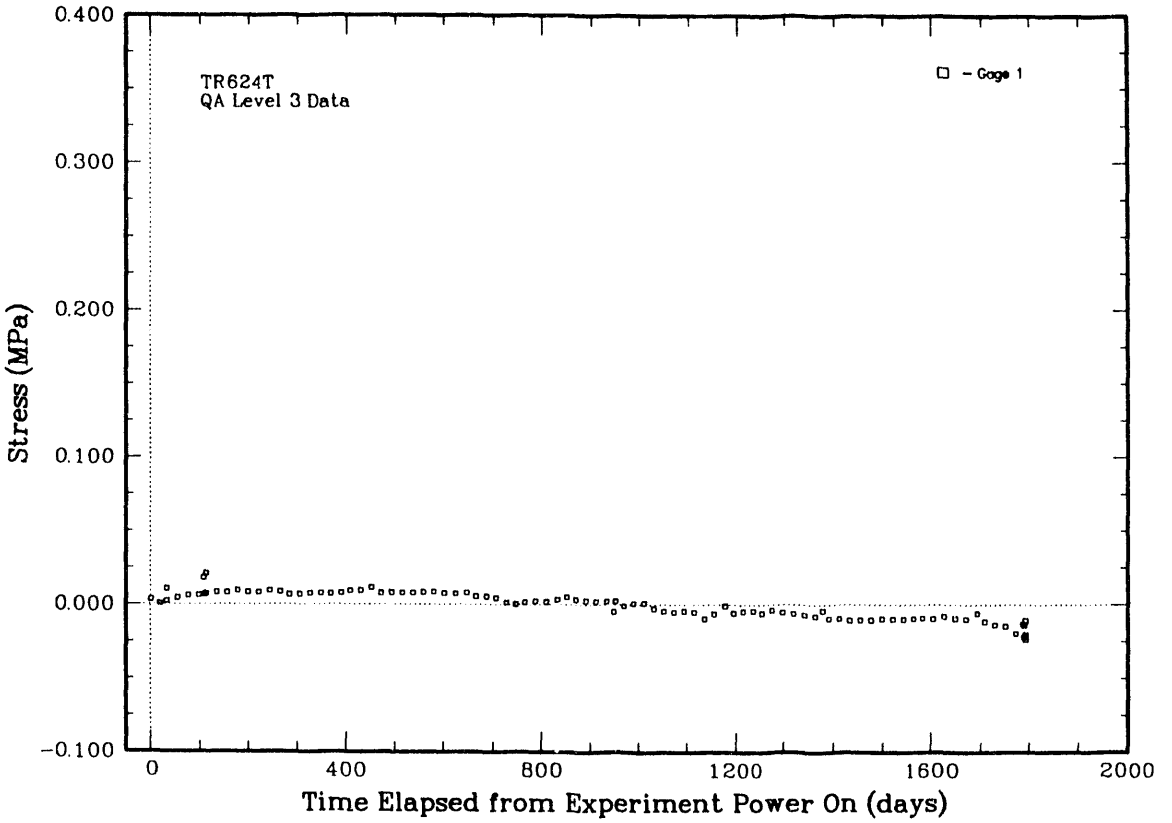

Figure 5.4-5T Pressure Gage TR624T History (TRH04)

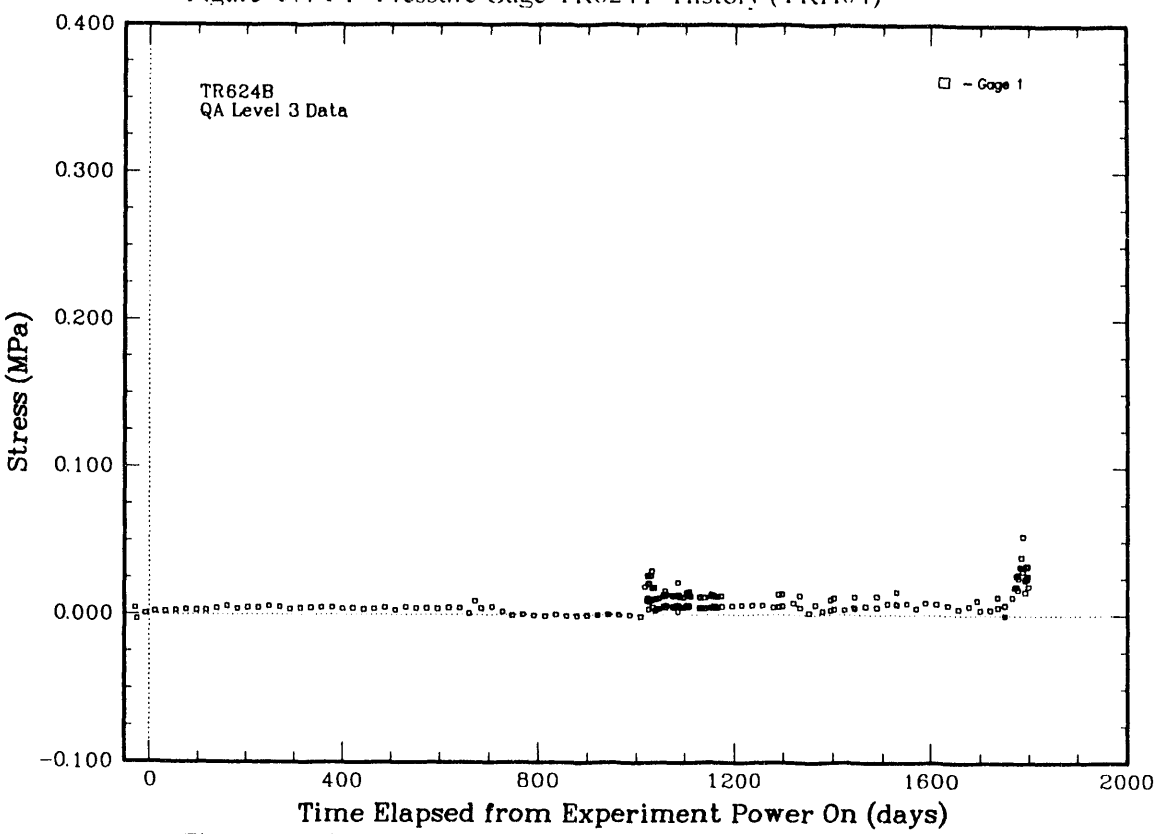

Figure 5.4-5B Pressure Gage TR624B History (TRH04)

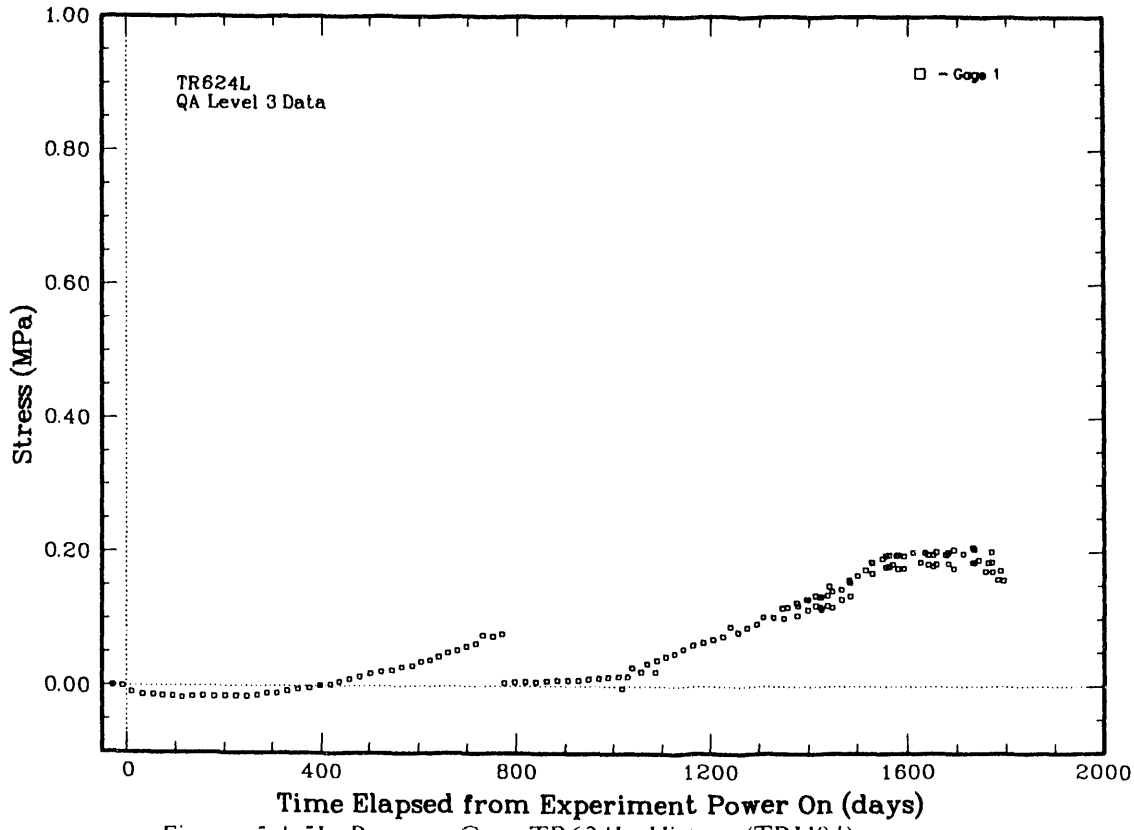

Figure 5.4-5L Pressure Gage TR624L History (TRH04)

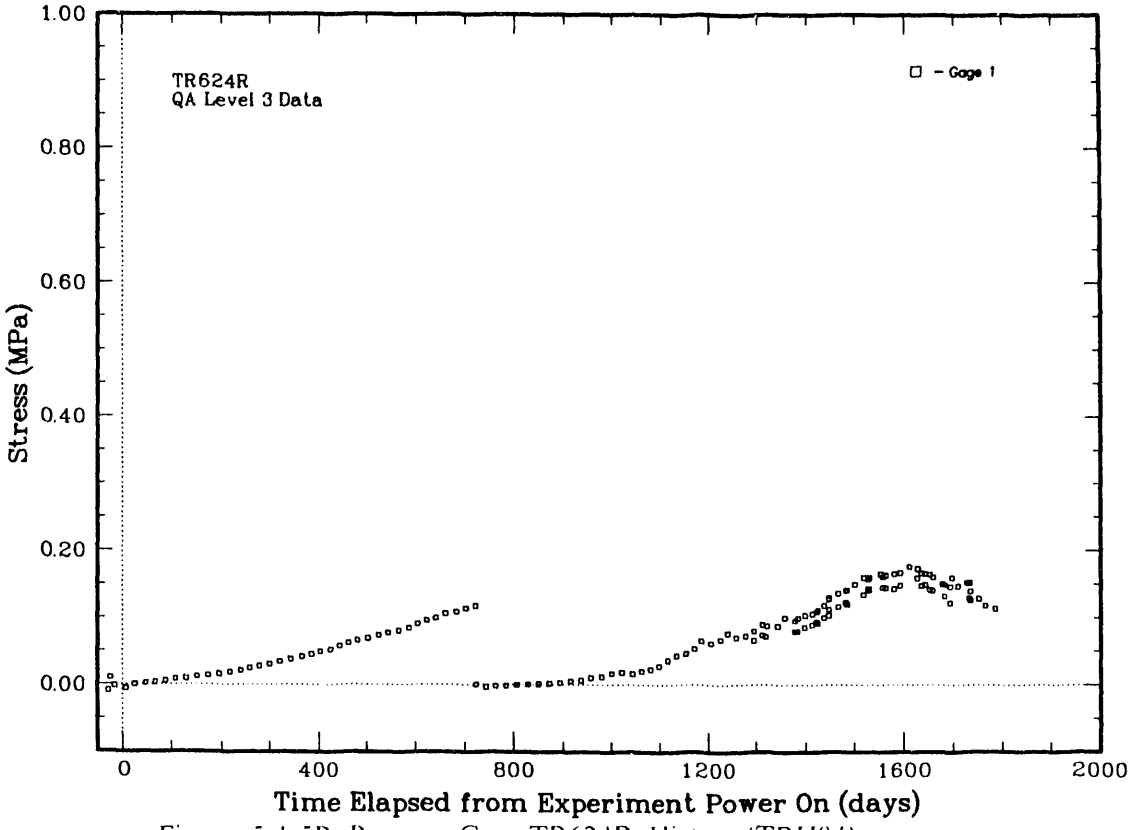

Figure 5.4-5R Pressure Gage TR624R History (TRH04)

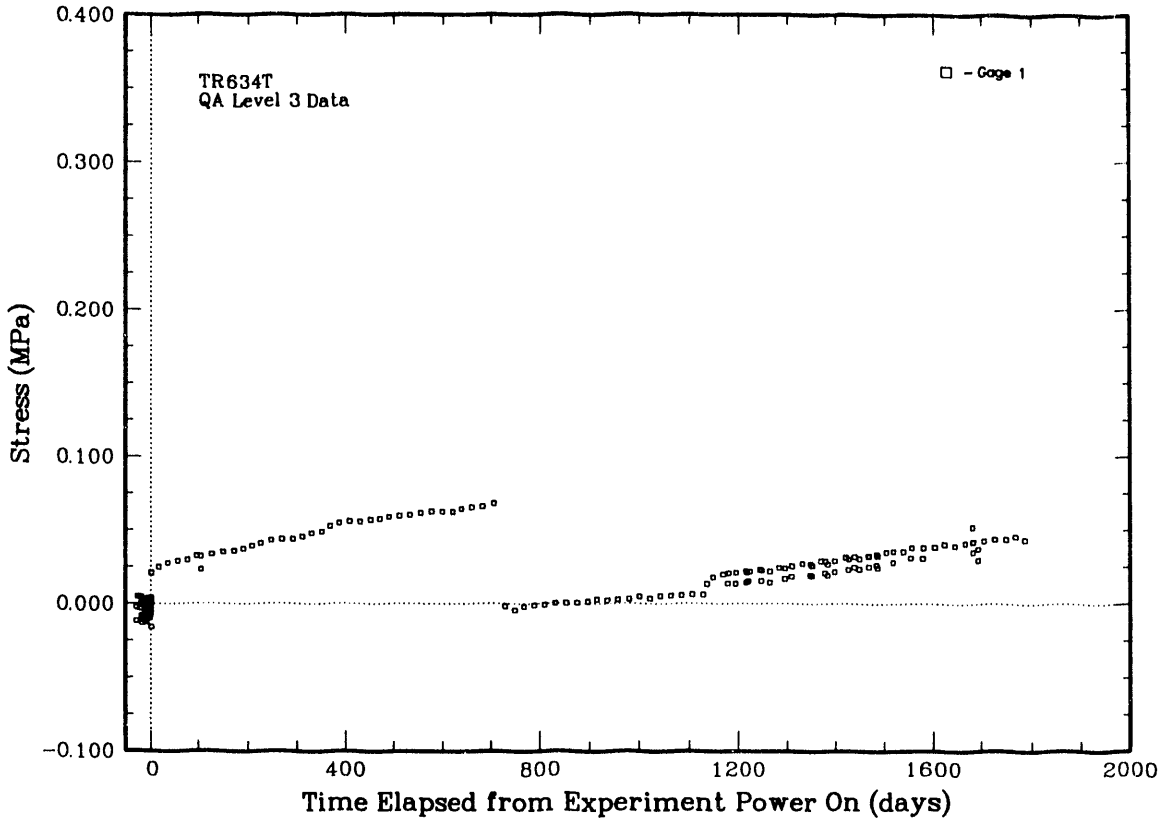

Figure 5.4-6T Pressure Gage TR634T History (TRH04)

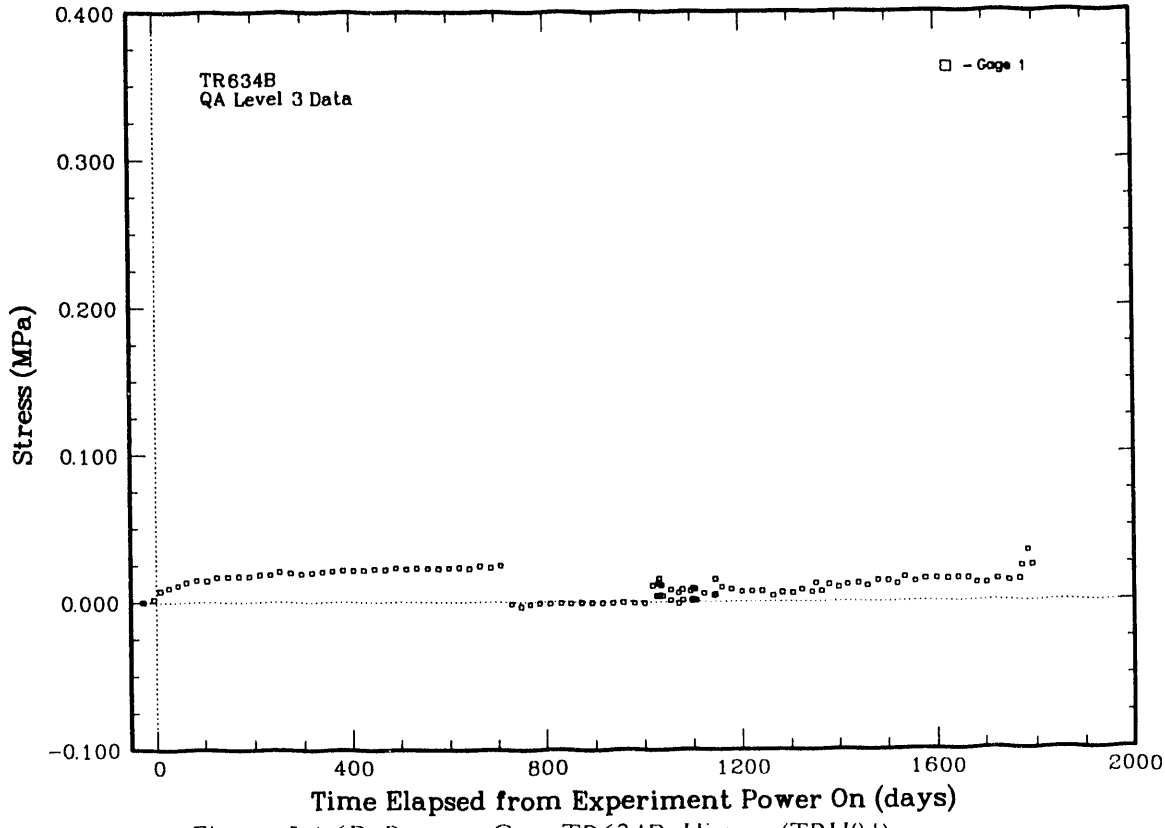

Figure 5.4-6B Pressure Gage TR634B History (TRH04)

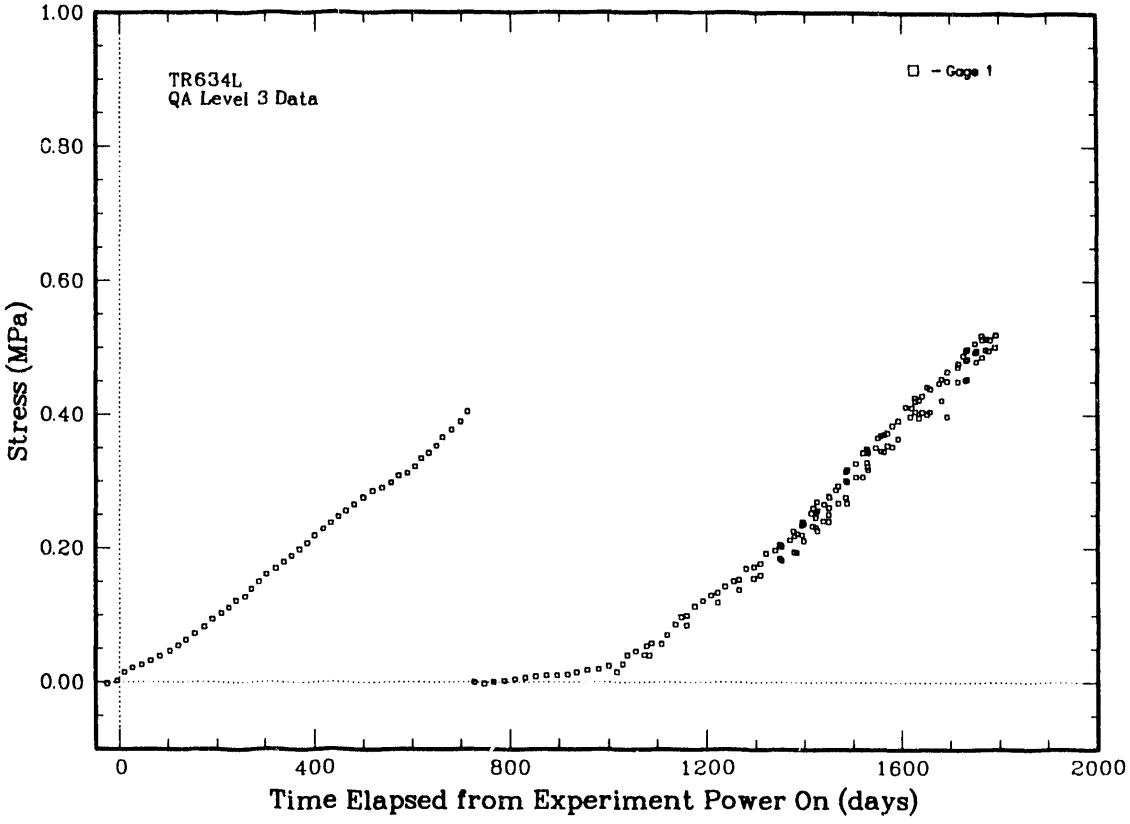

Figure 5.4-6L Pressure Gage TR634L History (TRH04)

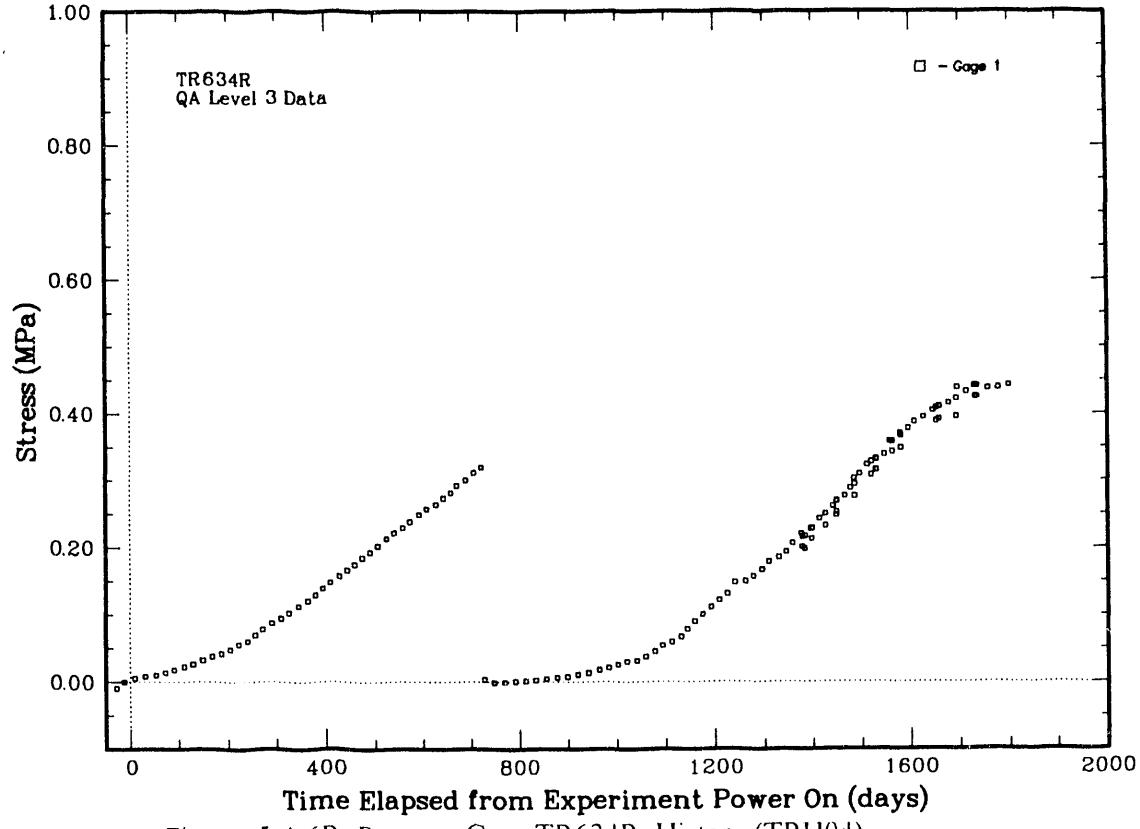

Figure 5.4-6R Pressure Gage TR634R History (TRH04)

5.5 Borehole Closure Measurements

We have obtained both manual and remote-instrument measurements of individual RH TRU test borehole closures during the course of heated test operations. Two main types of borehole closure have been monitored. We measured vertical-displacement borehole closure from the top of the horizontal test container to the top-center of the borehole surface. Results from these measurements are presented in Section 5.5.1. Also, we measured the changes in overall borehole diameters, both vertical and horizontal, as a function of time. These measurements are reported on in Section 5.5.2.

5.5.1 Vertical-Displacement Borehole Closure

The installed, vertical-displacement, borehole-closure gages monitor vertical displacement from the top of the test container to the borehole top surface in test emplacements TRH01, TRH02, TRH03, and TRH04. Such measurements include not only the downward displacement of the top of the borehole, but also the upward displacement of the bottom of the borehole, pushing the test container upward. We monitored data at three separate locations within these boreholes: at 2.18 m, 2.95 m, and 3.71 m in from the rib-face of the 4.88 m-long boreholes. These distances correspond to the locations of closure gages TR21X, TR22X, and TR23X, respectively, where X represents borehole 1, 2, 3, or 4; refer to **Figures 3.5-1** through **3.5-4.** A sample of these data is provided in **Table 5.5.1** for the maximum recorded vertical-displacement borehole closures from each gage at 12, 18, 24, and 36 months after heater turn-on.

Periodically, we also obtained manual vertical-displacement closure measurements made with a snap-type caliper gage, as described in Section 3.5.5. These manual measurements were taken directly adjacent to (in front of) the installed closure gages (in test emplacements TRH01, TRH02, TRH03, and TRH04, only), from the top of the horizontal container to the top-center of the borehole surface. Test containers were left in place, undisturbed during these measurements. We also obtained manual measurements in test boreholes TRH05, TRH06, TRH07, and TRH08, even though there were no installed closure gages for comparison. All results obtained from these measurements, after 12, 18, 24, and 36 months after heater turn-on, are presented in **Table 5.5.1** and are also compared to the remote-instrument data, as appropriate. The assumptions we made, to convert the periodic manual closure measurements (raw data) to the "manual vertical closure" measurements that are directly comparable to the remote measurements, are presented as notes at the bottom of **Table 5.5.1**.

Table 5.5.1 RH TRU Vertical-Displacement Borehole Closure Measurements [units of mm]
(* notes follow) (without spacer ♦ with initial spacer height of 30.2 mm)

	12 - Month		18 - Month		24 - Month		36 - Month		Days to Spacer Contact
Test Hole: Gage/Location	Rc note Closure	Manual * Closure	Remote Closure	Manual * Closure	Remote Closure	Manual * Closure	Remote Closure	Manual * Closure	
TRH01:									
TR211	15.6	20.1	22.4	28.7	29.4	35.6	42.6	49.5	0
TR221	5.2 ♦ 35.4	25.7	12.6 ♦ 42.8	32.0	19.5 ♦ 49.7	38.6	33.5 ♦63.7	53.0	220
TR231	2.0 ♦ 32.2	32.0	10.8 ♦ 41.0	38.4	18.3 ♦ 48.5	42.4	33.1 ♦63.3	61.2	330
TRH02:									
TR212	13.9	20.1	20.5	24.6	27.1	31.2	39.5	44.6	0
TR222	0.0	10.7	0.0	16.0	0.0	23.9	5.3 ♦ 35.5	32.5	920
TR232	0.0	25.9	0.9 ♦ 31.1	29.5	6.4 ♦ 36.6	35.1	16.2 ♦46.4	45.9	510
TRH03:									
TR213	14.2	24.4	21.7	30.5	29	36.6	43.3	50.0	0
TR223	1.1 ♦ 31.3	25.2	8.4 ♦ 38.6	34.3	16.0 ♦ 46.2	41.2	30.9♦ 61.1	56.1	340
TR233	0.0	28.5	1.4 ♦ 31.6	30.7	8.1 ♦ 38.3	37.3	20.6♦ 50.8	52.8	510
TRH04:									
TR214	16.3	27.2	24.5	34.5	32.6	38.9	45.7	51.1	0
TR224	0.0	25.9	3.4 ♦ 33.6	31.5	11.2 ♦ 41.4	37.3	24.3♦ 54.5	48.3	470
TR234	4.2 ♦ 34.4	28.5	10.9 ♦ 41.1	32.0	17.4 ♦ 47.6	38.9	28.9♦ 59.1	54.4	240
TRH05:									
- 2.2 m		- - -		27.7		34.3		49.0	
- 3.0 m		- - -		26.7		32.3		48.5	
- 3.7 m		- - -		26.4		30.7		42.9	
TRH06:									
- 2.2 m		- - -		30.7		37.3		42.4	
- 3.0 m		- - -		29.0		31.5		45.2	
- 3.7 m		- - -		30.7		32.3		50.0	
TRH07:									
- 2.2 m		- - -		26.8		31.8		42.8	
- 3.0 m		- - -		25.2		30.0		39.8	
- 3.7 m		- - -		25.2		29.2		37.6	
TRH08:									
- 2.2 m		- - -		30.5		36.8		47.9	
- 3.0 m		- - -		35.1		41.4		52.5	
- 3.7 m		- - -		34.3		39.1		48.6	

* Assumptions made for converting manual measurements to "Manual Vertical Closure:"
  1. Initial borehole diameter = 918.7 mm (36.17");
  2. Container top-to-borehole distance = 156.7 mm (6.17"); and,
  3. Manual Vertical Closure = (156.7 mm - measured distance).
  4. Reproducibility of manual measurements is ≈ 1 mm (0.03")

  Note: Gage TR21X is 2.2 m in from rib face
  Gage TR22X is 3.0 m in from rib face
  Gage TR23X is 3.7 m in from rib face

We replicated the manual closure measurements to support precision. When a test container was removed for examinations, then reemplaced, the manual measurements were made both before removal and after reemplacement, then averaged. The reproducibility of these measurements nominally was ± 1 mm (± 0.03 in.). This level of reproducibility is a good indicator of how well the containers can be replaced to their original, undisturbed position within the borehole, as facilitated by the roller assembly on the bottom of the hole.

Test gages TR21X, where X = test borehole #1, 2, 3, or 4, made use of Teflon spacers (as described in Section 3.5.3) and recorded borehole closures as soon as these gages were activated. However, gages TR22X and TR23X did not record any closure until the borehole(s) had closed the approximate distance of the spacer, about 30.2 mm (1.19 in.). The time, in days, it took for this amount of closure to occur, and for the gages to record actual displacements, is listed in **Table 5.5.1**; data from these remote-gages are also marked with a "♦" in the Table. The closure to the left of the ♦ is the gage-indicated value, the number to the right is the total, corrected value (with 30.2 mm added), and can be directly compared to the manual closure data values. The 30.2 mm "correction" was added to these remote closure values only if they were obtained after the number of "days to spacer contact" days listed in **Table 5.5.1**.

The remote-reading (gage) vertical-displacement borehole closure data histories for test emplacements TRH01, TRH02, TRH03, and TRH04 (for gages TR21X, TR22X, and TR23X, where X = 1 to 4) are presented in **Figures 5.5-1** through **5.5-12,** respectively. The data plots shown for TR211, TR212, TR213, and TR214 (**Figures 5.5-1**, **5.5-4, 5.5-7,** and **5.5-10**, respectively) are somewhat finer in detail than the "Level 3" data quality plots used for all other gage data. These particular plots were made with a somewhat smaller "sieving factor," but still only include quality assurance-approved Level 3 data. The added level of visual detail will be useful for the interpretations of early data, in the -27 day to + 2-year range, to be discussed in Section 7.3.

As a first approximation, we have assumed that the observed vertical-displacement borehole closures shown in **Figures 5.5-1** through **5.5-12** are linear, i.e., that the slope(s) of the displacement histories are constant. Consequently, **Table 5.5.2** lists the calculated linear rates of vertical-displacement borehole closure in units of mm/year, over almost the entire period of heated-test operations. Our assumption of linearity, however, may be somewhat incorrect in that there could be some slight, non-linear decrease in slope (rate) over the last several hundred days of each observation period, e.g., in the 900 to 1,100 day or the +1,600 day periods of observation. If there are decreases in closure rates with time, the calculated linear rates listed in **Table 5.5.2** may be slightly greater in magnitude, i.e., conservative, than actual or calculated (Section 6.3) rates over an approximate five-year time period.

In some instances, linear closure rates from the period from about -27 days through day t = 0 are also listed in **Table 5.5.2**, in order to include all measured data. We calculated these closure rates or slopes over a selected time period using both "sieved" remote-gage data and manual measurements. Calculations of gage data from 0 through about 1,800 days were performed with the same linear regression analysis program, LINREGS, as described in Section 5.4. Slopes for the periods of about -27 through 0 days, and 0 through 50 days, were manually calculated. Vertical-displacement closure rates for the -27 through 0-day period were preliminarily reported (Tyler et al., 1988) to be in the range of 22 to 42 mm/year. Closure gage calibrations and gage polarities used previously were corrected and modified since that time, resulting in somewhat different, lower-magnitude results. All closure measurements and rates reported herein are based on certified, Quality Assurance Level 3 approved data.

The closure rate, or slopes, of the manual data was computed by a separate linear regression analysis (by Tech Reps, Inc.) that also uses the method of least squares.

Table 5.5.2 Calculated Vertical-Displacement Borehole Closure Rates for RH TRU Test Emplacements

Test Hole: Gage/Location	Closure Rate (gage data)	Linear Slope Period	Closure Rate (manual data)	Linear Slope Period
TRH01:	mm/yr (in./yr)		mm/yr (in./yr)	
TR211/ -2.2m	18.6 (0.73")	-27 to -10 d		
TR211/ -2.2m	19.5 (0.77")	0 - 50.5 d		
TR211/ -2.2m	13.8 (0.54")	50 - 1826 d	14.5 (0.57")	12 - 36 mo.
TR221/ -3.0m	14.1 (0.56")	250 - 1826 d	13.7 (0.54")	12 - 36 mo.
TR231/ -3.7m	14.8 (0.58")	400 - 1650 d	14.5 (0.57")	12 - 36 mo.
TRH02:				
TR212/ -2.2m	17.3 (0.68")	-25 to 0 d		
TR212/ -2.2m	18.5 (0.73")	0 to 50 d		
TR212/ -2.2m	13.1 (0.52")	50 - 1826 d	12.5 (0.49")	12 - 36 mo.
TR222/ -3.0m	12.1 (0.48")	970 - 1826 d	11.1 (0.44")	12 - 36 mo.
TR232/ -3.7m	10.3 (0.41")	520 - 1826 d	10.2 (0.40")	12 - 36 mo.
TRH03:				
TR213/ -2.2m	11.2 (0.44")	-27 to 0 d		
TR213/ -2.2m	16.9 (0.67")	0 to 50 d		
TR213/ -2.2m	14.8 (0.58")	50 - 1826 d	12.8 (0.51")	12 - 36 mo.
TR223/ -3.0m	15.3 (0.60")	350 - 1826 d	15.2 (0.60")	12 - 36 mo.
TR233/ -3.7m	13.1 (0.52")	520 - 1826 d	12.6 (0.50")	12 - 36 mo.
TRH04:				
TR214/ -2.2m	16.9 (0.67")	-27 to 0 d		
TR214/ -2.2m	20.0 (0.79")	0 to 50 d		
TR214/ -2.2m	14.6 (0.58")	50 - 1826 d	11.7 (0.46")	12 - 36 mo.
TR224/ -3.0m	14.6 (0.58")	500 - 1430 d	11.2 (0.44")	12 - 36 mo.
TR224/ -3.0m	12.9 (0.51")	1450 -1826 d		
TR234/ -3.7m	12.7 (0.50")	270 - 1826 d	13.3 (0.52")	12 - 36 mo.
TRH05: - 2.2 m			14.3 (0.56")	18 - 36 mo.
- 3.0 m			14.4 (0.57")	18 - 36 mo.
- 3.7 m			11.2 (0.44")	18 - 36 mo.
TRH06: - 2.2 m			**7.41 (0.29")**	18 - 36 mo
- 3.0 m			11.2 (0.44")	18 - 36 mo.
- 3.7 m			13.6 (0.53")	18 - 36 mo.
TRH07: - 2.2 m			10.7 (0.42")	18 - 36 mo.
- 3.0 m			9.74 (0.38")	18 - 36 mo.
- 3.7 m			8.29 (0.33")	18 - 36 mo.
TRH08: - 2.2 m			11.5 (0.45")	18 - 36 mo.
- 3.0 m			11.5 (0.45")	18 - 36 mo.
- 3.7 m			9.53 (0.38")	18 - 36 mo.

[Note: **bold** value suspicious, probably inaccurate]

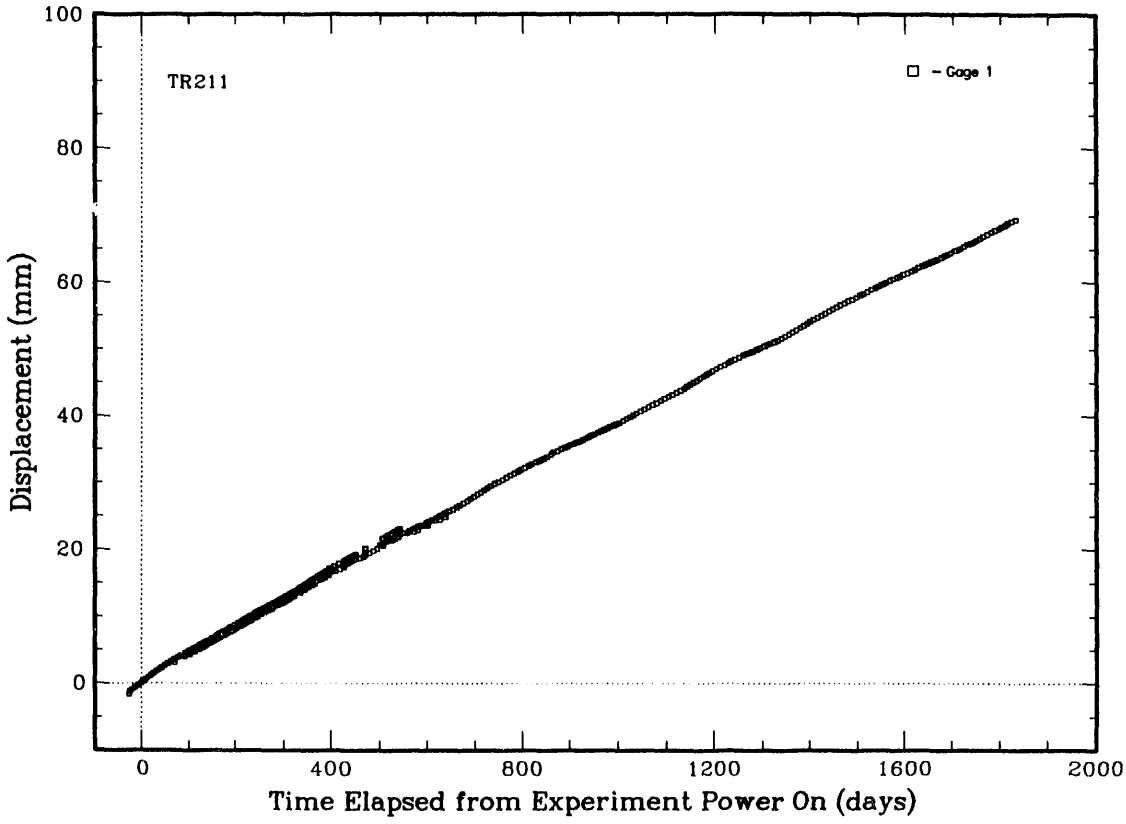

Figure 5.5-1 Vertical Displacement Gage TR211 History (TRH01)

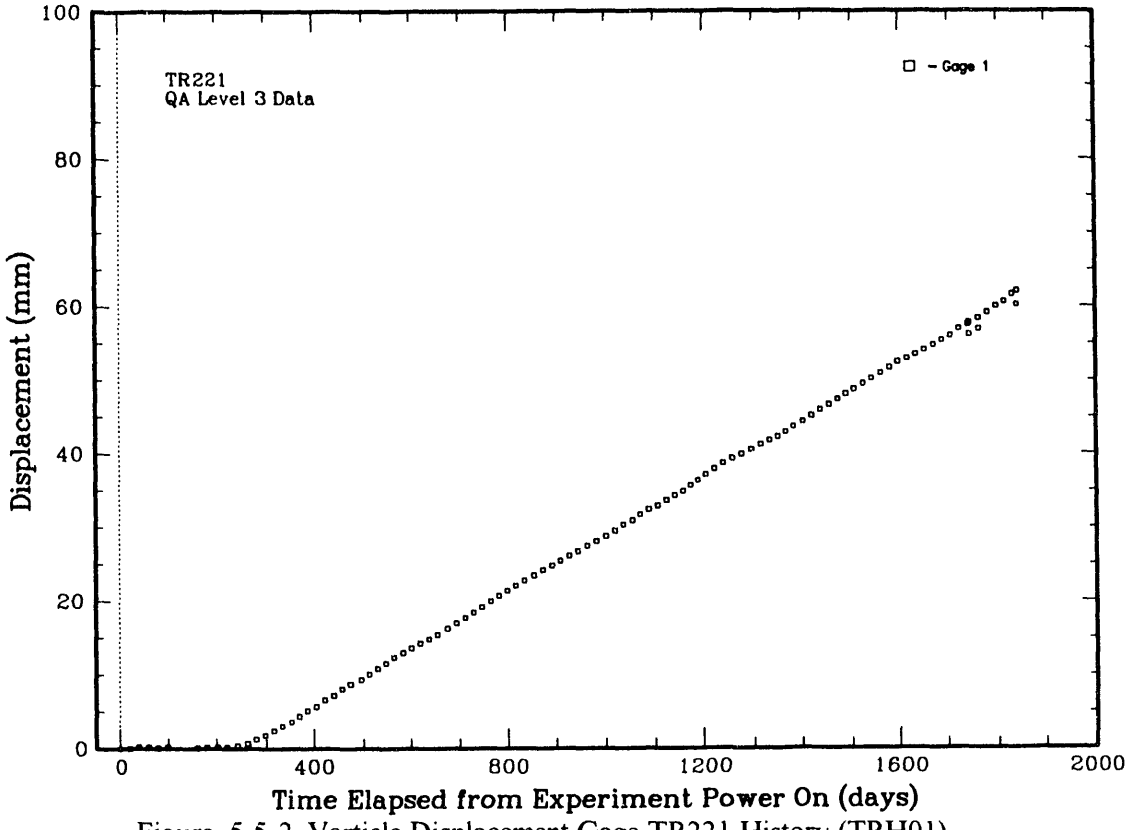

Figure 5.5-2 Verticle Displacement Gage TR221 History (TRH01)

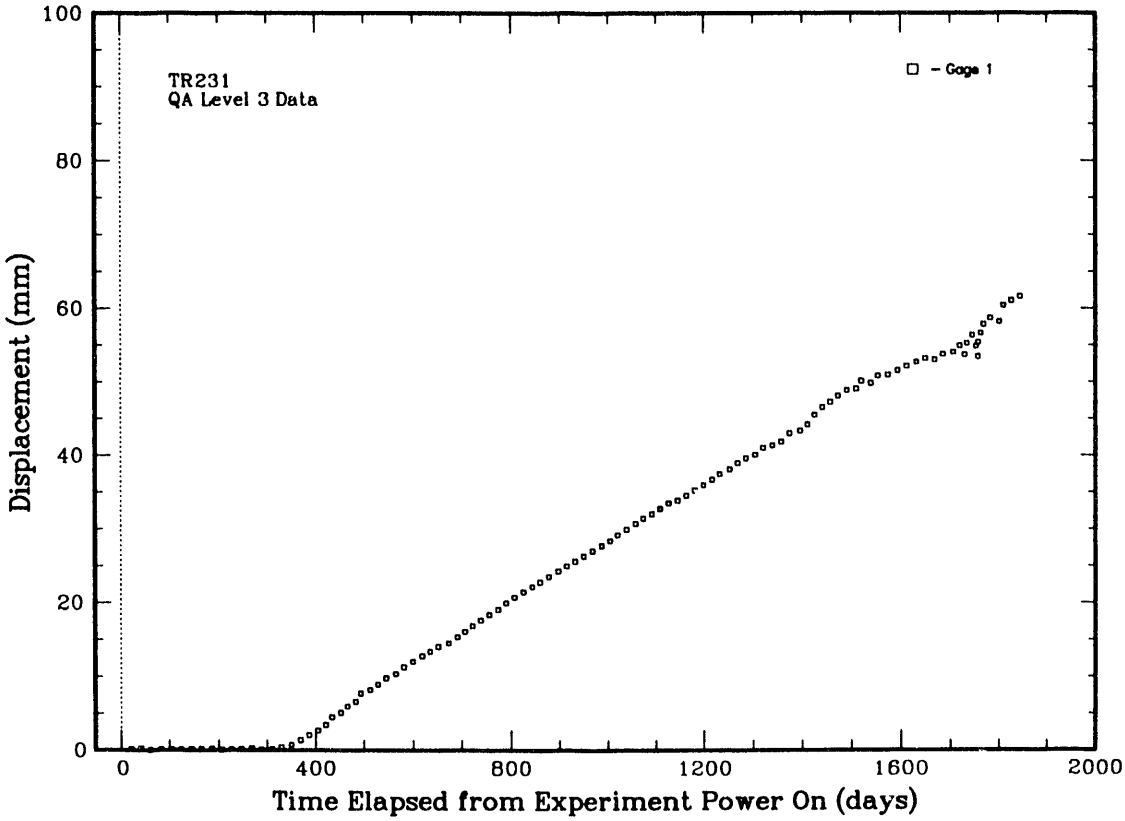

Figure 5.5-3 Vertical Displacement Gage TR231 History (TRH01)

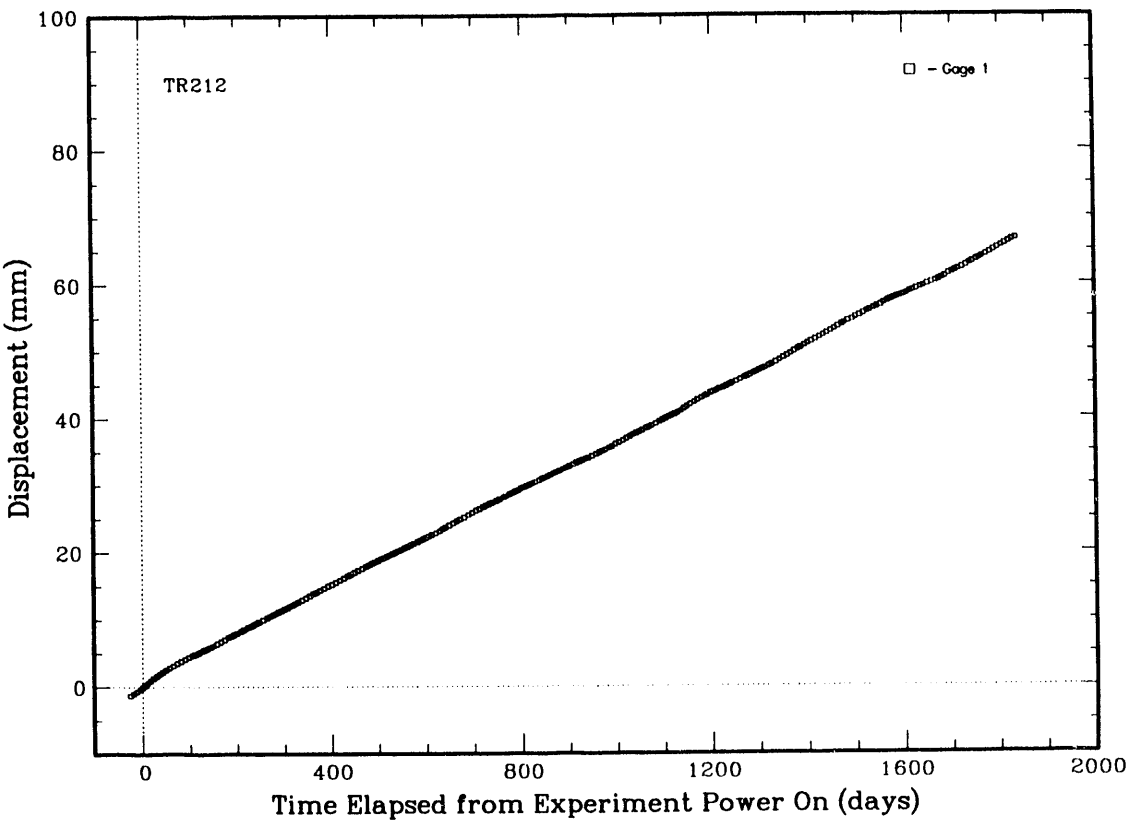

Figure 5.5-4 Verticle Displacement Gage TR212 History (TRH02)

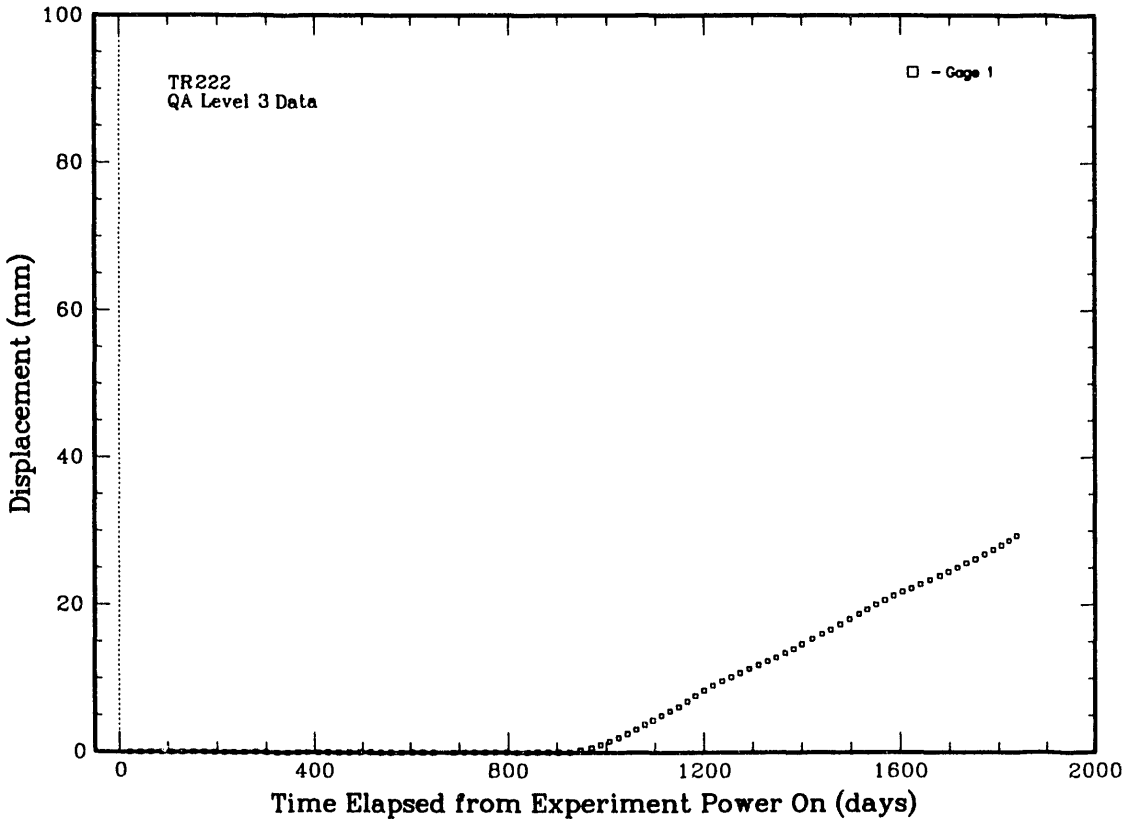

Figure 5.5-5 Vertical Displacement Gage TR222 History (TRH02)

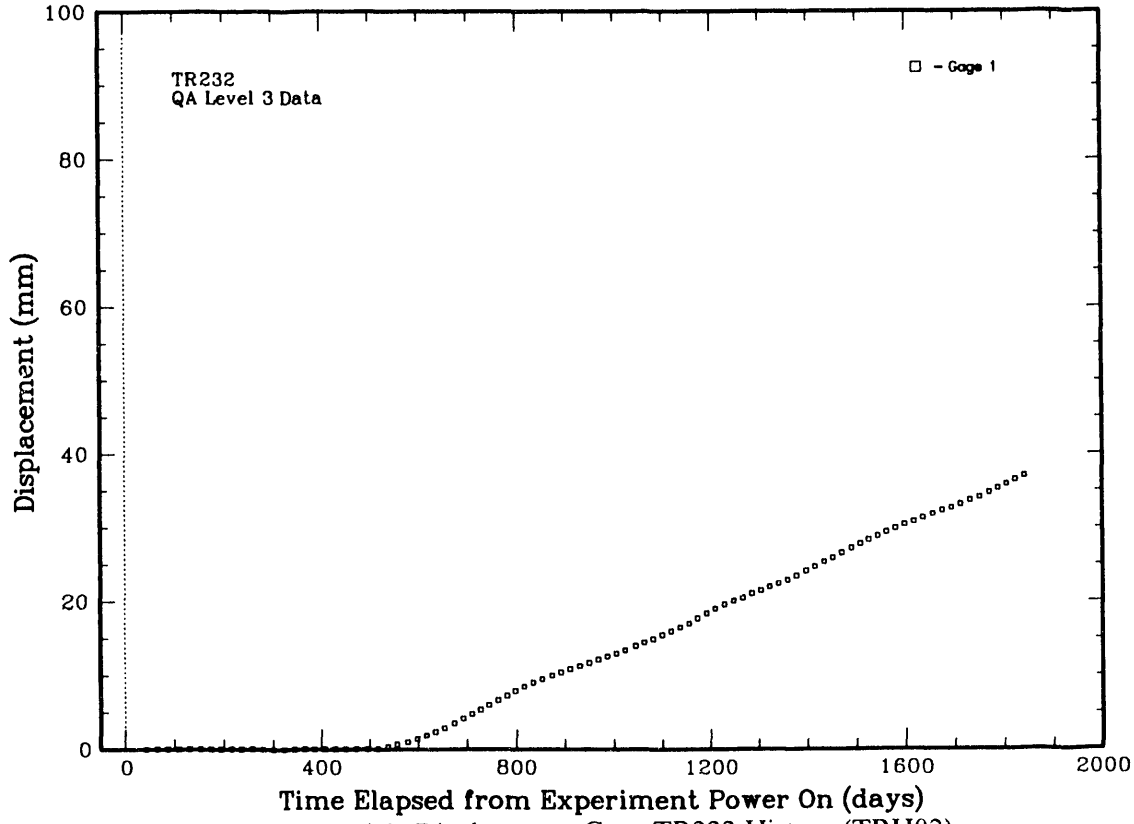

Figure 5.5-6 Verticle Displacement Gage TR232 History (TRH02)

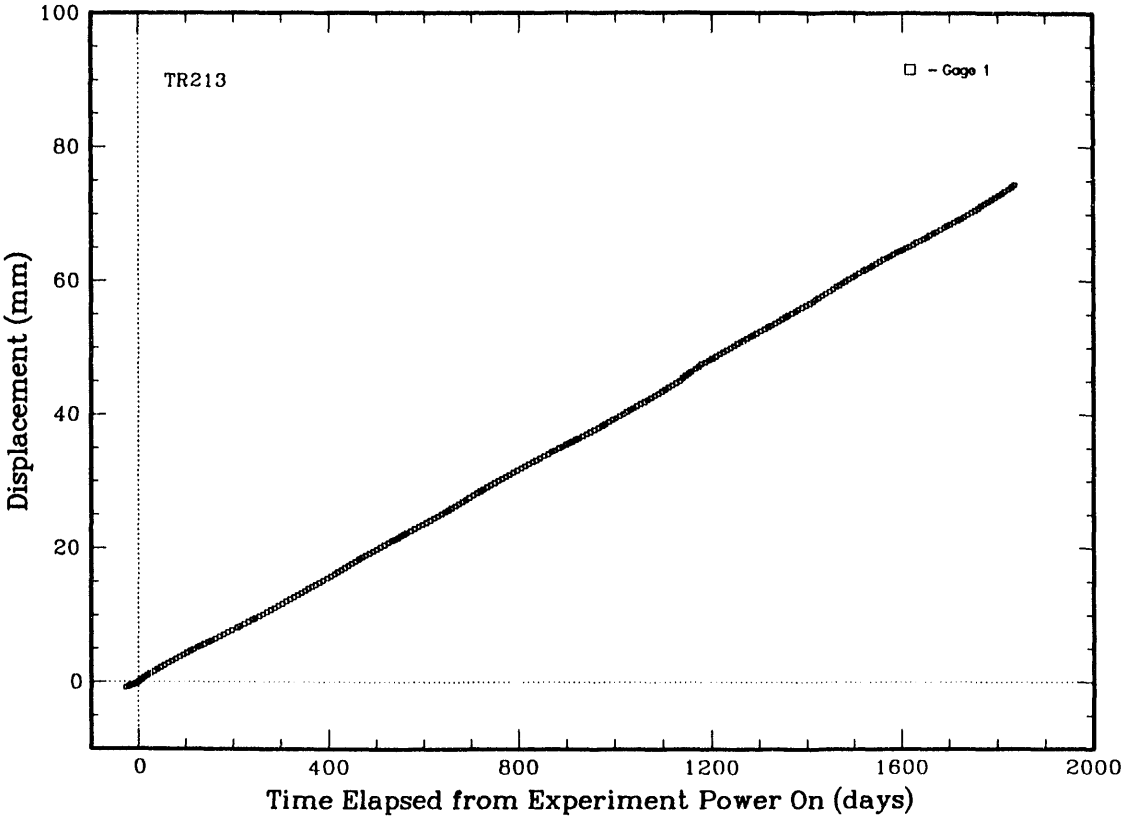

Figure 5.5-7Vertical Displacement Gage TR213 History (TRH03)

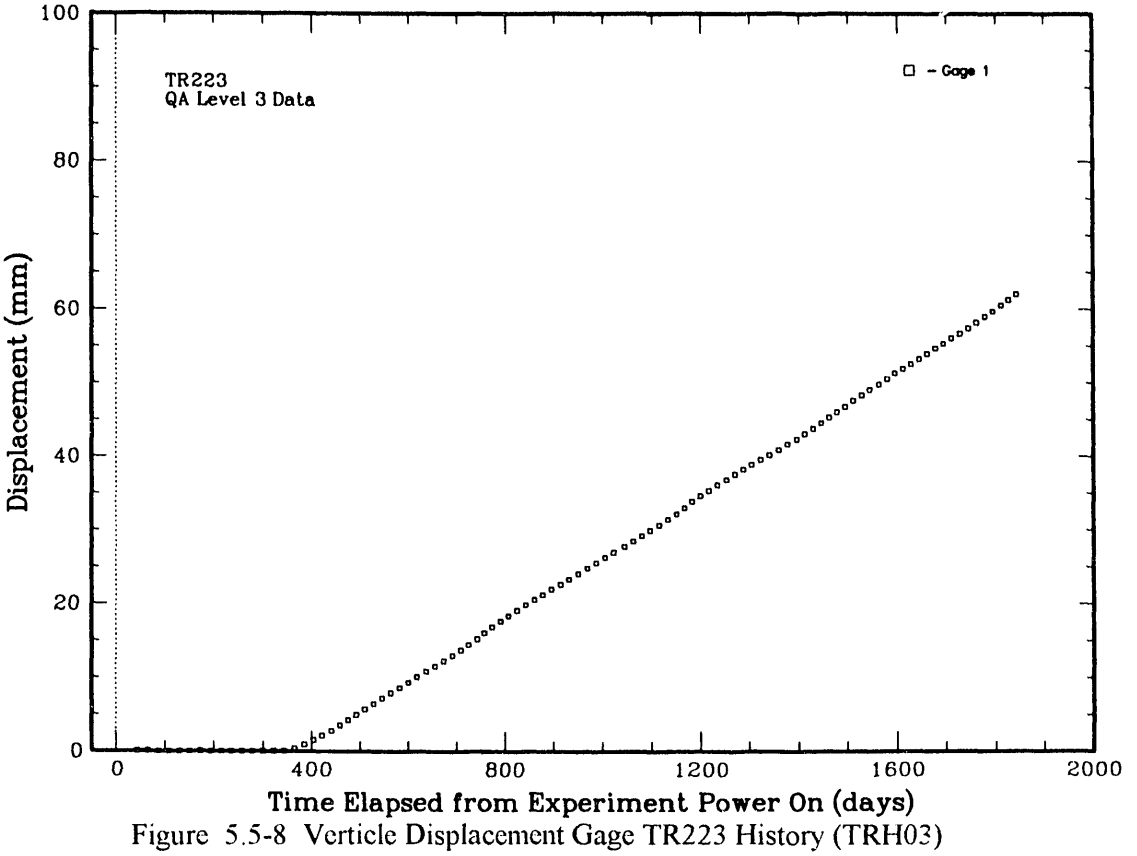

Figure 5.5-8 Verticle Displacement Gage TR223 History (TRH03)

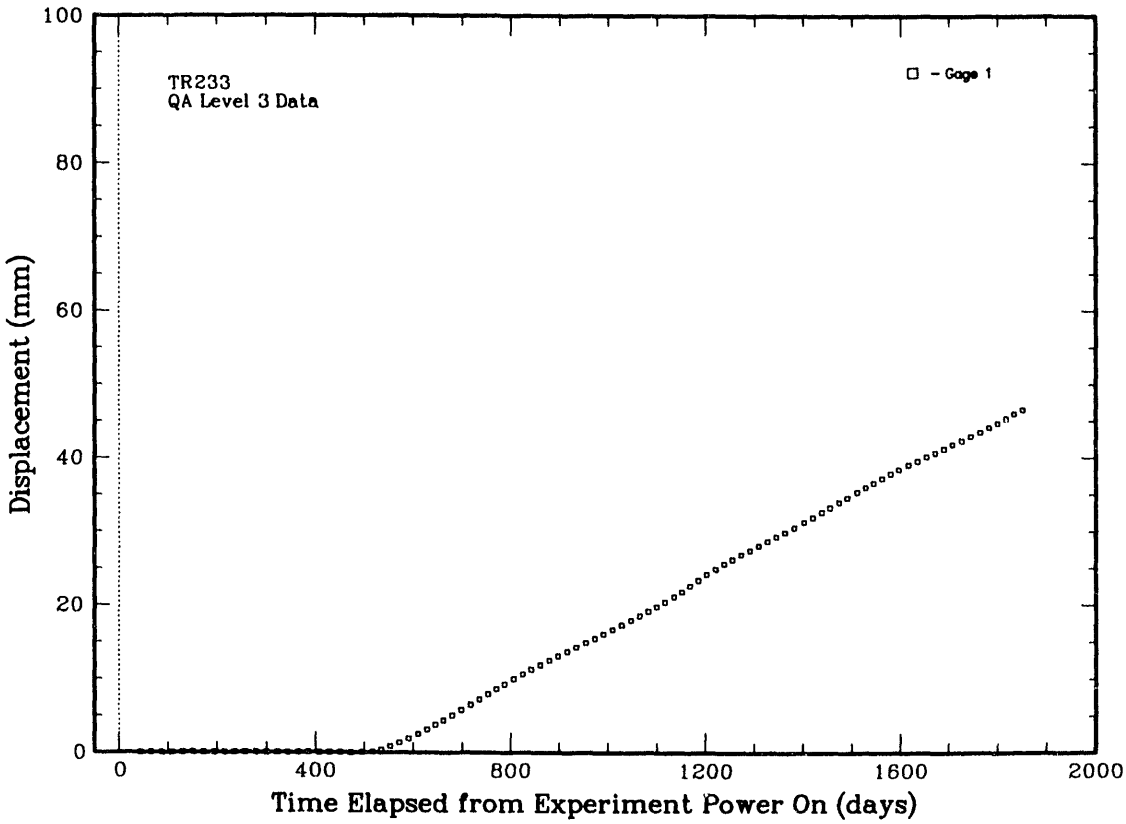

Figure 5.5-9 Vertical Displacement Gage TR233 History (TRH03)

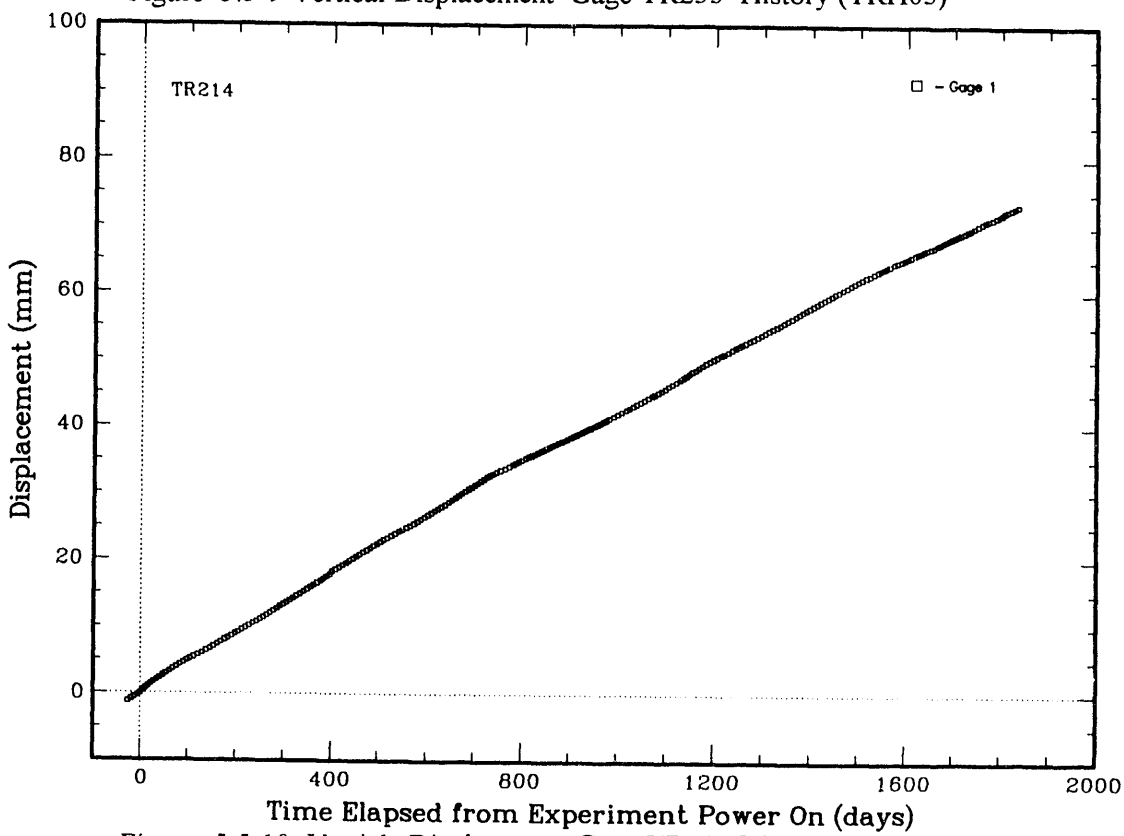

Figure 5.5-10 Verticle Displacement Gage TR214 History (TRH04)

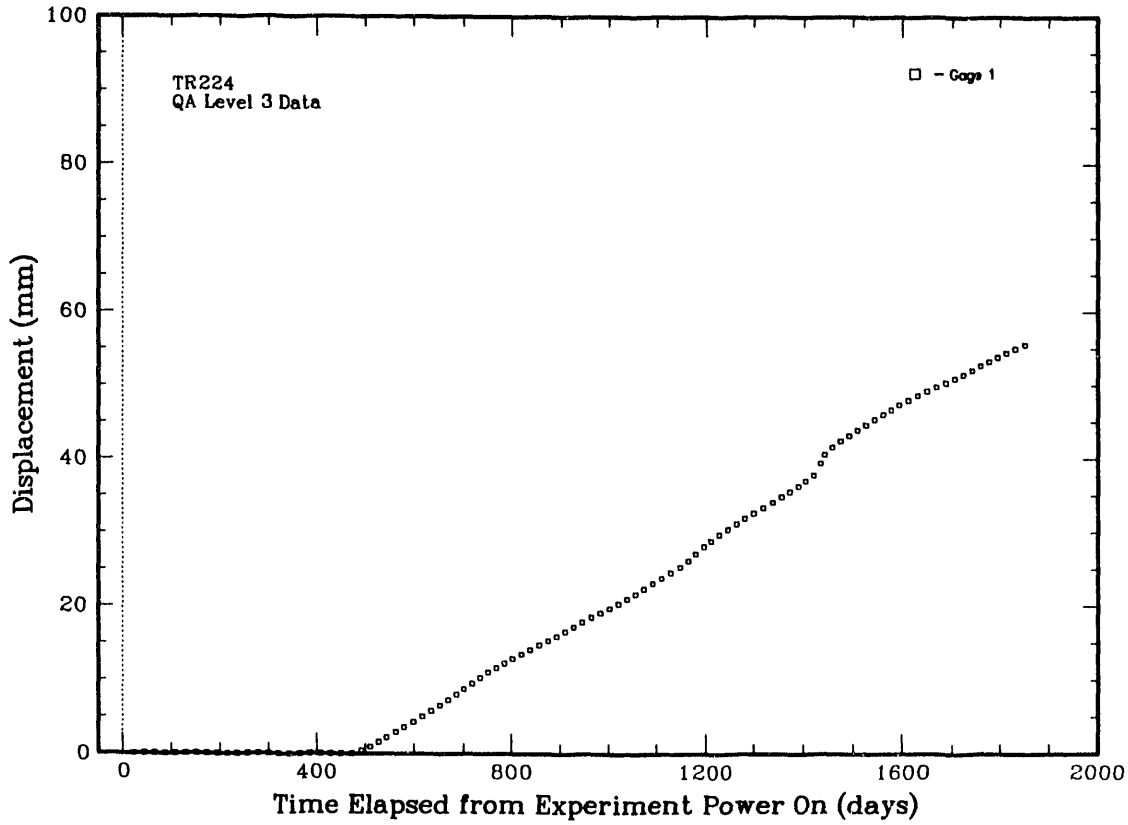

Figure 5.5-11 Vertical Displacement Gage TR224 History (TRH04)

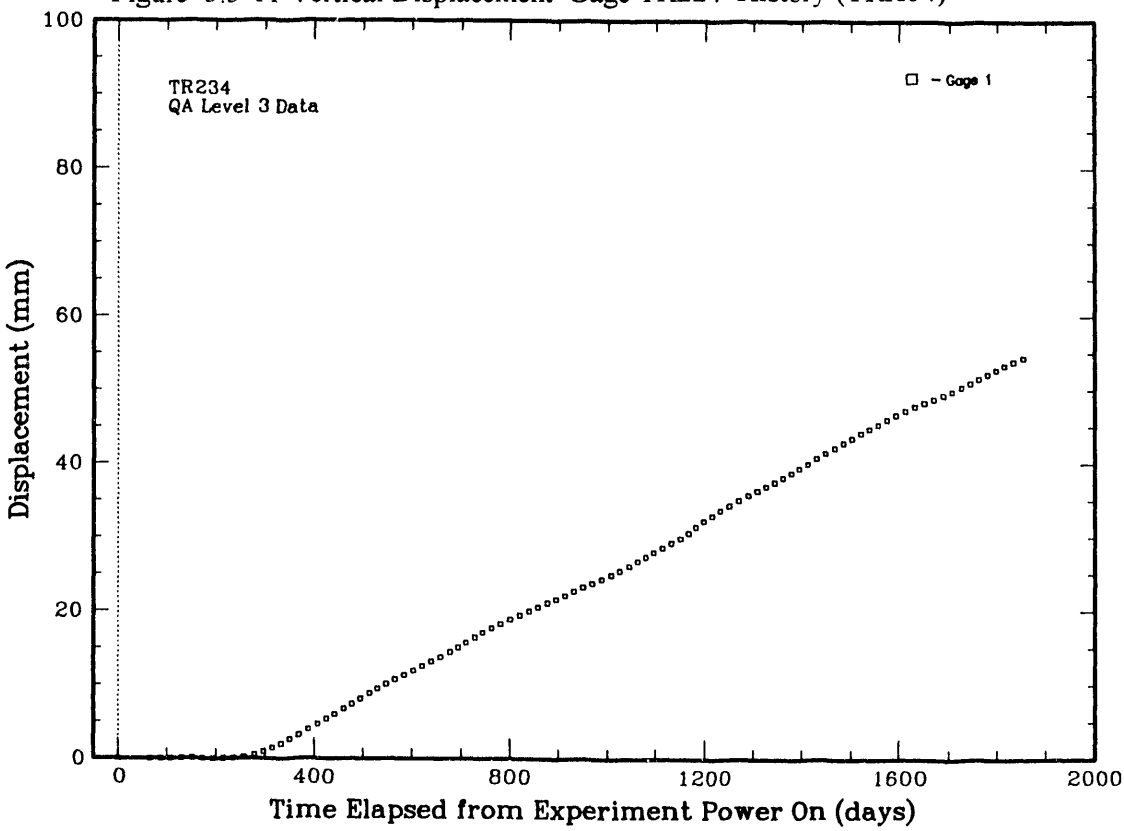

Figure 5.5-12 Verticle Displacement Gage TR234 History (TRH04)

5.5.2 Borehole Diameter Closure

We acquired manual measurements of both horizontal and vertical borehole diameters periodically -- if the particular RH TRU test container was removed from the emplacement borehole for detailed examinations. These measurements were made at three locations within the borehole that corresponded to the positions of the vertical closure gages, i.e., at 2.18 m, 2.95 m, and 3.71 m in from the rib. The precision of these diameter measurements is about ± 1.6 mm (± 1/16 in.). All of the manual borehole-diameter measurements obtained are listed in **Table 5.5.3.** As described in Section 3.1, the assumed, initial borehole diameters, immediately after coring, were about 919 mm (36.17 in.)

Table 5.5.3. RH TRU Manual Borehole-Diameter Measurements
(in units of mm)

	6 - Month		12 - Month		18 - Month		24 - Month		36 - Month	
Test Hole: *	Horiz. Diam.	Vert. Diam.	Horiz. Diam.	Vert. Diam.	Horiz. Diam.	Vert. Diam.	Horiz. Diam.	Vert. Diam.	Horiz. Diam.	Vert. Diam.
TRH01:										
-2.2 m	---	---	---	---	881	890	887	886	867	879
-3.0 m	---	---	---	---	882	890	886	891	872	879
-3.7 m	---	---	---	---	872	895	876	894	876	870
TRH02:										
-2.2 m	---	---	---	---	---	---	893	891	868	883
-3.0 m	---	---	---	---	---	---	902	901	890	898
-3.7 m	---	---	---	---	---	---	885	892	884	879
TRH06:										
-2.2 m	---	---	889	895	---	---	---	---	---	---
-3.0 m	---	---	889	895	---	---	---	---	---	---
-3.7 m	---	---	891	895	---	---	---	---	---	---
TRH07:										
-2.2 m	910	914	892	903	888	892	883	892	868	887
-3.0 m	908	914	892	903	889	893	882	896	869	880
-3.7 m	895	914	891	903	887	899	884	888	872	876
TRH08:										
-2.2 m	910	913	899	899	894	894	893	891	874	887
-3.0 m	908	911	897	902	891	895	888	895	876	883
-3.7 m	910	914	897	902	888	898	887	896	883	876

* = distance in from rib face

To supplement the manual borehole diameter measurements, we added eight remote-reading wire-extensometer, displacement (closure) transducers to measure both horizontal and vertical diameters and diameter-closure rates. These gage additions were not included in the Test Plan (Molecke, 1986). The physical coordinates of each added gage are listed in the final, "as-built" NOS instrument file in **Table 3.5**. We installed and activated these gages about 722 days, or 24 months, after the initiation of test heating.

We added the wire-extensometer gages to boreholes TRH01, TRH02, TRH07, and TRH08 to monitor both the vertical and horizontal diameter changes as a function of time. We selected these specific boreholes for monitoring because they have no backfill materials present and also have been opened and examined the greatest number of times. The extensometer gages are designated TR291 -1 (vertical) and -2 (horizontal), TR292-1 and -2, TR297-1 and -2, and TR298-1 and -2, respectively. These gages span the boreholes 1.23 m in from the rib face, about 16.5 cm in front of the emplaced test containers. The borehole-diameter closure data histories are illustrated in **Figures 5.5-13 through 5.5-16**.

Diameter closure rates calculated from the manual measurements of borehole diameters, listed in **Table 5.5.3**, and the calculated slopes of the extensometer-gage measured diameters, as illustrated in **Figures 5.5-13 through 5.5-20**, are summarized and compared in **Table 5.5.4.** We have made the same assumption of borehole closure rate linearity as discussed for vertical-displacement closures, as described in Section 5.5.1. The same caveats on linear rate conservatism apply to borehole diameter closures.

Table 5.5.4 Calculated Borehole-Diameter Closure Rates and Initial Diameters for RH TRU Test Emplacements

Test Hole: Gage # [in from rib]	1-Vertical Diameter Closure Rate	t = 0 Diam.	2-Horizontal Diameter Closure Rate	t = 0 Diam.	Linear Slope Period
TRH01:	mm/year (in./year)	Vert.	mm/year (in./year)	Horiz	
TR291 [-1.23m]	11.9 (0.47")		4.39 (0.17")		24 - 60 mo.
* manual [-2.2 m]	7.29 (0.29")	901	10.9 (0.43")	902	18 - 36 mo.
* manual [-3.0 m]	8.00 (0.32")	904	7.71 (0.30")	**897**	18 - 36 mo.
* manual [-3.7 m]	17.7 (0.70")	925	**non valid**	- - -	18 - 36 mo.
TRH02:					
TR292 [-1.23m]	11.7 (0.46")		6.19 (0.24")		24 - 60 mo.
** manual [-2.2 m]	8.00 (0.32")	907	**25.0 (0.98")**	**943**	24 - 36 mo.
** manual [-3.0 m]	**3.00 (0.12")**	907	12.0 (0.47")	**926**	24 - 36 mo.
** manual [-3.7 m]	13.0 (0.51")	918	**non valid**	- - -	24 - 36 mo.
TRH07:					
TR297 [-1.23m]	11.0 (0.43")		5.31 (0.21")		24 - 60 mo.
manual [-2.2 m]	10.2 (0.40")	914	15.3 (0.60")	913	6 - 36 mo.
manual [-3.0 m]	12.5 (0.49")	917	14.5 (0.57")	911	6 - 36 mo.
manual [-3.7 m]	15.0 (0.59")	920	9.03 (0.36")	**900**	6 - 36 mo.
TRH08:					
TR298 [-1.23m]	11.1 (0.44")		4.82 (0.19")		24 - 60 mo.
manual [-2.2 m]	9.43 (0.37")	912	13.2 (0.52")	915	6 - 36 mo.
manual [-3.0 m]	10.4 (0.41")	914	12.0 (0.47")	911	6 - 36 mo.
manual [-3.7 m]	13.9 (0.55")	920	10.0 (0.39")	909	6 - 36 mo.

Notes: **bold** values considered suspicious, possibly inaccurate
* only 3 data points available to calculate closure rates, slope
** only 2 data points available to calculate closure rates, slope

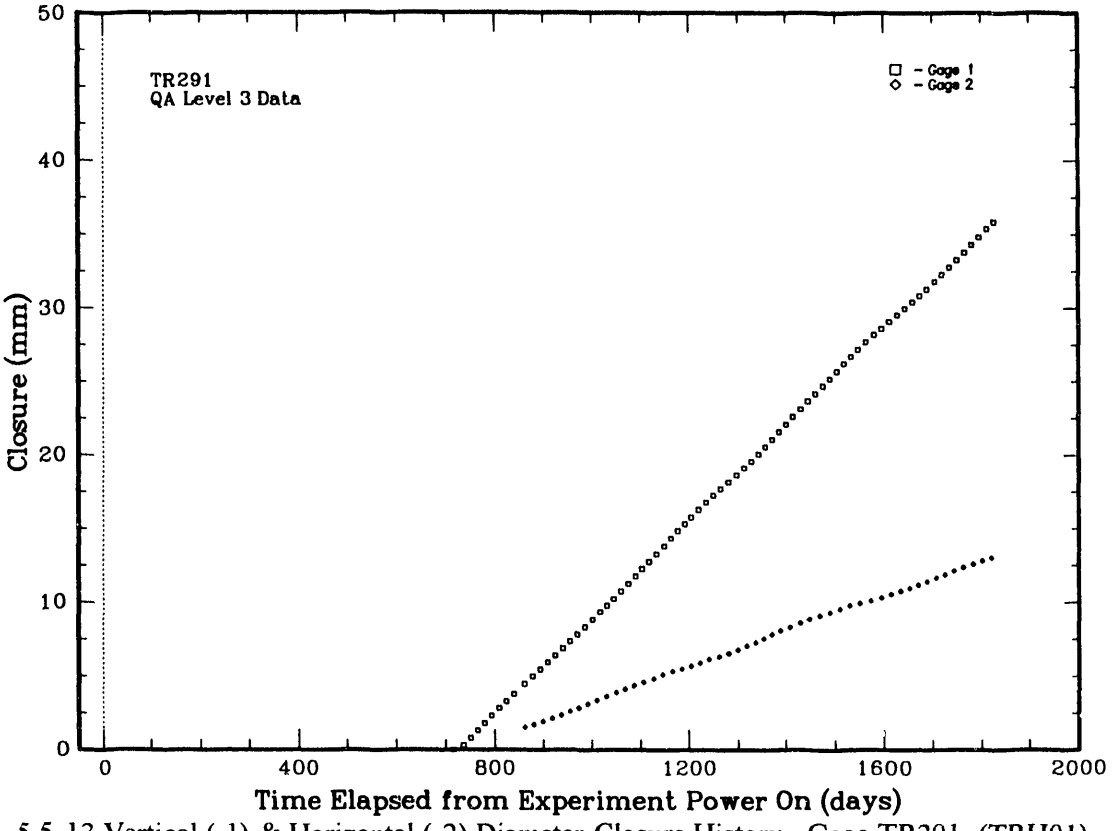

Figure 5.5-13 Vertical (-1) & Horizontal (-2) Diameter-Closure History, Gage TR291 (TRH01)

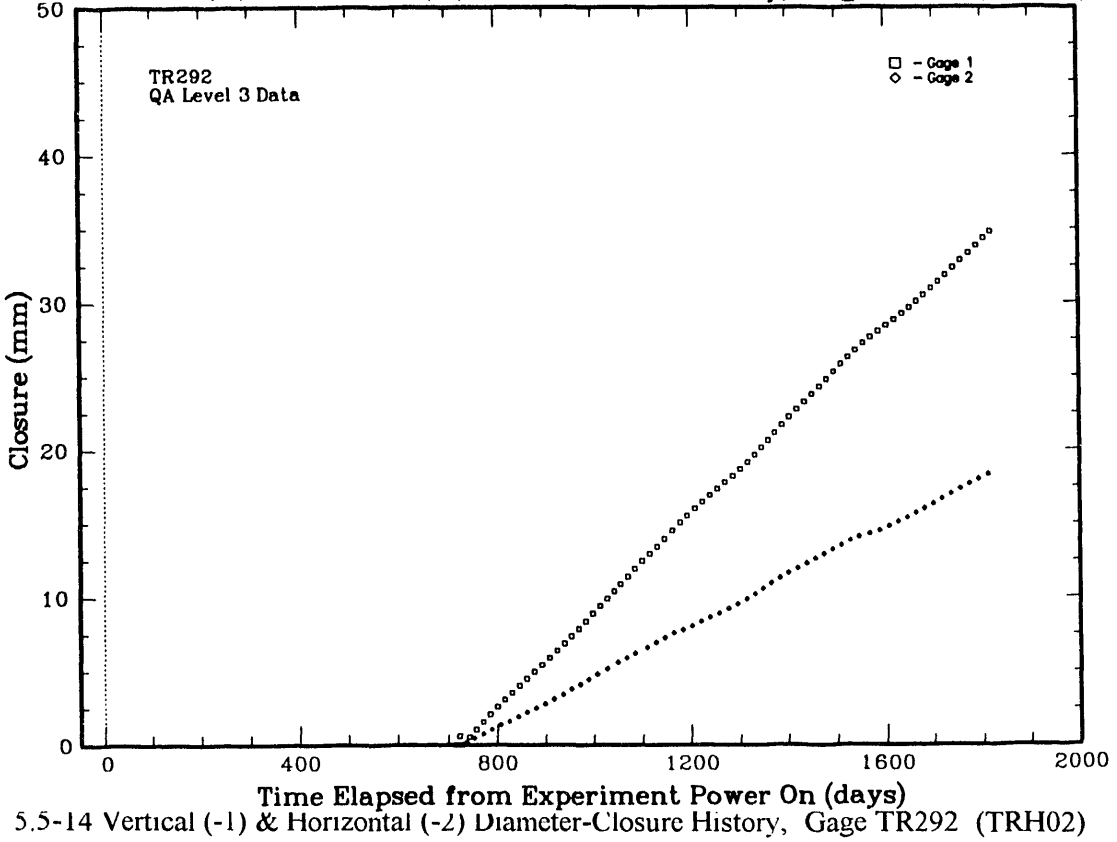

Figure 5.5-14 Vertical (-1) & Horizontal (-2) Diameter-Closure History, Gage TR292 (TRH02)

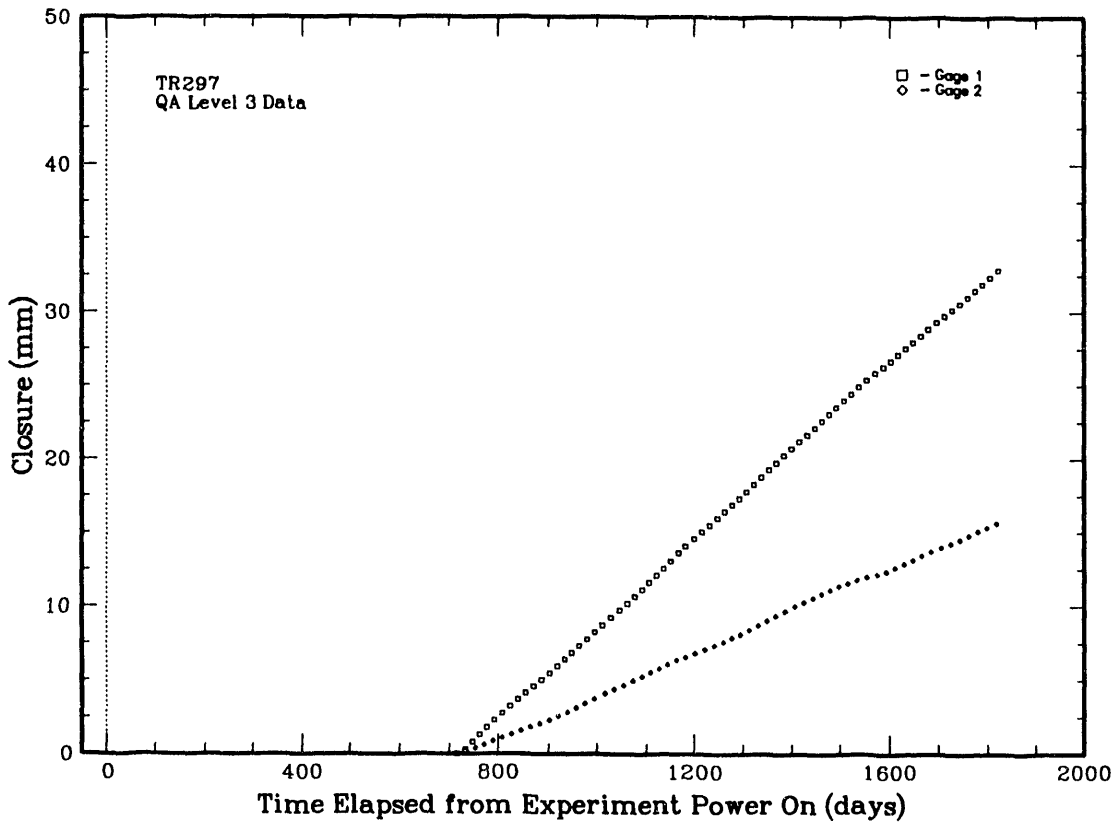

Figure 5.5-15 Vertical (-1) & Horizontal (-2) Diameter-Closure History, Gage TR297 (TRH07)

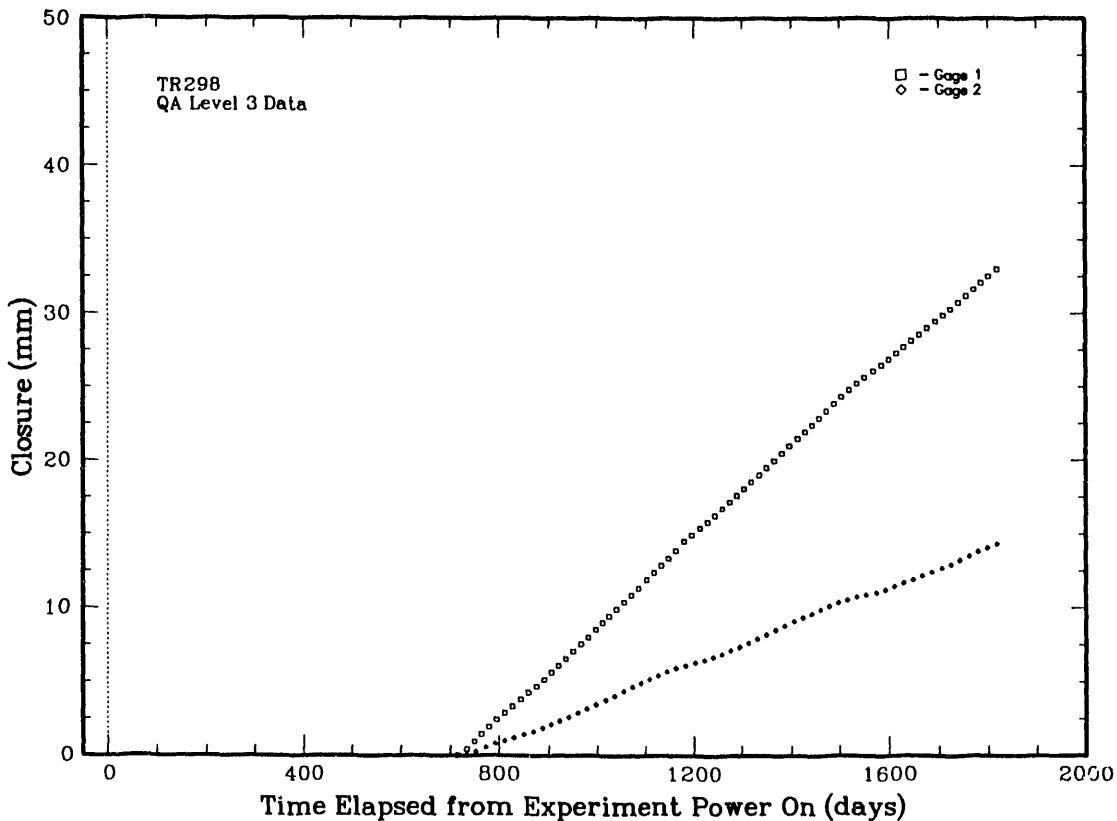

Figure 5.5-16 Vertical (-1) & Horizontal (-2) Diameter-Closure History, Gage TR298 (TRH08)

5.6 Assorted Test Observations and Analyses

We have opened all of the test emplacement boreholes for visual examinations and, occasionally, materials sampling from one to five times over the first 36 months of heated test operations, during the period of test room accessability. Boreholes TRH05, TRH07, and TRH08 were examined after 6 months; TRH01, TRH02, TRH03, TRH04, TRH06, TRH07, and TRH08 were examined after 12 months; and, all eight boreholes were examined after 18, 24, and 36 months. We conducted visual examinations for geochemical evidence of brine intrusion. Samples of salt and mineral efflorescences were taken for geochemical laboratory analyses. We also obtained samples of backfill material for determination of sorbed brine or residual moisture content. These geochemical evaluations are described in Section 5.6.1. Evaluations of the effects of brine and slightly elevated temperatures on test container corrosion are discussed in Section 5.6.2. In Section 5.6.3, we describe observations of salt fracturing adjacent to test boreholes as a function of time . A brief summary of in situ durability of the installed test instrumentation is discussed in Section 5.6.4.

5.6.1 Geochemical Sampling and Analyses

We frequently observed indications of minor brine intrusions, to varying degrees, into all of the unlined test boreholes. This was primarily evidenced by the presence of occasional, small blob-shaped efflorescences or stalactite drips on the top-half of the borehole surfaces, and of blob-precipitates, small stalagmites, and drip paths onto small areas of the top surface of the test containers, and occasionally, onto the closure gages. These efflorescences are illustrated in **Figure 5.6-1**, in a photo taken inside of test borehole TRH02 at the 36-month examination period. The population and size of these evaporated-brine occurrences in most boreholes increased somewhat with time.

We obtained several samples of the salt efflorescences for geochemical analyses. These samples ranged in color from clear-white to yellowish-brown. This coloration was due primarily to minor corrosion of some Ramset steel nails and steel clips that were used to hold instrumentation leads onto the top surface of the boreholes. X-ray diffraction analyses (by J.L. Krumhansl, Sandia National Laboratories) of these samples indicated that they are primarily halite, NaCl. Other minor X-ray peaks have been observed but are unidentified. Petrographic and SEM (scanning electron microscope) examinations of similar specimens revealed a variety of minor phases. Likely identification, based on an elemental content, are carnallite [$KMg(Cl)_3 \cdot 6H_2O$], sylvite [KCl], magnesium chloride, clays, and iron sulfate or chloride.

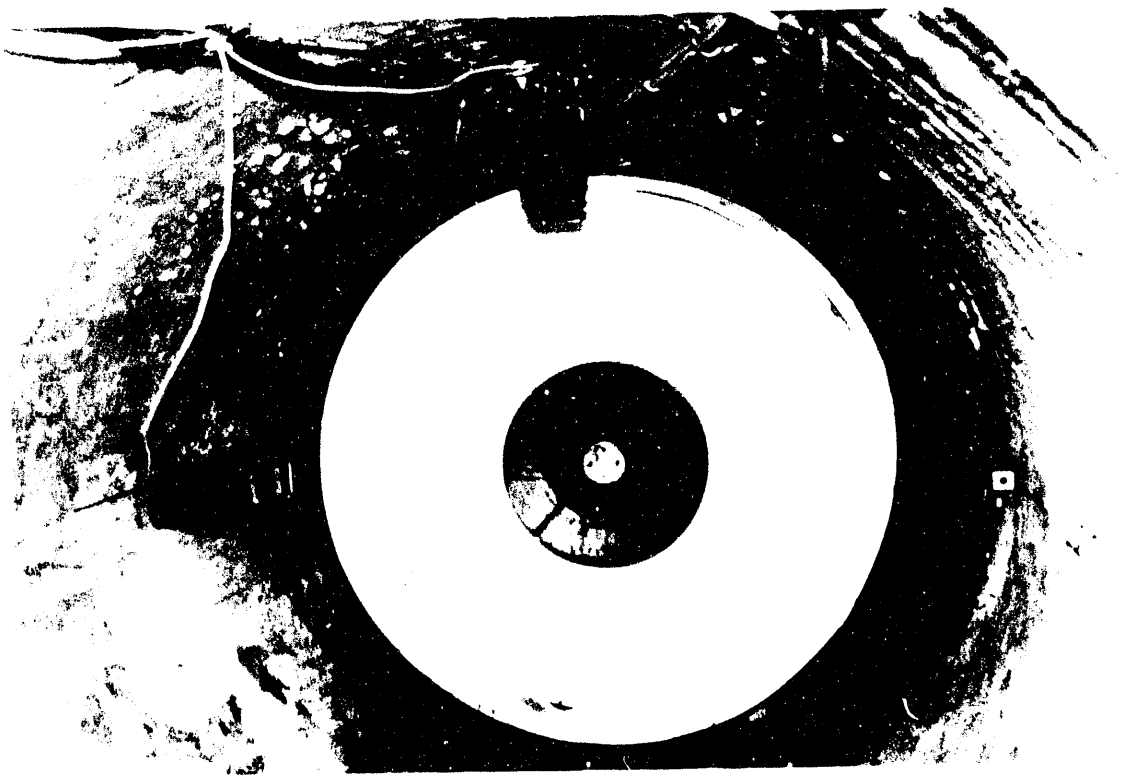

Figure 5.6-1 Brine effloresecences in borehole TRH02 at 36 months

We never observed any appreciable brine accumulations in the boreholes, except for borehole #1. Traces of brine on the bottom of borehole #1 appeared as a damp streak at 12 months; the damp spot had apparently evaporated and was not visible at the 18 month examination period. At 24 months, however, the brine had returned as a crusted-over salt "puddle," about 6 mm-deep, at the back end of this hole, underneath the test container. We obtained a 25 ml sample of this brine for analysis. A partial analysis of the major anions in this brine (257 parts per thousand, ppt, of Cl^-, 30.2 ppt of SO_4^{2-}, and 8.36 ppt of Br^-) indicated that this fluid was a partially evaporated, typical WIPP weep brine (Krumhansl et al., 1991). At the 36 month examination period, this "puddle" had evaporated, with only a salt "mush" remaining visible. We also observed some similar salt "mush" in borehole # 2 at 36 months.

Four of the 8 RH TRU waste test emplacements are partially filled with 70 wt. % bentonite/30 % silica sand backfill material. We also observed some indications of brine intrusion into these boreholes, as damp-appearing, slightly darker-colored regions in the backfill. We obtained "damp-appearing" backfill samples for laboratory moisture analyses. These samples were manually collected in small jars at the

backfill-salt-air interface, near the front (rib) end of the hole, or at the backfill-salt interface, when backfill was vacuumed out of test holes #4 and #6, for test canister removal and examination. Very little backfill material adhered to the sides of the heated canister in this situation, indicating a lack of dampness, and very little stuck to the sides of the borehole surfaces. The backfill material apparently sorbed essentially all brine drips intruding into the hole, or wicking into the hole from the sides. After sampling, we reemplaced the canister(s) and the original backfill material , and then turned-on the test again for continued exposure. These backfill samples were dried at 110 °C and yielded a sorbed-moisture content range of 5.38 % to 6.68 %. A dry-appearing 24-month backfill sample from directly in front of the container pintle in TRH04 yielded a 4.47% moisture content. Damp-appearing "lumps" from the same test emplacement, but near the borehole salt surfaces yielded somewhat higher moisture values of 6.2% through 8.2%. All of these measured moisture values are somewhat less than the nominal, maximum-allowable moisture value of backfill material, about 7 % (Pfeifle, 1987a). However, these measured values are all slightly above the nominal moisture value of about 3.9% for actual, initial bentonite/sand backfill, as described in Section 3.3.

Observations of "damp-appearing" backfill materials varied as a function of time. Boreholes with damp spots evident at the 6 or 12-month sampling period appeared to decrease in moisture level after 24 or 36 months. This decrease in damp backfill, similar to the decrease in the brine "puddle" reported for borehole # 1, is probably due to heat-assisted volatilization of the water and subsequent escape out of the borehole or, possibly, more uniform sorption into the bulk of the backfill.

We also obtained backfill sample cores in several boreholes by driving a "coring tube," a 38 mm to 76 mm-diameter, 1.5 to 3.0 m-long pipe, into the emplaced backfill, very near the salt-backfill interface, at the 3 o'clock position in the borehole. Analyzed moisture levels from a 6-month sample core in hole #5 ranged from 5.7 % to 5.9 %. Several 24-month sample cores ranged from 4.57 % through 6.03 %, 4.90 through 5.25%, and 4.45 through 5.24% over the sample length of 1.5 m.

We observed the interior, mid-height, horizontal side-surfaces of most of the boreholes to have hairline fractures in a region of appreciable clayey content. This grayish, clayey material coated the borehole walls in a somewhat scaly layer that was in some instances up to about 3 mm- to 6 mm- (0.25 in.) thick after 36 months. In some cases, the top layer of this sloughing, clayey material appears to overlap the bottom, lower portion. We obtained samples of this grayish, clayey material for laboratory evaluations. Geochemical analyses indicate that the samples consist of a mixture of a white fine-grain salt deposit and a

dark, reddish-brown mixture of clay and salt. The X-ray diffraction pattern of the white material indicated only halite. The clay yielded a diffraction pattern indicative of a small amount of anhydrite [$CaSO_4$], along with a complex mixture of clays. The clay peaks were identified as a mixture of chlorite, saponite, vermiculite, illite, and various interlayered mixtures of these phases. Although these clays do not have the capability of expanding nearly as much as bentonite (primarily montmorillonite), the presence of significant interlayering makes these clays plastic enough to be readily extrudable under applied stresses. It is important to note that these clays are typical of the argillaceous materials at the WIPP repository horizon, so that similar features may be expected elsewhere in the facility.

5.6.2 Corrosion Observations

Periodically, we have qualitatively evaluated all of the RH TRU test containers for signs of surface corrosion. Containers that were emplaced in boreholes containing no backfill material were simply rolled out of the hole, on their roller support assembly, and visually examined. Photographs were also taken, if appropriate. We also retrieved (and then reemplaced) two test containers, TRH04 and TRH06, for examination after 12 and/or 24 months from their 70 wt. % bentonite/30 % silica sand-backfilled holes. In several cases, brine had dripped from the top surface of the hole onto the top or sides of the painted RH TRU containers. There were either small blobs of salt crystals remaining on the cans, or, at the worst, slightly yellowish-colored stains and salt crystals on the paint. Basically, corrosion on the painted areas of all of the containers was insignificant, for at least the first 36 months of heated testing, in the relatively mild-corrosive, borehole-environment experienced. The unpainted, mild steel pintles of all test containers exhibited superficial rusting. This rusting has become more "flaky" as a function of time, but is still not considered significant. This superficial pintle rusting is evident in **Figure 5.6-1**. The RH TRU containers appear to have adequate physical integrity to remain unbreached by corrosion for more than the proposed initial five-years of a pilot-phase retrieval period.

There is a NUCFIL HEPA filter assembly installed in the pintle top of every RH TRU waste container, in order to vent any internally generated gases. After 24 months of heated testing, we observed that essentially all of the filters had appreciable corrosion on the top cover plate of the filter housing. This corrosion was directly on, and adjacent to the heat affected zones of four spot welds that attach the "splash" cover (fabricated out of 30 gage tinplate) over the vent passage. At the 36 month examination period, several of these "splash" covers had small corrosion holes adjacent to the spot welds, in addition to flaky uniform corrosion.

We observed few visible signs of corrosion on other support equipment and instrumentation within the RH TRU emplacement holes. The Inconel 600 bottom roller assemblies (visible in **Figures 3.1-3** and **3.2-5**) and the Inconel-600 clad instruments appeared untouched. The borehole plugs used in these tests, as visible in **Figure 3.1-4**, were painted with a coal tar epoxy paint (Molecke, 1986) and also appeared to be totally unaffected by corrosion -- when not mechanically abraded. We noted some minor uniform corrosion on plug areas that had been abraded during the test removal, examination, and retrieval cycles. The coal tar epoxy paint or coating was shown to be superior (in laboratory testing of anti-corrosion effectiveness, scratch testing, and blistering adhesion) to the enamel used for TRU containers, under salt repository-relevant conditions (Braithwaite and Molecke, 1979). However, based on the laboratory testing, the enamel paint used for TRU waste containers was also judged to be quite adequate for its intended application.

5.6.3 Observations of Borehole Fracturing

We examined almost all of the RH TRU emplacement holes at the 12, 18, 24, and 36 month times for signs of salt fracturing and cracking along the length of the holes. Only a few of the boreholes were examined at the 6 month period. We first observed cracks along the top of the borehole circumference, parallel to the rib-face, in many of the boreholes at 12 months, and in all the boreholes after 18 months. In all boreholes, these circumferential cracks appear to grow, to be increasing in size (both width and length) and number as time progressed. Our observations on these circumferential cracks as a function of time are summarized in **Table 5.6.1,** along with several other observations of salt slabbing at the hole-face.

Most of these cracks are along the top half of the hole, about 0.36 to 0.53 m in from the rib surface; most are centered at 0.46 m (18 inches) in, and in a few cases there are two cracks. We also noticed one crack 3 m in from the rib. These cracks range from 3 mm wide, initially, growing up to 51 mm after 36 months at their maximum opening. Crack depths also grew as a function of time, from 1.3 cm up to about 30 cm-deep. Cracks in the bottom surface of most of the boreholes became noticeable after 36 months. These bottom cracks were closer to the rib-face, about 0.20 to 0.33 m in, and in all instances tended to connect to the top crack through a series of minor fractures along the borehole sides. These bottom cracks also tended to extend toward the hole, or rib-face, resulting in the formation of salt "slabbing." The most obvious example of slabbing started at the near-bottom edge of hole #6, then extended toward adjacent hole #4. These observations of fracturing can be compared directly with other studies (Borns and Stormont, 1988) made of similar excavation effects and "disturbed rock zones" in the WIPP. It would be quite bene-

Table 5.6.1 Observations of Circumferential Borehole Fracturing, Slabbing

Borehole	Examination Period	Observations:
# 1	12 mo.	Top crack, ~0.46 m in from rib, ~3 to 12 mm-wide, over top 180° of hole.
	18 mo.	Top crack now ≤ 12 mm-wide, ~ 10 cm-deep; minor bottom crack at ~ 0.33 m in.
	36 mo.	Top crack ≤ 25 mm-wide, ≥ 15 cm-deep. Bottom crack, ~0.33 m in from rib, ≤ 25 mm-wide, over bottom 45° of hole, almost connecting to top crack.
# 2	12 mo.	Observed top circumerential crack at ~ 3 m in from rib, but not measured.
	18 mo.	Top crack, ~0.46 m in from rib, ≤ 5 mm-wide, ~12 mm-deep, ~0.4 m-long.
	24 mo.	Top crack now ~6 mm-wide. Several minor bottom cracks seen, ~15 cm in from rib.
	36 mo.	Top crack ≤ 10 mm-wide, ~10 cm-deep, ~35 cm-long, top 45° of hole; second, minor top crack ~0.43 m in from rib. Bottom crack, ~0.20 m in, extending almost to hole face and also almost connecting to top cracks; some hole-front slabbing evident.
# 3	12 mo.	Top crack, minor, ~0.46 m in from rib.
	18 mo.	Top crack , ~0.38 m in from rib, ≤ 3 mm-wide, ≤ 2.5 cm-deep.
	36 mo.	Top crack, at ~0.46 m in, ≤ 6 mm-wide, top 45° of hole; second top crack at ~0.38 m in, ≤ 10 mm-wide, top 90°.
# 4	12 mo.	Top crack , ~0.46 m in from rib, ≤ 25 mm-wide.
	18 mo.	Top crack , ~0.46 m in from rib, ≤ 10 mm-wide, ≤ 7 mm-deep; second top crack, ~0.34 m in, ≤ 44 mm-wide, ≤ 18 cm-deep.
	24 mo.	Top crack at ~0.46 m in from rib, top 60° of hole, with interconnecting small-fracture pattern to bottom crack, ~0.20 m in from rib. Brownish, overlapping clay at sides.
	36 mo.	Top crack , ~0.36 m in from rib, ≤ 32 mm-wide, ≤ 23 cm-deep, top 180° of hole. Bottom crack now ~19 mm-wide, ≤ 10 cm-deep, almost connecting to top cracks.
# 5	18 mo.	Top crack, at ~0.46 m in, ≤ 22 mm-wide, ≤ 10 cm-deep, top 90° of hole.
	24 mo.	Top crack now ≤ 25 mm-wide, ≤ 15 cm-deep, top 180° of hole.
	36 mo.	Top crack now ≤ 25 mm-wide, ≤ 18 cm-deep.
# 6	18 mo.	Top cracks at ~0.37 m and 0.43 m in, ≤ 6 mm-wide, ≤ 25 mm-deep. Significant rib slabbinging at hole face, at 8 O'clock position; slab ~ 10 to 15 cm-thick and ~46 cm-long, with crack parallel to the rib and extending toward hole # 4.
	36 mo.	Top crack at ~0.37 m in now ≤ 20 cm-deep, top 120° of hole. Bottom crack at ~0.22 m in, ≤ 10 cm-deep, connects to hole-face slab at 8 O'clock position.
# 7	12 mo.	Observed slight hairline fracturing at the sides of hole in a region of high-clay content; hole sides are somewhat "flakey."
	18 mo.	Top crack, at ~0.53 m in, ≤ 41 mm-wide, ≤ 19 cm-deep.
	24 mo.	Top crack now ≤ 51 mm-wide, ~ 15 to 20 cm-deep. Clayey hole-side coating 3 - 6 mm-thick.
	36 mo.	Top crack now ~ 30 cm-deep, top 120° of hole. Bottom crack at ~0.25 m in, ≤ 19 mm-wide, ≤ 25 mm-deep, bottom 45° of hole.
# 8	12 mo.	Observed slight hairline fracturing at the sides of hole in a region of high-clay content; hole sides are somewhat "flakey."
	24 mo.	Top crack ~0.48 m in from rib, ≤ 20 cm-deep.
	36 mo.	Top crack now ≤ 25 mm-wide, ~ 10 cm-deep, top 120° of hole, almost connecting to bottom crack. Bottom crack ~0.23 m in from rib, ≤ 32 mm-wide, ≤ 10 cm-deep, bottom 90° of hole, and extending to hole-face with some slabbing. The slabbing is parallel to the bottom 180° of hole.

ficial to make further, time-dependent observations on the growth of fractures in and around test boreholes #1 through #6 during the final test termination operation, approximately six years after test turn-on.

It appears that the horizontal salt surfaces may be separating somewhat, with the innermost surfaces moving inward, decreasing the hole diameter, while slightly deeper, adjacent portions of the salt are moving outward. In some cases, the top, higher portion of the horizontal surfaces of mixed salt and clay (refer to Section 5.6.1) appear to slightly overlap the bottom, lower surfaces. These observations help explain why the measured horizontal hole diameters are somewhat smaller than the vertical diameters, as shown in **Table 5.5.3**). The horizontal holes may indeed be ovalling as we originally assumed, but the salt surface layers are fracturing, with innermost (side) layers either staying in place or not moving outward as fast as the deeper layers. Although the observed salt and clay mixtures do not expand nearly as much as the smectite material bentonite (montmorillonite), the presence of significant interlayering makes these clays plastic enough to be readily extruded into or out of small fractures under applied rock salt stresses. This could essentially help seal or plug small fractures.

5.6.4 Instrumentation Durability and Maintenance

The remote-reading thermocouples, pressure gages, and borehole closure gages installed in the RH TRU test emplacement holes have survived very well for more than 60 months of active operations. Most maintenance activities were conducted during the first three years of testing, when we periodically opened test boreholes for inspections, with container removals and reemplacements. Gages were most likely to be pulled loose, damaged, or have their signal and power leads disconnected during these inspection periods. All maintenance and repair activities were documented on "Measurand Action Data" (MAD) sheets. These MAD sheets were signed, quality assurance approved, and are stored in WIPP QA files.

None of the "near-field" thermocouples failed during the entire period of test service. One "heater" thermocouple, TR004T1, no longer provided output signals after about 1070 days. The exact cause of failure was not determined since no examination and repair of this test system could be conducted; test room access was no longer available at this time. One other heater thermocouple, TR002T2, inside of test container TRH02, was received from the fabricator in the failed condition; this TC could not be accessed for repair.

All of the pressure gages have performed adequately for more than five years of heated test service. These gages have experienced some periods of noisy signal output or brief losses of data output due to disconnections in their power or data leads. Most of these problems were due to loose connections in leads or splices, dirty contacts in relay boards, or failure of power supplies. Most of these problems occurred and were corrected during the first two years of operations, during the period of canister retrievals and examinations. Twice, a pressure gage was broken loose from a test container during the canister retrieval activities. These gages were subsequently re-epoxied or strapped in place, then reactivated.

Several of the borehole-closure displacement gages have generated a somewhat noisy, but still usable data output signal. Most of this noise was found to be due to bad splices in leads, dirty connections, or noise from the power supplies. One LVDT (linear variable displacement transducer) required replacement at the two-year point. Some of the vertical closure gages have also required a small amount of periodic maintenance due to brine drips and salt blob growth either on top of the gages or onto the scissors jack mechanism of the apparatus; refer to **Figure 3.5-9**. Salt growths were scraped off of the affected closure gages, the gages were mechanically exercised, reset, then put back into service. Several times during the first two years, the closure gages were recalibrated in place, or had their lead polarities reversed or

corrected. All data impacts resulting from these repairs, resets, and recalibrations have been incorporated into the WISDAAM and UNDERDOG database processing system, in a QA approved manner; refer to Section 3.6.

The borehole-diameter wire extensometer gages were not affected by salt drips. They did, however, have to be removed, then reinstalled whenever test containers were retrieved for periodic examinations. One extensometer also was affected by a slipping wire-anchor point; this resulted in a "stair-step" displacement signal. The Ramset (nailed) anchor point was replaced by a shallow mechanical anchor and the problem was resolved.

All remote-reading gages have continued to operate satisfactorily over the last several years with very limited maintenance, even though no "in hole" or test room access has been available since just after the 3-year retrieval, sampling, and inspection period. Maintenance on cabling, power supplies, and other test equipment located outside of the test room or within the instrumentation and control shed is still possible. Slightly noisy data signal output can be accommodated in data interpretations. In comparison, the lack of room access has resulted in the total loss of acquisition of further manual measurements, borehole inspections, and maintenance activity.

6.0 GEOMECHANICAL MODELING RESULTS

In this section, we present and discuss a series of preliminary results from the geomechanical model described in Section 4.1 . We first present thermal results in the form of temperature contours, to show the thermal load on the configuration. Next, we will present results of vertical and horizontal room closure and pillar shortening . These are included to show the effects on room closure from drilling the boreholes and emplacing the heat-producing waste-simulation heaters in Room T. Then, modeling results for borehole closure itself are presented. Borehole closure was the response of our primary interest in this modeling study because of the comparison to the available, measured in situ data on borehole closure, as summarized in Section 5.5. Concluding this section, we discuss the modeling considerations that led to the choice of the finite element idealization used in this study. We will provide comparisons of the experimentally measured temperatures and borehole closures with calculated values in Sections 7.1 and 7.3.

6.1 Room and Borehole Thermal Predictions

Figures 6.1-1a, b, c, and **d** show the calculated temperature contours at 3.5, 4, 5 and 6 years for the modeled configuration, in the area of the room and borehole. (NOTE: Recall from Section 4.1 that thermal "power" is applied to this system at 3.48 years, the model time = 0 for the in situ experiments.) At the end of the 6-year simulation, about 2.5 years after power-on, most of the material immediately adjacent to the room and borehole has undergone a temperature increase of at least 3.5 K (°C), but the maximum temperature rise is only about 6 K at the borehole wall. These temperature increases are very small, and imply that the effect of the thermal load on borehole closure response will also be small for the power level of about 117 W/container. This is consistent with the results of other studies (Argüello and Torres, 1988) of the RH TRU "reference" emplacement scheme in which power output levels of this magnitude were shown to affect room and borehole closure response by very small amounts.

6.2 Room Closure Predictions

Figure 6.2-1 shows the computed vertical and horizontal closure histories of the modeled room configuration, as well as the pillar shortening history. Vertical closure and pillar shortening refer to the closure at the center and at the outer edge of the room, respectively. In all three curves, it is easy to see the effect of borehole coring at 3 years. This is evident by the increase in rate of closure, as seen by the marked increase in slopes in the curves at 3 years. The increase in closure rate is larger for horizontal closure than it is for vertical closure or pillar shortening. At the end of the 6-year simulation period, or 3 years after bore-

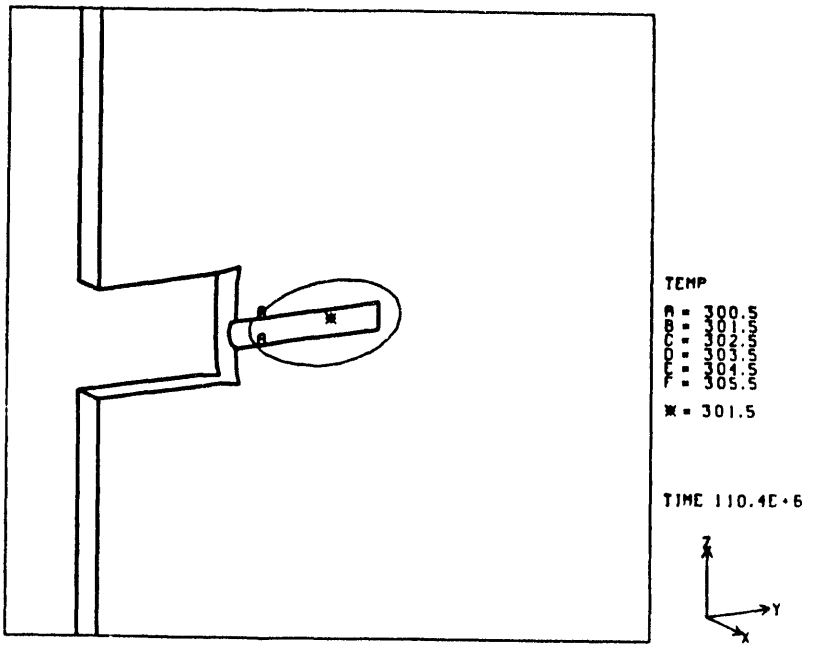

Figure 6.1a Calculated Room and RH Borehole Temperature Contours at 3.5 Years

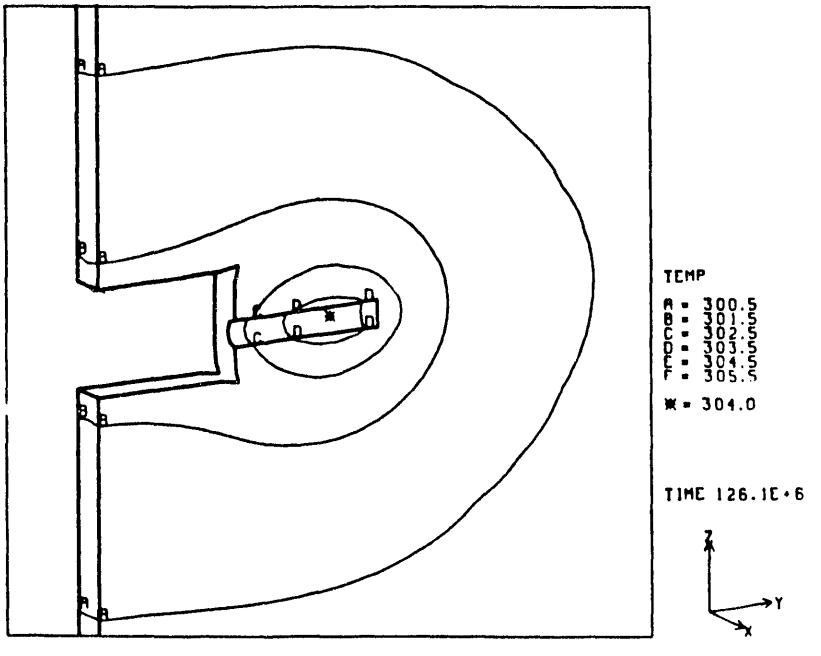

Figure 6.1b Calculated Room and RH Borehole Temperature Contours at 4 Years

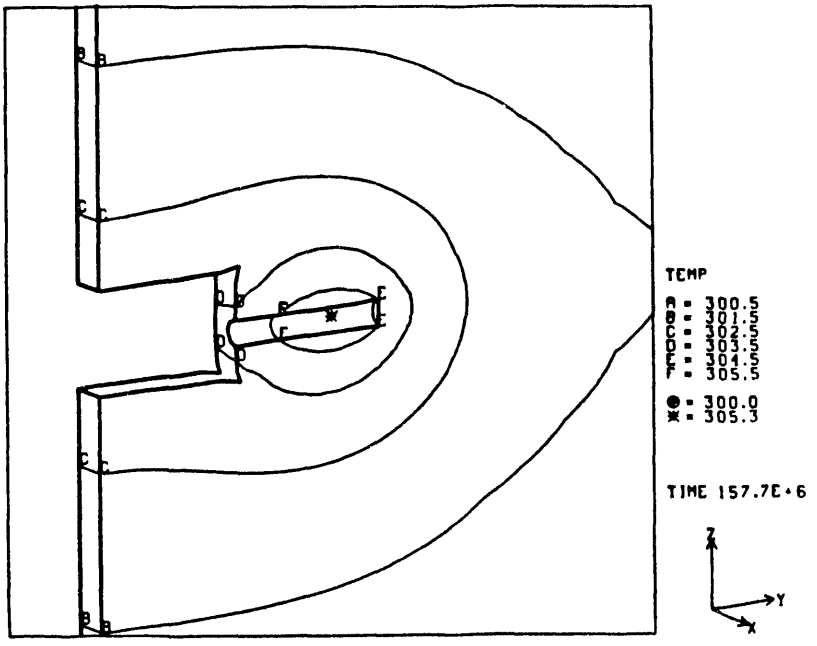

Figure 6.1c Calculated Room and RH Borehole Temperature Contours at 5 Years

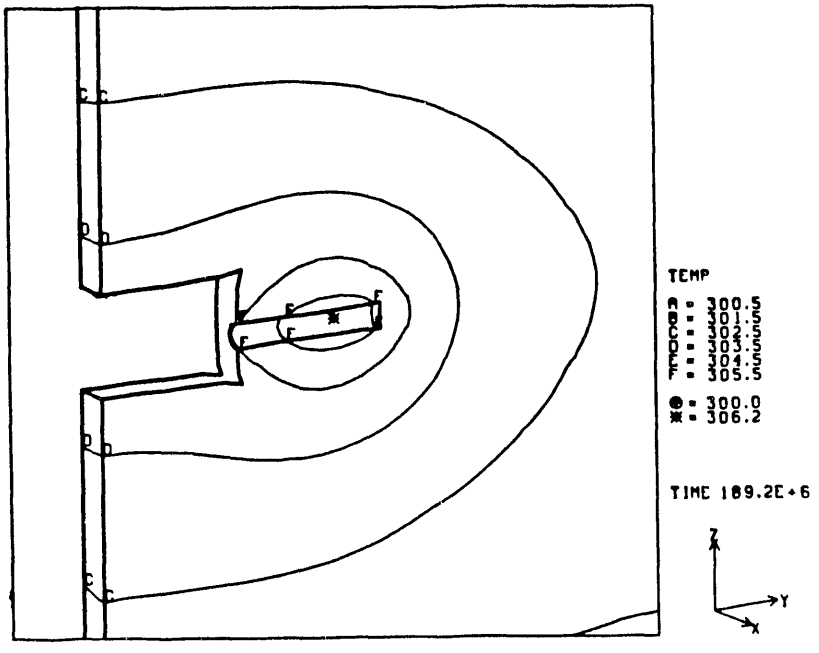

Figure 6.1d Calculated Room and RH Borehole Temperature Contours at 6 Years

hole creation, the values of vertical and horizontal room closure are almost equivalent, 0.6 m and 0.58 m, respectively. The value of the pillar shortening is approximately 0.26 m. These values represent a modest 15 % decrease in the original 3.96 m room height at the room centerline and a 6.6 % decrease in height at the rib. In addition, the original room width of 10.0 m decreases by 5.8 %. Based on these values, it does not appear that the coring of the boreholes and the subsequent emplacement of heat-producing waste containers in these boreholes will adversely affect the closure of a typical waste storage room during at least the first three years of the waste retrieval (5-year) period. It must be kept in mind, however, that the response of the room will depend on the time at which the boreholes are drilled after excavation of the room. These effects were specifically evaluated by Argüello and Beraún; basically, the sooner the boreholes are drilled into the rib after excavation of the room, the more significant the effect on room closure response will be. Such results and implications of these calculations will be discussed in Section 8.

A comparison of computed horizontal room closure results with available in situ data, presented elsewhere (Argüello and Torres, 1988; Argüello et al., 1989) indicates that there is a slight overprediction of room closures and closure rates by these computations. This was expected because the configuration modeled herein represents an infinite number of rooms as opposed to the four-room array in which Room T is actually located and the creation of an infinite number of boreholes in the ribs as opposed to the eight that

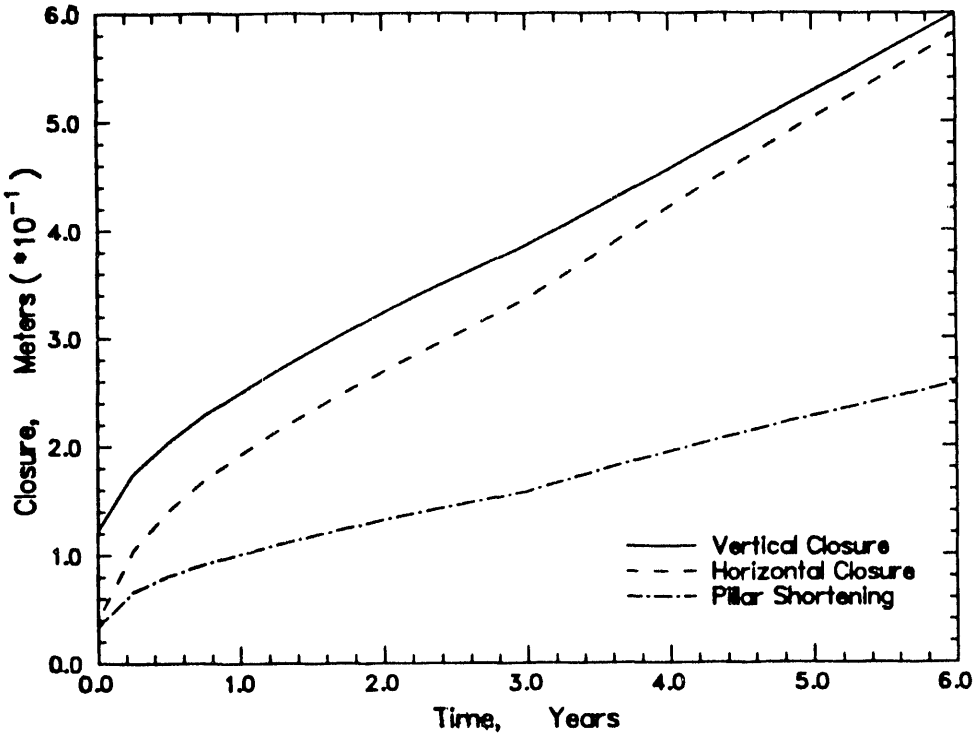

Figure 6.2-1 Computed RH TRU room closure histories

were actually cored in Room T. A more detailed discussion of these results, including an evaluation of different RH TRU container power outputs, is presented elsewhere (Argüello and Torres, 1988; Argüello et al., 1989).

6.3 Borehole Closure Predictions

Computed vertical and horizontal closure profiles of the RH borehole are shown in **Figures 6.3-1** and **6.3-2,** respectively, for times of 3, 3.5, 4, 4.5, 5, and 6 years. These are actually the profiles of relative displacement between two diametrically opposed points in either the vertical or horizontal directions. The vertical profiles shown in **Figure 6.3-1** indicate that there is significant relative displacement occurring between the two points prior to excavation of the borehole! This is illustrated by the nonzero response at 3 years. Basically, this means that there is room closure following excavation. If there had been a borehole in the room rib at the initial time, it also would have decreased in the vertical direction because of the room closure; the "virtual" borehole experienced vertical closure before it was actually cored at calculation time t = 3 years. On the other hand, the horizontal profile at 3 years, shown in **Figure 6.3-2**, indicates that an insignificant amount of relative displacement occurred between those two points prior to excavation of the boreholes. This is important because comparisons of measured closure should be made with computed closure only after the relative displacement of the computed response, that existed between those two points at the time of hole excavation, about 1.5 cm, has been subtracted out. On this basis, the horizontal relative displacement profiles shown in **Figure 6.3-2** also correspond quite closely to the closure of the borehole, but the vertical relative displacement profiles shown in **Figure 6.3-1** need to be adjusted appropriately before being compared to the measured borehole closures. The profiles shown are useful, however, in that they indicate that larger closures will be seen near the center (for vertical closure) and toward the back or blind end of the borehole (for horizontal closure) rather than near the rib, front end. This makes sense because the stresses around the room opening relax after room excavation, and as time passes, the peak stress location moves deeper into the pillar where the boreholes are located. Comparisons of calculated, diametrical closures with in situ measured vertical and horizontal borehole-diameter closure measurements will be made in Section 7.3.

Computed borehole vertical and horizontal closure histories, along with measured vertical and horizontal closure measurements (from Section 5.5), are shown in **Figures 6.3-3, 4,** and **5,** for three locations along the borehole length where the in situ closure measurements were made at depths of 2.19 m (7.17 ft), 2.95 m (9.67 ft), and 3.71 m (12.17 ft) in from the rib face, respectively. [Note: the measured vertical

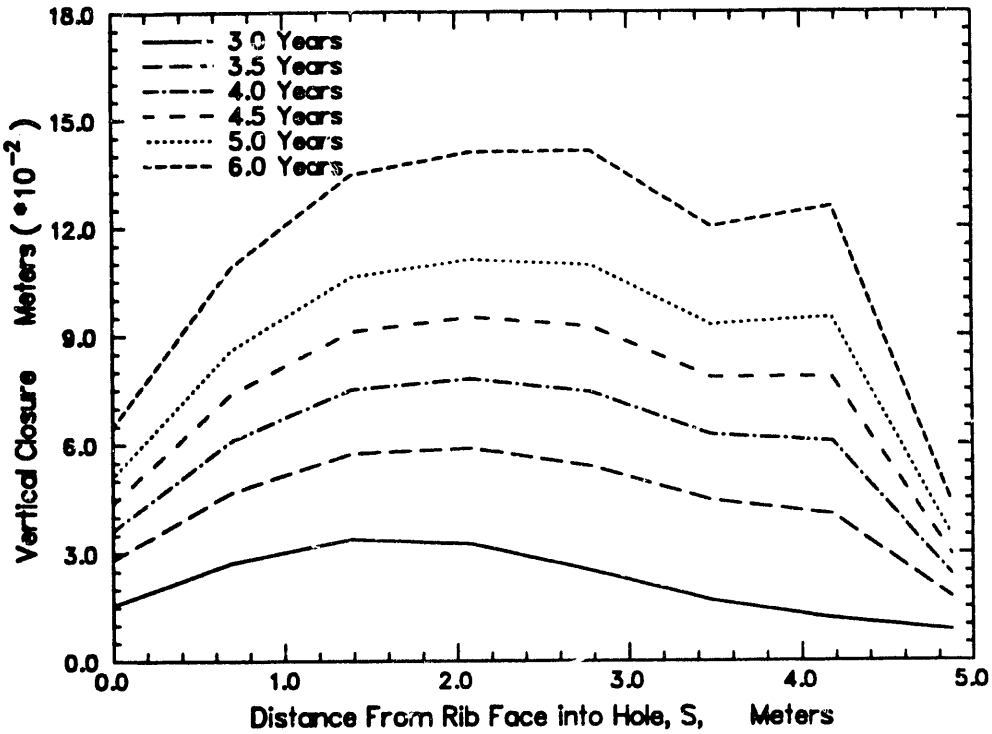

Figure 6.3-1 Computed Borehole Vertical Closure Profiles

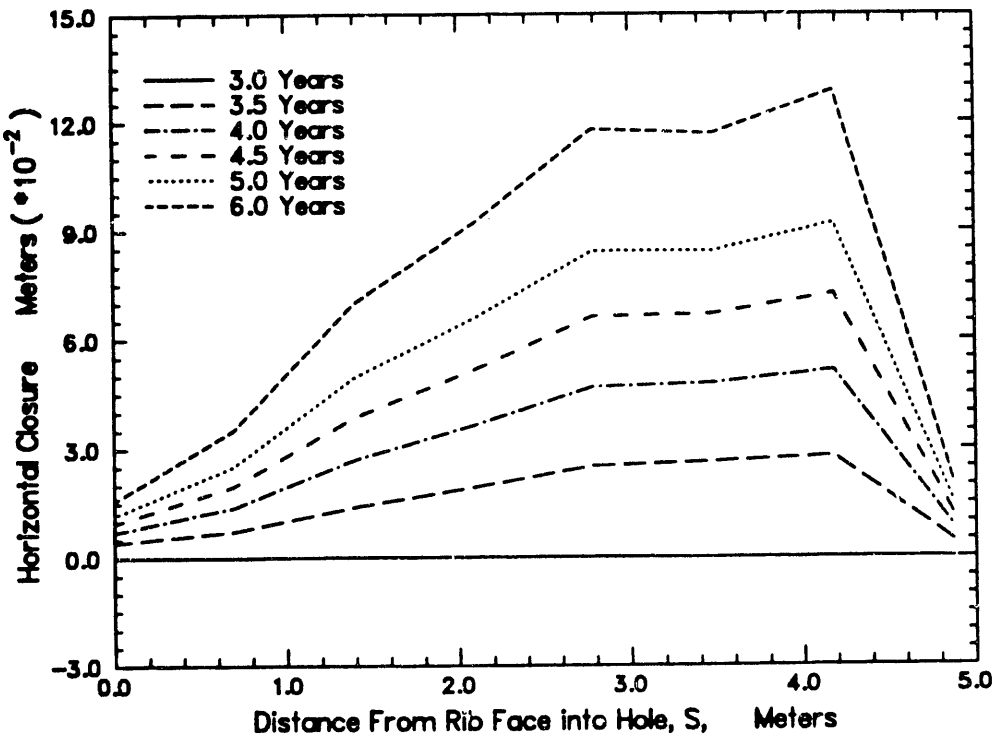

Figure 6.3-2 Computed Borehole Horizontal Closure Profiles

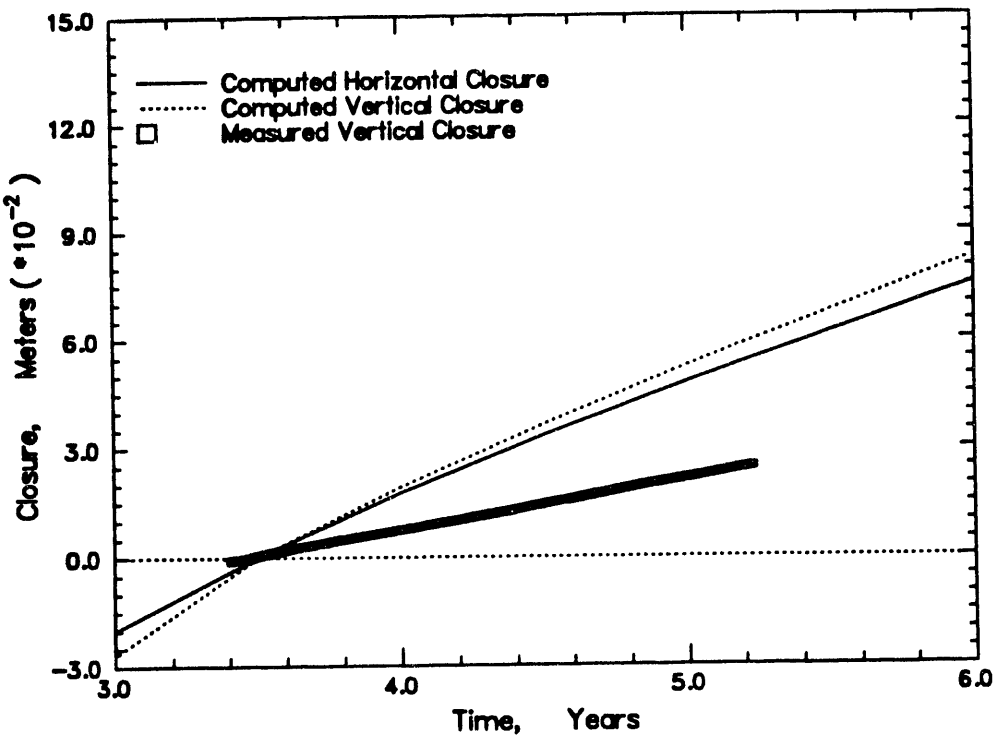

Figure 6.3-3 Computed vs. Actual Borehole- Closure Histories, 2.19 m in from Rib Face

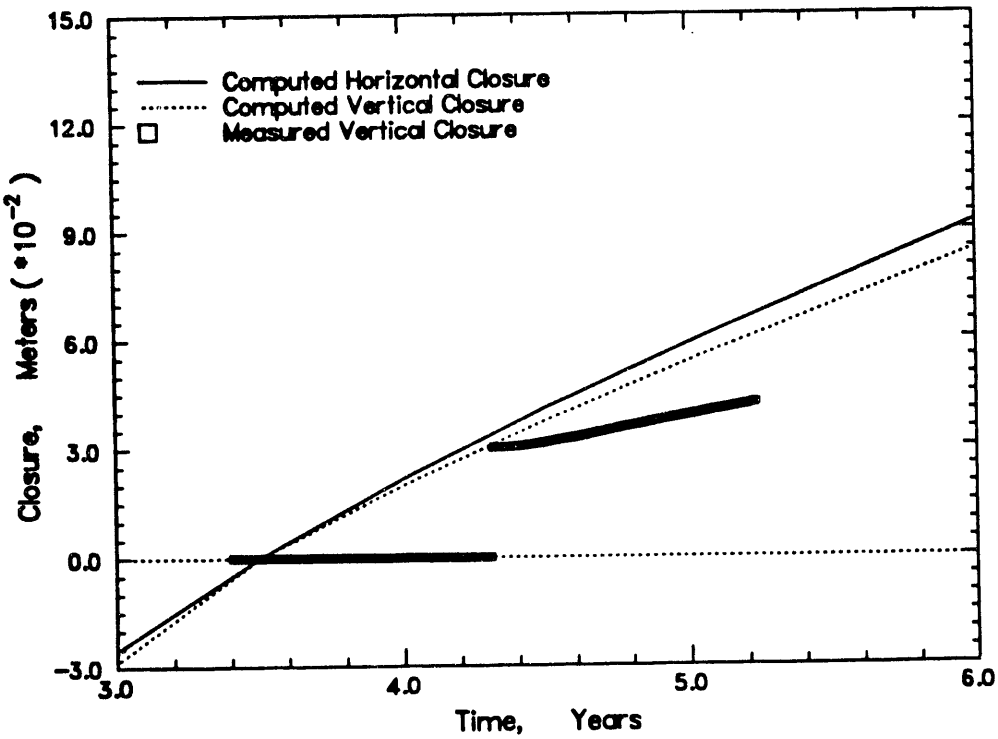

Figure 6.3-4 Computed vs. Actual Borehole- Closure Histories, 2.95 m in from Rib Face

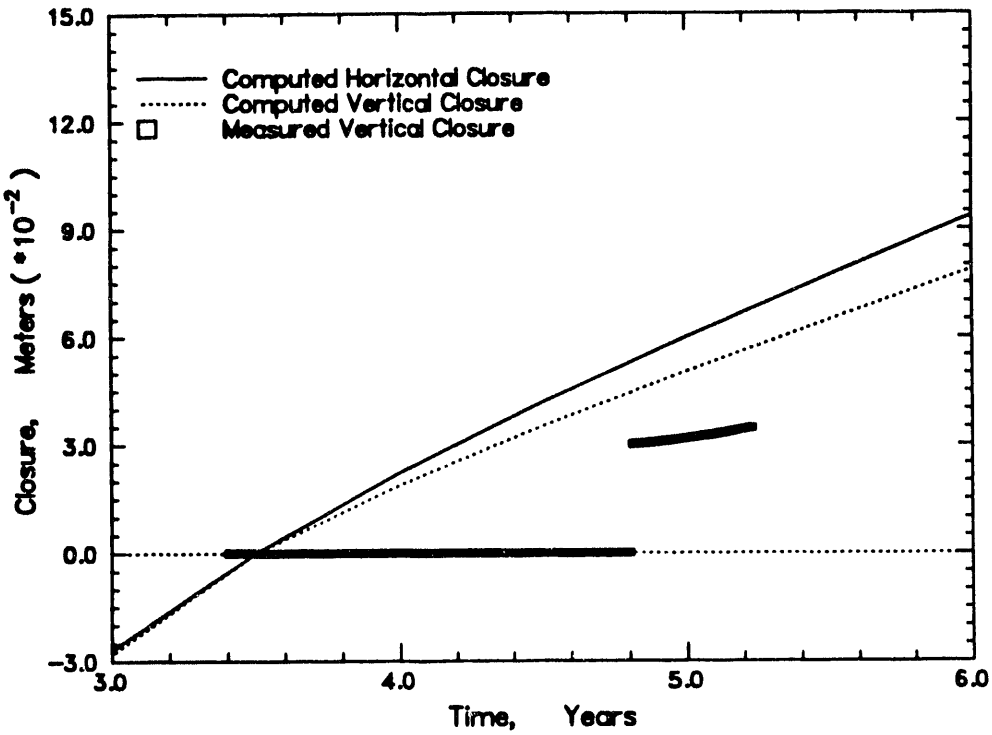

Figure 6.3-5 Computed vs. actual borehole-closure histories, 3.71 m in from rib face

closure data points in **Figures 6.3-3, 4,** and **5** are indicated by a "□" symbol; these "□" symbols are so close together that they do not appear distinguishable.] The computed closure results in **Figures 6.3-3, 4,** and **5** have been shifted downward so that the zero values corresponds to the zero values of the measured data; the computed values were arbitrarily zeroed so that the time of heater turn-on equals time t = 0. The measured vertical closure values correspond to those from emplacement TRH03 (see **Figures 5.5-1, 2,** and **3**). The discontinuous measurement curves in **Figures 6.3-3, 4,** and **5** are the result of the existence of a 30 mm gap between the gage and the top of the borehole, as explained in Section 5.5.1; these gaps are not indicated in **Figures 5.5-1, 2,** and **3** where the data are shown as a smooth, continuous curve. **Figure 6.3-3** is for a borehole cross-section at 2.19 m in from the rib face, **Figure 6.3-4** is for one at 2.95 m, and **Figures 6.3-5** is for one at 3.71 m. Because there were no nodal points on the computational mesh corresponding to the exact locations of the closure stations along the length of the borehole, the computed histories shown were obtained by interpolating between closure information at the available nodal locations. We will present further comparisons of these calculated results with measured borehole closures in Section 7.3.

7.0 DISCUSSION

The purpose of this section is to provide an initial interpretation of all available WIPP simulated RH TRU technology experiment data, observations, and calculations, as presented in Section 5. We will also compare measured data to the modeling results presented in Section 6. The intent of this discussion is to display as many correlations as possible, to extract as much meaning out of the test results as possible. Other analysts may then also be able to provide further interpretations, or to use the data for further modeling studies. Only then can the significance of these results be fully assessed for both the operational -phase safety and long-term performance of the WIPP facility. This data report should, therefore, not be considered as the only, or as the definitive data interpretation report for this test program.

7.1 Temperature Histories

7.1.1 Heater-Thermocouple Temperatures

We observed maximum, heater-thermocouple temperatures (i.e., of the container metal surface) in the range of about 36° to 42°C, with the heater power output of 114.9 ± 4.5 watts, and in the range of about 45° up to 58°C, with the heater power output of 298.9 ± 9.5 watts. Refer to **Table 5.2** and **Figures 5.2-1** through **5.2-8**. These temperatures should be compared to the observed borehole ambient temperature of 28° to 28.3°C, recorded over a 27 day period prior to heated test turn-on. Heater temperatures appear to reach a plateau level after about 10 days, even though there are minor fluctuations as a slow function of time; these fluctuations have a range of up to 2°C. Test container temperatures in non-backfilled boreholes (i.e., for test containers TRH01, -02, -07, and -08) generally occupy the lower end of these ranges. This may be due to the fact that the non-backfilled test boreholes are located on the ends of the installed test array; they only experience heating from their own internal heater and one near-neighbor, not two.

The maximum measured temperature differential over the length of an individual test heater-container, as measured by thermocouple gages #1, #2, and #3, is only about 1°C at the lower heater-power output and up to 3°C at the higher heater-power level. The later, near steady temperature increases noted for test heater TRH05, and to a lesser degree TRH06, as illustrated in Figures **5.2-5** and **5.2-6**, are the result of an unexplained thermal power step increase for these heaters, as shown in Figures **5.1-5** and **5.1-6**.

Brief heater power outages, particularly in the 3- to 5-year time period, yielded brief, but sharp measured temperature drops of 3°C or more.

7.1.2 Near-Field Temperatures

The observed near-field salt temperatures (i.e., at the borehole top-air interface) increased from the measured, pre-turn-on baseline of 28° to 28.3°C up to a range of about 31° to 32°C, with the heater power output of 114.9 ± 4.5 watts, and up to the range of about 35° to 37°C, with the heater power output of 298.9 ± 9.5 watts. Refer to **Table 5.3** and **Figures 5.3-1** through **5.3-8**. Maximum temperatures were achieved in a time period of about 1 to 2 weeks, somewhat slower than the observed temperature rise for the heater-TC values. Since all the measured near-field temperatures occupy such a narrow temperature range (of < 3°C per heater-power range), no specific comments can be made about the effects of gage locations within the boreholes or about backfilled or non-backfilled impacts on temperature.

7.1.3 Periodicity of Near-Field Temperatures

While there is a slow, steady increase over time for the first five years of heated test operation, there is also an obvious, distinct cyclical or near-sinusoidal nature that is not related to thermal power increases. There is a recurrent near-field temperature increase of up to about 2°C, with a periodicity of about 350 to 400 days over the five-year period of observation. We also noted these temperature fluctuations for the heater-thermocouple temperatures, but to a somewhat lesser extent. We conjecture that this temperature periodicity is caused by yearly temperature fluctuations in the mine-ambient air temperature in the test room, as influenced by a combination of both aboveground seasonal variations and underground mine ventilation patterns. The maximum observed temperatures in these cycles all occur in the September through October time frame. The minimum observed temperatures occur in the February through April time frame.

For validation of this conjecture on yearly temperature periodicity, we compared the near-field temperature histories with the measured Room T ambient air temperatures, as recorded by thermocouples TC898 and TC899. These two thermocouples are illustrated in **Figure 3.2-1**, and are labeled as CT898 and CT899. These thermocouples are attached to the salt ribs in Room T, with their sensing tips extending slightly into the room air space, not in contact with the rock salt, in order to monitor ambient room air temperatures, not salt temperatures. These TCs are located closer to the northern end of Room T and are a

part of the simulated CH TRU waste technology experiments (Molecke, 1986). Temperature data from these two thermocouples are illustrated in **Figures 7.1-1** and **7.1-2**. We have shifted the elapsed (CH TRU) test times shown on the X-axes of these two figures to correspond with the time axes for all of the simulated RH TRU test data (figures). The measured room air temperatures over the specified five-year time period ranged from about 23°C to 33°C. This test room has one end closed (with a bulkhead) at the north and one totally open end at the south; as such, it is affected directly by mine ventilation changes. There is little doubt that the observed temperature periodicity of the borehole salt near-field thermocouples is essentially identical to, and effected by the periodic nature of the room ambient temperatures.

7.1.4 Comparison of Measured vs. Calculated Temperatures

Calculated temperatures of the RH TRU reference configuration were illustrated in **Figures 6.1-1a, b, c**, and **d**. The heater-wall temperatures, illustrated as the centralized "*" temperature in these figures, range from 301.5 K to 306.2 K over the calculated time period of 3.5 to 6 years. These values are equivalent to 28.35° to 33.05°C, for test times of 0.02 to 2.5 years, at the thermal output power of 117 W/heater. The measured heater-wall temperatures, as illustrated in Figures 5.2-1 through 5.2-8 and summarized in Table 5.2, are all about 3° to 8°C higher in magnitude, but do follow an approximately similar, slow rise with time. The differences between measured and calculated heater temperatures are probably due to approximations made in the thermal properties of the RH container material, as discussed in Section 4.2, as compared to the actual materials of the test heaters. These discrepancies are expected to be most acute at the surface of the heaters.

The calculated temperature contours immediately adjacent to the RH boreholes, are illustrated in **Figures 6.1-1a, b, c**, and **d**, as contours "b, " "d," "e," or "f," depending on the time. These calculated near-field temperatures range from 301.5 K to 305.5 K (28.35° to 32.35°C), for test times of 0.02 to 2.5 years, at the thermal output power of 117 W/heater. These calculations can be compared directly with the near-field temperature values measured by thermocouples TRH8XX, as illustrated in **Figures 5.3-1a** through **5.3-8a,** and summarized in **Table 5.3**. In essentially all cases, the calculated near-field temperatures match the measured near-field temperatures very well, in both magnitude and time dependence. This good modeling-test agreement provides satisfactory validation as to the correctness of the model used.

It should also be noted that the temperature rise experienced by the near-field rock salt is only about 4°C (compared to the stated pretest baseline of 28°C), when power output of these RH TRU test heaters

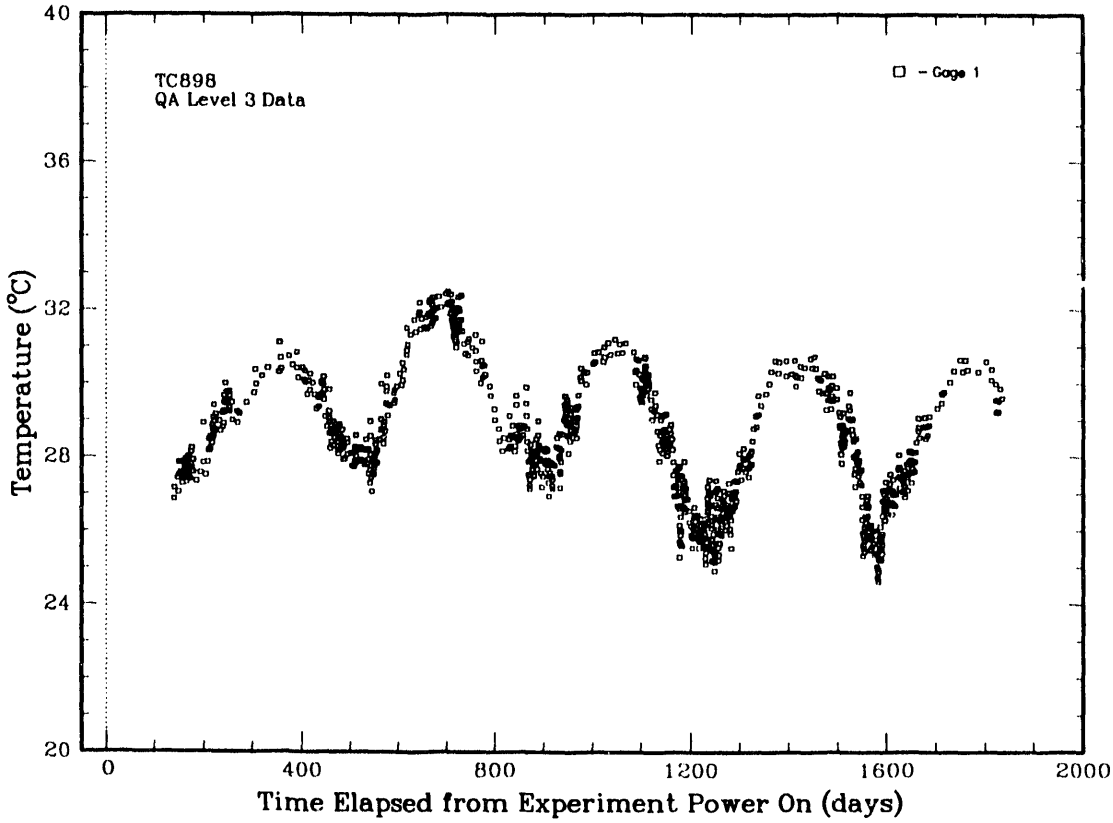

Figure 7.1-1 Ambient Room T Temperature History, Gage TC898

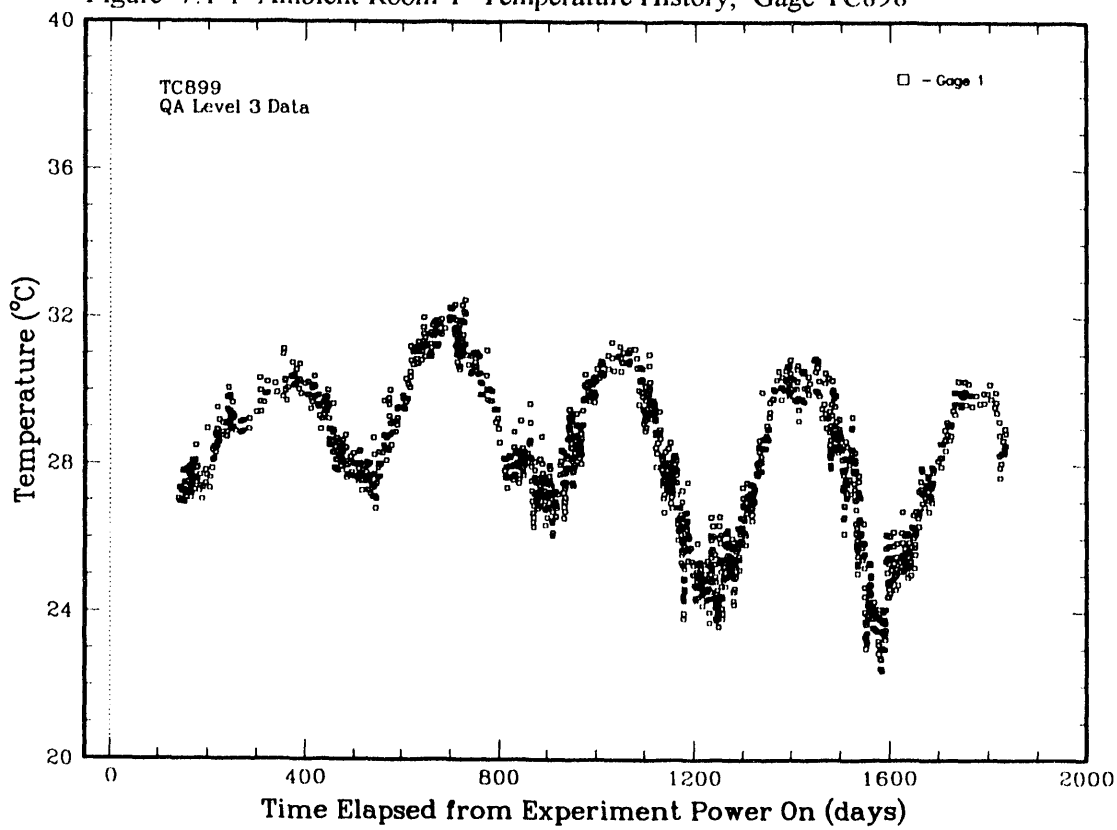

Figure 7.1-2 Ambient Room T Temperature History, Gage TC899

was held at about 120 watts/each, and 7° to 9°C at the overtest thermal output of about 300 watts/each. A thermal output of 120 watts is about 2 to 4 times greater than that expected from actual, "reference" RH TRU wastes currently expected to be shipped to, and isolated in, the WIPP facility. Separate thermal modeling calculations were also performed by Argüello and Beraún with RH TRU containers having the "reference" 60 W/container thermal output. Based on these calculations, actual "reference" RH TRU waste containers isolated in the WIPP (for a limited number of RH TRU containers per room) should be expected to only raise the ambient rock salt temperature a very small amount, less than 3°C. Note that this temperature rise is about of the same magnitude as that caused by cyclical variations in the mine-ambient air temperature in a continuously vented room.

7.2 Pressure Measurements

The pressure gages located on the top, horizontal surface of the test containers, and designated as TR6XXT, should theoretically indicate zero pressure; there is only an air void above them. As listed in **Tables 5.4.1** and **5.4.2**, very low pressure values (mostly in the range of ± 0.02 to 0.08 MPa, 3 to 12 psi) were recorded, with extremely low rates of increase, or decrease for TR633T and TR624T, mostly in the range of ± 0.005 to 0.017 MPa/year, 0.7 to 1.7 psi/year. These low values, approximately 10% or less of similar pressures measured by the TR6XXL or **R** gages, indicate an acceptable, very low, long-term drift for these gages.

Pressure gages on the bottom, horizontal surface of the test containers, and designated as TR6##**B**, also measured very minimal pressures and pressure rates of increase, similar in magnitude to the TR6XXT gages. Refer to the values listed in **Tables 5.4.1** and **5.4.2**. These pressures are probably also the result, predominantly, of minimal gage drift. The bottom gages would have measured appreciable applied pressures if vertical borehole-closure stresses were transferred to the container via the backfill. That was not the case in these partially backfilled emplacement holes. Two of the gages, TR613B and TR623B, indicated minor rates of decreasing pressures; this decrease is ascribed to either downward drift, similar to gages TR633T and TR624T, or, possibly, minor (gravity) settling of the backfill material beneath these gages.

We measured pressures applied to the left and right sides of test containers TRH03 and TRH04 at three separate distances along the container, at 2.18 m, 2.95 m, and 3.71 m in from the rib face. The

maximum pressures were always recorded at the furthest distance in, nearer the closed or blind end of the borehole; refer to the values listed in **Tables 5.4.1** and **5.4.2**. The minimum pressures were always observed at the midpoint of the container, at 2.95 m in from the rib face.

The highest pressure values we observed, e.g., 0.72 and 0.87 MPa (104 to 126 psi) for gages TR633R and TR633L, were always followed by a subsequent pressure decrease. There were also occasions of two maximum peaks; refer to **Figures 5.4-3L** and **R**, for example. It appears that the not-totally-confined, granular bentonite/silica sand backfill material is quite capable of transferring stress loading due to borehole closure onto the RH container. This capability is limited, however. In the test boreholes, only partially filled with backfill, the backfill reached a certain amount of consolidation, transferring pressures, before it shifted or crumbled somewhat, thereby temporarily decreasing its load-bearing capacity. The largest observed rates of pressure increase, up to 0.23 MPa/year (33 psi/year) for gage TR613L and 0.25 MPa/year (36 psi/year) for gage TR614L, would yield a maximum pressure of about 1.2 to 1.3 MPa (170 to 180 psi) if linearly extrapolated over an undisturbed 5-year emplacement-retrieval cycle, and assuming no backfill slippage. The 6 mm- (0.25 inch) thick wall of the RH TRU container should have little difficulty in withstanding this pressure loading without deformation. Visual confirmation of this assertion will have to await the next, final test container retrieval and examinations.

A visual evaluation of the observed pressure histories in boreholes TRH03 and TRH04, as illustrated in **Figures 5.4-1** through **5.4-2**, does not reveal any obvious correlation between heater thermal output (about 120 watts and 300 watts per heater) and pressure increase. However, a comparison of the calculated slopes (rates of pressure increase) in **Table 5.4.2**, for the **L** and **R** gages in test emplacement TRH04 both before and after the increase in thermal power at day 1122, indicates that there is an increase of between about 20% to about 50%. Care must be taken for this comparison, however. The identical backfill material was used in this borehole both before and after its vacuum removal then reemplacement at the 24-month examination period. But, the in situ backfill compaction density, not just the thermal load increase, may have been different enough to cause the observed differences in pressure rates of increase. Minor differences in sorbed-moisture content of the backfill material both before and after reemplacement, and resultant assumed differences in compaction behavior, may also have played a minor part in the observed pressure increase differences.

7.3 Borehole Closure Measurements

7.3.1 Vertical Displacement Borehole Maximum Closures

The maximum measured, vertical-displacement borehole closure after approximately 1800 days of test operation is about 75 mm (3.0 inches); refer to **Figures 3.5-1** through **3.5-4**. We last made manual vertical-closure measurements at the 36-month borehole examination period, as indicated in **Table 5.5.1.** The degree of correlation or comparison of manual measurements (with the spacer height of 30.2 mm added to the manual measurements, denoted by the value to the right of the "♦" in **Table 5.5.1**) to the gage closure-measurements up through this point in time is very good. This good correlation lends further validity to the maximum manually measured closures (and calculated closure rates) obtained in test boreholes #5, 6, 7, and 8 -- where no remote closure gages were present. The extent of observed variances between the two types of closure measurements ranged from 0.2 mm up to 11.1 mm (0.01 to 0.44 inch), with the majority of variances at the lower end of this range. The variances may be partially explained by:

1. inaccuracies in the assumptions made in converting manual measurements to manual vertical closure, as listed after **Table 5.5.1**;
2. uncertainties in the exact height of the Teflon spacers used; [Many of spacers were remeasured when they were removed. Most were within 0.2 mm of the stated 30.2 mm-height, usually being shorter in height. One spacer measured only 29.3 mm-high.]
3. inaccuracies in vertical closure gages, e.g., gage drift, as a function of time or temperature; [Observations of the data from gages TR22X and TR23X indicate that the gages drifted much less than a total of 1 mm, for the extended time period prior to the contact of the top of the spacer with the borehole salt.]
4. local variations in the initial borehole diameter, as cored; [In borehole #2, for example, there was an observable, abrupt change in hole diameter between the distances of 2.95 to 3.71 m in from the rib face. This change was probably due to a switch in the core barrel, or modifications to the core barrel cutting surface, during the initial coring operation.]
5. inaccuracies in making the manual measurement at the exact same location every measurement period; or,
6. changes in borehole diameter due to minor, localized salt growths as a function of time.

No clear-cut trends could be observed for vertical-closure vs. distance (in from the rib face) along the borehole. There were just too many observed variations in both the remote or manual measurements of closure.

7.3.2 Vertical Displacement Borehole Closure Rates

We assumed the vertical-displacement closures to be linear with time, as described in Section 5.5.1, and linear slopes or closure rates were appropriately calculated for the specified time periods, as listed in **Table 5.5.2**. The remote-gage vertical-displacement closure rates ranged from 10.3 to 15.3 mm/year (0.41 to 0.60 inches/year), over about the 50 to 1826 day period. For the manual measurements, the calculated vertical-displacement closure rates ranged from about 8.3 to 15.2 mm/year (0.33 to 0.60 inches/year), over the 12 or 18 through 36-month period. The agreement between the calculated gage and remote closure rates is very good, usually better than ± 1 mm/year (0.04 inch/year).

There does not appear to be a significant difference in vertical closure rates as a function of heater power, over the approximate 120 to 300 W/heater range, as seen in **Figures 5.5-1** through **5.5-12**. This apparent lack of influence is similar to that observed for pressure increases, as described in Section 7.2. We calculated the closure rates, therefore, over time periods spanning both power outputs. We initially assumed that the higher level of thermal output, with resultant slightly higher borehole near-field temperatures, would yield increases in the closure rates. This does not seem to be the case. As we described in Section 5.5.1 on the caveats of assumed linear vertical-closure rates, there possibly could be a minor decrease in observed closure histories (rates) in the (approximate) 900 to 1,122 day period, immediately before the heater power increase, and again in the +1,600 day period. It is possible that the power increase at day 1,122 overwhelmed any decrease in rates, thereby smoothing out the slope or linearity of the closure rates.If the closure rates were broken into two time periods of approximately 50 to 1,122 days at about 120 W/heater, and 1,122 to 1,800 days at about 300 W/heater, the slope of the gage closure histories, or closure rate for the later period in some cases appears to be slightly lower than the slope, or rate, for the initial time period. Minor temperature increases did not increase the observed rates.

Borehole vertical closure data, and rates, were also obtained for the almost one-month period, for 25 to 27 days, before heater turn-on, as shown in **Figures 5.5-1** through **5.5-12**. These ambient-temperature closure rates are listed in **Table 5.5.2** and are (with the exception of TR213 data) between 16.9 to 18.6

mm/year (0.69 to 0.73 in./year). This range of rates is generally about 2 to 5 mm/year faster than the observed ranges over the 50 to 1,826 day period. Immediately after turn-on of the 120 W canister heaters, the vertical closure rates increased slightly, for a period of about 0 through 50 days, presumably in response to the thermal output and temperature increase; refer to **Table 5.5.2**. The initial increases over the pre-turn-on closure rates were in the range of +0.9 to 5.7 mm/year (0.04 to 0.22 inch/year) greater. These rates all decreased after about 50 days, down to the reported 50 to 1,826 day rates. Both of these observations indicate that minor borehole temperature increases are less important than elapsed time for controlling the observed vertical closure rates.

7.3.3 Comparisons of Vertical-Diameter to Vertical Borehole-Closure Rates

The measured vertical diameter-closure rates listed in **Table 5.5.4** are generally within the range of 7.3 to 17.7 mm/year (0.29 to 0.70 inch/year). These rates appear to be greatest near the back, or blind end of all boreholes, as measured at 3.7 m in from the rib face. There is a secondary maxima in the vertical-diameter closure rates near the front, open end of the hole, as monitored at 1.23 m in from the rib face. There is a minimum in the observed rates near the middle of the hole, between about 2.2m and 3.0 m in from the rib face. By comparison, there is no apparent, significant difference in vertical-displacement closure rates with distance, as measured both by manual measurements and the remote-gage borehole (top) vertical-displacement gages, over the 50 to 1,826 day test period; refer to **Table 5.5.2**. These borehole-top gage closure rates ranged from 10.3 to 15.3 mm/year (0.41 to 0.60 inches/year) and the manual measurement, calculated vertical-displacement (top) closure rates ranged from about 8.3 to 15.2 mm/year (0.33 to 0.60 inches/year). Overall agreement is very good between the vertical-diameter closure rates and the top, vertical displacement closure-rates. This agreement indicates that the same vertical closure rates were being measured, albeit at different positions within the boreholes.

7.3.4 Comparison of Measured to Predicted Vertical Borehole Closures

We briefly described a comparison of appropriately adjusted, computed vertical borehole closures versus measured vertical closures in Section 6.3; this is illustrated in **Figures 6.3-3, -4**, and **-5** at three locations along the borehole lengths. We shifted the computed closure results downward so that the zero closure value corresponds to the zero data value at the time of heater turn-on, time t = 0. The measured vertical closure values are from emplacement TRH03. Because there were no nodal points on the

computational mesh corresponding to the locations of the closure stations (for gages TR213, 223, and 233) along the length of the borehole, we obtained the computed histories shown by interpolating between closure information at the available nodal locations.

Quantitatively, the computed vertical closures and closure rates (slopes of the curves) are larger than the measured values. **Figure 6.3-3** shows that the computed vertical closure at the station closest to the rib face is 0.06 m at 5.2 years (test time = 1.7 years, about 620 days) while the measured value is 0.025 m. Similarly, **Figure 6.3-4** shows that the computed value is 0.063 m, and the measured value is 0.042 m, at the same time, and Figure **6.3-5** shows the computed value to be 0.057 m while the measured value is 0.033 m. Thus, the computed vertical closures are seen to be about 1.5 to 2.5 times larger than the measured values at 5.2 years. We *expected* this discrepancy because the idealization used in this analysis represents one room of infinite length in an infinite array of equally spaced similar rooms and is, therefore, only an approximation to the actual configuration of Room T, which is only one finite-length room in a series of four. Furthermore, Room T is the only one of the four with boreholes drilled into its ribs -- a finite number of boreholes as opposed to the infinite number assumed in the idealized configuration. Because the actual configuration is stiffer than the idealization, the closure results we obtained from the analysis were expected to provide an upper bound to the actual Room T closures.

We can make several general qualitative observations regarding these results. As seen in **Figures 6.3-1** and **6.3-5**, the largest computed and measured vertical closures occur near the mid-station of TRH03, at 2.95 m in from the rib, near the borehole mid-length. Although a quantitative agreement does not exist between computed and measured values, a qualitative agreement is evident. However, the measured vertical closures for all eight boreholes do not indicate a maximum closure at the borehole mid-length. There was no clearly evident trend for measured vertical closure(s) vs. borehole depth. In addition, the change in slope is seen to be relatively small in both the measured and computed vertical closure curves of **Figure 6.3-3** as the heat is turned on at 3.48 years. This implies that the effects on closure due to drilling the holes, and time, are much more significant than that arising from the thermal load imposed by the canisters.

7.3.5 Comparisons of Vertical-Diameter to Horizontal-Diameter Closure Rates

We have only a limited data base on measured horizontal-diameter closure rates, as listed in **Table 5.5.4**. The data seem to indicate a maximum in horizontal-diameter closure rates near the borehole mid-point position, between about 2.2 to 3.0 m in from the rib face. There is also a distinct minimum in horizontal closure rates nearer the open end of the boreholes, at 1.23 m in from the rib face.

Observed horizontal-closure histories are distinctly different than the observed vertical closure histories, as described in Sections 7.3.2. and 7.3.3. Vertical diameter-closure rates at 1.23 m in from the rib face are in the range of 11.0 to 11.9 mm/year (0.43 to 0.47 inch/year) . These are approximately a factor of two greater than the horizontal closure rates at the same location, in the range of 4.4 to 6.2 mm/year (0.17 to 0.24 inch/year). At 3.0 m to 3.7 m in from the rib face, however, the horizontal-diameter and vertical-diameter closure rates appear to be comparable in range, with no major differences.

We cannot make any unequivocal comparisons between the manually measured horizontal- and vertical-diameter closures within borehole TRH02; only two data points were available to calculate each of the respective rates. The closure behavior of the boreholes is obviously different as a function of depth into the hole.

7.3.6 Comparison of Measured to Predicted Borehole Diameter Closures

We can make several general observations regarding the comparison of computed horizontal-diameter closures (refer to Section 6.3) and measured horizontal closure rates. First of all, calculated horizontal borehole closures in **Figures 6.3-3, -4,** and **-5** indicate that these values increase in magnitude with depth into the borehole with a maxima at about 4.0 m in from the rib face,so that the horizontal closure of the borehole is larger (i.e., the diameter is smaller) nearer the blind end than it is at the rib end. The mea sured horizontal closures (and rates) are indeed the smallest at 1.23 m in from rib, the measurement location nearest the rib face. However, based on the limited available data in **Table 5.5.4**, the measured horizontal closures have maximized values near the mid-length of the boreholes, between 2.2 m and 3.0 m in from the rib face, not at 4.0 m -- closer to their blind ends. At this time, we cannot resolve nor interpret this discrepancy between observed and calculated horizontal closures.

7.4 Materials Data and Observations

7.4.1. Corrosion Integrity

We have used laboratory and field studies and results thereof as the precursors to, and foundations of, the current WIPP in situ simulated RH (and CH) TRU waste technology experiments (Tyler et al., 1988). Laboratory studies on the corrosion behavior of TRU waste container materials (i.e., mild steel) and on the protectiveness of several coatings (paints), were conducted at Sandia (Braithwaite and Molecke, 1979) and completed in the late 1970's. More advanced laboratory studies on the anoxic corrosion of TRU waste container (and waste material) steels in brine and vapor are currently in progress (Brush et al., 1992) and have the primary aim of quantifying hydrogen gas generation as a function of time and several gas-composition environments. These current corrosion studies are being conducted by Battelle Pacific Northwest Laboratory, as an important part of the Sandia-WIPP gas generation program.

Laboratory measured mild steel corrosion rates were in the range of near zero in dry crushed salt, up to about 50 μm/year in aerated, saturated NaCl brine, at 25°C (Braithwaite and Molecke, 1979). Observed mild steel corrosion rates in anoxic brine at 30°C, initially about 2 μm/year after three months of testing, decreased down to about 1 μm/year after twenty four months (Brush et al., 1992). We have not observed pitting corrosion in these laboratory tests; pitting could potentially penetrate waste containers at a much faster rate if the appropriate environmental conditions would be present in situ (Tyler et al., 1988). Pitting has not been observed on RH TRU container bodies at this time. Our only significant observation relative to RH TRU container-body integrity concerns the reference enamel paint (Hertelendy, 1984). The corrosion-prevention capability of the enamel paint appears adequate for at least the observed three years in the relatively mild corrosive environment of a RH TRU salt borehole, and is probably also adequate for the planned, initial five-year waste retrievability period. However, the mechanical abrasion resistance (paint hardness, durability) of this paint on the tested containers was less than ideal. During initial canister handling and emplacement activities at the WIPP, several test containers had areas of paint scraped off or appreciably scratched. These areas were spot painted or touched-up with more of the original paint, prior to test emplacement. Such spot painting might prove difficult if the container had included actual, radioactive RH TRU wastes rather than nonradioactive test simulants. A further evaluation of more (mechanically) durable paints might be worthwhile. For example, coal tar epoxy paints have been successfully tested in the laboratory under WIPP-relevant conditions (Braithwaite and Molecke, 1979) and have also shown excellent mechanical and chemical durability (in 40°C backfill and air, and in 90°C brine for periods up to

3.75 years) in in situ simulated CH TRU waste tests in WIPP Room J (Molecke, 1986; Tyler et al., 1988).

Overall, our qualitative observations on the in situ RH TRU waste tests in WIPP Room T certainly tend to indicate that RH containers should have no difficulty whatsoever in withstanding corrosive attack, with full mechanical integrity, during the anticipated, initial five-year WIPP retrievability period. This integrity or durability conclusion applies to both the near-reference and overtest thermal conditions, as used in these RH TRU tests.

However, the above conclusion does not apply to the HEPA filter assembly on each RH TRU container. The observed flaky corrosion buildup and small holes on the HEPA filter splash cover, as described in Section 5.6.2, could become detrimental with time. Although this corrosion was first noticed after only two years of salt "repository" environment testing, the extent or degree of corrosion would be expected to become greater as a function of time, as was observed at the three-year point. The filter splash cover serves to prevent moisture or dirt from coming in contact with the top surface of the filter medium. This steel (tinplate) cover essentially caps the only access route for internal gas escape from the waste container, through small groove, vent-passages in the pintle-cover region. The splash cover has a 5 cm. (2 inch) inside diameter, that is intended to provide a vent area more than 50% greater than the central 12 mm- (0.5 inch) diameter hole that it covers. Potential plugging of these vent passages could be caused by appreciable corrosion-product buildup, possibly hindering gas release and causing unwanted pressure buildup within the waste container. This could be a valid concern to RH-container performance adequacy, possibly within the first 5 years of WIPP operation, or certainly during the operational lifetime of the facility.

This HEPA filter splash cover corrosion concern was brought to the attention of the WIPP facility operating contractor when the corrosion first became apparent, after 24 months of testing. The RH TRU container designers at the Hanford facility (Hertelendy, 1984) and Waste Handling Engineering personnel at the WIPP facility (J. E. Stumbaugh, WID) reviewed the filter design from the point of view of corrosion impacts. Their conclusion was that the filter vent passages are ample enough to preclude filter plugging without a design change. However, the extent of corrosion still is continuing to increase with time. A further in situ examination for container, pintle, and filter assembly corrosion after more than six years of in situ testing would appear to be quite valuable in this regard; investigations will be conducted if personnel access to Room T is restored. The potential for a filter blockage due to corrosion should not be totally

dismissed; further evaluations seem prudent. There appear to be several simple resolutions to this corrosion concern, to eliminate any potential problems on future filters before they occur. As discussed with WIPP personnel (J.E. Stumbaugh, WID), our recommendations are to:

1. Replace the (tinplate) steel filter cover plate with a non-metallic (e.g., plastic or other) cover with appropriate gas channels. Due to unknown, multi-year corrosion in the slightly moist, dusty salt environment found at the WIPP, the use of bare steel in the filter manufacture appears to be a questionable choice.
2. Use a more corrosion-resistant metal on the pintle-cover area. Based on previous laboratory and WIPP in situ tests (Tyler et al., 1988), we would recommend Inconel 600 or 625 components for ambient-temperature WIPP applications. Stainless steel components are not recommended for use in a damp, salt environment because of chloride-induced stress corrosion cracking (Sorensen and Molecke, 1992; Molecke et al., 1993).

7.4.2 Backfill Material Considerations

As previously mentioned, we frequently observed indications of minor brine intrusions, to varying degrees, into all of the unlined test boreholes. We also observed some indications of brine intrusion into the four borehole emplacements that were partially filled with the 70 wt. % bentonite/30 % silica sand backfill material. The backfill material appeared to sorb essentially all of the brine drips intruding into the hole, or wicking into the hole from the sides. This backfill sorption can be considered to help shield the waste container from potential short-term, brine-enhanced corrosion. Brine-moistened bentonite in the backfill can also help to fill or seal small rock salt fractures adjacent to the waste container. One perceived negative, short-term contribution of backfill is the transference of pressure, induced by borehole closure, onto the container. This can be mitigated over the period of five or so years by only partial filling the borehole emplacement void with backfill material. Another short-term negative is the increase in operational difficulty due to installing the backfill material in the borehole, over and around the waste container. This increased difficulty needs to be balanced against the longer-term gains due to brine-sorption effectiveness and the known effectiveness of bentonite for sorbing transuranic species in a brine solution (Tyler et al., 1988), thereby hindering potential long-term transuranic radionuclide migration or dispersal.

8.0 SUMMARY AND CONCLUSIONS

This report summarizes laboratory and in situ data, in situ observations, and preliminary conclusions on the WIPP Simulated RH TRU Waste Experiments. These experiments involve the testing of eight full-size, nonradioactive RH TRU containers emplaced into horizontal, unlined rock salt boreholes in the ribs of WIPP underground Room T. Most of the test emplacements are fully instrumented with remote-reading thermocouples, pressure gages, borehole vertical-closure gages, and vertical and horizontal borehole-diameter closure gages. In situ test conditions were designed to be "near-reference" with respect to anticipated thermal outputs of RH TRU containers and their geometrical spacing or layout in WIPP repository rooms. The effects of heat on borehole closure and near-field materials interactions were closely monitored. Each test borehole was opened periodically for visual inspections, manual closure measurements, maintenance, and materials sampling.

These simulated RH TRU waste experiments have been in heated operation since September 1986 and are presently continuing in a state of instrument monitoring and passive maintenance -- no instrument maintenance, test observations, or sampling within the test room due to the current lack of access. We have documented herein a comprehensive presentation of all results acquired over the first five years of test operation and initial interpretations of all data. A schedule for final in situ test visual inspections, manual measurements, and experiment termination has not as yet been set. We anticipate that this final examination, if conducted, could provide valuable, additional WIPP Project information on RH TRU borehole stability, brine intrusion potentials, waste package materials performance, and associated handling and retrieval operations. These data should be relevant to the originally planned WIPP initial retrievability period for actual TRU wastes.

Temperatures: The maximum observed heater-thermocouple temperatures were in the range of 36° to 42°C with the heater power output of 115 ± 4.5 W, and in the range of 45° to 58°C with the later heater power output of 299 ± 9.5 W. Similarly, the observed near-field salt temperatures, at the borehole top - air interface, were in the range of 31° to 32°C at the lower heater power output, and in the range of about 35° to 37°C at the higher heater power output. These temperatures should be compared to the observed borehole salt initial ambient temperature of 28° to 28.3°C and the observed room air ambient temperature range of about 23 to 33°C, over five years. In both heater- and near-field temperature cases, there are also minor fluctuations in temperature histories with a range of up to 2°C, and a near-sinusoidal periodicity of about one year, due to mine-ambient air seasonal temperature and ventilation fluctuations in the test room.

We also conducted extensive thermal analyses to predict near-field and far-field thermal behavior, to compare to the experimentally measured temperature histories, and to aid in accomplishing the objectives of these WIPP simulated RH TRU waste tests. These thermal calculations, with each RH TRU container having a thermal output of 117 W, were utilized as input to the 3D thermal-structural study also conducted to help in the interpretation of the borehole closure measurements obtained experimentally. The analytical thermal results appear, in general, to agree well with the experimentally measured temperatures in both magnitude and time dependence, particularly for the near-field temperatures. The largest calculated temperature rise was only ~6°C at the borehole wall surface, implying that the room thermal load is very small. However, some discrepancies between the measured and calculated temperature responses at the heater (container) wall surfaces are noticeable. These discrepancies are believed to be due to approximations made in the thermal properties of the RH TRU container material as compared to the actual materials of the test heaters and, perhaps, due to the presence of air and moisture initially present in the backfill material near the heater-backfill interface. These approximations effectively result in smaller thermal conductivity values, making the interface region act more as an insulator. Before this interface region becomes thermally stable, the heater-surface temperature would rise rapidly. Once the backfill material in the interface region attains a quasi-stable condition, the heat is conducted more efficiently through the region.

Pressures: The not-totally-confined, granular bentonite/silica sand backfill material in the test boreholes is quite capable of transferring stress loading due to borehole creep-closure onto the RH containers. Pressures applied to the left and right sides of test containers were monitored as a function of time and location within the boreholes. The maximum observed pressures were always at the furthest distance in, nearer the closed or blind end of the borehole. The minimum pressures were always observed at the midpoint of the container, at 2.95 m in from the rib face. Monitored pressures increased almost continuously from the time of backfill material emplacement. The highest pressure values observed, e.g., 0.72 and 0.87 MPa (104 to 126 psi) were always followed by subsequent pressure decreases. There were also several occasions of two pressure maxima. This pressure transference capacity is limited, however. In the test boreholes, only partially filled with backfill, the backfill reached a certain amount of consolidation, transferring pressures, before it shifted somewhat, thereby temporarily decreasing its load-bearing capacity. The largest observed rates of pressure increase, up to 0.25 MPa/year (36 psi/year), would yield a maximum calculated pressure of about 1.3 MPa (180 psi) if linearly extrapolated over an undisturbed 5-year test emplacement-retrieval cycle, assuming a fully backfilled waste emplacement hole and no backfill slippage.

Visual evaluations of the observed pressure histories in the test boreholes do not reveal any obvious correlation between heater thermal output and pressure increase, between 0 (ambient) to 115 and 300 watts/heater.

Borehole Closures: The maximum measured, vertical-displacement borehole closure after approximately five years of test operation is about 75 mm (3.0 in.). The vertical closure rates were very close to linear with time, with rates ranging from 10.3 to 15.3 mm/year (0.41 to 0.60 in./year) over the 50- to 1826-day test period. There does not appear to be a significant impact on vertical closure rates over the heater-power range used. Borehole vertical closure data and rates were also obtained for an about-one-month period prior to heater turn-on. These ambient-temperature closure rates were between 16.9 to 18.6 mm/year (0.69 to 0.73 in./year), generally about 2 to 5 mm/year faster than the observed ranges over the 50- to 1826-day heated period. Immediately after turn-on of the 115 W heaters, vertical closure rates increased slightly for about 50 days, presumably in response to the thermal output and temperature increase. The initial increases over the pre-turn-on closure rates were in the range of +0.9 to 5.7 mm/year (0.04 to 0.22 in./year) greater. These rates all decreased after about 50 days, down to the reported 50- to 1826-day rates. Both of these observations indicate that minor borehole temperature increases are less important than elapsed time and salt creep for controlling the observed vertical closure rates.

We also conducted a series of three-dimensional geomechanical, thermal/structural analyses to evaluate the effects of emplacing the RH TRU wastes in the ribs of a typical waste storage room at the WIPP, and to help answer basic concerns regarding retrievability of the wastes during the planned initial five-year retrievability period. We investigated a "reference" emplacement configuration, in which 60 W canisters of RH TRU waste are emplaced at 2.44 m (8 ft) centers one year after room excavation; we also performed similar calculations with 117 W canisters, to better model the simulated RH TRU tests. We then performed additional calculations to investigate the relative importance of the heat load versus the drilling of the boreholes on structural response. Finally, we performed a series of calculations to evaluate the effect of timing for borehole drilling on structural response. Results of these analyses, primarily for the "reference" configuration show that:

- Drilling of the boreholes and application of the heat load at 1 year produces a marked increase in room closure rate, with the effect on closure of drilling the boreholes being about twice that due to the heat load from the RH TRU.

- The effect of heater turn-on at 3.48 years after room excavation, as was the case for the simulated RH TRU tests, has a lesser effect on room closure, and is almost imperceptible in both computed and measured borehole closure results. This implies that the effect of drilling the holes is much more significant than that arising from the thermal load imposed by the canisters.
- Larger borehole closures occur near the center and towards the blind end of the hole than near the rib end. Although the computed vertical closure results provide an upper bound estimate on borehole closure that is 1.5 to 2.5 times larger than the measured in situ values, the computed and measured vertical closure results are in qualitative agreement.
- The computed vertical borehole closure is larger near the rib-end of the hole than the horizontal closure, but the reverse is true toward the middle and the blind end of the hole.
- Despite the significant increase in room closure rate at 1 year, the closure of the room at the end of 6 years (i.e., 5 years after waste container emoplacements) is a moderate 16% for vertical closure and 7% for horizontal closure.

In addition, Argüello and Beraún have calculated that both the vertical and horizontal closures of the boreholes are appreciably greater if the time between room excavation and hole drilling is short (e.g., 1 year) compared to the case where there is a longer time (e.g., 3 years) between these events. This was *expected* because those holes drilled earlier in time after room excavation are subjected to longer periods of loading than those drilled later in time. What was more significant, however, was that for boreholes open for the same length of time, but drilled at different times, the closure is significantly greater for the ones drilled earlier in time. This suggests that time to drilling of the boreholes is an important parameter in borehole closure response and that drilling of the boreholes should be deferred until just prior to emplacement of the RH TRU waste containers. This finding is important because of its implications on waste emplacement operations -- the recommendation is that drilling of the boreholes should be deferred preferably until just prior to emplacement of wastes in a room.

Borehole Closure Implications: When the RH TRU test canisters were initially emplaced into the bare salt unlined boreholes, there was an approximately 152 mm (6 in.) space between the top of the canister and the borehole surface. Based on the measured closure data, it does not seem reasonable to assume that a 66 cm (26 in.)- diameter RH canister emplaced into a 91 cm (36 in.)-diameter borehole, even with a 10 cm (4 in)-high bottom spacer, would be seized by salt creep-closure of the hole during an initial 5-year WIPP retrievability period. Creep-closusure seizing would also not occur even if the retrievability period is extended to include a 5-year retrieval "decision" period plus an additional 2-year period for actual retrieval

operations. This 7-year total period is described in an operational Demonstration Plan for the RH TRU Waste Mock Retrieval Demonstration (DOE, 1986a). Based on the *largest* observed vertical borehole closure rate of 20.0 mm/year (0.79 inch/year), it would require more than 7.5 years before the salt would contact the top of the RH TRU container. The thermal/structural calculations of borehole closure (the upper bound estimates) yielded an equivalent annular clearance of 1.5 cm (0.6 inch) between the borehole wall and the canister at 5 years after emplacement.

Actual borehole closure measurements and thermal/structural calculations suggest that emplacement of thick-walled sleeves in the boreholes to prevent potential borehole-container creep seizure, per current operational proposals (DOE, 1986a; Nair et al., 1986; DOE, 1987), should not be necessary. Additional "insurance" against borehole-container seizure could, if desired, be obtained by using a slightly larger-diameter borehole. The proposed thick sleeves were also intended to prevent any potential rock chunks falling or scaling from the salt borehole surfaces, thus hindering retrieval operations. Neither of these occurrences have yet been observed. Another round of in situ test borehole visual examination, after more than six years of heated testing would be extremely beneficial to check for rock salt fracturing, scaling, rock fall, and brine intrusion into the unlined test holes. This observation would be conducted as a part of the overall test termination.

We previously proposed (Molecke and Munson, 1987) the WIPP in situ testing of thin "rock fall" borehole liners, in order to protect RH TRU canisters in the boreholes from potential impacts from rock salt fracturing and cracking. These thin liners also would prevent any potential rock chunks falling or scaling from the salt borehole surfaces. These "rock fall" borehole liners would be 30 in. in OD and 0.5 in. thick (0.76 m x 12.7 cm), and are adequate to surround and protect either a 26 in.-OD RH TRU canister or a 28 in.-OD overpacked RH TRU waste container. In essence, these liners are an alternative "safety blanket" to the use of thick borehole sleeves, to guarantee the easy retrieval of RH TRU containers from the emplacement holes. The testing of such liners was not, however, initiated. Based on our borehole closure measurements and calculations, neither the thin liners nor the thick borehole sleeves are required or really necessary during the initial period of retrievability. After the 5-year, or even 7-year period of retrievability, there does not appear to be any technical justification for RH TRU borehole sleeves or liners. The potential future use of any liners in the WIPP facility could be eliminated, for the benefit of overall cost effectiveness for RH TRU waste disposal. These statements are not intended to cover the use of a short, e.g., < 1 m-long cylinder for anchoring and aligning the borehole shield-cover in place.

An additional WIPP repository performance assessment issue exists that also supports the recommendation not to use thick borehole sleeves, thin liners, or other massive shielding components fabricated from steel. In the long-term, anoxic corrosion of low-carbon steels in the presence of potentially intruding brines can yield an appreciable quantity of hydrogen gas, and resultant pressures in a sealed repository. Ongoing laboratory corrosion studies (Brush et al., 1992) are quantifying the gas generation potentials and rates for hydrogen production from steels used in WIPP CH TRU waste applications. These studies and results (Brush et al., 1992) are also directly applicable to RH TRU waste containers and associated steel components that are planned to be stored in the same repository rooms as the CH TRU wastes. There should be a concerted WIPP Project effort, coupled with performance assessment evaluations, to minimize the emplacement of unnecessary steel components, particularly thick borehole liners. The specific objective is to minimize the overall gas generation potential, quantities, and pressures in the WIPP.

Materials Related Information: Indications of minor brine intrusions were frequently observed, to varying degrees, in all of the unlined test boreholes. This was primarily exhibited by the presence of occasional small, blob-shaped efflorescences or stalactite drips on the top-half of the borehole surfaces, and of blob-precipitates, small stalagmites, or drip paths onto small areas of the top or side surfaces of the test containers. The population and size of these evaporated-brine occurrences in most boreholes has increased somewhat with time. However, we never observed any appreciable liquid brine accumulations. Indications of brine intrusion were observed as damp-appearing, slightly darker-colored regions of the backfill. The backfill material sorbs or wicks essentially all brine intruding into the hole from either hole-top drips or side seeps. "Damp-appearing" backfill samples had an analyzed, sorbed-moisture content within the range of 4.5 % to 8.2 wt. %, somewhat greater than the nominal moisture value of about 3.9 wt. % for unused, initial bentonite/sand backfill. Moisture content within the emplacements decreased somewhat as a function of time, as the available brine dried out in the slightly warm boreholes. These in situ test results support the use of tailored, i.e., bentonite-containing backfill materials in WIPP TRU waste storage, particularly for the short-term sorption of brine and, in the long-term, to hinder potential transuranic radionuclide migration or dispersal away from the waste emplacement borehole (Tyler et al., 1988).

Overall, the qualitative observations on the in situ RH TRU waste tests in WIPP Room T certainly tend to indicate that RH containers should have no difficulty whatsoever in withstanding corrosive attack, with full mechanical integrity, during the early years of WIPP operations. This integrity or durability conclusion applies to both the near-reference and overtest thermal conditions, as used in these RH TRU tests. These containers are not intended to be long-term (i.e., decades to centuries), corrosion-resistant barriers.

Corrosion on the painted areas of all containers is considered insignificant, for at least the first 36 months of heated testing in the relatively mild, corrosive test borehole environment. The corrosion-prevention capability of the reference enamel paint used on the containers is adequate, but the mechanical abrasion resistance (paint hardness, durability) of the paint was less than ideal. The unpainted, mild steel pintles of all containers exhibited superficial rusting, which has become more "flaky" as a function of time, but is still not considered significant. As a portion of the test termination activity, it would be very worthwhile to re-examine the corrosion behavior or condition of the test containers at the present time, after more than six years, to see if our conclusions are still valid.

Based on in situ observations, however, the above conclusion on container corrosion adequacy may not apply to the HEPA filter assembly on each RH TRU container. The observed flaky corrosion buildup and small holes on the HEPA filter splash cover potentially could become detrimental with time. Possible plugging of vent passages in the HEPA filter could be caused by appreciable corrosion-product buildup, potentially hindering gas release and causing unwanted pressure buildup within the waste container. This could be a valid concern to RH TRU container-performance adequacy, possibly within the initial WIPP waste retrievability period, or certainly during the operational lifetime of the facility. Again, a visual examination of these HEPA filter assemblies after more than six years, during test termination activities, would be quite beneficial to resolve this question of adequacy.

In conclusion, our current data, results, and observations from the WIPP simulated RH TRU waste experiments have addressed and quantified essentially all of our initial objectives, as described in Section 2. In situ results on the interactions of heat, waste package materials, limited amounts of intruding brine, and the quantified rates of salt borehole closure and resultant pressures indicate that similar, but radioactive (actual) RH TRU containers should be adequate and safe for repository-phase isolation in unlined, horizontal salt boreholes in the WIPP. There should be no restrictions on WIPP RH TRU waste acceptance due to observed waste package performance.

Our in situ, simulated RH TRU waste test conduct should not be viewed as an isolated waste package performance experiment. The RH TRU test results, interpretations, and recommendations can be combined with ongoing WIPP mechanistic modeling and performance assessment studies, with separate RH TRU operational demonstrations, with planned actual CH TRU waste tests on brine-leaching, source-term evaluations (in the laboratory) and waste degradation, gas-generation tests (both in the laboratory and at the WIPP). The sum total of experimental, operational, and modeling analyses will help provide the

WIPP Project the overall scientific and technical bases needed to demonstrate the short-term performance behavior, and predict the long-term safety performance, of radioactive waste packages emplaced in WIPP salt. These resolutions will be important in assuring both the general public and the technical community that the concept of nuclear waste disposal in WIPP salt will be both valid and safe.

9.0 REFERENCES

Adams, C. R. 1985. *GRAFAID Code User Manual.* SAND84-1725. Albuquerque, NM: Sandia National Laboratories.

Argüello, J. G. and T. M. Torres. 1988. *Thermal Effects of RH-TRU Waste Emplacement on WIPP Storage Room Thermal/Structural Response.* SAND88-2217. Albuquerque, NM: Sandia National Laboratories.

Argüello, J. G., R. Beraún, and M. A. Molecke. 1989. *3D Thermal Stress Analysis of WIPP Room T RH TRU Experiments.* SAND88-2734. Albuquerque, NM: Sandia National Laboratories.

Ball, J. R., and L. K. Shepard, Re/Spec, Inc. 1987. *User's Manual for the UNDERDOG Data Reduction Software.* SAND87-7149. Albuquerque, NM: Sandia National Laboratories.

Beraún, R. and M. A. Molecke. 1987. *Thermal Analysis of the WIPP In Situ Room A1 DHLW Package Experiments.* SAND86-0681. Albuquerque, NM: Sandia National Laboratories.

Biffle, J. H. 1984. *JAC - A Two-Dimensional Finite Element Computer Program for the Non-Linear Quasistatic Response of Solids With the Conjugate Gradient Method.* SAND81-0998. Albuquerque, NM: Sandia National Laboratories.

Borns, D. J. and J. C. Stormont. 1988. *An Interim Report on Excavation Effect Studies at the Waste Isolation Pilot Plant: The Delineation of the Disturbed Rock Zone.* SAND87-1375. Albuquerque, NM: Sandia National Laboratories.

Braithwaite, J. W. and M. A. Molecke. 1979. *Corrosion and Anti-Corrosion Coatings Studies for TRU Waste Containers, Section 7, in Summary of Research and Development Activities in Support of Waste Acceptance Criteria for WIPP.* SAND79-1305. Albuquerque, NM: Sandia Laboratories.

Brush, L.H., M.A. Molecke, R.E. Westerman, A.J. Francis, J.B. Gillow, D.T. Reed, and R.H. Vreeland. *1993.* "Laboratory Studies of Gas Generation for the Waste Isolation Pilot Plant." SAND92-2160C. Published in *Scientific Basis for Nuclear Waste Management XVI, MRS Volume 294.* Eds. C.G. Interrante and R.T. Pabalan. Pittsburgh, PA: Materials Research Society. 335-340.

Bulmer, B. M. 1990. *Pretest Thermal Analysis of the Tuff Water Migration/In Situ Heater Experiment.* SAND79-1278. Albuquerque, NM: Sandia National Laboratories.

Hertelendy, N. A. 1984. *Users Manual for Remote Handled Transuranic Waste Container.* RHO-RE-MA-7. Hanford, WA: Rockwell Hanford Operations.

Krieg, R. D. 1984. *Reference-Stratigraphy and Rock Properties for the Waste Isolation Pilot Plant Project.* SAND83-1908. Albuquerque, NM: Sandia National Laboratories.

Krumhansl, J. L., K. M. Kimball, and C. L. Stein. 1991. *Intergranular Fluid Compositions from the Waste Isolation Pilot Plant, Southeastern New Mexico.* SAND90-0584. Albuquerque, NM: Sandia National Laboratories.

Matalucci, R. V., C. L. Christensen, T. O. Hunter, M. A. Molecke, and D. E. Munson. 1979. *Waste Isolation Pilot Plant (WIPP) Research and Development Program: In Situ Testing Plan.* SAND81-2628. Albuquerque, NM: Sandia National Laboratories.

McIlmoyle, J. T., R. V. Matalucci, and H. C. Ogden. 1987. *The Data Acquisition System for the Waste Isolation Pilot Plant In Situ Tests.* SAND86-1031. Albuquerque, NM: Sandia National Laboratories.

Molecke, M. A. 1986. *TEST PLAN: WIPP Simulated CH and RH TRU Waste Tests: Technology Experiments (TRU TE).* Albuquerque, NM: Sandia National Laboratories.

Molecke, M. A. 1984. *TEST PLAN: Waste Package Performance Technology Experiments for Simulated DHLW.* Albuquerque, NM: Sandia National Laboratories.

Molecke, M. A. and D. E. Munson. 1987. *TEST PLAN APPENDIX: WIPP Simulated RH TRU Waste Add-On Tests.* Albuquerque, NM: Sandia National Laboratories.

Molecke, M.A., N.R. Sorensen, J.R. Harbour, and D.M. Ferrara. 1993. *Post-Test Evaluations Of Waste Isolation Pilot Plant-Savannah River Simulated Defense HLW Canisters And Waste Form.* SAND91-2038C. To be presented at 1993 International Conference on High-Level Radioactive Waste Management, Las Vegas, NV, April 26-30, 1993.

Morgan, H. S. 1987. "Estimate of the Time Needed for TRU Storage Rooms to Close," memo to D. E. Munson, Sandia National Laboratories, Albuquerque, NM, June 2, 1987.

Mufti, I. R. 1971. "Geothermal Aspects of Radioactive Waste Disposal Into the Surface." *J. Geophysics Research.* Vol. 26, no. 35.

Munson, D. E. 1983. *TEST PLAN: Overtest for Simulated DHLW, Thermal- Structural Interactions.* Albuquerque, NM: Sandia National Laboratories.

Munson, D. E., R. L. Jones, J. R. Ball, R.M. Clancy, D.L. Hoag, and S.V. Petney. 1989. *Overtest for Simulated Defense High-Level Waste (Room B): In Situ Data Report (May 1984 - February 1988), Waste Isolation Pilot Plant (WIPP) Thermal/Structural Interactions Program.* SAND89-2671. Albuquerque, NM: Sandia National Laboratories.

Munson, D. E., J. R. Ball, and R. L. Jones. 1990. *DataQuality Assurance Controls Through the WIPP In Situ Data Acquisition, Analysis, and Management System.* SAND88-2845. Albuquerque, NM: Sandia National Laboratories.

Nair, B.R., R.J. Maloney, and J.E. Stumbaugh. 1986. *"Horizontal Emplacement and Retrieval Equipment for Remote Handled Transuranic Wastes at the Waste Isolation Pilot Plant." Proceedings of Waste Management '86, Vol. 2.* Eds. R. G. Post and M. E. Wacks. Tucson, AZ: University of Arizona.

PDA Engineering INC., Software Products Division. 1984. *PATRAN User's Guide, Volume I and II.* Santa Ana , CA.

Pfeifle, T. W., RE/SPEC, Inc. 1987a. *Backfill Material Specifications and Requirements for the WIPP Simulated DHLW and TRU Waste Technology Experiments.* SAND85-7209. Albuquerque, NM: Sandia National Laboratories.

Pfeifle, T. W., RE/SPEC, Inc. 1987b. *Mechanical Properties and Consolidation of Potential DHLW Backfill Materials: Crushed Salt and 70/30 Bentonite /Sand.* SAND85-7208. Albuquerque, NM: Sandia National Laboratories.

Rockenbach, F. A. 1987. *P/THERMAL Application Module User Manual, Version 1.1.* P/N-2192006. Costa Mesa, CA: PATRAN Division of PDA Engineering.

Rohsenow, W. M. and J. P. Hartnett. 1973. *Handbook of Heat Transfer.* New York, NY: McGraw-Hill Book Company.

Sorensen, N.R. and M.A. Molecke. 1992. *Summary of the WIPP Materials Interface Interactions Test - Metal Corrosion,* SAND92-1921C. Albuquerque, NM: Sandia National Laboratories. Presented at the Workshop on In Situ Tests on Waste Packages and Engineered Barriers, in Corsendonk, Belgium, October 1992.

Tyler, L. D., R. V. Matalucci, M. A. Molecke, D. E. Munson, E. J. Nowak, and J. C. Stormont. 1988. *Summary Report for the WIPP Technology Development Program for Isolation of Radioactive Waste.* SAND88-0844. Albuquerque, NM: Sandia National Laboratories.

U. S. Department of Energy. 1986a. *Demonstration Plan for the Remote Handled (RH) Transuranic Waste Mock Retrieval Demonstration.* DOE/WIPP-86-011. Carlsbad, NM: prepared by Westinghouse Electric Corporation.

U. S. Department of Energy. 1986b. *Waste Isolation Pilot Plant Validation Final Report.* DOE/WIPP-86-010. San Francisco, CA: prepared by Bechtel National, Inc.

U. S. Department of Energy. 1987. *Report of the Remote Handled (RH) Transuranic Waste Mock Retrieval Demonstration.* DOE/WIPP-87-009. Carlsbad, NM: prepared by Westinghouse Electric Corporation.

DISTRIBUTION

Federal Agencies

US Department of Energy (6)
Office of Civilian Radioactive Waste Management
Attn: Deputy Director, RW-2
Associate Director, RW-10/50
Office of Program and Resources Management
Office of Contract Business Management
Director, Analysis and Verification Division, RW-22
Associate Director, RW-30
Office of Systems and Compliance
Associate Director, RW-40
Office of Storage and Transportation
Director, RW-45
Office of Strategic Planning and International Programs
Office of External Relations
Forrestal Building
Washington, DC 20585

US Department of Energy
Albuquerque Operations Office
Attn: National Atomic Museum Library
PO Box 5400
Albuquerque, NM 87185-5400

US Department of Energy (4)
WIPP Project Integration Office
Attn: W.J. Arthur III
L.W. Gage
P.J. Higgins
D.A. Olona
PO Box 5400
Albuquerque, NM 87115-5400

US Department of Energy (2)
WIPP Project Integration Satellite Office
Attn: R. Batra
R. Becker
PO Box 3090
Carlsbad, NM 88221-3090

US Department of Energy (3)
WIPP Project Site Office (Carlsbad)
Attn: V. Daub
J. Lippis
J.A. Mewhinney
PO Box 3090
Carlsbad, NM 88221-3090

US Department of Energy
Research & Waste Management Division
Attn: Director
PO Box E
Oak Ridge, TN 37831

US Department of Energy
Attn: E. Young
Room E-178
GAO/RCED/GTN
Washington, DC 20545

US Department of Energy
Office of Environmental Restoration and Waste Management
Attn: J. Lytle, EM-30
(Trevion II)
Washington, DC 20585-0002

US Department of Energy (3)
Office of Environmental Restoration and Waste Management
Attn: M. Frei, EM-34
(Trevion II)
Washington, DC 20585-0002

US Department of Energy
Office of Environmental Restoration and Waste Management
Attn: S. Schneider, EM-342
(Trevion II)
Washington, DC 20585-0002

US Department of Energy (2)
Office of Environment, Safety and Health
Attn: C. Borgstrom, EH-25
R. Pelletier, EH-231
Washington, DC 20585

US Department of Energy (2)
Idaho Operations Office
Fuel Processing and Waste Management Division
785 DOE Place
Idaho Falls, ID 83402

US Environmental Protection Agency (2)
Radiation Protection Programs
Attn: M. Oge
ANR-460
Washington, DC 20460

US Geological Survey (2)
Water Resources Division
Attn: R. Livingston
4501 Indian School NE
Suite 200
Albuquerque, NM 87110

US Nuclear Regulatory Commission
Division of Waste Management
Attn: H. Marson
Mail Stop 4-H-3
Washington, DC 20555

Boards

Defense Nuclear Facilities Safety Board
Attn: D. Winters
625 Indiana Ave. NW, Suite 700
Washington, DC 20004

Nuclear Waste Technical Review Board (2)
Attn: Chairman
S.J.S. Parry
1100 Wilson Blvd., Suite 910
Arlington, VA 22209-2297

Advisory Committee on Nuclear Waste
Nuclear Regulatory Commission
Attn: R. Major
7920 Norfolk Ave.
Bethesda, MD 20814

State Agencies

Environmental Evaluation Group (3)
Attn: Library
7007 Wyoming NE
Suite F-2
Albuquerque, NM 87109

NM Bureau of Mines and Mineral Resources
Socorro, NM 87801

NM Energy, Minerals, and Natural Resources Department
Attn: Library
2040 S. Pacheco
Santa Fe, NM 87505

NM Environment Department (3)
Secretary of the Environment
Attn: J. Espinosa
1190 St. Francis Drive
Santa Fe, NM 87503-0968

NM Environment Department
WIPP Project Site
Attn: P. McCasland
PO Box 3090
Carlsbad, NM 88221

Laboratories/Corporations

Battelle Pacific Northwest Laboratories
Attn: R.E. Westerman, MSIN P8-44
Battelle Blvd.
Richland, WA 99352

INTERA Inc.
Attn: J.F. Pickens
6850 Austin Center Blvd.
Suite 300
Austin, TX 78731

INTERA Inc.
Attn: W. Stensrud
PO Box 2123
Carlsbad, NM 88221

IT Corporation
Attn: R.F. McKinney
Regional Office
5301 Central NE, Suite 700
Albuquerque, NM 87108

Los Alamos National Laboratory
Attn: B. Erdal, CNC-11
PO Box 1663
Los Alamos, NM 87544

RE/SPEC, Inc.
Attn: W. Coons
4775 Indian School NE
Suite 300
Albuquerque, NM 87110-3927

RE/SPEC, Inc.
Attn: J.L. Ratigan
PO Box 725
Rapid City, SD 57709

Southwest Research Institute (2)
Center for Nuclear Waste Regulatory Analysis
Attn: P.K. Nair
6220 Culebra Road
San Antonio, TX 78228-0510

SAIC
Attn: D.C. Royer
101 Convention Center Dr.
Las Vegas, NV 89109

SAIC
Attn: H.R. Pratt
10260 Campus Point Dr.
San Diego, CA 92121

SAIC (2)
Attn: M. Davis
J. Tollison
2109 Air Park Rd. SE
Albuquerque, NM 87106

Tech Reps Inc. (3)
Attn: J. Chapman
C. Crawford
T. Peterson
5000 Marble NE, Suite 222
Albuquerque, NM 87110

TRW Environmental Safety Systems
Attn: L. Wildman
2650 Park Tower Dr., Suite 1300
Vienna, VA 22180-7306

Westinghouse Electric Corporation (5)
Attn: Library
C. Cox
L. Fitch
B.A. Howard
R. Kehrman
PO Box 2078
Carlsbad, NM 88221

Westinghouse-Savannah River
Technology Center (4)
Attn: N. Bibler
J.R. Harbour
M.J. Plodinec
G.G. Wicks
Aiken, SC 29802

National Academy of Sciences, WIPP Panel

Howard Adler
Oak Ridge Associated Universities
Medical Sciences Division
PO Box 117
Oak Ridge, TN 37831-0117

Ina Alterman
Board on Radioactive
Waste Management, GF456
2101 Constitution Ave.
Washington, DC 20418

Fred M. Ernsberger
250 Old Mill Road
Pittsburgh, PA 15238

John D. Bredehoeft
Western Region Hydrologist
Water Resources Division
US Geological Survey (M/S 439)
345 Middlefield Road
Menlo Park, CA 94025

Rodney C. Ewing
Department of Geology
University of New Mexico
Albuquerque, NM 87131

Charles Fairhurst, Chairman
Department of Civil and
Mineral Engineering
University of Minnesota
500 Pillsbury Dr. SE
Minneapolis, MN 55455-0220

B. John Garrick
PLG Incorporated
4590 MacArthur Blvd., Suite 400
Newport Beach, CA 92660-2027

Leonard F. Konikow
US Geological Survey
431 National Center
Reston, VA 22092

Peter B. Myers
National Academy of Sciences
Board on Radioactive
Waste Management
2101 Constitution Ave.
Washington, DC 20418

Jeremiah O'Driscoll
Jody Incorporated
505 Valley Hill Drive
Atlanta, GA 30350

Christopher G. Whipple
Clement International
160 Spear St., Suite 1380
San Francisco, CA 94105

Individuals

P. Drez
8816 Cherry Hills Rd. NE
Albuquerque, NM 87111

D.W. Powers
Star Route Box 87
Anthony, TX 79821

Universities

University of New Mexico
Geology Department
Attn: Library
Albuquerque, NM 87131

University of Washington
College of Ocean
and Fishery Sciences
Attn: G.R.Heath
583 Henderson Hall
Seattle, WA 98195

Libraries

Thomas Brannigan Library
Attn: D. Dresp
106 W. Hadley St.
Las Cruces, NM 88001

Government Publications Department
Zimmerman Library
University of New Mexico
Albuquerque, NM 87131

Hobbs Public Library
Attn: M. Lewis
509 N. Ship St.
Hobbs, NM 88248

New Mexico Junior College
Pannell Library
Attn: R. Hill
Lovington Highway
Hobbs, NM 88240

New Mexico State Library
Attn: N. McCallan
325 Don Gaspar
Santa Fe, NM 87503

New Mexico Tech
Martin Speere Memorial Library
Campus Street
Socorro, NM 87810

WIPP Public Reading Room
Carlsbad Public Library
Attn: Director
101 S. Halagueno St.
Carlsbad, NM 88220

Foreign Addresses

Studiecentrum Voor Kernenergie
Centre D'Energie Nucleaire (2)
Attn: A. Bonne
P. Van Iseghem
SCK/CEN Boeretang 200
B-2400 Mol, BELGIUM

Atomic Energy of Canada, Ltd. (3)
Whiteshell Research Estab.
Attn: B. Goodwin
M. Stevens
D. Wushke
Pinewa, Manitoba, CANADA ROE 1LO

Francois Chenevier (2)
ANDRA
Route du Panorama Robert Schumann
B.P. 38
92266 Fontenay-aux-Roses, Cedex
FRANCE

Jean-Pierre Olivier
OECD Nuclear Energy Agency
Division of Radiation Protection
and Waste Management
38, Boulevard Suchet
75016 Paris, FRANCE

Claude Sombret
Centre D'Etudes Nucleaires
De La Vallee Rhone
CEN/VALRHO
S.D.H.A. B.P. 171
30205 Bagnols-Sur-Ceze, FRANCE

Gesellschaft fur Reaktorsicherheit
(GRS) (2)
Attn: B. Baltes
W. Muller
Schwertnergasse 1
D-5000 Cologne, GERMANY

Bundesanstalt fur Geowissenschaften
und Rohstoffe
Attn: M. Langer
Postfach 510 153
3000 Hanover 51, GERMANY

Bundesministerium fur Forschung und
Technologie
Postfach 200 706
5300 Bonn 2, GERMANY

Institut fur Tieflagerung (2)
Attn: K. Kuhn
Theodor-Heuss-Strasse 4
D-3300 Braunschweig, GERMANY

Kerfurschungszentrum Karlshruhe Gmbh (2)
Institut fur Nukleare Entsorgungstechnik
Attn: W. Lutze
E. Smailos
Postfach 3640
D-7500 Karlsruhe 1, GERMANY

Physikalisch-Technische Bundesanstalt
Attn: P. Brenneke
Postfach 3345
D-3300 Braunschweig, GERMANY

Shingo Tashiro
Japan Atomic Energy Research Inst.
Tokai-Mura, Ibaraki-Ken, 319-11
JAPAN

Netherlands Energy Research Foundation ECN
Attn: L.H. Vons
3 Westerduinweg
PO Box 1
1755 ZG Petten, THE NETHERLANDS

Svensk Karnbransleforsorjning AB
Attn: F. Karlsson
Project KBS
Karnbranslesakerhet
Box 5864
10248 Stockholm, SWEDEN

Nationale Genossenschaft für die Lagerung radioaktiver Abfälle (2)
Attn: S. Vomvoris
P. Zuidema
Hardstrasse 73
CH-5430 Wettingen, SWITZERLAND

AEA Technology
Attn: J.H. Rees
D5W/29 Culham Laboratory
Abington, Oxfordshire OX14 3DB
UNITED KINGDOM

AEA Technology
Attn: W.R. Rodwell
044/A31 Winfrith Technical Centre
Dorchester, Dorset DT2 8DH
UNITED KINGDOM

AEA Technology
Attn: J.E. Tinson
B4244 Harwell Laboratory
Didcot, Oxfordshire OX11 0RA
UNITED KINGDOM

D.R. Knowles
British Nuclear Fuels, plc
Risley, Warrington, Cheshire WA3 6AS
1002607 UNITED KINGDOM

Internal

1502	J.C. Cummings
1561	J.G. Arguello (3)
6000	D.L. Hartley
6119	E.D. Gorham
6119	Staff (14)
6121	J.R. Tillerson
6121	Staff (7)
6300	D.E. Ellis
6302	L.E. Shephard
6303	S.Y. Pickering
6303	W.D. Weart
6305	S.A. Goldstein
6305	A.R. Lappin
6306	A.L. Stevens
6342	D.R. Anderson
6342	Staff (20)
6343	V. Harper-Slaboszewicz
6343	Staff (2)
6345	R.C. Lincoln
6345	Staff (9)
6347	D.R. Schafer
6348	J.T. Holmes
6348	M.A. Molecke (10)
6348	Staff (4)
6351	R.E. Thompson
6352	D.P. Garber
6352	S.E. Sharpton
6352	WIPP Central Files (10) (WPP/TRU, 1.1.1.3.1)
6411	R. Beraun (3)
7141	Technical Library (5)
7151	Technical Publications
7613-2	Document Processing for DOE/OSTI (10)
8523-2	Central Technical Files

* U.S. GOVERNMENT PRINTING OFFICE 1992—775-122/80168

DATE

FILMED

9/27/93

END